Vol.: 49(1)
March, 2025
ISSN: 0250-4758
Online ISSN: 0973-970X

IJVP-2025

INDIAN JOURNAL OF VETERINARY PATHOLOGY

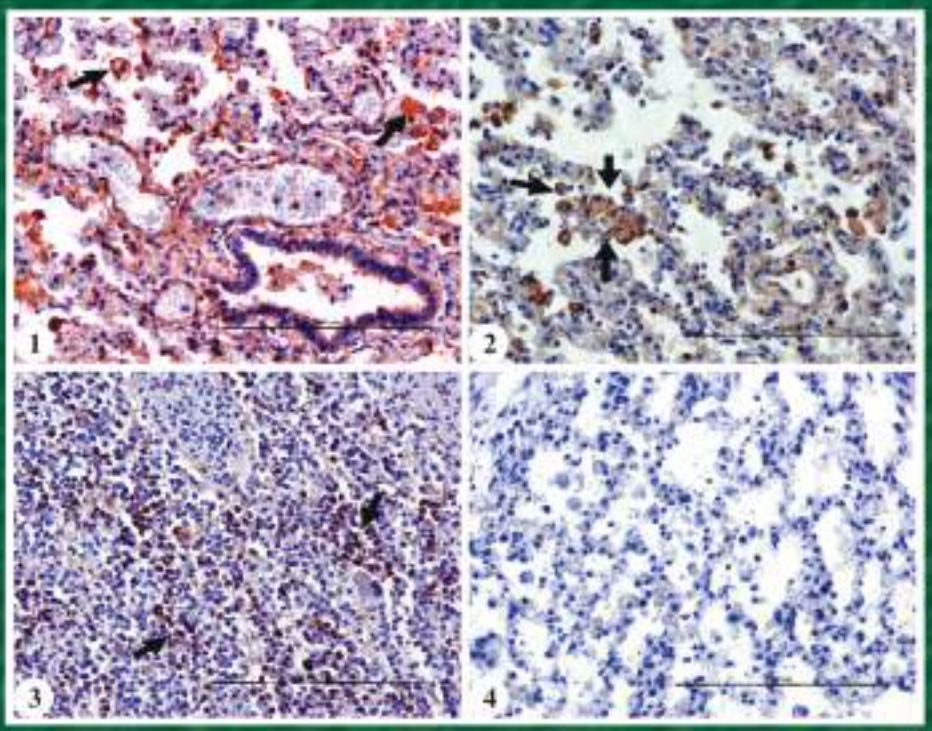

INDIAN ASSOCIATION OF VETERINARY PATHOLOGISTS
(Registered under article 21 of Societies Act 1860)

Visit us at: **www.iavp.org**
Journal available at: **www.indianjournals.com**

Vol. 49 (1)
March, 2025
ISSN: 0250-4758

INDIAN JOURNAL OF VETERINARY PATHOLOGY

Chief Editor
A. Anand Kumar

Editor
K.S. Prasanna

Managing Editor
Vidya Singh

Department of Veterinary Pathology, College of Veterinary Science,
Sri Venkateswara Veterinary University, Tirupati-517502, Andhra Pradesh
Mobile: +91-9441185383; E-mail: 7aakumar@gmail.com

INDIAN JOURNAL OF VETERINARY PATHOLOGY

Chief Editor

A. Anand Kumar

Editor

K.S. Prasanna

Managing Editor

Vidya Singh

Editorial Board

C. Balachandran, Chennai
Rajendra Singh, Bareilly
T.V. Anil Kumar, Kerala
D.V. Joshi, Gujrat
P. Krishnamoorthy, Karnataka
M.R. Reddy, Telangana
Nitin Virmani, Haryana
K. Dhama, Bareilly
A.K. Sharma, Bareilly
N. Divakaran Nair, Kerala
N.P. Kurade, Maharastra
Kuldeep Gupta, Punjab
S.M. Tamuli, Assam
J. Selvaraj, Tamil Nadu
Hemanth Dadhich, Rajasthan

Membership Fee and Subscription of Journal

- Individual life membership — Rs. 3,000/- (India) — US$ 600/- (Foreign)
- Individual Annual Membership (for foreign only) — US $ 60/- (with free online access; no hard copy of journal)
- Library, Institutions, etc. (Annual) — Rs. 12,000/- (India) — US$ 400/- (Foreign)
- Individual Patron of IAVP — Rs. 1,00,000/- (Life member - paid patron for 5 years)
- Govt./Non-Govt./Corporate/ Institution Patrons — Rs. 5,00,000/ (for 5 years)

Advertisement Tariff

	Black and White	Full Colour
Regular full page	Rs. 4,000	Rs. 6,000
Regular half page	Rs. 2,000	Rs. 3,000
Inside front & back cover page	–	Rs. 10,000
Back cover page	–	Rs. 15,000

Note:

- Those submitting advertisement for two/four/six issues of the IJVP will be extended 15%/20%/25% discounts, respectively, on the above rates.
- The membership fee must be paid through Cash/Online/Crossed cheque or DD in favour of Treasurer "Indian Association of Veterinary Pathologists" payable at SBI, CARI Branch, Bareilly.

- No part of this publication should be reproduced or transmitted in any form (electronic, mechanical or otherwise including photocopy) without written permission from the Chief Editor.

Contents

INDIAN JOURNAL OF VETERINARY PATHOLOGY

INDIAN ASSOCIATION OF VETERINARY PATHOLOGISTS
(Estd. 1974)

PATRONS : D.D. Heranjal
N.C. Jain
D.L. Paikne
U.K. Sharma

EXECUTIVE COMMITTEE (w.e.f. 2023)

President	:	Dr B.N. Tripathi, Jammu
Vice-Presidents	:	Dr K.P. Singh, Izatnagar Dr S.K. Mukhopadhyay, Kolkata
Secretary General	:	Dr G.A. Balasubramaniam, Namakkal
Joint Secretary	:	Dr M. Saminathan, Izatnagar
Treasurer	:	Dr Pawan Kumar, Izatnagar
Chief Editor	:	Dr A. Anand Kumar, Tirupati
Editor	:	Dr K.S. Prasanna, Mannuthy
Managing Editor	:	Dr Vidya Singh, Izatnagar
Web Manager	:	Dr R. Somvanshi, Izatnagar
Zonal Secretary	:	Dr R.C. Ghosh, Durg (Central) Dr Seema Rani Pegu, Guwahati (North-East) Dr S.K. Panda, Bhubaneshwar (East) Dr R.D. Patil, Palampur (North) Dr Manjunatha S.S., Shivamogga (South) Dr Arvind Ingle, Mumbai (West)
Executive Members	:	Dr Pankaj Goswami, Jammu Dr C.K. Jana, Mukteswar Dr Kamal Purohit, Udaipur Dr Rajeev Ranjan, Bhubaneshwar Dr Ashwani Kumar Singh, Bagpat Dr Asok Kumar M, Izatnagar

Cover Page Photo : PCV-2 infection in pigs. Fig. 1. Photomicrograph of the tissue sections of lungs and lymph nodes shadowing alveolar macrophages and inflammatory cells in the lumen. **Fig. 2.** The presence of dark brown immunopositive signals for PCV-2 in the alveolar macrophages and lungs. **Fig. 3.** Mononuclear cells and histiocytes. **Fig. 4.** Absence of immunopositive signals for PCV-2 in the negative control of the lung tissue section.

Indian J. Vet. Pathol., 49(1) : 1-12, 2025: DOI: https://doi.org/10.5958/mavjsy67

REVIEW ARTICLE

Current Status of Ovine Pulmonary Adenocarcinoma (Jaagsiekte)

C. Balachandran
Tamil Nadu Veterinary and Animal Sciences University, Chennai, India

Address for Correspondence
C. Balachandran, Professor, Former Vice-Chancellor, Tamil Nadu Veterinary and Animal Sciences University, Chennai, India, E-mail: balachandran.path@gmail.com

Received: 11.2.2025; Accepted: 14.2.2025

How to cite this article : Balachandran, C. 2025. Current Status of Ovine Pulmonary Adenocarcinoma (Jaagsiekte). Indian J. Vet. Pathol., 49(1) : 1-12.

Ovine pulmonary adenocarcinoma (OPA) / Jaagsiekte (Afrikaans: Jaag: Chasing, Driving; Siekte: Sickness - because affected sheep have the appearance of having being chased and the disease is most noticeable when sheep are being herded), earlier known as ovine pulmonary adenomatosis/ovine pulmonary carcinoma. OPA, a progressive respiratory disease, principally affecting adult animals, is a transmissible contagious tumour of lung, brocnchoalveolar carcinoma, caused by exogenous beta *retrovirus* which has an oncogenic protein that develops lung tumor in sheep and rarely, of goats and moufflons OPA was first described early 19th century in South Africa. OPA was first reported from India in Tamil Nadu State in 1960[1].

With India holding 74.26 million of sheep and 148.89 million of goat (Livestock Census, 2019), contributes nearly 5% and 10% of total meat (chevon and mutton) required in the world respectively implying economic importance. Occurrence of diseases leads to heavy economic losses to meat industry, wool and milk production. In sheep and goats, the most commonly affected system the respiratory system. Pneumonia inflicts heavy mortality and therefore adversely affects the profit in sheep and goat production.

The lungs are exposed to the external environment. The feed dust, pollutant, microorganism and noxious chemicals present in the air will cause respiratory disorder and distress to the animals. Pneumonia in sheep is one of the complex syndromes with multifactorial etiology, usually precipitated by physiological factors and stress in combination with infectious agents. OPA causes respiratory distress to the animal resulting in huge economic loss worldwide. Unlike antemortem diagnosis post mortem diagnosis has significant lesion in the lung like tumor growth and accumulation of fluid in the air ways. OPA has wide range of distribution in the world. Sheep and goat importing country from infested areas are largely at risk. Since the virus has a wide range of transmission it takes little time to infect the whole flock[2]. Hence, OPA is an important economic and animal welfare problem[3].

Aetiology

OPA is caused by a beta-retrovirus that cannot yet be cultured *in vitro,* but the virus has been cloned[4] and sequenced. The term Jaagsiekte sheep retrovirus (JSRV) is used in referring to this virus[5]. OPA caused by a betaretrovirus, JSRV, is distinct from the non-oncogenic ovine lentiviruses.

Exogenous JSRV (ExJSRV), responsible for lung cancer in sheep[6], is a single-stranded, positive sense RNA virus in the genus Beta-retrovirus, family Retroviridae, having approximately 7,460 nucleotides in length and as with other retroviruses four genes encode for essential viral proteins. These are i. gag encoding the structural internal virion proteins comprising matrix (MA), capsid (CA) and nucleocapsid (NC); ii. pro for an aspartic protease (PR); iii. Pol for the RT and integrase (IN) enzymes; and env the surface (SU) and transmembrane (TM) envelope glycoproteins. The viral proteins synthesized initially as large precursors and are later processed into the mature proteins by proteolytic cleavage. The genome also contains several cis-acting elements required for expression of the viral proteins[7-10].

JSRV also has a further open reading frame (orf-x) which overlaps the pol gene with undefined function. orf-x has a codon usage markedly different from that of other genes within JSRV and the predicted amino-acid sequence is extremely hydrophobic. Expression of the putative orf-x protein has not been demonstrated, although there appears to be a specific orf-x mRNA transcript in JSRV-transfected cells and in lung tumours[11]. The sequence is highly conserved in JSRV isolates collected from the UK, Italy, Spain, South Africa and the USA, which is consistent with the notion that orf-x encodes an authentic viral protein[12,13]. Sequence similarity with the adenosine 3A receptor that may give a clue to its function[12], but as most of the 'homologous' regions are in hydrophobic domains, the significance of this similarity is uncertain. orf-x is not essential for cellular transformation *in vitro*[14]

or for oncogenesis *in vivo*[3,15-17].

ERVs (Endogenous retroviruses) are important in the OPA as the sheep genome contains many proviruses that are closely related to JSRV[10,11,18-20]. Twenty-seven endogenous JSRV-related proviruses (denoted enJSRV) have been identified. enJSRV was expressed in the ovine uterus[11].

Completely sequenced three strains of JSRV, including a South African isolate, denoted as JSRV-S[10,21]. The etiological agent of OPA is exogenous JSRV (exJSRV). A specific U3 long terminal repeat (LTR) sequence of exJSRV was detected in lungs from affected animals. U3 sequence and restriction profiles of the virus suggest that there are two types of exJSRV sequences: type I (Kenyan and South African) and type II (Wyoming, USA and UK isolates). exJSRV having a specific tropism for the differentiated epithelial cells, type II pneumocytes and non-ciliated bronchiolar Clara cells of the lung, is the only virus known to cause pulmonary adenocarcinoma in naturally infected animals[22].

The env protein induces oncogenic transformation due its interaction with cell growth pathways such as Hya12-RON, PI3K/Akt and Ras-MEK-ERK[6]. Though enJSRV genes were similar to exJSRV, but not associated with the development of tumors[3,8,9]. Despite this high homology, genetic differences are evident in the viral promoter region (U3) that allowed the development of the exJSRV-specific U3PCR. The genetic similarity is also smaller in the intracytoplasmic tail of the transmembrane protein encoded by the env gene[23] the latter being related to the mechanism of oncogenesis induced by env[11,23].

Epidemiology

Incidence: OPA has been reported in many sheep rearing countries of the world (Fig. 1), Europe, Africa, Asia and America, except in Australia, New Zealand and Falkland Islands. OPA was eradicated in Iceland in the 1950s, following a rigorous slaughter policy[3]. OPA was described in UK in 1888 by Dykes and McFadyean in the first volume of the Journal of Comparative Pathology and Therapeutics (1: 139-146), without knowing true nature of the disease, as lung disease in sheep, caused by the *Strongylus rufescens*. OPA reported in sheep or goats since 2015: UK[24], India[25-29], Ireland[30], Iraq[31,32], Algeria[33], Romania[22] and Mexico[34] using pathological and molecular studies.

Prevalence, morbidity and mortality: The prevalence of OPA appears to vary among the countries but, Peru, Scotland, South Africa, Spain are endemic[35]. In India, Jaagsiekte was first reported in Bikaneri breed of sheep. Two rams were aged one year four months each and two ewes, one aged two years eleven months and other ewe was seven years old[1]. Four Jaagsiekte cases were reported out of 1610 sheep, aged between 2-3 years, by examining the lung lesions obtained from slaughter house[36]. It was reported that the incidence in sheep was 0.060% (117/19342) and in goat was 0.13% (34/25467) from slaughter house samples[37]. Further, it was reported as the occurrence 0.57% (1/174) of Jaagsiekte in sheep and 0.54% (2/367) in goat[38]. Then, OPA has been reported in various parts of India[39-42].

The morbidity and mortality rates vary, but reported high in the first years after the emergence of the disease in a flock can reach up to 50% (Iceland in the 1930s), but as the disease becomes endemic the mortality rate falls to around 1-5%[3,43]. But, many cases of OPA can remain

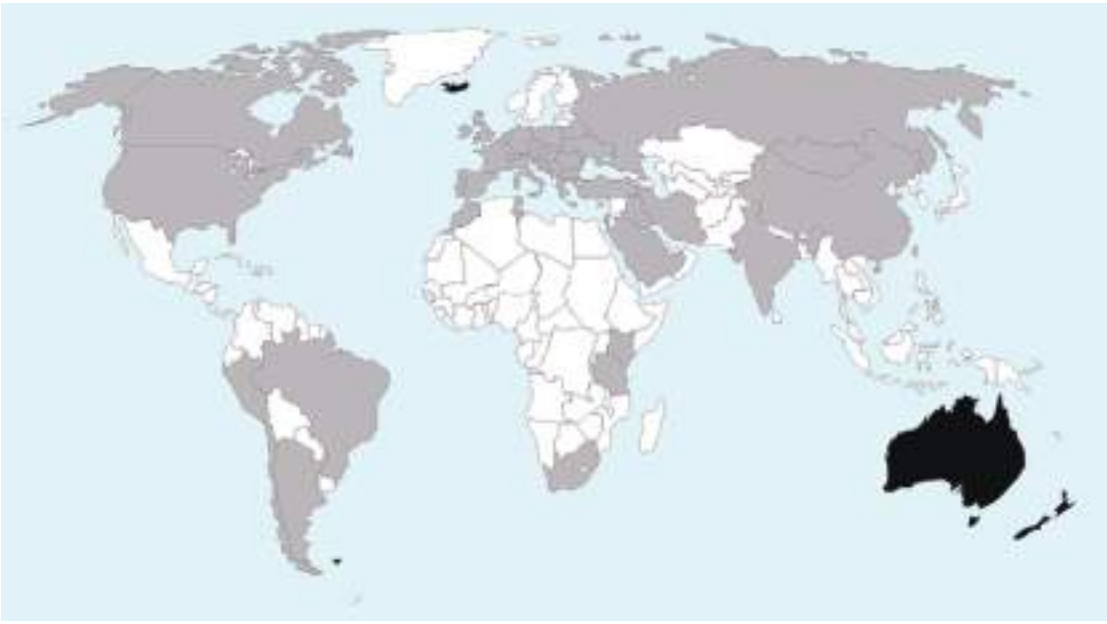

Fig. 1. Distribution of OPA. OPA present is shown in grey; Absent in black; Unknown in white.

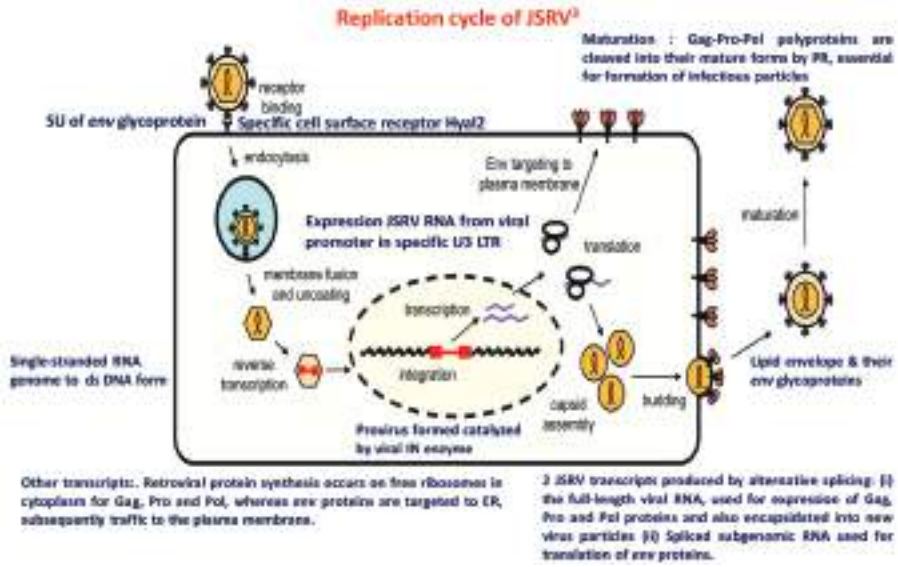

Fig. 2. Replication cycle of JSRV.

subclinical. Studies in flocks with endemic OPA in Scotland and Spain revealed that approximately 30% of the sheep had histologically confirmed lesions while the annual losses attributable to OPA were quite lower[35] and that 40% of animals with OPA lesions at necropsy were not clinically affected[3,9,23]. In our earlier slaughterhouse study conducted, because of limited sample size (n=95), we found 31.20% incidence of OPA[41]. In a later extensor study conducted with large sample size, out of 110000 sheep, 5000 goats studied, 247 affected lung tissues collected showed a prevalence of Jaagsiekte in 9.77% (21/215) in sheep and 6.25% (2/32) in goats[44].

In Europe, the classical OPA has been reported in several countries, such as Ireland, UK, Scotland, Italy, Germany and Spain. The incidence of OPA is usually low, but in some locations it reaches up to 30% and mortality is >50%, causing important economic losses[45]. It can cause about 80% loss of flock for first exposure and 20% for endemic area[2]. Species: OPA mainly affects domesticated sheep *(Ovis aries)*. Sardinian moufflon (*Ovis musimon*, a species of wild sheep) can also become ill, and a few cases were reported in domesticated goat[5,28,44]. Breed and sex: Animals of either gender are affected. Although, there are no evidences that sex or breed can affect sensitivity, many sheep breeds around the world are susceptible to OPA. While some breeds or families seem more resistant to OPA[22,43], some breeds are more susceptible. In Iceland, Gottorp breed showed greater susceptibility, with some producers losing about 90% of the sheep, whereas only up to 10% of Adalbol sheep present in those farms presented clinical signs[23]. Age: In natural conditions, clinical disease is more often detected in sheep aged 1-4 years but age ranged from 2 months to 11 years, or even more, indicating a long incubation period. However, it seems shorter, 6-8 months, in previously unaffected flock. However, experimental data showed that sheep of all ages are susceptible and newborn lambs can develop OPA in 3-4 weeks. Season: Winter seems registering more cases[3,43].

Transmission

Portal of entry and source of virus: Epidemiological study showed that the OPA retrovirus is transmitted by droplets from respiratory fluid via aerosols or droplets, milk, and colostrum tumors, lung fluids, peripheral blood leucocytes and lymphoid organs; as a result, the agent has high chance of contaminating the environment from excess respiratory discharge. Horizontal transmission is demonstrated among sheep of all ages, but neonates appear particularly susceptible to the infection. There was no evidence that *in utero* vertical transmission is significant in the epidemiology of this disease; however, JSRV might be spread in milk or colostrum[46]. JSRV reaches Peyer's patches and mesenteric lymph nodes of lambs nursed by infected mothers[47] and further studies showed the presence of JSRV in milk macrophages but not in milk lymphocytes or mammary gland epithelia of naturally infected sheep[48]. Before tumors develop, the virus is detected in lymphoreticular cells. JSRV found in macrophages of infected mother's milk cross to cross the gut barrier of newborn lambs and spread from mesenteric lymph nodes and Peyer's Patch. The transplacental pathway does not appear to have any epidemiological significance[23,46-48].

The virus has long incubation period that varies according to age of the host. The period between infection and the appearance of clinical signs may be several months or years and many JSRV infected sheep do not exhibit clinical signs at all during their lifespan. This allows the spread of OPA into new flocks through contact

with infected but apparently normal animals. This is due to the absence of an immunological response to JSRV in infected animals, which has hindered the development of serological diagnostic tests and vaccines. JSRV does not survive for long periods in the environment[49]. However, JSRV was reportedly present at high concentration in lung fluid produced by OPA affected sheep and can survive for several weeks at ambient temperatures[50]. In goats, few reports of natural infection, mostly unconvincing, possibly because of misdiagnosis[51]. However, in this species, the OPA acquires significant differences and virus replication does not take place within sensitive lung cells[23,52,53].

Incubation period

The incubation period of natural infections is prolonged, likely for several months to several years, 6 months to 3 years. The incubation period can be shorter in non-endemic herds (6-8 months) and in experimentally infected young lambs[11]. It appears to be age-dependent, and is longer in older sheep. The presence of tumours was detected in animals from 2 months to 11 years of age, although cases of natural disease are rarely observed in sheep less than 9 months old[43,50,54]. In herds where the disease is endemic, the mortality rate is generally low (1-5%), but can reach higher values (>30%) in newly infected herds[3,50]. In an experimental infection 1-week-old lambs developed clinical signs in 70 to 74 days, 1-month-old lambs in 92 to 209 days and 1 to 6-month-old lambs in approximately 160 days or longer. Experimentally infected adult sheep become ill in several months to years[55].

Pathogenesis

JSRV is transmitted primarily by the respiratory route and once inhaled the virus may infect a variety of cells including lymphocytes and myeloid cells[56], in addition to the epithelial cells of the lung. The functional consequences of infection of non-epithelial cells are unclear as very little virus gene expression appears to occur there. Within type II pneumocytes and Clara cells (or their precursors), expression of the JSRV env protein activates signaling cascades that promote cellular proliferation and drive malignant transformation of the cells. Initially, the tumour cells grow along the alveolar walls in a pattern reminiscent of human BAC, but subsequently become more invasive and metastasize to the local lymph nodes. In rare cases, extrathoracic metastases may occur. Larger tumours may be necrotic and fibromatous at their centre. For the weeks to months while the tumour grows, there may be little outward indication and most infected animals show no clinical signs. As the tumour grows, fluid production in the lung increases and this is likely to promote virus spread to other sheep. Only when the tumour reaches a size large enough to compromise lung function, or when fluid production reaches a noticeable level, do clinical signs appear. Critically, the majority of infected animals in endemic areas never show outward signs of infection, but they may be shedding virus, thus promoting inadvertent introduction of the disease into previously unaffected flocks and new geographical areas. Virus life cycle[3] is given in Fig. 2.

Clinical signs

The first indicator of OPA in a flock is often an increased number of deaths in adult sheep from pneumonia that does not respond to antibiotic treatment. Affected animals are afebrile, febrile in secondary bacterial infections, struggle to breathe, especially when exercised[57] and may become very thin despite having a normal/good appetite. Initially, affected animals are less active and have the appearance to have been chased and later dyspnoea and moist respiratory sounds, caused by the accumulation of fluid in the respiratory airways. A pathognomonic sign of OPA is the production of copious amounts of fluid in the lung that is frothy, clear, milky or at times pinkish and drains from the sheep's nostrils when it lowers its head. In the final stages of the disease variable amounts of frothy seromucous pulmonary fluid, from 10 to 40 mL up to 400 mL, are discharged from the nostrils when the sheep head is lowered or the rear limbs are raised (the 'wheelbarrow' test-raising/lifting the hind legs to lower the head of the animal-can be used to check for excess fluid in the lungs), although 40 mL per day is more common[50]. Once the clinical signs are seen the sheep usually lives for only a few more days and may die abruptly following exercise or exposure to cold. The severity of the signs reflects the extent of tumour development in the lung. Despite the unique clinical signs in some affected animals, in many cases no lung fluid is seen[2,3,9,58].

OPA occurs in domestic and wild sheep species and affects no other livestock except goats, in which natural cases have been described only subclinically in affected animals[3]. As the OPA has a long incubation period, clinical disease is encountered most commonly in sheep over 2 years of age, with a peak occurrence at the age of 3-4 years. In exceptional cases, the disease occurs in animals as young as 2-3 months of age. The cardinal signs are those of a progressive respiratory embarrassment, particularly after exercise; the severity of the signs reflects the extent of tumour development in the lungs. Death is often precipitated by a super imposed bacterial pneumonia, particularly that due to *Mannheimia* (formerly *Pasteurella multocida*) *haemolytica*. In clinically affected animals, a peripheral lymphopenia characterized by a reduction in CD4+ T lymphocytes and a corresponding neutrophilia may assist clinical diagnosis, but the changes are not pathognomonic and are not detected during early experimental infection. Moist rales may be heard

on auscultation, but coughing is not usually prominent. The clinical signs are slowly progressive, ending in severe dyspnea. Death usually occurs in days to a few months, often from secondary bacterial pneumonia[2]. Not with standing, this period is shortened and fever appears in the case of secondary bacterial infections[9,43,50,58]. As the pulmonary tumor burden increases, the production of surfactant-containing fluid by the transformed epithelial cells increases, resulting in copious pulmonary effusion, nasal discharge, and progressive dyspnea, which can be accentuated by exercise[58].

Cytology

Cytopathology show high epithelial cellularity seen as individual, acinar or papillary arrangements. Leishman-Giemsa stained smears revealed high cellularity as individual to acinar or papillary arrangements. Neoplastic cells were round. Acinar pattern of neoplastic cells showed pleomorphism with variable sized nuclei and nucleoli. Nuclei showed coarse chromatin. Nucleoli were basophilic. Cytoplasm was scanty to moderate in amount and pale basophilic. Columnar type of cell, showed basally placed spherical to oval nucleus[44]. Both classical and atypical forms of OPA reveal numerous well differentiated cuboidal or polygonal neoplastic epithelial cells arranged in small acini, clusters or individually. The neoplastic cells had a moderate amount of pale blue, finely granular cytoplasm, moderate nuclear: cytoplasmic (N/C) ratio and round to oval, centrally located, nuclei with finely stippled chromatin and 1-2 distinct blue nucleoli. Anisocytosis and anisokaryosis were mild to moderate with rare mitotic figures. Large numbers of macrophages and mature lymphocytes were admixed with the neoplastic cells. OPA containing MGs were poorly cellular and composed of spindle, stellate and elongated cells with round to oval nuclei and inserted in a pale blue slightly vacuolar extracellular myxoid material[22].

Types of OPA

There are two recognized forms of OPA which show gross, histological and immunohistochemical (IHC) differences. Although mixed or intermediate forms of OPA have also been reported. i. Classical OPA: Clinically, the affected sheep develop chronic and progressive respiratory distress, especially when exercised. A common sign of classical OPA is mucous nasal discharge because of production of large fluids amounts in the lung. The lesions in classical OPA predominantly affect all pulmonary lobes and are located in the cranioventral area. They can be either nodular or exhibit a diffuse growth type, showing a grey moist appearance on the cross section. The classical form is more common than the atypical type. ii. Atypical OPA: The atypical OPA is less contagious than classical form. The atypical OPA has been reported in Spain, Peru, Iran and India, but there is no evidence of its occurrence in other countries where OPA is commonly found. Due to the restricted tumour development in atypical OPA and the lack of overproduction of lung fluid, the atypical form of OPA occurs only as a subclinical finding in abattoir studies or when the animal is necropsied for unrelated reasons. Lesions consist of hard nodules, pearly-white that have a dry cut surface; the tumors are well-delimited by the surrounding pulmonary tissue[3,22,45]. However, nodules resembling atypical lesions have been noted in the same lungs in which the classical form of the tumour is present. Therefore, these two forms of OPA appear to represent two extremes of a spectrum of histological presentations in this disease[3]. No molecular differences have been found between JSRV associated with these two forms which may represent two extremes of the OPA disease spectrum rather than two separate forms, and atypical OPA might constitute the initial lesions of this spectrum[43,45].

Gross pathology

In over 100 years of OPA reports two pathological forms of OPA are recognized, classical and atypical[43]. In the classical form the lungs appear considerably enlarged, heavy, oedematous and they do not collapse when the chest is opened. On necropsy, naturally infected animal in the advanced stages of disease will show a thin carcass with frothy fluid filling the trachea and exuding from the nares. Careful palpation will reveal consolidated foci or diffuse areas within the bulk of some or all of the lung lobes. This represents tumour, which, when extensive, can grossly distort the normal architecture of the organ. Externally, affected areas appear darker (purple/greyish) than adjacent normal tissue, but the smooth contour of the overlying pleura generally remains uninterrupted. Sectioning the lesion displays the solid, grey, granular surface of the tumour, which frequently exudes frothy fluid. There is a clear boundary between this and adjacent normal aerated, pink, functional lung tissue. Affected lungs have variably sized, coalescing neoplastic nodules (Fig. 3)[44], associated with regions of pulmonary atelectasis and the tumors fail to protrude from the cut surface of the lung. Affected lungs may exude clear fluid on sectioning; additional frothy fluid may be present in the bronchi and trachea and concurrent pneumonia is often present. In larger masses, the centre is more resistant to the knife and may feel gritty. In addition, firm foci of fibrosis or soft pockets of necrosis and abscessation are also frequently found. Mediastinal and tracheobronchial lymph nodes may be enlarged and occasionally contain metastasis. Extrathoracic spread of the tumour has been occasionally reported (Up to 10% in the liver, kidney, heart and skeletal muscle), but are generally rar[3,45]. Animals that have died naturally often have a secondary bacterial pneumonia, detailed dissection is important as

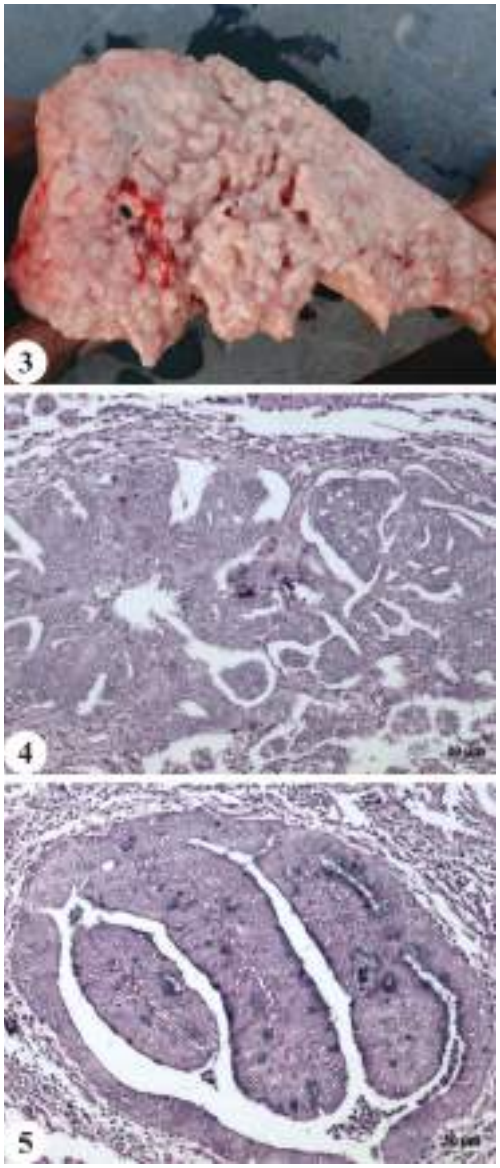

Fig. 3. Jaagsiekte-Diffuse multiple variable sized grayish-white nodules; **Fig. 4.** Jaagsiekte-Alveoli-Pulmonary papillary adenocarcinoma-Cuboidal cells (H&E Bar = 20 μm); **Fig. 5.** Jaagsiekte-Bronchogenic adenocarcinoma-Columnar cells (H&E Bar = 50 μm).

extensive pleurisy and adhesions can mask the underlying pathology of OPA[3].

The neoplastic lesions occur particularly in the cranioventral parts of the lungs, although any part may be involved. They are diffuse or nodular, grey or purple in colour and have an increased consistency. The neoplastic areas vary from small discrete nodules, in the early stages, to diffuse extensive lesions, which often are bordered by small satellite nodules. The cut surface of the tumour lesion has a granular appearance, is moist and frequently exudes frothy fluid. Concurrent lesions of other lung diseases are frequent and may hide the tumour lesion pattern[42,58,59].

Atypical form tends to be more nodular, well-demarcated from surrounding parenchyma, solitary, or multifocal nodules, dry sectioned surface, distributed primarily in the caudal pulmonary/diaphragmatic lobes. Such nodules may be present either underneath the pleura or deep in the lung tissue, and fluid is absent in the bronchi. The neoplastic foci are more solid than in the classical form, and tend to exude less fluid. Atypical and classical OPA may coexist in a flock and in individual sheep. Little is known about possible differences in the pathogenesis of classical and atypical OPA[3,42,45].

Histopathology

OPA reveals several non-encapsulated neoplastic foci that emanate from the alveolar and bronchiolar epithelia, forming acinar and papillary proliferations predominantly that expand into adjacent structures and compressing the adjacent structures. These are supported by a fibrovascular connective tissue framework that can dominate the centre of large tumour nodules. OPA were composed of a single layer of neoplastic cuboidal, columnar or polyhedral epithelial cells lining the alveolar lumina or bronchioles, surrounded by a fine to moderate fibrovascular stroma (Figs. 4-5)[44]. Tumour cells vary in shape and malignancy both within and between tumour nodules. Classically, they are cuboidal or columnar, with or without cytoplasmic vacuolation, and have a low mitotic index (0.002% in any tumour). In areas of increased malignancy, solid masses of pleomorphic cells with a high mitotic rate and scattered foci of necrosis are found. Occasionally, nodules of loose mesenchymal tissue appear admixed with tumour, as part of the fibrovascular core or on their own, which are also assumed to be neoplastic tissue. The fibrovascular connective tissue acts as a scaffold for infiltrating inflammatory cells, which vary according to the size and age of tumour and the presence of secondary infectious agents[3,45].

Natural stroma of the tumour may show variable amounts of lymphocytes, plasma cells and connective tissue fibres. Another common feature of OPA is the infiltration of large numbers of macrophages in and around the neoplastic alveoli and bronchioles. In secondary bacterial infection, neutrophils can also be often found. Mesenchymal tissue foci (myxoid nodules or growths) in a variable proportion of tumours interming led with the neoplastic epithelial component may be seen[3,43].

The diameter of individual neoplastic epithelial cells ranged from 20 to 30 μm, showed moderate amount of pale acidophilic, finely granular cytoplasm and intermediate N/C ratio. Anisokaryosis and anisocytosis were low to moderate; the nuclei were round to oval, centrally located, with a fine granular to lacy chromatin with and 1-2 distinct, basophilic nucleoli. The average of mitotic rate was 2 per 10 HPF without atypical features. The adjacent parenchyma of the neoplastic mass show atelectasis, and at the periphery of the tumors, the neoplastic cells were occasionally arranged in a lepidic growth pattern. The myxoid growths consisting of sparsely cellular structures of spindles cells embedded in an abundant extracellular matrix were observed. The MGs were admixed with the neoplastic epithelial component, or in some areas were disposed as multiple poorly demarcated masses. In some cases,

the neoplastic epithelial component was absent. The neoplasm is composed of short bundles and streams of spindle, stellate or individual cells. These mesenchymal cells were embedded into an abundant myxoid matrix that contains moderate amounts of foamy, amphophilic, AB-PAS positive material (mucin). The individual cells had variable distinct borders, intermediate N/C ratio and moderate amounts of pale acidophilic, homogenous cytoplasm. The nuclei were oval to elongated, 20-30 μm in diameter, in transverse section, centrally located with clumped chromatin and indistinct nucleoli. No mitotic figures were present; anisocytosis and anisokaryosis were low. Presumptive diagnosis is pulmonary myxomas. Overall, mesenchymal proliferations and myxomatous changes, named as myxoid growths (MGs), were identified (myxoma-like nodules)[22].

Histologically, OPA lesions are consistent with a well-differentiated, multicentric, bronchioloalveolar carcinoma (adenocarcinoma). Based on predominant architectural patterns OPA is classified as lepidic, papillary, acinar, or mixed. The lepidic subtype was characterized by a layer of cuboidal epithelium following an alveolar pattern. The papillary subtype presented exophytic growths of cuboidal-to-columnar cells arranged around a fibrovascular core. The acinar subtype was characterized by palisades of taller columnar cells that formed tubular structures often surrounded by fibrovascular stroma. Some of the acinar structures showed mucous differentiation. Mixed patterns were the most frequently identified, and they were composed of a combination of the previously described subtypes or the intermediate forms between them. In sheep with subtle 1-2 mm diameter pulmonary lesions (the mixed form of OPA), the diagnosis of OPA was only confirmed after histological examination. In several cases, proliferative pulmonary nodules were composed of neoplastic cells associated with a moderate amount of extracellular matrix, with myxoid differentiation (fibromyxoid nodules)[58].

Atypical OPA

Atypical forms though essentially similar in histological appearance as that of classical OPA, the pattern of epithelial neoplasia is more often acinar and the stroma is more heavily infiltrated by mononuclear cells, mostly lymphocytes and plasma cells and connective tissue fibres. Lymphoid proliferations are also consistently seen around the bronchioles of neoplastic areas. The distinguish of atypical OPA features were represented by more prominent limits between normal tissue and neoplastic masses due to higher fibroblast proliferation and inflammatory infiltrates, predominated by mature lymphocytes and macrophages[43,45].

Electron microscopy

Electron microscopy document the early growth of the tumour, to identify ultrastructural characteristics of neoplastic cells and to support the histological findings. The tumours appear to originate from cells resembling fetal pneumocytes and type II pneumocytes. These cells proliferate to line alveoli with cuboidal or columnar cells, before forming papilliform or varicose clusters that can extend into bronchioles. Tumour cells have microvilli, basal or centrally located nuclei and are connected by desmosomes. They contain variable numbers of secretory granules appearing as electron-dense structures or are filled with myelinoid whorls, in comparison with the electron-lucent granules found in normal granular pneumocytes. The cells have rough endoplasmic reticulum, large numbers of free polysomes, a well-developed Golgi apparatus and hypertrophic mitochondria. Cytoplasmic glycogen granules have also been identified, sometimes in large quantities and confirmed using periodic acid-Schiff staining. The macrophages identified by histology are highly 'ruffled' and enlarged, confirming their activated state. They either attach to the surface of normal or neoplastic cells, or form separate clusters. In addition to lysosomes and phagolysosomes, they contain ingested JSRV particles, bacteria and mycoplasma-like organisms[3]. Ultrastructurally, proliferation of type II pneumocytes (Type B cells) having microvilli and well-developed junctional complexes. Non-ciliated bronchiolar epithelial cells (Clara cells) with electron dense cytoplasmic granules without any surrounding membrane and microvilli and no virus particles were traced[27].

Diagnosis

A definitive diagnosis of OPA is made based on the characteristic gross and histopathological lesions. Lack of antibody development against the virus in infected sheep limits the use of serological test and vaccine production; due to this the diagnostic option becomes minimum. Further, the virus can't grow in any laboratory animal except sheep and goat. JSRV cannot yet be propagated *in vitro*, therefore routine diagnostic methods, such as virus isolation, are not available for diagnosis. Diagnosis relies, at present, on clinical history and examination, as well as on the findings at necropsy and by histopathology and IHC. Viral DNA or RNA can be detected in tumour, draining lymph nodes, and peripheral blood mononuclear cells by polymerase chain reaction. Lambs become persistently infected by JSRV at an early age, and, in an OPA-affected flock, most sheep are infected. Transthoracic ultrasound diagnosis of ovine pulmonary adenocarcinoma in adult sheep can be helpful in natural cases and experimental sequential study[60].

Serological tests

Antibodies to the retrovirus have not been detected in infected sheep; therefore, serological tests are not available for diagnosis.

Serum biochemical markers

Among the serum markers tested, CEA levels remained similar, whereas CA 125, CA 19-9, CA 15-3, and AFP-3 levels were significantly higher in the OPA group than the control group. In all OPA animals, CA 125 levels were higher than 1 U/mL[61].

Oxidative stress, apoptosis and autophagy

To elucidate pathogenic mechanism, effects of OPA infections on lung tissue oxidative DNA damage, inflammation, apoptosis and autophagy with IL1-β, TNF-α, 8-OHdG, Bcl-2, BAX, Caspase3, LC3B and LC3A levels investigated in sheep showed that severe OPA cases showed more severe levels of IL1-β, Tnf-α, 8-OHdG, BAX, Caspase3, LC3A and LC3B expressions than mild cases did. Thus, where the severity of tumor foci due to OPA in lung tissues increased, oxidative stress, inflammation, apoptosis and autophagy were found to be significantly increased[62].

Immuno-histochemistry/fluorescence

Epithelial tumour cells in the lungs of sheep with OPA are the major sites of replication for JSRV[63]. As defined by IHC, type II alveolar epithelial cells are the principal neoplastic cell type (82%), with Clara cells (7%) and undifferentiated cells (11%) making up the remainder[3]. JSRV proteins were demonstrated in myxoid nodules and infiltrating interstitial cells of some OPA initial lesions suggesting that the participation of lymphoreticular cells may form part of the sequence of events leading to lung cell infection and tumour development[64]. JSRV nucleic acids can be also detected in the tumour tissue by specific PCR techniques[9,23]. Antibodies raised against JSRV proteins confirms the presence of JSRV in the transformed cells by IHC. LTR and ENV genes are targeted. The long terminal repeats of Jaagsiekte sheep retrovirus (JSRV) are preferentially active in type II pneumocytes[65]. IHC showed expression of *env* antigen in the cytoplasm of neoplastic epithelium by specific *env* oncogene monoclonal antibody. Cytokeratin identified epithelial component and vimentin fibroblasts of neoplasm by cytoplasmic expression[44]. IHC analysis reveals fewer JSRV-positive cells in atypical tumours than in the classical form of OPA[43,45].

JSRV protein is detected in all tumor epithelial cells, histologically normal alveolar type II cells and few bronchiolar epithelial cells, alveolar macrophages, lymphocytes and plasma cells[2]. A comparative study was conducted by IHC differential expression of JSRV capsid antigen and tumour biomarkers in classical and atypical OPA[66]. OPA cases were positive for MCK and TTF-1. MGs showed IHC reaction to vimentin, desmin and SMA; Ki67 expression of classical OPA was higher than atypical OPA and MGs. JSRV-MA was identified by IHC in both epithelial and mesenchymal cells of OPA. IHC and EM also confirmed the JSRV within the neoplastic cells[22].

Angiogenesis

The bFGF; VEGF-C and PDGF-C have roles in the pathogenesis of OPA. The bLF may activate macrophages and plasma cells in these lesions, but limited expression of bLF by neoplastic cells may be a consequence of defective or impaired function of this molecule[2].

Apoptosis marker studies

Immunofluorescence staining of lung tissues revealed no BAX, Caspase 3, LC3A and LC3B expression in negative controls, whereas moderate and severe BAX, Caspase 3, LC3A, and LC3B expression was observed in OPA positive cases[62]. Apoptosis, known as programmed cell death, can cause differentiation in cells and tissues by going beyond the body's control mechanisms in cases such as oxidative stress, inflammation and cancer[67]. Apoptosis and carcinogenesis mechanism work together. In the occurrence of apoptosis in cancer formation, apoptosis occurs faster in the cell as a result of decreased Bcl-2 molecule level and increased BAX molecule level[68,69]. Bcl-2 molecule level decreased significantly in the lung tissues with OPA, as in the tumoral mechanism and BAX increased severely and increased Caspase 3 expression in the cells. Thus, the tumoral foci developed and grew faster than normal due to the acceleration of the apoptotic process, especially in severe cases. Autophagy increases in cells under oxidative stress and starvation[70]. Although studies revealed that OPA causes oxidative stress[71], no study evaluated in terms of autophagy. OPA infections increased autophagy in cells depending on the severity of the disease in lung tissues.

In immunofluorescence staining revealed that LC3A and LC3B expression levels in anaplastic cells increased severely in advanced cases. Oxidative stress caused by the disease in the tissue is the cause of such an increase in autophagy in the cells. OPA infection triggered oxidative stress in sheep lung tissues, causing DNA damage and autophagy in cells and increased inflammation due to cancer. Apoptosis is also accelerated in cells according to the severity of the tumor and accordingly, the tumor spread to larger areas. These findings will be useful in further clarifying the pathogenesis of OPA[62].

PCR

PCR with primers specific for JSRV is always positive when applied to samples of OPA lesions in lung tissue. ExJSRV was identified by PCR in 97.05% of analyzed samples. Phylogenetic analysis revealed the presence of the exJSRV type 2 in Romanian sheep affected by lung cancer and showed a high similarity with the UK strain. PCR using *ltr* and *env* nucleotides were done[22,44]. NA (enzootic nasal adenocarcinoma) associated with JSRV infection was reported first time in a sheep of Ireland origin, which shows the necessity of using PCR in combination with IHC to reach an accurate etiologic diagnosis, which is of importance in countries currently

free of ENTV-1[72]. ENA, a neoplasia of glands of the nasal mucosa associated with enzootic nasal tumour virus 1 (ENTV-1), is similar to JSRV. ENA enzootically occurs in many countries of the world with the exception of Australia and New Zealand[73].

Transcriptional response to JSRV

In a RNA sequencing study conducted for the transcriptional response of ovine lung tissue to infection by JSRV, 1,971 ovine genes were differentially expressed in JSRV-infected lung compared to non-infected lung, including many genes with roles in carcinogenesis and immunomodulation, confirmed using IHC and reverse transcription-quantitative PCR. There was activation of anterior gradient 2, yes-associated protein 1 and amphiregulin in OPA tumor cells, indicating a role for this oncogenic pathway in OPA. There was also differential expression of genes related to innate immunity, including genes encoding cytokines, chemokines and complement system proteins; also macrophage function reflecting the increased abundance of these cells in OPA-affected lung tissue. There was little evidence for the upregulation of genes involved in T-cell immunity. Comparison of the genes differentially regulated in OPA with the transcriptional changes occurring in human lung cancer revealed important similarities and differences between OPA and human lung adenocarcinoma. This provided valuable new information on the pathogenesis of OPA and strengthens the use of this naturally occurring animal model for human lung adenocarcinoma[74].

Treatment, control measures and vaccines

Since effective treatment and a vaccination procedure are not currently possible and control and eradication of the disease are difficult[9]. Till date there is no effective methods of controlling its spread and OPA remains an important problem sheep farming countries[61]. There are no vaccines available[75].

In silico analysis for vaccine development: An attempt was made to construct an effective multi-epitopes vaccine against JSRV eliciting B and T lymphocytes using immunoinformatics tools. The designed vaccine was composed of 499 amino acids. Before the vaccine was computationally validated, antigenicity, allergenicity, toxicity and stability were considered. The physiochemical properties of the vaccine displayed an isoelectric point of 9.88. According to the Instability Index (II), the vaccine was stable at 28.28. The vaccine scored 56.51 on the aliphatic index and -0.731 on the GRAVY, indicating that the vaccine was hydrophilic. By applying the RaptorX server for vaccine's tertiary structure, Galaxy WEB server refined the structure, and the Ramachandran plot and the ProSA-web server validated the vaccine's tertiary structure, Protein-sol and the SOLPro servers showed the solubility of the vaccine. The high mobile regions in the vaccine's structure were reduced and the vaccine's stability was improved by disulfide engineering. The vaccine construct was docked with an ovine MHC-1 allele and showed efficient binding energy. Immune simulation remarkably showed high levels of immunoglobulins, T lymphocytes, and INF-γ secretions. The molecular dynamic simulation provided the stability of the constructed vaccine. Finally, the vaccine was back-transcribed into a DNA sequence and cloned into a pET-30a (+) vector to affirm the potency of translation and microbial expression. A novel multi-epitopes vaccine construct against JSRV, was formed from B and T lymphocytes epitopes, and was produced with potential protection. This study might help in controlling and eradicating OPA[76].

Ovine JSRV induced OPA model

Necessity of JSRV to induce a lung cancer in sheep is reported[4,54]. Experimental induction of OPA in sheep results in pathological changes similar to those observed in natural conditions and are compatible with the classical form, whereas atypical presentations have not been recorded in these cases[9,43]. Such studies will improve OPA research by providing novel insights into JSRV infectivity and OPA disease progression[77]. In experimentally induced OPA JSRV replicates actively in the transformed cells (type II pneumocytes and club cells) where viral antigen can be shown by IHC methods[3,43].

Human lung cancer model

Similarities in pulmonary anatomy and physiology potentially make sheep better models for studying human lung function and disease. OPA shares many histological similarities with the human pulmonary adenocarcinoma, representing an important animal model for understanding the mechanisms of viral oncogenesis. Although JSRV was found in human pulmonary neoplastic cells, its role in the development of lung cancer in humans is not fully elucidated[22]. The potential for OPA to be used as a pre-clinical animal model for assessing human lung cancer treatment strategies are yet to be fully exploited.

Antibodies against JSRV capsid were identified in human lung adenocarcinoma, but an association between JSRV and this neoplasm in humans could not be demonstrated[23,53]. Since, natural infection of Jaagsiekte is common in sheep caused by retrovirus globally, OPA is considered as model for human adenocarcinoma especially pneumonic type bronchioalveolar carcinoma[23,78,79]. JSRV can infect human cells but it plays little if any role in human lung cancer[80]. We can integrate techniques commonly used in the treatment of human lung cancer patients to further strengthen the effectiveness of OPA as a pre-clinical cancer research model[7,81]. Comparison of transcriptional changes in the genes differentially regulated in OPA and human lung cancer revealed important and OPA can be a model

for studying pathogenesis of OPA for human lung adenocarcinoma[74].

Virus entry into cells is initiated by binding of the viral envelope (env) protein to a specific cell-surface receptor, Hyal2. Unlike almost all other retroviruses, the JSRV env protein is also a potent oncoprotein and is responsible for lung cancer in animals. Of concern, Hyal2 is a functional receptor for JSRV in humans. JSRV is fully capable of infecting human cells, as measured by its reverse transcription and persistence in the DNA of cultured human cells. Role for JSRV in human lung cancer both agreed and disputed. A highly-specific mouse monoclonal antibodies and a rabbit polyclonal antiserum against JSRV env to test for JSRV expression in human lung cancer was done. JSRV env expression was undetectable in lung cancers from 128 human subjects, including 73 cases of bronchioalveolar carcinoma (BAC; currently reclassified as lung invasive adenocarcinoma with a predominant lepidic component), a lung cancer with histology similar to that found in JSRV-infected sheep. Neutralizing antibodies in sera from 138 Peruvians living in an area where sheep farming is prevalent and JSRV is present, 24 of whom were directly exposed to sheep and found none. While JSRV can infect human cells, JSRV plays little if any role in human lung cancer[81].

Naturally occurring OPA cases are readily available from infected flocks due to the endemic nature of the disease in many countries and pre-clinical cases can be identified by the use of ultrasound scanning programmes. The use of naturally occurring cases could decrease the use of experimentally induced OPA tumors in lambs, reducing ethical concerns with this model. Future studies that can integrate techniques commonly used in the treatment of human lung cancer patients, such as ultrasound, general anesthesia, CT and surgery, would further strengthen the effectiveness of OPA as a pre-clinical cancer research model and in ovine natural cases model[7] and is comparable to TTNB in human patients in terms of procedure duration, radiation exposure and complication rate. This model can be developed further for other pre-clinical uses, such as the procurement of biopsy specimens, the development of medical devices for the local delivery of chemotherapeutic agents, monitoring the tumor microenvironment and in the assessment of the effectiveness of RT or systemic chemotherapeutic agents and has a great potential to not only advance the molecular understanding of human lung cancer[81].

Recommendations

1. Herd replacement from infected area should be banned to avoid spread of infection in naïve population.
2. Avoiding OPA introduction: Need for stringent bio-security measures and replacements only from flocks free from respiratory diseases including OPA.
3. Environmental hygiene to be maintained from discharges and any virus reserving matter.
4. To prevent OPA transmission through milk, weaning and feeding neonates with milk replacement and colustrum from cow rather than sucking their dam.
5. Stamp out the affected flocks to eradicate the diseases from the area.
6. Research fields for the future: Mechanism of tumor production, vaccine development, public health importance and nature of tumor.
7. Considering lack of diagnostics, development of better preclinical diagnostic tools is essential to control[2,24].
8. Cell culture studies suggested a new mechanism of retroviral transformation having direct relevance to design JSRV-based vectors targeting the differentiated epithelial cells of the lungs[11].
9. Novel methodologies to explore the possibility of generating transgenic sheep resistant to JSRV infection by redirecting enJSRVs expression in type II pneumocytes and Clara cells with caution[19].

REFERENCES

1. Damodaran S. 1960. Ovine pulmonary adenomatosis (Jaagsiekte). *Ind Vet J* **37:** 127-138.
2. Gebeyehu DT. 2017. A review on sheep pulmonary adenocarcinoma. *J Adv Allergy Immunol Dis* **2:** pp. 9.
3. Griffiths DJ, Martineau HM and Cousens C. 2010. Review: Pathology and pathogenesis of ovine pulmonary adenocarcinoma. *J Comp Path* **142:** 260-283.
4. Palmarini M, Sharp JM, Lee C and Fan C. 1999. *In vitro* infection of ovine cell lines by Jaagsiekte sheep retrovirus (JSRV). *J Virol* **73:** 10070-10078.
5. CFSPH (Centre for Food Security & Public Health, Coll Vet Med, Iowa State University, USA). 2009. Ovine pulmonary adenocarcinoma. pp. 1-4.
6. Palmarini M, Cousens C, Dalziel RG, Bai J, Stedman K, DeMartini JC and Sharp JM. 1996. The exogenous form of Jaagsiekte retrovirus is specifically associated with a contagious lung cancer of sheep. *J Virol* **70:** 1618-1623.
7. Gray ME, Meehan J, Sullivan P, Marland JRK, Greenhalgh SN, Gregson R, Clutton RE, Ward C, Cousens C and Griffiths DJ. 2019. Ovine pulmonary adenocarcinoma: A unique model to improve lung cancer research. *Front Oncol* **9:** 335.
8. Zhang K, Kong H, Liu Y, Shang Y, Wu B and Liu X. 2014. Diagnosis and phylogenetic analysis of ovine pulmonary adenocarcinoma in China. *Virus Genes* **48:** 64-73.
9. Ortín A, De las Heras M, Borobia M, Ramo MA, Ortega M and Ruíz de Arcaute M. 2019. Ovine pulmonary adenocarcinoma: A transmissible lung cancer of sheep, difficult to control. *Small Rumin Res* **176:** 37-41.
10. York DF, Vigne R, Verwoerd DW and Querat G. 1992. Nucleotide sequence of the Jaagsiekte retrovirus, an exogenous and endogenous Type D and B retrovirus of sheep and goats. *J Virol* **66:** 4930-4939.
11. Palmarini M, Maeda N, Murgia C, De-Fraja C, Hofacre A and Fan HA. 2001. Phosphatidylinositol 3-kinase docking site in the cytoplasmic tail of the Jaagsiekte sheep retrovirus transmembrane protein is essential for envelope-induced transformation of NIH 3T3 cells. *J Virol* **75:** 11002-11009.

12. Bai J, Bishop JV, Carlson JO and DeMartini JC. 1999. Sequence comparison of JSRV with endogenous proviruses: envelope genotypes and a novel ORF with similarity to a G-protein-coupled receptor. *Virol* **258:** 333-343.
13. Rosati S, Pittau M, Alberti A, Pozzi S and York DF. 2000. An accessory open reading frame (orf-x) of Jaagsiekte sheep retrovirus is conserved between different virus isolates. *Virus Res* **66:** 109-116.
14. Maeda N, Palmarini M, Murgia C and Fan H. 2001. Direct transformation of rodent fibroblasts by Jaagsiekte sheep retrovirus DNA. *Proc Natl Acad Sci USA* **98:** 4449-4454.
15. Wootton SK, Halbert C and Miller AD. 2005. Sheep retrovirus structural protein induces lung tumours. *Nature* **434:** 904-907.
16. Caporale M, Cousens C, Centorame P, Pinoni C and De las Heras M. 2006. Expression of the Jaagsiekte sheep retrovirus envelope glycoprotein is sufficient to induce lung tumors in sheep. *J Virol* **80:** 8030-8037.
17. Cousens C, Maeda N, Murgia C, Dagleish MP and Palmarini M. 2007. *In vivo* tumorigenesis by Jaagsiekte sheep retrovirus (JSRV) requires Y590 in env TM, but not full-length orfX open reading frame. *Virol* **367:** 413-421.
18. Palmarini M, Hallwirth C, York D, Murgia C and de Oliveira T. 2000. Molecular cloning and functional analysis of three type D endogenous retroviruses of sheep reveal a different cell tropism from that of the highly related exogenous Jaagsiekte sheep retrovirus. *J Virol* **74:** 8065-8076.
19. Palmarini M, Mura M and Spencer TE. 2004. Endogenous beta-retroviruses of sheep: teaching new lessons in retroviral interference and adaptation. *J Genl Virol* **85:** 1-13.
20. Arnaud F, Caporale M, Varela M, Biek R and Chessa B. 2007. A paradigm for virus-host coevolution: sequential counter-adaptations between endogenous and exogenous retroviruses. *PLoS Pathogens* **3:** 170.
21. York DF, Vigne R, Verwoerd DW and Querat G. 1991. Isolation, identification and partial cDNA cloning of genomic RNA of Jaagsiekte retrovirus, the etiological agent of sheep pulmonary adenomatosis. *J Virol* **65:** 5061-5067.
22. Toma C, Valentin AB, Septiumiu T, Trifa A, Rema A, Amorim I and Pop RM. 2020. Exogenous Jaagsiekte Sheep Retrovirus type 2 (exJSRV2) related to ovine pulmonary adenocarcinoma (OPA) in Romania: Prevalence, anatomical forms, pathological description, immunophenotyping and virus identification. *BMC Vet Res* **16:** 296.
23. Quintas H, Pires I, Garcês A, Prada JU, Silva F and Alegria N. 2021. The diagnostic challenges of ovine pulmonary adenocarcinoma. *Ruminants* **1:** 58-71.
24. Cousens CL, Gibson J, Finlayson I, Pritchard MP and Dagleish. 2015. Prevalence of ovine pulmonary adenocarcinoma (Jaagsiekte) in a UK slaughterhouse sheep study. *Vet Rec*.
25. Rama Devi V, Manasa BB, Samatha V, Mahesh M, Srikanth KVT and Yathiraja Rao T. 2016. Pathology of natural cases of ovine pulmonary adenocarcinoma (Jaagsiekte) in goats. *Braz J Vet Pathol* **9:** 108-112.
26. Sonawane GG, Tripathi BN, Kumar R and Kumar J. 2016. Diagnosis and prevalence of ovine pulmonary adenocarcinoma in lung tissues of naturally infected farm sheep. *Vet World* **9:** 365-370.
27. Naik HS, Srilatha Ch, Sujatha K, Kumar RVS and Ramanamurthy RV. 2015. Histopathological and ultrastructural studies of ovine pulmonary adenocarcinoma (Jaagsiekte). *Ind J Vet Pathol* **39:** 81-83.
28. Mishra SP, Kumar JA, Dar V, Singh K, Pandit and Mahanta D. 2018. A rare case of pulmonary adenocarcinoma in goat. *J Entomo Zool Studies* **6:** 981-982.
29. Shah Z, Mir AQ, Kawoosa M, Badroo G, Qureshi S, Bhat MA and Hussain I. 2024. First evidence of exogenous Jaagsiekte Sheep Retrovirus-induced pulmonary adenocarcinoma in Kashmir. Conference Paper in National Symposium IAVP. p. 299.
30. Lee AM, Wolfe A, Joseph P, Cassidy, Locksley L, Messam, John P, Moriarty, O'Neill R and Fahy C. 2017. First confirmation by PCR of Jaagsiekte sheep retrovirus in Ireland and prevalence of ovine pulmonary adenocarcinoma in adult sheep at slaughter. *Irish Vet J* **70:** 33.
31. Jassim A, Al-Husseiny SH, Mansou KA and Kshash QH. 2017. First molecular diagnosis of ovine pulmonary adenocarcinoma in Awassi sheep in Iraq. AL-Qadisiyah *J Vet Med Sci* **16:** 105-110.
32. Mansour KA, Al-Husseiny SH, Kshash QH and Jassim A. 2019. Clinical-histopathological and molecular study of ovine pulmonary adenocarcinoma in Awassi sheep in Al-Qadisiyah Province, Iraq. *Vet World* **12:** 454-458.
33. Belalmi NEH, Sid N, Bennoune O, Ouhida S, Heras MDL and Leroux C. 2020. Evidence of Jaagsiekte sheep retrovirus-induced pulmonary adenocarcinoma in Ouled Djellal breed sheep in Algeria. *Vet Res Forum* **11:** 93-95.
34. Ruíz-Ramírez JA, Jossue B, Chávez-Ramírez, García-Valle JL, Heras MDL López-Mayagoitia A and García-Márquez LJ. 2023. Ovine pulmonary adenocarcinoma in Mexico. *Rev mex de cienc pecuarias* **14**.
35. Sharp JM and DeMartini JC. 2003. Natural history of JSRV in sheep. *Curr Top Microbiol Immunol* **275:** 55-79.
36. Gupta PP and Rajya BS. 1968. Morphology of pulmonary adenomatosis in sheep and its histochemical differentiation from other epithelizing lung affections. *Ind J Vet Sci* **38:** 67-73.
37. Sharma DN, Rajya BS and Dwivedi JN. 1975. Metastasaizing pulmonary adenomatosis (Jaagsiekte) in sheep and goats. Pathoanatomical studies. *Ind J Vet Sci* **45:** 363-370.
38. Banerjee M and Gupta PP. 1979. Note on Maedi and Jaagsiekte in sheep and goats in Ludhiana area of Punjab. *Ind J Anim Sci* **49:** 1102-1105.
39. Ramadevi V, Srilatha Ch, Sujatha K and Ahmed MN. 2001. Pulmonary adenomatosis in sheep-A case report. *Ind Vet J* **78:** 853-854.
40. Pawaiya RVS and Kumar R. 2007. Ovine pulmonary adenocarcinoma: evaluation of molecular tumour markers. *Ind J Vet Pathol* **31:** 99-107.
41. Tamizharasan S. 2009. Pulmonary pathology in ovines with special emphasis on Jaagsiekte. MVSc thesis approved by Tamil Nadu University of Veterinary and Animal Sciences, Chennai, India.
42. Kumar MA, Kumar R, Varshney KC, Palanivelu M, Sridhar BG and Sivakumar M. 2014. Incidence of ovine pulmonary adenocarcinoma in Southern parts of India: A slaughter house-based study. *Indian J Vet Pathol* **38:** 149.
43. De las Heras M, Gonza´lez L and Sharp JM. 2003. Pathology of ovine pulmonary adenocarcinoma. *Curr Top Microbiol Immunol* **275:** 25-54.
44. Nilakanth MM, Balachandran C, Maroudam V and Dhinakar Raj G. 2014. Pathology and molecular characterization of Jaagsiekte Retro Virus (JSRV) in naturally infected small ruminants. Conference Paper IAVP 2014, Anand, Gujrat.
45. García-Goti M, González L, Cousens C, Cortabarría N, Extramiana AB, Minguijón E, Ortín A, Heras DLM and Sharp JM. 2000. Sheep pulmonary adenomatosis: characterization of two pathological forms associated with Jaagsiekte retrovirus. *J Comp Pathol* **122:** 55-65.
46. Grego E, De Meneghi D, Álvarez V, Benito AA, Minguijón E and Ortín A. 2008. Colostrum and milk can transmit Jaagsiekte retrovirus to lambs. *Vet Microbiol* **130:** 247-257.
47. Borobia M, Heras DLM, Ramos JJ, Ferrer LM, Lacasta D and

De Martino. 2016. Jaagsiekte sheep retrovirus can reach Peyer's patches and mesenteric lymph nodes of lambs nursed by infected mothers. *Vet Pathol* **53:** 172-1179.
48. Borobia M, Heras DLM, Godino J, Ferrer LM and Lacasta D. 2021. Jaagsiekte sheep retrovirus found in milk macrophages but not in milk lymphocytes or mammary gland epithelia of naturally infected sheep. *J Vet Diagn Invest* **34:** 112-115.
49. Sanna MP, Sanna E, Heras MD, Leoni A, Nieddu Am, Pirino S, Sharp JM and Palmarini M. 2001. Association of Jaagsiekte sheep retrovirus with pulmonary carcinoma in Sardinian Moufflon *(Ovis Musimon). J Comp Pathol* **85:** 3319-3324.
50. Cousens C, Thonur L, Imlach S, Crawford J, Sales J and Griffiths DJ. 2009. Jaagsiekte sheep retrovirus is present at high concentration in lung fluid produced by ovine pulmonary adenocarcinoma-affected sheep and can survive for several weeks at ambient temperatures. *Res Vet Sci* **87:** 154-156.
51. Rai SK, DeMartini JC and Miller AD. 2000. Retrovirus vectors bearing Jaagsiekte sheep retrovirus env transduce human cells by using a new receptor localized to chromosome. *J Virol* **74:** 4698-4704.
52. Caporale M, Martineau H, Heras MDL, Murgia C, Huang R and Centorame P. 2013. Host Species barriers to Jaagsiekte sheep retrovirus replication and carcinogenesis. *J Virol* **87:** 107 52-10762.
53. Yousem SA, Finkelstein SD, Swalsky PA, Bakker A and Ohori NP. 2001. Absence of Jaagsiekte sheep retrovirus DNA and RNA in bronchiolo alveolar and conventional human pulmonary adenocarcinoma by PCR and RT-PCR Analysis. *Hum Pathol* **32:** 1039-1042.
54. Salvatori D, González L, Dewar P, Cousens C, Heras M, Dalziel RG and Sharp JM. 2004. Successful induction of ovine pulmonary adenocarcinoma in lambs of different ages and detection of viraemia during the preclinical period. *J Gen Virol* **85:** 3319-3324.
55. Kahn CM and Line S. 2006. Pulmonary Adenomatosis. Editors The Merck Veterinary Manual White House Station, NJ: Merck and Co., pp. 123-243.
56. Palmarini M, Holland MJ, Cousens C, Dalziel RG and Sharp JM. 1996. Jaagsiekte retrovirus establishes a disseminated infection of the lymphoid tissues of sheep affected by pulmonary adenomatosis. *J Gen Virol* **77:** 2991-2998.
57. York DF and Querat G. 2003. A history of ovine pulmonary adenocarcinoma (Jaagsiekte) and experiments leading to the deduction of the JSRV nucleotide sequence. *Curr Top Microbiol Immunol* **275:** 1-23.
58. Ortega J, Corpa JM, Castillo D and Murphy BG. 2023. Pathological spectrum of ovine pulmonary adenocarcinoma in small ruminants: A focus on the mixed form. *Animals* **13:** 2828.
59. Minguijón E, González L, Heras MDL, Gómez N, García-Goti M, Juste and Moreno RAB. 2013. Pathological and aetiological studies in sheep exhibiting extrathoracic metastasis of ovine pulmonary adenocarcinoma (Jaagsiekte). *J Comp Pathol* **148:** 139-47.
60. Cousens S and Scott PR. 2015. Assessment of transthoracic ultrasound diagnosis of ovine pulmonary adenocarcinoma in adult sheep. *Vet Rec.*
61. Özkan C, S. Yıldırım S, Huyut Z and Özbek M. 2020. Selected tumour biomarker levels in sheep with pulmonary adenomatosis. *J Vet Res* **64:** 39-44.
62. Bolat I, Yildirim S, Sa˘glam S, Çomakli M, Kiliçlio˘glu and Dereli E. 2024. Investigation of the effects of pulmonary adenomatosis on oxidative DNA damage, inflammation, apoptosis, and autophagy in lung tissues in sheep. *Small Ruminant Res* **230:** 107-171.
63. Palmarini M, Dewar P, Heras LM, Inglis NF, Dalziel RG and Sharp J. 1995. Epithelial tumour cells in the lungs of sheep with pulmonary adenomatosis are major sites of replication for Jaagsiekte retrovirus. *J Gen Virol* **76:** 2731-2737.
64. De las Heras MA, de Martino, Borobia M, Ortín A, Álvarez R, L Borderías and JA Giménez-Más. 2014. Solitary tumours associated with Jaagsiekte retrovirus in sheep are heterogeneous and contain cells expressing markers identifying progenitor cells in lung repair. *J Comp Pathol* **50:** 138-147.
65. Palmarini M, Datta S, Omid R, Murgia C and Fan H. 2000. The long terminal repeats of Jaagsiekte sheep retrovirus (JSRV) are preferentially active in type II pneumocytes. *J Virol* **74:** 5776-57 87.
66. Mishra S, Kumar P, Dar JA, George N, Singh V and Singh R. 2019. Differential immunohistochemical expression of JSRV capsid antigen and tumour biomarkers in classical and atypical OPA: a comparative study. *Biol Rhythm Res* **1:** 11.
67. Carneiro BA and El-Deiry WS. 2020. Targeting apoptosis in cancer therapy. *Nat Rev Clin Oncol* **17:** 395-417.
68. Greten FR and Grivennikov SI. 2019. Inflammation and cancer: triggers, mechanisms and consequences. *Immunity* **51:** 27-41.
69. Hafezi S and Rahmani M. 2021. Targeting BCL-2 in cancer: advances, challenges and perspectives. *Cancers (Basel)* **13:** 1292.
70. Kiffin R, Bandyopadhyay U and Cuervo AM. 2006. Oxidative stress and autophagy. *Antioxid Redox Signal* **8:** 152-162.
71. Karakurt E, Beytut E, Da˘g S, Nuho˘glu H, Yıldız A and Kurtbas E. 2022. Assessment of MDA and 8-OHdG expressions in ovine pulmonary adenocarcinomas by immunohistochemical and immunofluorescence methods. *Acta Vet Brno* **91:** 235-241.
72. Jahns H and Cousens C. 2020. Nasal adenocarcinoma associated with Jaagsiekte sheep retrovirus infection in a sheep. *J Vet Diag Invest* **32:** 152-155.
73. De las Heras M, Borobia M and Ortín A. 2021. Neoplasia-associated wasting diseases with economic relevance in the sheep industry. *Animals* **11:** 381.
74. Karagianni AE, Vasoya D, Finlayson J, Martineau HM, Wood AR, Cousens C, Dagleish MP, Watson M and Griffiths DJ. 2019. Transcriptional response of ovine lung to infection with Jaagsiekte sheep retrovirus. *J Virol* **93:** e00876-19.
75. OIE Terrestrial Manual. 2018. Ovine pulmonary adenocarcinoma.
76. Mahmoud NA, Abdelmajeed M, Elshafei and Yassir AA. 2022. A novel strategy for developing vaccine candidate against Jaagsiekte sheep retrovirus from the envelope and gag proteins: an in-silico approach. *MC Vet Res* **18:** 343.
77. Cousens C, Meehan J, Collie D, Wright S, Chang Z, Todd H and Moore J. 2024. Tracking ovine pulmonary adenocarcinoma development using an experimental Jaagsiekte sheep retrovirus infection model. *Genes* **15:** 1019.
78. Palmarini M, Fan H and Sharp JM. 1997. Sheep pulmonary adenomatosis: a unique model of retrovirus-associated lung cancer. *Trends Microbiol* **5:** 478-483.
79. Palmarini M and Fan H. 2001. Retrovirus-induced ovine pulmonary adenocarcinoma: an animal model for lung cancer. *J Natl Cancer Inst* **93:** 1603-1614.
80. Miller AD, las Heras MD, Yu JF, Zhang, Shan-Lu Liu, Andrew E Vaughan and Vaughan TL. 2017. Evidence against a role for Jaagsiekte sheep retrovirus in human lung cancer. *Retrovirol* **14:** 3.
81. Gray ME, Sullivan P, Marland JRK, Greenhalgh SN, Meehan J, Gregson R, Clutton RE, Cousens C, Griffiths DJ, Murray A and Argyle D. 2019. A novel translational ovine pulmonary adenocarcinoma model for human lung cancer. *Front Oncol* **9:** 534.

Indian J. Vet. Pathol., 49(1) : 13-22, 2025: DOI: https://doi.org/10.5958/9jdf6y53

RESEARCH ARTICLE

Occurrence of Pneumonia based on histopathology in domestic ruminants - A seasonal record

Sourabh Babu, S.D. Vinay Kumar, C.P. Singh, Vidya Singh*, Pawan Kumar, Rohit Singh and R.V.S. Pawaiya

Division of Pathology, ICAR-Indian Veterinary Research Institute (IVRI), Izatnagar, Bareilly-243 122, India

Address for Correspondence

Vidya Singh, Division of Pathology, ICAR-Indian Veterinary Research Institute (IVRI), Izatnagar, Bareilly-243 122, India, E-mail: vidyasingh100@gmail.com

Received: 7.9.2024; Accepted: 28.9.2024

ABSTRACT

A total of 120 fallen ruminants (64 cattle, 09 buffaloes, 15 sheep and 32 goats), received for necropsy at the Division of Pathology, ICAR-IVRI, Izatnagar were included in the study. Among animals, higher mortality rate was observed in adult animals followed by 3 to 12 months old animals and young animals upto 3 months age. In the present study was conducted to assess the types of pneumonia in ruminants based on gross and histopathological findings. Further, C categorization of pneumonia was primarily based on histopathology finding of the lung tissue. Tissue sections were stained with special stains such as Periodic Acid Schiff (PAS), Masson Trichrome Stain (MTS) and Brown and Brenn (B&B) respectively for demonstration of goblet cell hyperplasia, fibrous tissue proliferation and bacteria, respectively. Histopathological examination of lungs tissue sections was carried out for 120/123 cases as due to autolytic changes in 3 cases. Histopathological examination revealed one or more lesions associated with pneumonia in 97.56% (120/123) cases. Bronchointerstitial pneumonia 65.831% (79/120) was the most common type followed by interstitial (16.66%, 20/120), bronchopneumonia 7.5% (9/120) and granulomatous pneumonia (0.83%, 1/120). Bronchointerstitial pneumonia included chronic (1.66%, 2/120), sub-acute (55.83%, 67/120) and acute forms (8.33%, 10/120). Interstitial pneumonia (16.66%, 20/120) was sub categorized into acute (4.16%, 5/120) and subacute interstitial pneumonia (12.5%, 15/120). The lesions of bronchopneumonia was diagnosed in 7.5% (9/120) animals, which included acute (0.83%, 1/120), fibrinous (0.83%, 1/120) and subacute bronchopneumonia 5.83% (7/120) and granulomatous pneumonia (0.83%, 1/120). Besides, miscellaneous conditions were diagnosed in 9.16% (11/120) animals, which included congestion and edema in 6/120 (5%) and emphysema in 5/120 (4.16%) cases. Other miscellaneous conditions like congestion, edema, emphysema, atelectasis, etc. were observed in 9.16% (11/120) animals.

Keywords: Bronchopneumonia, brown and brenn, Masson Trichrome, periodic acid schiff

INTRODUCTION

Pneumonia is an acute, subacute or chronic infection of the lungs characterized by the inflammation of the lung parenchyma and inflammatory cell infiltration into the alveoli and bronchioles[1]. Bronchopneumonia, Interstitial pneumonia, Embolic pneumonia and Granulomatous pneumonia are the four major types of pneumonia based on the etiological factors, gross and microscopic abnormalities. Further, pneumonia is divided into three categories the include chronic, subacute and acute, based on duration, as well as pathogens such as bacterial, viral and mycoplasma based on etiology[2]. Respiratory disease complex (RDC) is one of the primary causes of mortality in domestic animals contributing up to 20-40% of cases in India[3]. Bovine respiratory disease (BRD) is one of the most serious and costly illnesses affecting cattle around the world and symptoms generally appear soon after arrival in the feedlot[4]. The morbidity risk of respiratory illness cases in feedlot cattle is highest in the first 45 days after arrival and is highest in 1 to 3 weeks. Further, the morbidity decreases until the end of the 12-week period[5]. High temperature (about 40-41.5^{O}C), depression, decreased appetite, nasal and ocular discharge, coughing and variable degrees of dyspnea are the most typical clinical symptoms that has been described. In young domestic animals, respiratory and digestive illnesses are the leading causes of death. Pneumonia, along with diarrhea is one of the leading causes of morbidity and mortality in dairy ranging from 17.1% to 39% and 43.2% to 58%, respectively. In feed-lot farms, calves mortality associated with respiratory illnesses has been found 10-61% in Canada and 44-67% in United States[6]. The combination of many respiratory pathogens, stress and the environment has a synergistic effect and disease severity increases in mixed infections[7]. In all respiratory diseases of ruminants, bacterial pneumonia has drawn much attention due to the variable clinical manifestations and severity of diseases[8]. Viruses are the most common pathogens, causing damage to the epithelium and cilia[9], as well as increasing vulnerability to other diseases by impairing the host's immune system[10] by suppressing or killing

How to cite this article : Babu, S., Kumar, S.D.V., Singh, C.P., Singh, V., Kumar, P., Singh, R. and Pawaiya, R.V.S. 2025. Occurrence of Pneumonia based on histopathology in domestic ruminants - A seasonal record. Indian J. Vet. Pathol., 49(1) : 13-22.

Table 1. Details of samples collected.

Species	Place	No. of Samples	Sample Types
Cattle	PM Facility, IVRI	64	Lungs
Buffalo	PM Facility, IVRI	09	Lungs
Sheep	PM Facility, IVRI	15	Lungs
Goat	PM Facility, IVRI	32	Lungs
	Total	120	

alveolar macrophages[11].

Bronchipneumonia is the most prevalent type of pneumonia in domestic animals is characterized by the consolidation of cranio-ventral pulmonary lobes and inflammation of the bronchi, bronchioles and alveolar lumen[12]. Mainly pathogens enter through the airways, resulting in exudative lesions at the bronchiolar-alveolar junction[13].

Viruses such as BRSV, BPI-3, BVDV, BCV and BHV-1, as well as septicemia/toxemia, fungal spores, various chemical substances like 3-methylindole, migratory parasitelarvae, immunological processes, toxic gases, hypersensitivity and possibly environmental factors cause interstitial pneumonia[14].

Broncho-interstitial pneumonia is frequently complicated by secondary bacterial infection, concealing the original viral symptoms. As a result, right broncho-interstitial pneumonia is occasionally reported[15] for example, in a feedlot cow, broncho-interstitial pneumonia was found in only 3 of 214 (1.4%) and 25 of 112 pneumonic lungs respectively[16,17]. However, 12.64% prevalence of broncho-interstitial pneumonia in pneumonic lungs of adult cattle in Punjab, India, has been reported[18].

MATERIALS AND METHODS

Collection of lungs samples from dead/fallen domestic ruminants

During necropsy examination, tissue samples (lungs) were obtained from a total of 120 fallen animals (64 cattle, 9 buffaloes, 15 sheep and 32 goats). For histopathology, representative tissue samples (1 cm thick) from the affected areas of the lungs were collected in 10% NBF. These samples were used to identify various types of Histopathological pneumonia conditions. The carcasses were received at the Post Mortem Facility of Division of Pathology, ICAR-IVRI, Bareilly during the period from January to December 2022. Detail of the animals and the samples are listed in the Table 1.

Tissues processing

Histopathology

Tissue samples collected in 10% NBF were stored for 48 hours for proper fixation at room temperature. Further, 0.5 cm thick tissue sections were cut from the fixed tissues,

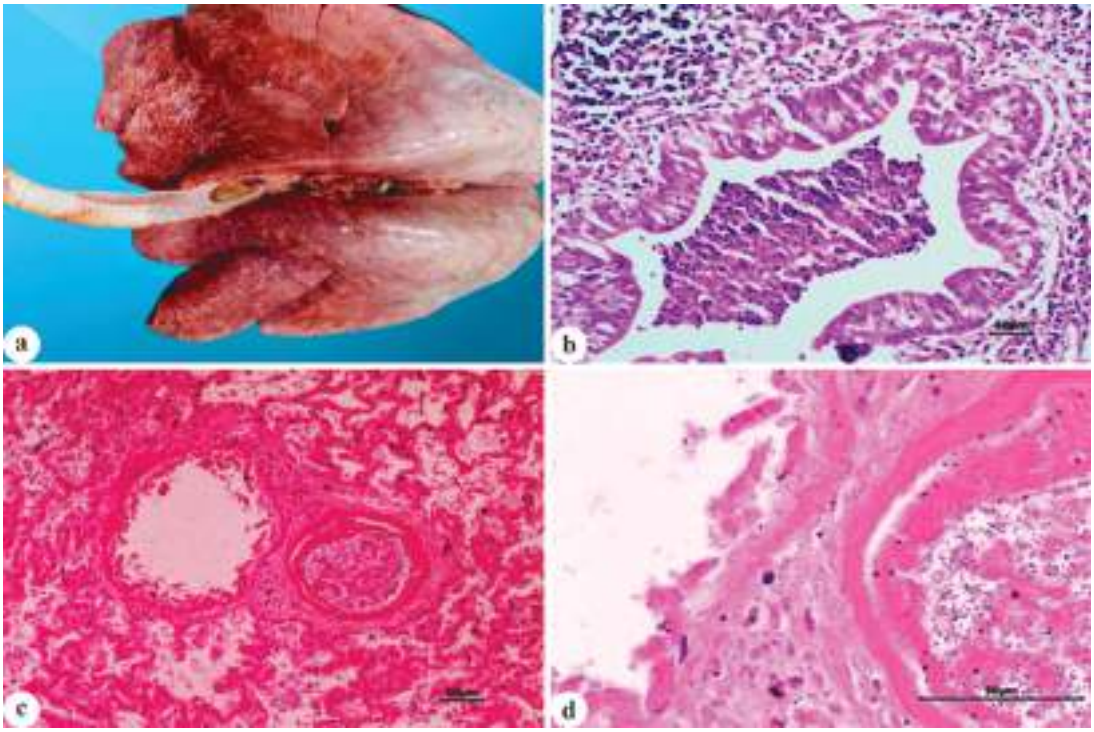

Fig. 1. Suppurative bronchopneumonia: Gross images of lungs **a.** Showing severe congestion and patchy consolidation in right cranial lobe; **b.** Microscopic image showing bronchiole with neutrophilic exudate (100x); **c.** Bronchiolar epithelial desquamation with bacteria in adjacent blood vessels (c) 40x and (d) H&E 400x/Lungs **a.** Severe congestion and patchy consolidation in right cranial lobe; **b.** Neutrophilic exudate in bronchiolar lumen (H&E Stain, bar = 50 μm); **c-d.** Bronchiolar epithelial desquamation with bacteria in adjacent blood vessels (H&E Stain, bar = 50 μm).

Table 2. Age wise mortality pattern in fallen animals.

Species	Cattle			Buffalo			Sheep			Goat		
Age (months)	0-3	3-12	>12	0-3	3-12	>12	0-3	3-12	>12	0-3	3-12	>12
Mortality ratio	9/64	15/64	40/64	1/9	2/9	6/9	1/15	0/15	14/15	2/32	11/32	19/32
% Mortality	14.06	23.43	62.5	11.11	22.22	66.66	6.66	0	93.33	6.25	34.4	59.37

and processed for routine histopathological examination. The cut section was dehydrated using ascending grades of the alcohol and cleared by two changes of the xylene. Further paraffin embedded tissue section was processed and 4 to 5 micron thick section was cut using semiautomatic microtome and taken on glass slide. The sections were stained using routine Haematoxylin and Eosin (H&E) staining following standard protocol[19].

Special staining methods used in histopathology

To demonstrate goblet cell hyperplasia, fibrous tissue proliferation and bacteria in tissue sections Periodic Acid Schiff (PAS), Masson Trichrome Stain (MTS) and Brown and Brenn (B&B) staining[19] were performed, respectively.

RESULTS

A total of 120 ruminants, including cattle (64), buffalo (9), sheep (15) and goats (32) were received at the post-mortem facility of the Division of Pathology for necropsy examination. To determine the pattern of mortality in animals with respect to age, gender and season, the data was analyzed for different animals during the period between January to December 2022 (Table 2-4).

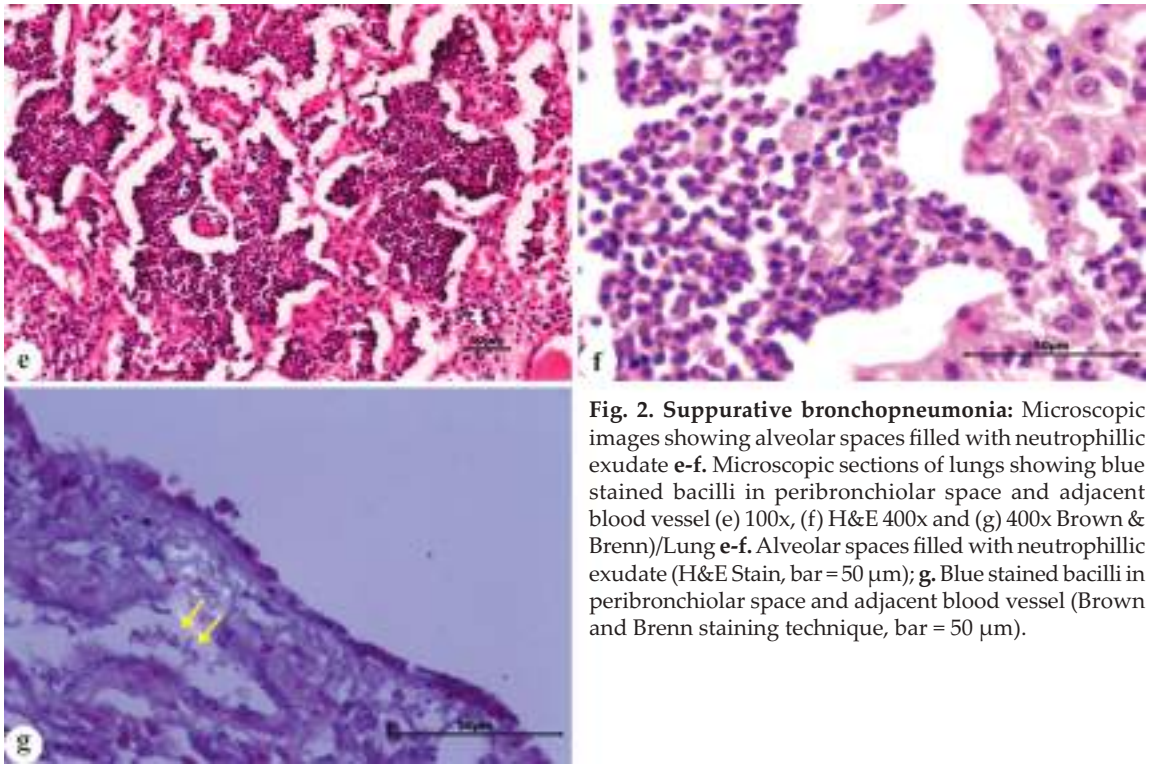

Fig. 2. Suppurative bronchopneumonia: Microscopic images showing alveolar spaces filled with neutrophillic exudate **e-f.** Microscopic sections of lungs showing blue stained bacilli in peribronchiolar space and adjacent blood vessel (e) 100x, (f) H&E 400x and (g) 400x Brown & Brenn)/Lung **e-f.** Alveolar spaces filled with neutrophillic exudate (H&E Stain, bar = 50 μm); **g.** Blue stained bacilli in peribronchiolar space and adjacent blood vessel (Brown and Brenn staining technique, bar = 50 μm).

The mortality rate in cattle was higher in males 67.18% (43/64) as compared to 32.82% (21/64) in female. Animals older than one year had a higher mortality rate (62.5%, 40/64), followed by 3 to 12 months old animals (23.43%, 15/64) and young animals upto 3 months age (14.06%, 9/64). Cattle mortality was highest during the post-monsoon (42.18%, 27/64) season, followed by the monsoon (29.68%, 19/64) and summer (18.75%, 12/64), and winter (9.37%, 6/64) season.

Among buffaloes, mortality was higher in female (77.77%, 7/9) than male buffaloes (22.22%, 2/9) received

Table 3. Sex wise mortality pattern in fallen animals.

Species/Sex	Cattle		Buffalo		Sheep		Goat	
	M	F	M	F	M	F	M	F
Mortality ratio	43/64	21/64	2/9	7/9	6/15	9/15	19/32	13/32
% Mortality	67.18	32.82	22.22	77.77	40	60	59.38	40.62

Table 4. Season wise mortality pattern in fallen animals.

Species/Sex	Monsoon			Post-Monsoon			Winter			Summer		
	Male	Female	Total %	Male	Female	Total %	Male	Female	Total %	Male	Female	Total %
Cattle	15	4	29.68	15	12	42.18	3	3	9.37	9	3	18.75
Buffalo	0	1	11.11	1	2	33.33	1	2	33.33	0	2	22.22
Sheep	1	1	13.33	5	3	53.33	0	3	20	0	2	13.33
Goat	4	3	21.87	5	3	25	5	3	25	5	4	28.15

for necropsy. The post monsoon and winter season (33.33, 3/9) had the highest and identical mortality rates, followed by summer (22.22%, 2/9) and monsoon season (11.11%, 1/9).

Mortality was higher in male goats (59.38%, 19/32) than females (40.62%, 13/32) during the study period. Animals older than 12 months had the highest mortality rate (59.37%, 19/32), followed by grower animals (34.4%, 11/22) and young animals (6.25%, 2/32). The summer season had the highest mortality rate (28.15%, 9/32), followed by the post monsoon and winter seasons (28%, 8/32). Lowest mortality (21.87%, 7/32) was observed during monsoon season.

In sheep, higher mortality was observed in female animals (60%, 9/15) than males (40%, 6/15). Animals older than 12 months had the highest rate of mortality (93.33%, 14/15), followed by those younger than 3 months (6.66%, 1/15) and no mortality was recorded in grower animals (3-12 months). Seasonal mortality showed that post-monsoon (53.33%, 8/15) had the highest rate, followed by winter (20%, 3/15) and summer and monsoon (13.33%, 2/15) had similar rates.

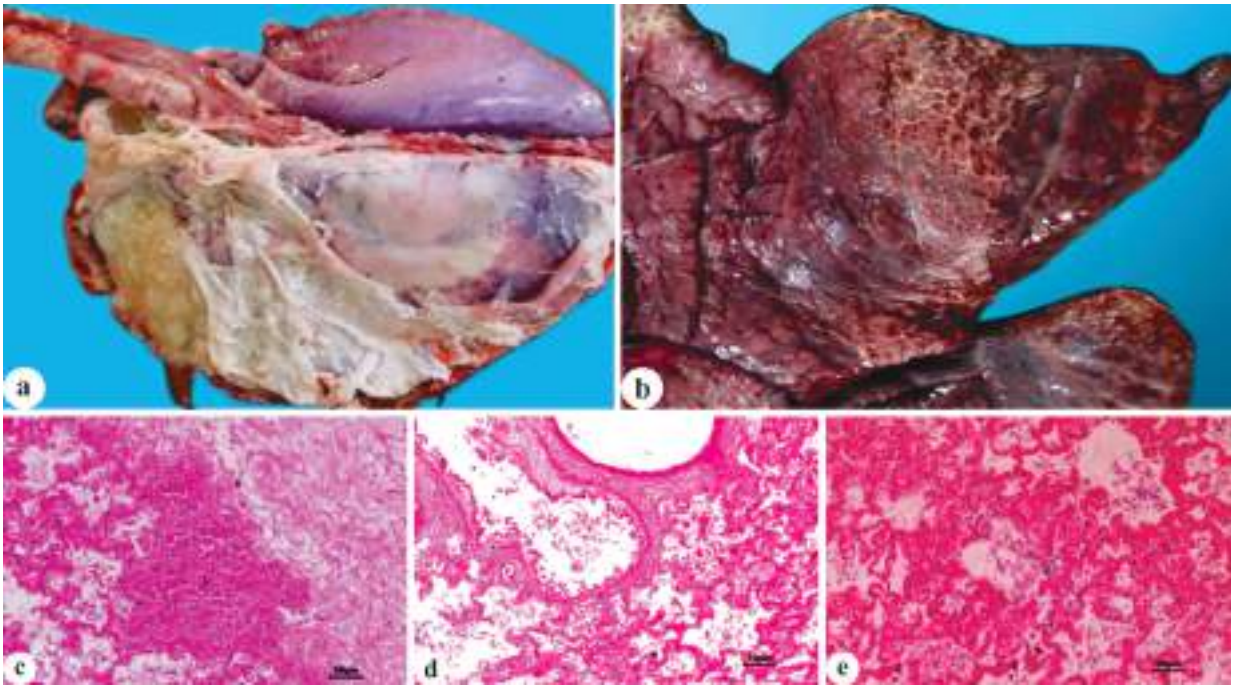

Fig. 3. Fibrinous bronchopneumonia: a-b. Gross images showing deposition of light yellowish layer of fibrinous exudate over the congested and consolidated lobes; **c-e.** Microscopic images of lungs showing eosinophilic fibrin strands in pleura, bronchiolar lumen and alveoli (c-e) H&E 100x/Lungs **a-b.** Deposition of light yellowish layer of fibrinous exudate over the congested and consolidated lobes; **c-e.** eosinophilic fibrin strands in pleura, bronchiolar lumen and alveoli (H&E Stain, bar = 50 μm).

Classification of Pneumonia

Tissue samples collected from all the necropsied carcasses during the period as well as few archieved samples were processed for the morphological and pathological diagnosis. Tissue

Table 5. Types of Pneumonia and frequency of their occurrence.

Type of Pneumonia	Frequency of Occurrence	Percentage Frequency (%)
Bronchopneumonia	9	7.50
Bronchointerstitial pneumonia	79	65.83
Interstitial pneumonia	20	16.66
Granulomatous pneumonia	1	0.83
Miscellaneous conditions	11	9.16
Total	120	

Table 6. Histological classification of Pneumonia and their occurrence.

Types of Pneumonia		Cattle	Buffalo	Sheep	Goat	Total	Total %
Bronchopneumonia (BP)	Acute BP	1	0	0	0	1/120	0.83
7.5% (9/120)	Sub acute BP	3	1		2	7/120	5.83
	Fibrinous BP	1	0	0	0	1/120	0.83
Bronchointerstitial pneumonia (BISP)	Acute BISP	5	1	2	2	10/120	8.33
65.83% (79/120)	Sub acute BISP	34	5	7	21	67/120	55.83
	Chronic BISP	2	0	0	0	2/120	1.66
Interstitial pneumonia (ISP)	Acute ISP	4	1	0	0	5/120	4.16
16.66% (20/120)	Sub acute ISP	10	0	1	4	15/120	12.5
Granulomatous pneumonia 0.83% (1/120)	-	0	1	0	0	1/120	0.83
Miscellaneous conditions	Congestions & Oedema	4	0	2	0	6/120	5
9.16% (11/120)	Emphysema	0	0	2	3	5/120	4.16
	Total	64	9	15	32	120/120	

samples of a total of 123 animals were examined histopathologically and out of which 120 cases were classified into different types of pneumonia and other miscellaneous lesions based on the histopathological lesions and nature of exudate in the airways and parenchyma. Microscopically, three cases were found to be in advance stage of autolysis. The lung lesions were categorized as bronchopneumonia, broncho-interstitial pneumonia, interstitial pneumonia, granulomatous pneumonia and miscellaneous conditions (Table 5).

Classification of pneumonic lungs was done based on cellular infiltration, into acute suppurative bronchopneumonia, chronic bronchopneumonia (cBP), fibrinous pneumonia, acute bronchointerstitial pneumonia (aBISP), subacute bronchointerstitial pneumonia (saBISP), chronic bronchointerstitial pneumonia (cBISP), acute interstitial pneumonia (aISP), chronic interstitial pneumonia (cISP), acute bronchointerstitial pneumonia (aBISP), sub acute bronchointerstitial pneumonia, granulomatous pneumonia and bronchitis. The miscellaneous conditions such as congestion, haemorrhages and congestion, edema, congestion and edema, emphysema and atelectasis, haemorrhages and emphysema, etc. were

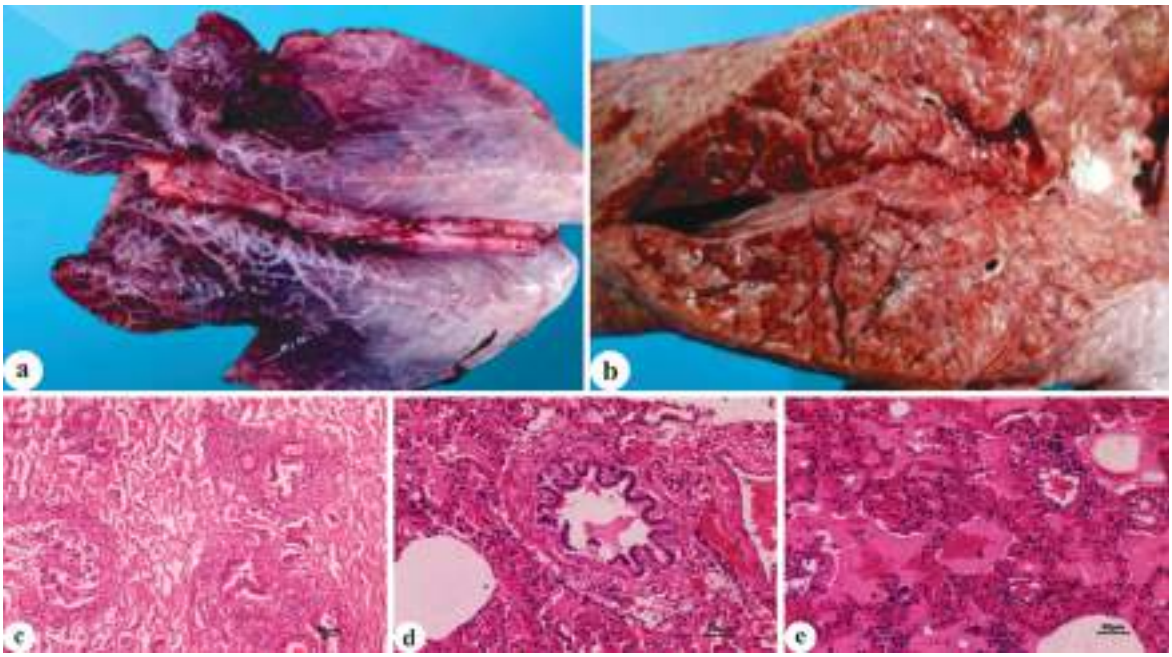

Fig. 4. Subacute bronchointerstitial pneumonia: a. Gross images of lungs showing severe congestion and consolidation cranio-ventral lobes with thickened and emphysematous interlobular septa; **b.** Cut section showing oedematous interlobular septa; **c-e.** Microscopic images of lungs section showing moderate to severe bronchiolar desquamation, peri-bronchiolar infiltration of MNCs, alveolar oedema and thickened alveolar septa (c) 4x and (d-e) H&E 10x/Lungs **a.** Severe congestion and consolidation cranio-ventral lobes with thickened and emphysematous interlobular septa; **b.** Cut section showing oedematous interlobular septa; **c-e.** Lungs: Moderate to severe bronchiolar desquamation, peri-bronchiolar infiltration of MNCs, alveolar oedema and thickened alveolar septa (H&E Stain, bar = 50 μm).

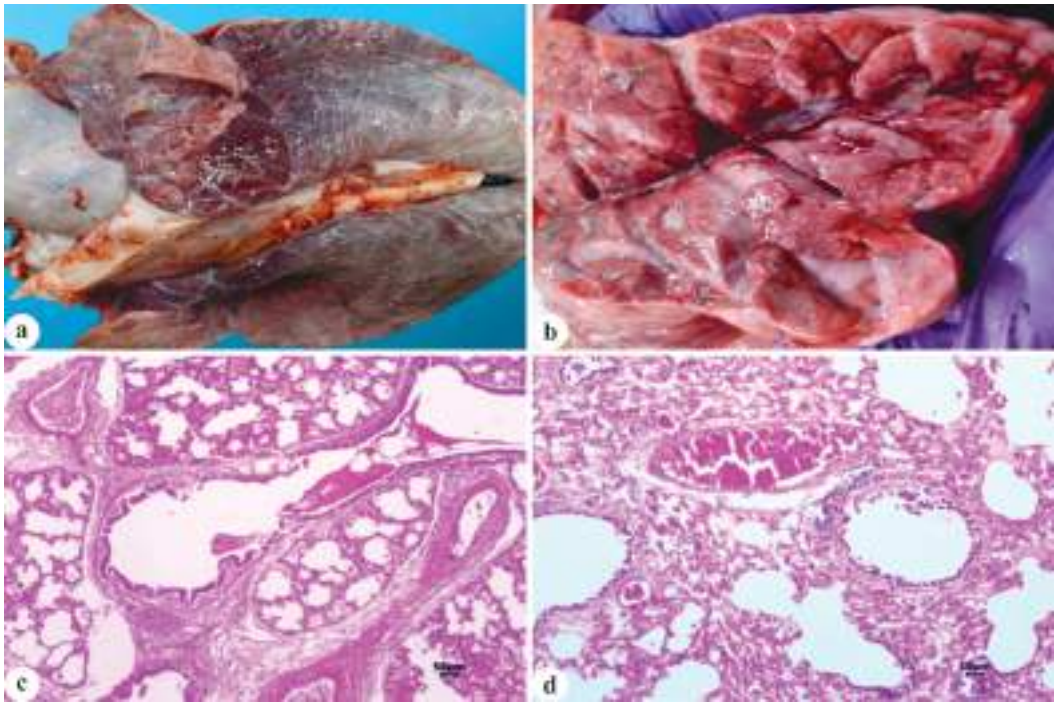

Fig. 5. Acute bronchointerstitial pneumonia: a. Gross images showing congestion and consolidation of pulmonary lobes with mild thickening of visceral pleura over the caudal lobes; **b.** Cut section showing thickening of interlobular septa and congested lobules; **c-d.** Microscopic images showing mild desquamation of bronchi and bronchioles with thickened alveolar septa (c-d) H&E 100x/Lungs **a-b.** Congestion and consolidation of pulmonary lobes with mild thickening of visceral pleura over the caudal lobes; **b.** Cut section showing thickening of interlobular septa and congested lobules; **c-d.** Mild desquamation of bronchi and bronchioles with thickened alveolar septa (H&E Stain, bar = 50 μm).

also identified (Table 6).

Suppurative Bronchopneumonia

Four out of 120 pneumonic cases had lesions suggestive of suppurative bronchopneumonia, one of which was acute and three of which were of sub acute nature. None of the cases had lesions suggestive of chronic bronchopneumonia. The affected lobes in acute suppurative bronchopneumonia were reddish or brown-grey in color, with mild to moderate interlobular edema (Table 6).

Gross examination of the lobes revealed firm texture and cranioventral consolidation. The majority of cases had consolidation in the left and right cranial lung lobes, with only a few cases having consolidation in the cranioventral aspect of the diaphragmatic lobes (Fig. 1a). A lobular pattern was observed, with oedema and hyperemia in the affected areas, as well as a mosaic of normal and affected lobules. When the affected lobes were cut open, the sections revealed mucopurulent exudate of a hemorrhagic type from the airways in areas that were both pale and dark in colour.

Histopathological examination of the affected lungs tissues revealed engorged alveolar capillaries with minor haemorrhages. The lumen of the bronchi and bronchioles, as well as in the alveolar spaces, had cellular exudate containing mostly neutrophils with denuded cellular debris and a few macrophages (Fig. 2e). The alveolar spaces were filled with a uniform pinkish edema fluid.

Some of the bronchioles and bronchi had necrosis and denudation of the epithelium. Acute bronchiolitis was observed, with suppurative exudates plugging the bronchiolar lumen and inflammatory cells infiltrating the peribronchiolar space.

The lungs had liver-like firmness and grayish to red consolidated areas in the right and left anterior lobes in the case of subacute suppurative bronchopeumonia; the cut surface had a nodular appearance, with purulent exudate oozing from the airways.

Pleural thickening was observed, as well as cellular infiltrates primarily composed of neutrophils and to a lesser extent, mononuclear cells (MNCs). Mild fibro-cellular proliferation around the bronchi and bronchioles, as well as thickened alveolar interstitium were observed as a result of MNC infiltration.

Fibrinous Bronchopneumonia

One out of 120 cases one had typical fibrinous bronchopneumonia lesions (Table 6). The lungs were grossly covered with a thin straw-yellow layer of fibrin, as well as watery serous fluid in the thoracic cavity. Consolidation was seen as patchy to diffuse areas of

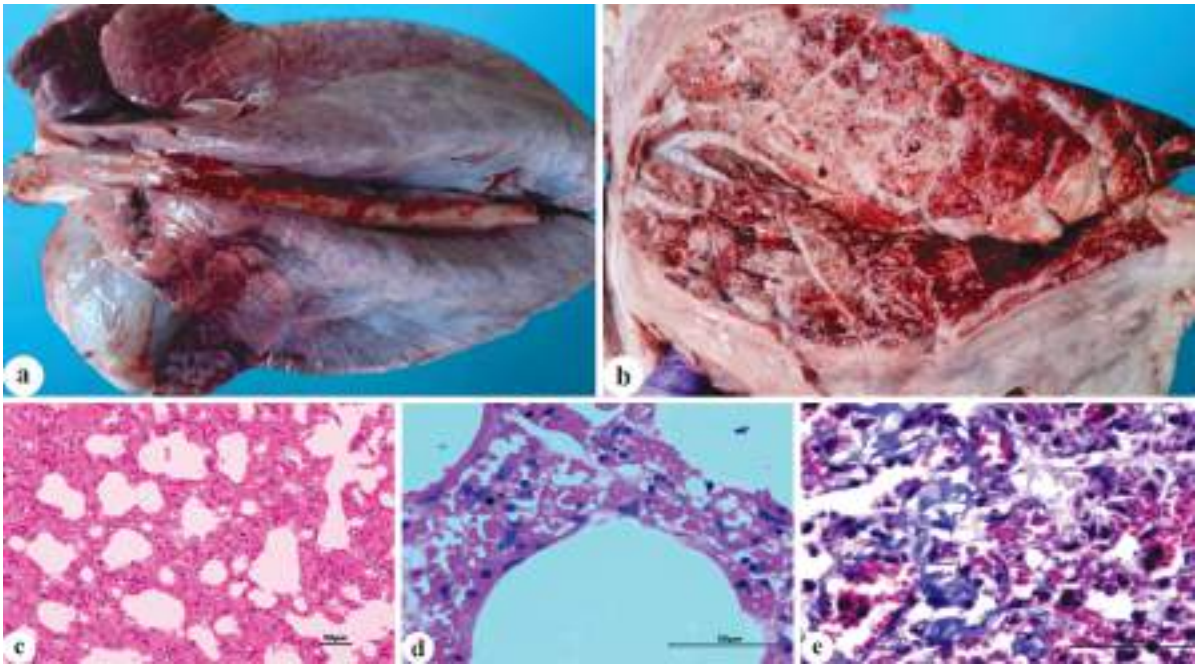

Fig. 6. Subacute interstitial pneumonia: a. Gross image of lungs with severe congestion of pulmonary lobes with prominent thickening of inter-lobular septa and visceral pleura; **b.** Cut-section showing widened interlobular septa; **c-d.** Microscopic images of lungs revealing severe thickening of interstitium as a result of congested capillaries and infiltration of MNCs (c) 100x and (d) H&E 400x; **e.** Lung section with thickened interstitium due to deposition of collagen fibres, stained blue (400x MTS)/Lungs **a.** Severe congestion of pulmonary lobes with prominent thickening of inter-lobular septa and visceral pleura; **b.** Cut-section showing widened interlobular septa; **c.** Lungs with severe thickening of interstitium as a result of congested capillaries and infiltration of MNCs (H&E Stain, bar = 50 μm); **d.** Thickened interstitium due to deposition of collagen fibres, stained blue (Masson Trichrome Stain, bar = 50 μm).

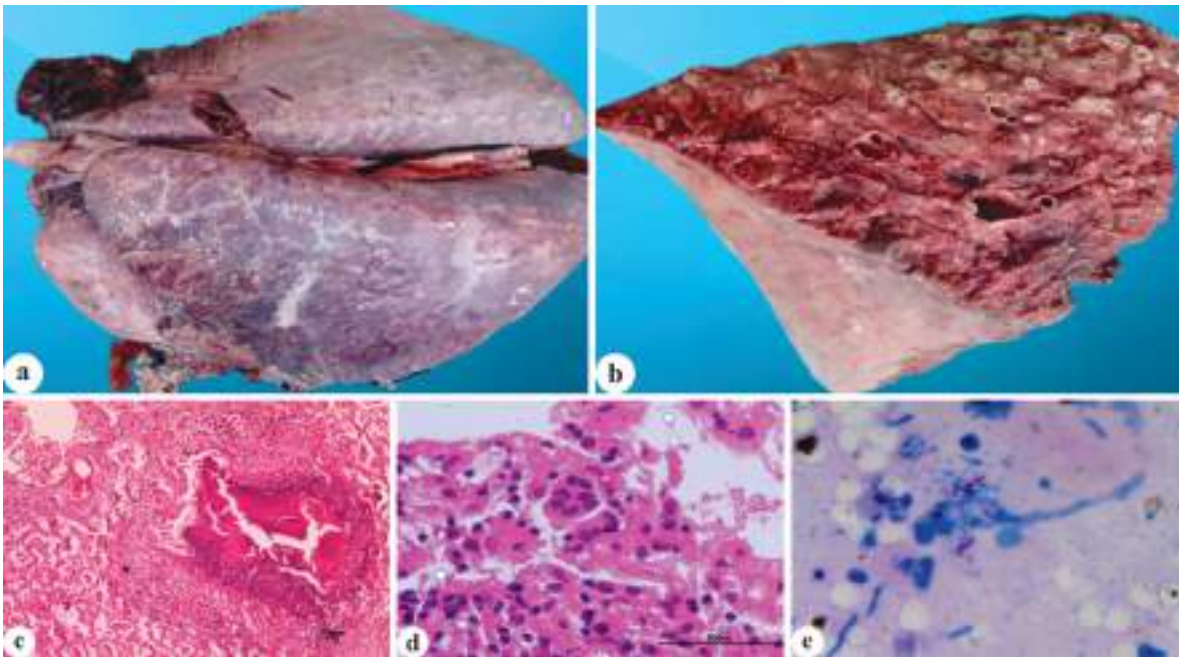

Fig. 7. Granulomatous pneumonia: a. Gross image of lungs showing inflated lobes with diffused nodules (2-4 cm diameter) over the surface; **b.** Cut section showing presence of diffused nodules and caseous exudate within bronchial lumen; **c-d.** Microscopic image of lungs showing granuloma with eosinophilic central necrotic debris surrounded by macrophages, MNCs and giant cells (c) 40x and (d) H&E 400x); **e.** Lungs impression smear showing red acid-fast bacilli (1000x, Modified Z-N Stain)/Lungs **a.** Inflated lobes with diffused nodules (2-4 cm diameter) over the surface; **b.** Cut section showing presence of diffused nodules and caseous exudate within bronchial lumen; **c-d.** Note the presence of granuloma with eosinophilic central necrotic debris surrounded by macrophages, MNCs and giant cells (H&E Stain, bar = 50 μm); **e.** Impression smear from cut surface of affected lungs showing red acid-fast bacilli (Modified Z-N Stain, bar = 10 μm).

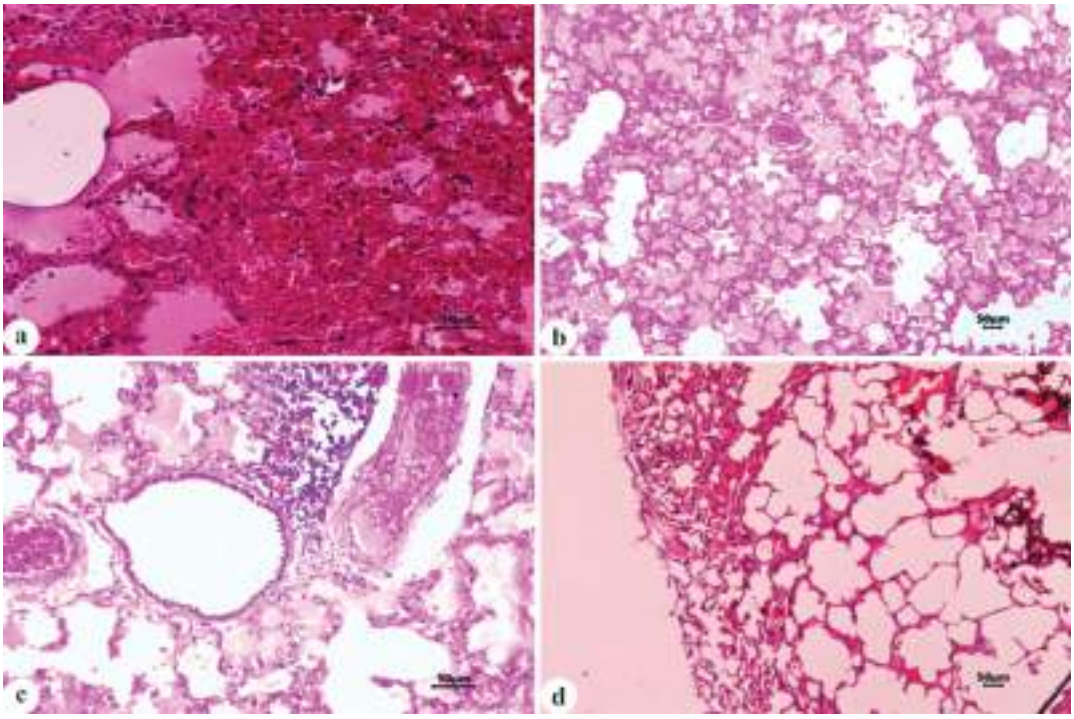

Fig. 8. Miscellaneous affections of lungs: a. Tissue section showing alveolar airspaces with erythrocytes and interstitial congestion (H&E 100x); **b-c.** Section showing congested pulmonary vessels with adjacent alveolar airspaces (b) 4x and (c) H&E, 100x; **d.** Thin, enlarged and ruptured alveoli indicating bullous emphysema and atelectasis (100x, H&E 4x)/Lungs **a.** Tissue section showing diffuse alveolar hemorrhages obliterating alveolar airspaces and interstitial congestion (H&E Stain, bar = 50 μm); **b-c.** Section showing marked congestion of pulmonary vessels adjacent alveolar airspaces and edema (H&E Stain, bar = 50 μm); **d.** Thin, enlarged and ruptured alveoli indicating bullous emphysema and atelectasis (H&E Stain, bar = 50 μm).

distribution, primarily in the anterioventral portion of the lungs, which were reddish-enlarged and liver-like in consistency. The parietal pleura was found to be adherent to the visceral pleura and diaphragm. The cut surface of the lungs revealed focal to diffuse lesions, as well as firm, hard-consolidated areas (Fig. 3a & b).

Microsscopic examination revealed the thickening of pleura with fibrinocellular exudate. The infiltration of fibrinous and cellular exudates enlarged the interlobular septae. The bronchi and bronchioles' lumens showed epithelial desquamation with cellular exudate containing MNCs and a few neutrophils. In the bronchioles and alveolar spaces, fibrinous exudate mixed with neutrophils was observed (Fig. 3c-e).

Bronchointerstitial Pneumonia

Bronchointerstitial pneumonia (BISP) was diagnosed histopathologically in 79 cases (65.83%) (Table 6). The majority of the cases revealed lungs with cranio-ventral distribution of lesions, with affected lobes exhibiting dark reddish to brown coloured consolidated areas. The majority of the cases had consolidated lesions in the left and right cranial lobes, as well as the right middle lobes. Further, the caudo-dorsal lobes were frequently distended with lobular, inter-lobular or sub-pleural edematous and emphysematous leseion. In severe cases, one or more entire lobes were involved and were consolidated with multifocal area to diffuse type of distribution. On palpation, atlectic areas revealed a rubbery consistency in some cases.

Necrosis and denudation of bronchiolar and bronchial epithelium were observed along with MNC infiltration around the bronchi, syncytia formation, type II pneumocyte hyperplasia and proliferative or exudative alveolitis. Fibrinous exudate containing RBCs and macrophages accumulated in the subpleura and interlobular septa, leading to the thickening of the septae.

Out of 48 cases, acute, sub-acute and chronic broncho-interstitial pneumonia (BISP) were diagnosed in 10 (8.33%), 67 (55.83%) and 2 (1.66%) cases, respectively.

Interstitial Pneumonia

Microscopic examination of lungs tissues revealed interstitial pneumonia (ISP) in 20 (16.66%) cases, of which 5 (4.16%) were diagnosed as acute interstitial pneumonia and 15 (12.5%) as sub-acute interstitial pneumonia (Table 6).

Grossly, bilateral deflation of the lungs, particularly the diaphragmatic lobes, was observed, along with varying degrees of interlobular emphysema and/or edema. In some cases, the caudo-dorsal portion of the lungs showed rubbery to firm dark red areas interspersed with pale pink areas (Fig. 6a & b). The dorsal surface

of inflated emphysematous lungs had rib impressions. Consolidation of the cranial lobes was associated with serous to mucopurulent exudate from the smaller airways in some cases. In some cases, pleuritis with focal to diffuse fibrin and adhesions to the adjacent thoracic wall was observed. Few cases had petechial haemorrhages on the surfaces of the lobes and the thoracic wall.

Microscopically, thickening of inter-alveolar septa due to the infiltration of variable numbers of neutrophils, MNCs and fiboblast cells (Fig. 6c & d) and in few cases inter-alveolar septa had hyperemia, oedema partial to complete hyperplasia of type 2 pneumocytes. In most of the cases, proliferative lesions were observed in sections of lungs. Interstitium showed macrophages with basophilic bacterial colonies. MTS staining revealed lung section with thickened interstitium due to deposition of blue stained collagen fibers (Fig. 6e).

Granulomatous Pneumonia

Granulomatous pneumonia was found in 1 (0.83%) out of 120 affected lungs examined. During gross examination, the affected lungs showed inflated lobes with diffused nodules (2-4 cm) over the surfaces and cut section showed presence of diffused nodules and caseous exudates within bronchial lumen (Table 6). There were numerous granulomas of varying sizes all over the surface of the lung. A number of small granulomas merged to form a larger granuloma with central caseating material. Pyogranuloma was focally extensive and limited to both cranial lobes in one case. Chronic granulomatous nodules of this type were also found in the parietal and visceral pleura. There was severe enlargement and caseation of the mediastinal and tracheobronchial lymph nodes (Fig. 7a & b).

Microscopically, granulomas were composed of a central eosinophilic necrotic area surrounded by epitheloid cells, lymphocytes, macrophages and characteristic Langhan's type of giant cells with horse shoe nuclei and an outer zone of proliferating fibrous connective tissue. In the center and periphery of granulomatous lesion, slender acid-fast bacilli were demonstrated by using Ziehl and Neelsen staining. Impression smear from the granulomatous lesion also revealed presence of acid-fast bacteria (Fig. 7c, d & e).

Congestion and Pulmonary Oedema

In 5% (6/120) of the cases, pulmonary congestion and edema were observed (Table 6). Grossly, the lungs had scattered regions of haemorrhage and congestion. When the thorax was opened, the lungs were pale and heavy and failed to collapse. Following the incision, frothy edematous fluid was observed in the lumen of trachea, bronchi and bronchioles.

Histopathological examination of the sections indicated blood vessel engorgement in the interalveolar, interlobular septa and peribronchiolar regions. Erythrocytes partially or totally filled the alveoli and interalveolar septa. In the alveoli and interlobular septa, homogeneous, eosinophilic fluid was found.

Emphysema and atelectasis

Five out of 120 cases (4.16%) of cases revealed atelectasis and emphysema (Table 6). Grossly, prominent foci of pale and large emphysematous regions in one or more pulmonary were detected. These areas were slightly raised from the nearby unaffected areas and showed depression and crepitation on applying pressure. Large emphysematous bullae were seen in the form of open distended alveoli in lungs sections that have breached alveolar interstitium. Dark reddish to bluish-grey discoloured, firm textured areas depressed below than the normal lobular surface were marked as atelectatsis in one or more lobes. On microscopic examination, atelectatic lesions with foci of emphysema nearby and collapsed alveoli that resembled a slit-like constricted lumen (Fig. 8). Alveolar walls looked parallel and in apposition and neither the alveoli nor the interstitium displayed any signs of inflammation.

DISCUSSION

The incidence of pneumonia in the present study was higher (97.56%) in comparison to the previous report, 89.13% in small and large ruminants by[20], 63.23% by[21], 64.7% in large ruminants by[22] and 14.82% in small ruminants by[23]. The differences in the results of incidence of cases of pneumonia could be attributed to the variables in the temporal and spatial parameters taken up by different researchers during their investigation work. In cases of interstitial pneumonia, the inflammatory processes were primarily in the alveolar epithelium, endothelium and were contiguous with bronchiolar epithelium. Progression of inflammatory changes from interstitium towards the alveoli, bronchiole and bronchi lead to broncho-interstitial pneumonia[24]. Bronchopneumonia are typically characterized by the cranio-ventral consolidation of the lobes and infiltration of inflammatory exudate within the lumen of bronchi, bronchioles and alveoli of different lobules was recorded in 6.7% (8/129) cases. The agents initially damage the broncho-alveolar epithelium and subsequently the inflammation spread distally and centrifugally, the earlier lesions being at the centre. Based on the vascular changes and type of predominant inflammatory cells, bronchopneumonia is arbitrarily categorized into acute, sub-acute, suppurative, fibrinous and chronic pneumonia. In the present study, the incidence of acute bronchopneumonia was recorded as 0.83% (1/120), which is in contrast to reports of higher incidence of upto 90%[25,26] and 26.28% to 33.33%[27,28]. Suppurative bronchopneumonia was observed in 3.3% (4/120) animals, wherein the gross

and microscopic lesions recorded were similar to those described in the literature[12,24]. The affected lobes had consolidation with necrotic cellular debris admixed with neutrophilic exudate and occasional few macrophages in the air spaces. The lungs exhibited a varying range of consolidation in the affected lobes, fibrinous exudate over the pleura and the airways were filled with fibrinous exudate along with the presence of inflammatory and denuded epithelial cells. Miscellaneous affections of lungs were also diagnosed in 9.16 (11/120) animals in the current study, which included congestion and oedema in 5% (6/120) animals and emphysema in 4.16% (5/120) animals.

CONCLUSION

Occurrence of bronchointerstitial pneumonia was found to be highest with 65.83% (79/120) incidence followed by interstitial pneumonia with 16.66% (20/120) and bronchopneumonia 7.5% (9/120).

ACKNOWLEDGEMENTS

The authors are thankful to the Head, Division of Pathology, Indian Veterinary Research Institute for providing the necessary facilities for this work and also gratitude for his whole-hearted encouragement, advice, expert suggestions and support for completing present case report and for providing the opportunity, scope and requisite administrative facilities for carrying out this work.

REFERENCES

1. McLuckie AM, Ratchford MA and Fridell RA. 2011. Regional desert tortoise monitoring in the Red Cliffs Preserve. *Utah Div Wild Res* **13:** 1-54.
2. Lopez A. 2012. Respiratory system, mediastinum and pleurae. In: Pathologic Basis of Veterinary Disease JF Zachary and MD McGavin, eds. Mos by Elsevier, *St Louis* 458-538.
3. Singh R, Kumar P, Sahoo M, Bind RB, Kumar MA, Das T, Kumari S, Kasyap G, Saminatham M and Singh KP. 2017. Spontaneously occurring lung lesions in sheep and goats. *Indian J Vet Pathol* **4:** 18-24.
4. Buhman MJ, Perino LJ, Galyean ML, Wittum TE, Montgomery TH and Swingle RS. 2000. Association between changes in eating and drinking behaviors and respiratory tract disease in newly arrived calves at a feedlot. *Am J Vet Res* **6110:** 1163-1168.
5. Smith KJ, White BJ, Amrine DE, Larson RL, Theurer ME, Szasz JI and Waggoner JW. 2023. Evaluation of First Treatment Timing, Fatal Disease Onset and Days from First Treatment to Death Associated with Bovine Respiratory Disease in Feedlot Cattle. *Vet Sci* **10:** 204.
6. Gagea MI, Bateman KG, Van Dreumel T, McEwen BJ, Carman S, Archambault M, Shanahan RA and Caswell JL. 2006. Diseases and pathogens associated with mortality in Ontario beef feedlots. *J Vet Diagn Invest* **18:** 18-28.
7. Snowder GD, Van Vleck LD, Cundiff LV and Bennett GL. 2006. Bovine respiratory disease in feedlot cattle: Environmental, genetic and economic factors. *J Anim Sci* **848:** 1999-2008.
8. Woldemeskel M, Tibbo M and Potgieter LND. 2002. Ovine progressive pneumonia Maedi-Visna: an emerging respiratory disease of sheep in Ethiopia. *Berl Munch Tierarztl* **109:** 486-488.
9. Jakab GJ. 1982. Viral bacterial interactions in pulmonary infection. *Adv Vet Sci Comp Med* **26:** 155.
10. Potgieter LN. 1995. Immunology of bovine viral diarrhea virus. *Vet Clinics North America Food Anim Prac* **11:** 501-20.
11. Sutherland AD. 1985. Effects of *Pasteurella haemolytica* cytotoxin on ovine peripheral blood leucocytes and lymphocytes obtained from gastric lymph. *Vet Microbiol* **105:** 431-438.
12. Jubb KVF, Kennedy PC and Palmer N. 2015. Pathology of Domestic Animals. 6th ed. US Acade Press.
13. Caswell JL and Archambault M. 2007. *Mycoplasma bovis* pneumonia in cattle. *Anim Health Res Rev* **8:** 161-186.
14. Griffin D, Chengappa MM, Kuszak J and McVey DS. 2010. Bacterial pathogens of the bovine respiratory disease complex. *Vet Clin Food Anim Pract* **26:** 381-394.
15. Gershwin LJ. 2007. Bovine respiratory syncytial virus infection: immunopathogenic mechanisms. *Anim Health Res Rev* **8:** 207.
16. Fulton RW, Blood KS, Panciera RJ, Payton ME, Ridpath JF, Confer AW, Saliki JT, Burge LT, Welsh RD, Johnson BJ and Reck A. 2009. Lung pathology and infectious agents in fatal feedlot pneumonias and relationship with mortality, disease onset and treatments. *J Vet Diagn Invest* **21:** 464-477.
17. Murray GM, More SJ, Sammin D, Casey MJ, McElroy MC, O'Neill RG, Byrne WJ, Earley B, Clegg TA, Ball H and Bell CJ. 2017. Pathogens, patterns of pneumonia and epidemiologic risk factors associated with respiratory disease in recently weaned cattle in Ireland. *J Vet Diagn Invest* **291:** 20-34.
18. Goswami P, Banga HS, Deshmukh S, Mahajan V, Singh ND and Brar RS. 2015. Pathological investigation of bovine lungs in naturally acquired *Pasteurella multocida* infection by immunohistological technique. *Indian J Vet Pathol* **39:** 304-310.
19. Luna LG. 1968. Manual of Histologic Staining: Methods of the Armed Forces Institute of Pathology. 3rd Edn. New York, McGraw Hill Book Co.
20. Roopa N. 2020. Etiopathology of respiratory disease complex in ruminants and molecular characterization of important pathogens. Thesis, MVSc Deemed University, IVRI, Izatnagar, India.
21. Sindhoora K. 2019. Etiopathology of pneumonia in ruminants and molecular characterization. Thesis, MVSc Deemed University, IVRI, Izatnagar, India.
22. Bhupesh PK. 2018. Patho-epidemiological studies and molecular characterization of important pathogens of calf pneumonia. Thesis, PhD Deemed University, IVRI, Izatnagar, India.
23. Neethu G. 2018. Pathomorphology of pneumoniain sheep and goat with special reference to parainfluenza virus. Thesis, MVSc Deemed University, IVRI, Izatnagar, India.
24. McGavin D and Zachary J. 2007. Pathologic basis of veterinary disease. Mosby-Elsevier, *St Louis* **4:** 490-495.
25. Ramachandran S and Sharma GL. 1969. Observations on the incidence and histopathology of pneumonia of sheep and goats in India. *Indian J Vet Pathol* **46:** 16-29.
26. Kumar MA, Kumar R, Varshney KC, Nair MG, Lakkawar AW, Sridhar BG and Palanivelu M. 2014. Pathomorphological studies of lung lesions in sheep. *Indian J Vet Pathol* **382:** 75-81.
27. Kumar AA, Shivachandra SB, Biswas A, Singh VP, Singh VP and Srivastava SK. 2004. Prevalent serotypes of Pasteurella multocida isolated from different animal and avian species in India. *Vet Res Comm* **288:** 657-667.
28. Ettore C, Sacchini F, Sacchia M and Salda DL. 2007. Pneumonia of lambs in the Abruzzo region of Italy: anatomopathological and histopathological studies and localization of *mycoplasma ovipneumoniae*. *Vet Ital* **43:** 149-155.

Indian J. Vet. Pathol., 49(1) : 23-29, 2025: DOI: https://doi.org/10.5958/mwkwvk54

RESEARCH ARTICLE

Pathological and molecular diagnosis of porcine Circovirus 2 in slaughtered pigs of India

Sourabh Babu, Dinesh Murali, Anbazhagan Subbaiyan[1], Pradeep Kumar, Sagar Patel, Jigarji Chaturji Thakor, Rajendra Singh, Saikumar, Tareni Das[2], Mamata Pasayat[2], Ramakant Acharya[2], Jagannath Prasad Tripathy[2], Prabin Kumar Sahoo[2], Nihar Ranjan Sahoo[2] and Monalisa Sahoo[2*]

Division of Pathology, ICAR-Indian Veterinary Research Institute (IVRI), Izatnagar, India, [1]ICAR-Division of Bacteriology & Mycology, Indian Veterinary Research Institute (IVRI), Izatnagar, India, [2]ICAR-National Institute on Foot and Mouth Disease (NIFMD), Arugul, Jatni, Bhubaneswar, Odisha, India

Address for Correspondence

Monalisa Sahoo, Scientist, ICAR-National Institute on Foot and Mouth Disease (NIFMD), Arugul, Jatni, Bhubaneswar, Odisha, India, E-mail: vety.lisa@gmail.com

Received: 19.8.2024; Accepted: 20.9.2024

ABSTRACT

Porcine Circovirus 2 (PCV2), an emerging viral pathogen of pigs is distributed worldwide causing huge economic loss to the swine industry. Despite its high prevalence globally, very little or no reports are available regarding the prevalence of porcine circovirus-2 (PCV-2) in slaughtered pigs. The objective of our study was to estimate the prevalence of PCV2 in Indian slaughtered pigs using pathological and molecular techniques. Out of 968 morbid tissue samples (lungs-484; lymph nodes-484) collected from slaughtered pigs showed the high prevalence of PCV2 (65.28%) by PCR targeting ORF2 gene showing the amplification of 481 bp. Among 632 positive morbid tissues, lungs (52.89%) showed higher detection of PCV2 DNA as compared to lymph nodes (12.39%). Microscopically, affected lungs showed the predominant lesions of subacute interstitial pneumonia, proliferative and necrotizing pneumonia with suppurative bronchopneumonia. The lymph nodes showed the predominant lesions of lymphoid depletion with infiltration of histiocytes and macrophages in the medullary cords and sinuses. PCV2 antigen was immunohistochemically demonstrated in the alveolar macrophages and mononuclear cells in the lymph nodes confirming the association of PCV2 with associated pathologies. The phylogenetic analysis revealed that the PCV2 isolates circulating in pigs belonged to PCV2d-2 genotype. In conclusion, this study shows that PCV2d-2 is an emerging genotype circulating in Indian slaughtered pigs, which warrants the immediate implementation of PCV2 vaccination to aid the development of prevention and control strategies.

Keywords: Histopathology, immunohistochemistry, molecular diagnosis, PCV-2, PCV2d-2 genotype, phylogenetic analysis

INTRODUCTION

Porcine circovirus (PCV), a single-stranded, circular DNA virus belonging to the Circovirus genus of the Circoviridae is an emerging ubiquitous viral pathogen confronting swine industry worldwide[1,2]. It is responsible for porcine circovirus virus-associated disease (PCVAD), which includes a number of diseases such as post-weaning multi-systemic wasting syndrome (PMWS), porcine dermatitis and nephropathy syndrome (PDNS), granulomatous enteritis, porcine respiratory disease complex, reproductive failure and acute pulmonary edema based on the virus, hostimmunity, co-infections and other environmental characteristics[3,4]. Its high prevalence has been reported in different swine rearing countries of the globe such as North and South America, Europe, Asia, Oceania, Middle East, and the Caribbean including India[1,4,5]. Currently, PCVs are classified into four genotypes such as PCV1, PCV2, PCV3 and identified recently PCV4; out of which PCV2 is frequently reported in global swine industry[1,6,7]. Recently, PCV2 is divided into eight different genotypes: PCV2a, PCV2b, PCV2c, PCV2d, PCV2e including recently reported PCV2f, PCV2g, and PCV2h genotypes based on ORF2 classification criteria[8]. Recent reports showed the continuous evolution of PCV2 leading to emergence of novel strains due to genetic shift[1,9]. The first identified PCV2a, the oldest genotype is used in available commercial PCV2 vaccines due to its predominance till 2003. Later on, global genotype shift was observed from PCV2a to PCV2b and recently to PCV2d in global swine production[1,9]. PCV2d is further classified to PCV2d-1 and PCV2d-2. Out of these 2 subtypes, PCV2d-2 is frequently reported worldwide with increased virulence[1,9]. The frequent reports of high prevalence of various genotypes of PCV2 along with intergenotypic recombination in different geographical regions of India suggest that PCV2 is likely to be endemic in India[10-15]. Moreover, PCV3 has been reported in a pig farm of Chhattisgarh with the history of severe reproductive failure, piglet mortality and dermatitis[5]. Out of its various genotypes, PCV2d genotype is frequently reported

How to cite this article : Babu, S., Murali, D., Subbaiyan, A., Kumar, P., Patel, S., Thakor, J.C., Singh, R., Saikumar, Das, T., Pasayat, M., Acharya, R., Tripathy, J.P., Sahoo, P.K., Sahoo, N.R. and Sahoo, M. 2025. Pathological and molecular diagnosis of porcine Circovirus 2 in slaughtered pigs of India. Indian J. Vet. Pathol., 49(1) : 23-29.

in Indian pig population[7,12,14,15]. However, majority of the cases were reported from the organized farms only. The use of histopathology and immunohistochemical (IHC) techniques in association with molecular diagnosis has been an important source of information for sanitary monitoring of pigs for the identification and monitoring the circulation of infectious pathogens[16]. Diagnosis of PCVAD is primarily based on clinical signs, histologic lesions, and detection of PCV-2 antigens or DNA within characteristic lesions. Despite continuous reports of newly emerging strains and global genotype shifts, there is little information available regarding the prevalence of PCV2 in slaughtered pigs of India. The objectives of this study were to broaden our knowledge of prevalence of PCV2 with associated pathologies in slaughtered pigs using pathological and molecular techniques.

MATERIALS AND METHODS

A total of 968 morbid tissue samples (lungs-484; mesenteric lymph nodes-484) from 484 sacrificed pigs (cross bred-302, desi-182) of aged < 6 months age (121) and adults (363) were collected out of 982 pig carcasses examined in the slaughterhouses at various slaughterhouses belonging to Chandigarh (Punjab, 78), Bareilly (Uttar Pradesh, 148), and Mumbai (Maharashtra, 258) using random sampling method. These slaughterhouses were targeted because of high the turnover of pigs from densely pig-rearing areas. After the evisceration, thin (< 5mm) tissue pieces from lungs and lymph nodes were aseptically removed and examined for gross pathological lesions. All the lungs (484) showed varying degrees of pulmonary lesions, while 29 lymph nodes were enlarged. The tissues were fixed in 10% neutral buffered formalin (NBF) for histopathology and immunohistochemistry (IHC) studies. The aseptically collected tissues were transferred to the laboratory in a sterile container on ice and stored at -20^{O}C for the molecular detection of PCV2.

Histopathological investigation

The 10% NBF fixed tissues were routinely processed followed by staining with routine Hematoxylin and Eosin (H&E) method[17]. The stained slides were examined under the microscope, and the alterations, if any were photographed (Olympus BX41, USA). The duplicate paraffin tissue sections of lungs and lymph nodes were taken on poly-L-lysin coated glass slides for the *in-situ* demonstration of PCV-2 antigen in lungs and lymph nodes.

Immunohistochemistry investigation

Briefly, the tissue sections were deparaffinized, rehydrated, and treated with proteinase-k solution (Abcam, USA) for 15 min to unmask the antigen, followed by washing with phosphate buffer saline - tween (PBST) for 2X of 5 min each. The quenching was done by adding 0.5% H_2O_2 for 30 min to block the endogenous peroxidase activity. The prediluted horse serum (Vectorlab, USA) was applied for 30 min at room temperature (RT) in the humid chamber to stop nonspecific binding. Then, the sections were incubated with PCV-2 capsid rabbit polyclonal antibody (1:200) for overnight at 4^{O}C in humidity chamber followed by incubating the sections with prediluted ImmPRESS® HRP universal secondary antibody (MP-7500, Vector laboratories, USA) for 30 min. Afterwards, the sections were added with ImmPACT® DAB Substrate, (HRP) (SK-4105, Vector laboratories, USA) for 30 sec till development of the color. After the color development, sections were counter stained with Mayer's haematoxylin, and mounted on the aqueous mountant (C9368, CC/Mount, Sigma-Aldrich, USA) for visualization of signals under the microscope. Negative controls were run for each block tested with substitution of similar dilutions of PBS with 1% BSA for primary antibody and mouse isotype control antibodies (ThermoFischer Scientific, USA) as secondary antibody to rule out the false positive staining.

Molecular investigation

The DNA was extracted from the lungs and mesenteric lymph nodes using commercially available DNeasy Blood and Tissue Mini Kit (Qiagen, USA) as per manufacture's protocol. The viral genomic DNA was further subjected to PCR using the previously reported primer sets targeting the ORF2 region of PCV2[18].

Sequencing and phylogenetic analysis

The amplified 4 PCR amplicons were purified by using Gene JET PCR purification kit (Thermo

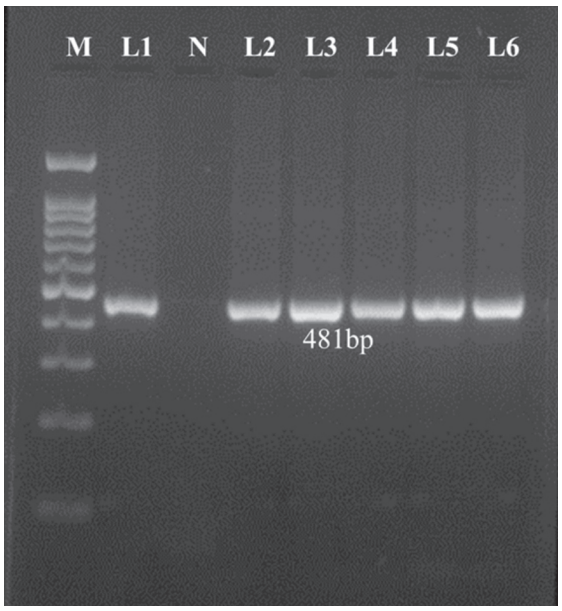

Fig. 1. Molecular detection of PCV2 showing amplified product of 481 bp for ORF2 gene, Lane M: Ladder (100 bp), L1: Positive control, L2: Negative control, L3: Lungs, L4: Lungs, L5: Lymph node, L6: Lymph node positive for PCV2.

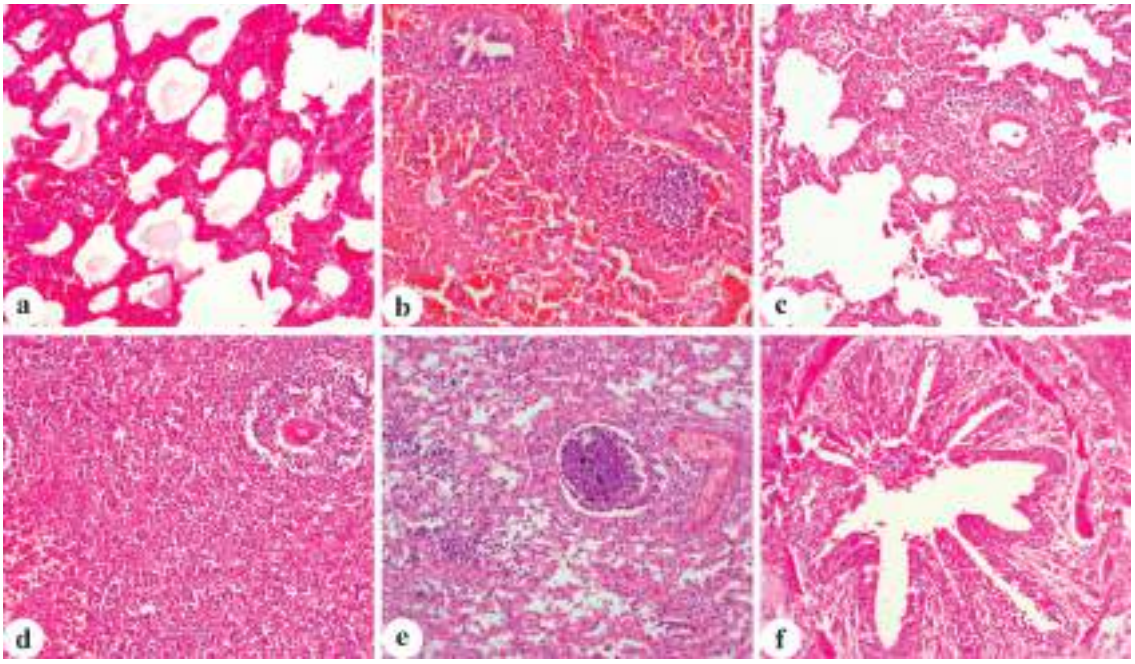

Fig. 2. Histopathological lesions in pigs of naturally infected with PCV2 showing **a.** Interstitial pneumonia with oedema (H&E X100); **b.** Extensive areas of haemorrhages in the pulmonary interstitium (H&E X100); **c.** Interstitial pneumonia with perivascular lymphocytic infiltrate (H&E X100); **d.** Proliferative and necrotizing pneumonia (H&E X100); **e.** Suppurative bronchopneumonia (H&E X100); **f.** Bronchiolitis fibrosa obliterans (H&E X200).

Fisher Scientific, USA) and then these got sequenced commercially (Eurofins, Bangalore). The sequence data (FASTA files) were analyzed using 'EditSeq' programme of 'Lasergene' version 10 (DNASTAR Inc, USA). The nucleotide sequences of the isolates belonging to different genotypes of PCV were retrieved from GenBank and aligned with nucleotide sequences of the study isolates by using the ClustalW method. The evolutionary history was

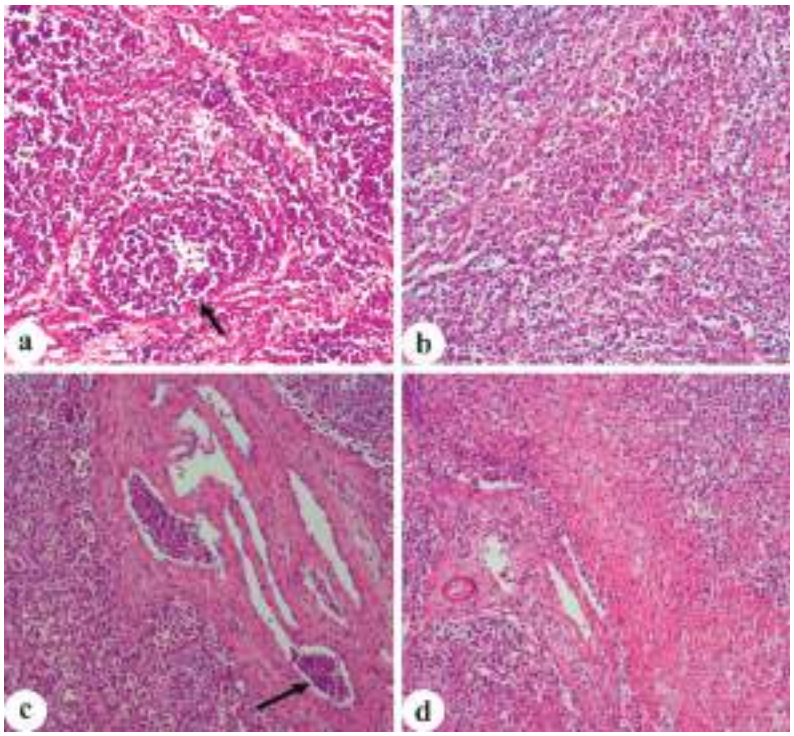

Fig. 3. Histopathological lesions in lymph nodes of naturally infected with PCV2 showing **a.** Lymphoid depletion (arrow) (H&E X100); **b.** Marked infiltration of macrophages and histiocytes in medullary sinus (H&E X100); **c.** Purulent lymphadenitis showing infiltration of neutrophilic exudates (arrow) within lumen of blood vesssel (H&E X100); **d.** Large area of necrosis in the medulla (H&E X100).

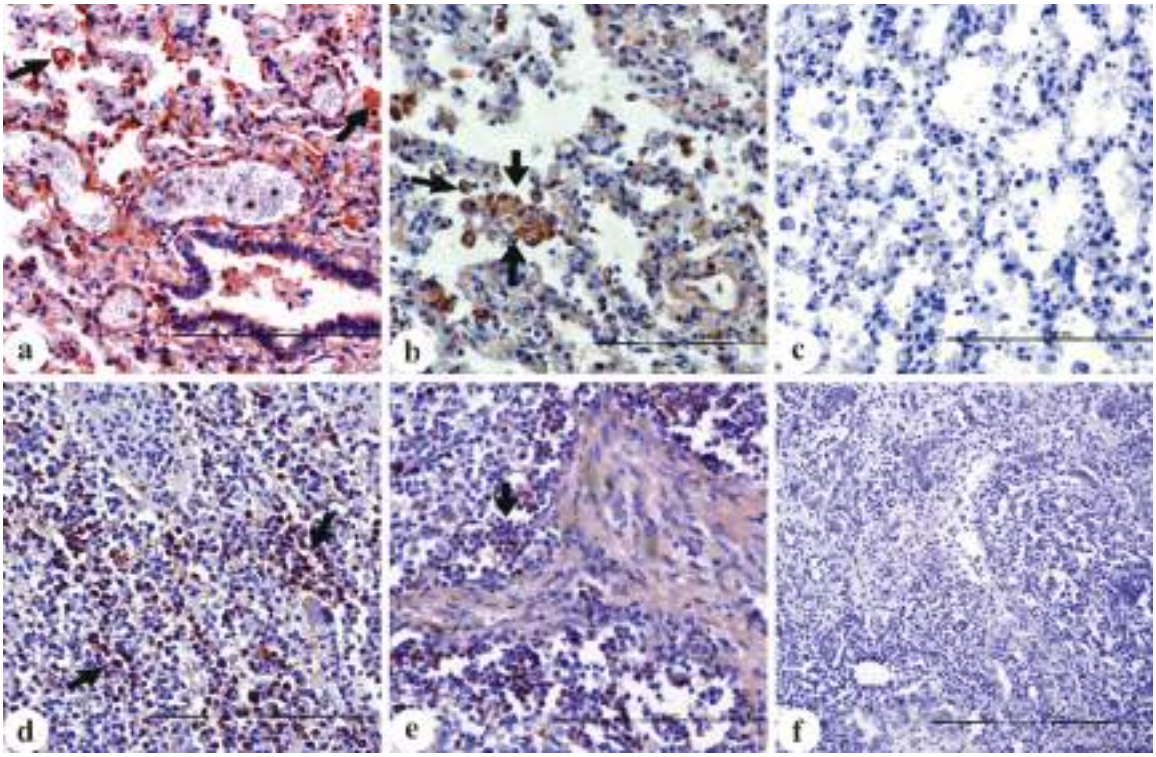

Fig. 4. The immunolocalization of PCV2 antigen in lungs and lymph nodes of naturally infected slaughtered pigs **a.** Alveolar macrophages (arrow), vessel wall and inflammatory cells in the vascular lumen, lungs; **b.** Alveolar macrophages, lungs; **c.** Absence of immunoreactivity, negative control, lungs; **d,e.** Mononuclear cells and histiocytes (arrow), lymph nodes; **e.** Negative control, lymph node (IHC X40 bar 1000 μm).

inferred using the Neighbor-Joining method. The optimal tree with the sum of branch length = 1.74952771. The percentage of replicate trees in which the associated taxa clustered together in the bootstrap test (1000 replicates) are shown next to the branches. The tree is drawn to scale, with branch lengths in the same units as those of the evolutionary distances used to infer the phylogenetic tree. The evolutionary distances were computed using the Jukes-Cantor method and are in the units of the number of base substitutions per site. The rate variation among sites was modeled with a gamma distribution (shape parameter = 4). The analysis involved 17 nucleotide sequences with codon positions included were 1st + 2nd + 3rd + Noncoding. All ambiguous positions were removed for each sequence pair. There were a total of 752 positions in the final dataset. Evolutionary analyses were conducted in MEGA7.

RESULTS

Out of 968 morbid tissues tested, 632 tissues from 354 pig carcasses showed the amplification of ORF2 gene with product size of 481 bp specific to PCV-2 (65.28%, 632/968) (Fig. 1). Out of 632 positive cases, lungs (52.89%) showed higher detection of PCV2 than lymph nodes (12.39%). Among the different states, Uttar Pradesh showed higher positivity (41.9%), while Chandigarh showed lowest (11.6%) detection of PCV2. The high prevalence was observed in adult age group (78.4%) than young age group (21.5%). The crossbred pigs (61.9%) showed higher detection of PCV2 as compared to desi breed.

Grossly, the PCV2-infected lungs were heavy, non-collapsible, diffusely mottled red to purple, and rubbery in majority of the cases (87.85%) with interlobular edema (60.74%). The mediastinal lymph nodes were enlarged and oedematous. The lungs showed the lesions of interstitial pneumonia (Fig. 2a) accompanied with diffuse congestion, hemorrhages in the interstitium (Fig. 2b), vasculitis (Fig. 2c) accompanied with infiltration of lymphocytes, macrophages in the alveolar lumen, alveolar septae and at places in the connective tissue of the bronchi/bronchioles. The bronchial and bronchiolar epithelium of the affected lungs showed hyperplasia, desquamation, and desquamated epithelium admixed with inflammatory cellular exudates within the lumen. The interalveolar septa was thickened with infiltration of mononuclear cells, and macrophages. The pleura was moderately thickened due to infiltrations of fibrino-cellular exudates. The predominant histologic diagnosis was interstitial pneumonia associated with proliferative and necrotizing pneumonia (58.24%) (Fig. 2d), suppurative bronchopneumonia (41.69%) (Fig. 2e), fibrinonecrotizing bronchopneumonia (21.85%),

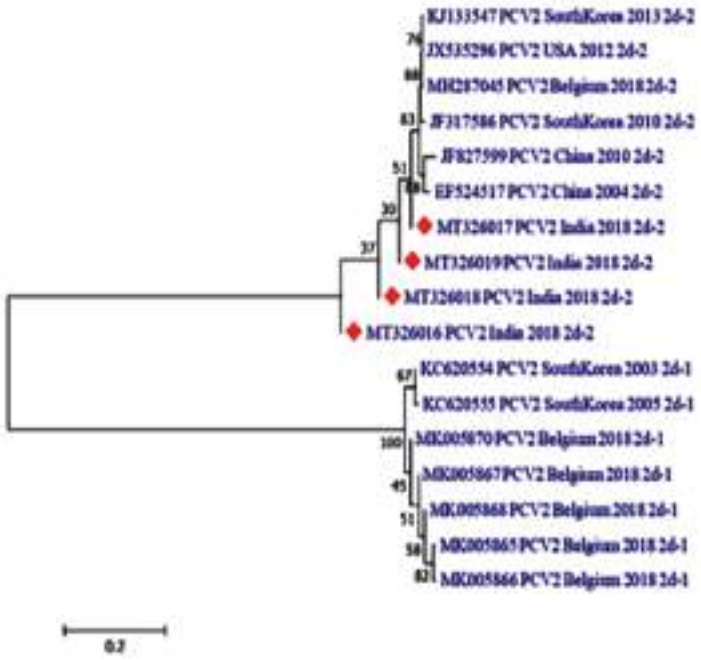

Fig. 5. Phylogenetic tree of the ORF2 nucleotide sequences of various genotypes of PCV2 using the Neighbor-Joining method in MEGA 7 showing the presence of PCV2d-2 genotype. Samples with solid Red coloured triangles represent Indian PCV2 isolates included in the present study.

peribronchiolar fibrosis and bronchiolitis fibrosa obliterans (Fig. 2f) were observed. In 49 cases, lymphoid depletion with histiocytic infiltration was observed in bronchus-associated lymphoid tissue (BALT). The majority of the lymph nodes did not show any appreciable gross lesions except multifocal areas of necrosis was observed in 13 lymph nodes (10.83%). Microscopically, majority of the lymph nodes (89.26%) showed variable degree of lymphocyte depletion (Fig. 3a) with loss of follicular architecture with infiltration of histiocytes in the medullary cords and sinuses (Fig. 3b). Majority of the lymph nodes showed mild to moderate degree of lymphoid depletion. A total of 11 lymph nodes showed indistinct lymphoid follicles in one or more lymph nodes. The purulent lymphadenitis (Fig. 3c) was also observed in 21 cases. Nine lymph nodes showed coagulation necrosis affecting the wide areas of lymph node parenchyma (Fig. 3d). Besides, various lesions like haemosiderosis, oedema, fibrosis and multinucleated giant cells in the lymphoid follicles were detected in few cases (5.73%).

Immunohistochemically, abundant immunosignaling of PCV2 antigens were detected consistently intracytoplasmically in the inflammatory exudates especially alveolar macrophages, lymphocytes (Figs. 4a, b) and rarely intranuclearly in epithelial cells. The immunoreactivity was also noticed in vessel wall with few inflammatory cells present in the vascular lumen (Fig. 4a). The alveolar, bronchial and bronchiolar epithelial cells also showed intracytoplasmic immunoreactivity for PCV2 antigen. The presence of PCV2 antigen was also detected in bronchial and vascular smooth muscle cells and in epithelial cells of bronchial submucosal glands. In lymph nodes, abundant immunosignaling for viral antigen was noticed in the lymphocytes, histiocytic and dendritic cells of the medullary region (Figs. 4d, e). The negative controls of lungs and spleen did not show any immunoreactivity for PCV2 antigen (Figs. 4c, f).

The comparative phylogenetic analysis of 4 PCV-2 positive Indian isolates (MT326016, MT326017, MT326018 and MT326019) with the sequences of PCV-2 in NCBI database showed 98% similarity with PCV2d sequences. Further, our sequences with the sequences of 2 different genotypes (PCV2d-1 and PCV2d-2) of PCV2d sequences downloaded from the database formed clad with PCV2d-2 genotype sequences while forming separate clad from PCV2d-1 sequences (Fig. 5). The sequences of Indian isolates belonging to PCV2d-2 genotype were closely related to the sequences of the isolates reported from China, South Korea, Belgium and USA isolates.

DISCUSSION

Porcine circovirus type 2 (PCV2), recognized as emerging global viral pathogen is frequently reported from slaughtered pigs worldwide[2,6,19]. Despite its high economic importance, the paucity of literatures regarding the prevalence of PCV2 with the associated pathologies in Indian slaughtered pigs prompted us to take the present investigation.

Slaughterhouse surveys are essential components of

infectious disease control and eradication programmes worldwide being the source being the source of providing helpful information on the prevalence of economically important animal diseases including diseases of zoonotic importance[20]. The detection of PCV2 by PCR is considered as a rapid tool in identifying PCV2 infections in pigs[21]. Therefore, the present study used PCR as PCV2 detection method. The overall prevalence of PCV2 in the slaughtered pigs was 65.28%. In our case, the possible reason for the higher prevalence in Uttar Pradesh might be due to slaughtering of pigs from different states of North as well as North-Eastern India. Uttar Pradesh has the second highest pig population (1.35 million) in India (19th Livestock Census, 2012), thus higher numbers of pigs being slaughtered. The high prevalence of PCV2 in slaughtered pigs was reported in earlier reports[2,6,19,22]. The complex interaction of multi-etiological factors such as infectious pathogens, environmental factors, and management and husbandry practices play pivotal role in the development of clinical disease. The high evidence of the disease in the older pigs (above 6 months of age) in comparison to the younger pigs (< 6 months of age) might be due to increased exposure of pigs (mainly horizontal transmission) to infection with the advancement of age. The higher detection of PCV2 in crossbred pigs as compared to desi breed might be due to more number of pigs received to the slaughterhouse for slaughtering. The higher prevalence of PCV2 was detected in lungs than lymph nodes suggest the major contribution of PCV2 in pneumonic lesions. PCV2 is the major viral pathogen associated with porcine respiratory disease complex in the slaughtered pigs[1,23-25]. The affected lungs showing the histopathological lesions of interstitial pneumonia, proliferative and necrotizing pneumonia with suppurative bronchopneumonia are in agreement with the previous reports[9,12,15,26,27]. The predominant lesions of lymphoid depletion with infiltration of macrophages and histiocytes in the lymph nodes were similar to previous observations in weaned pigs diagnosed with PMWS[11,28,29]. The lymphoid depletion might suggest the PCV2 associated immunosuppression which predisposes the animal to secondary bacterial infection[12,30].

The IHC study is a reliable method for confirmation of role of PCV-2 in swine diseases. The abundant immunoreactivity of PCV2 antigens in lungs and lymph nodes at the lesional sites confirm the role of PCV2 with the associated pathologies. The detection of PCV2 antigens in the bronchial, bronchiolar, alveolar epithelial cells and vascular smooth muscle cells in the present study was similar with the earlier observation[26,31]. The detection of PCV2 antigens in the alveolar macrophages suggest the replication of PCV2 in macrophages[31]. The immunodetection of abundant PCV2 antigens in the lymphocytes and histiocytes suggest the uptake of viral antigens in the antigen-presenting cells, which later on might be transported either intracellularly or free in lymph and/or blood. The predominant lesions of histiocytic infiltration in the lymph nodes in our case corroborated with the previous reports showing PCV2 associated lymphadenopathy[31]. The immunoreactivity of large amounts of PCV2 antigen in the wall of the blood vessels of lungs and lymph nodes suggests that the vascular system may be important in the pathogenesis of PCV2[32].

In the phylogenetic analysis, it was found that Indian PCV2 isolates matched 98% with PCV2d isolates from the database which suggest the prevalence of PCV2d genotype in Indian slaughtered pigs. The higher detection of PCV2d genotype in Indian pig population is similar with the previous findings[7,12,33]. Further, all 4 isolates forming clade (red, highlighted with red solid triangle marker) with PCV2d-2 genotype suggest that the PCV2d isolates belongs to PCV2d-2 genotype. The circulation of PCV2d-2 genotype in Indian pig population has been reported in previous reports[13,34]. The high prevalence of PCV2d-2 genotype suggests that the genotype PCV2d-2 is getting endemic within the slaughtered pigs of India.

CONCLUSION

From the present investigation, it may be concluded that PCV2d-2 genotype is prevalent in Indian slaughtered pigs based on pathological and molecular findings. This findings suggest the need for immediate use of PCV2 vaccine in pigs along with designing effective preventive and control strategies to minimise the economic loss to the farmers. However, investigation on large number of samples with continuous surveillance covering the slaughterhouses from various geographical regions of India will give the detailed insight into identification of newly emerging strains and genotype shifts in swine population which will pave the way for the effective control of the disease.

ACKNOWLEDGMENTS

Authors are thankful to the Head, Division of Pathology, Director and Joint Directors of ICAR-IVRI, Izatnagar for providing the necessary facilities to carryout this research work.

REFERENCES

1. Maity HK, Samanta K, Deb R and Gupta VK. 2023. Revisiting porcine Circovirus infection: recent insights and its significance in the piggery sector. *Vaccines* **11:** 1301-1308.
2. Park SC, Kim S, Jeong TW, Oh B, Lim CW and Kim B. 2024. Prevalence of porcine circovirus type 2 and type 3 in slaughtered pigs and wild boars in Korea. *Vet Med Sci* **10:** e1329.
3. Allan GM and Ellis JA. 2000. Porcine circoviruses: a review. *J*

Vet Diagn Invest **12:** 3-14.
4. Opriessnig T, Karuppannan AK, Castro AM and Xiao CT. 2020. Porcine circoviruses: Current status, knowledge gaps and challenges. *Virus Res* **286:** 198044.
5. Bera BC, Choudhary M, Anand T, Virmani N, Sundaram K, Choudhary B and Tripathi BN. 2020. Detection and genetic characterization of porcine circovirus 3 (PCV3) in pigs in India. *Transbound Emerg Dis* **67:** 1062-7.
6. Souza AE, de Menezes Cruz AC, Rodrigues IL, de Carvalho ECQ, Varella RB, Medina RM, Rodrigues RBR, Silveira RL and de Castro TX. 2023. Molecular detection of porcine circovirus (PCV2 and PCV3), torque teno swine virus 1 and 2 (TTSuV1 and TTSuVk2) and histopathological findings in swine organs submitted to regular slaughter in Southeast, Brazil. *Brazilian J Vet Med* **45:** 1-9.
7. Mukherjee P, Karam A, Barkalita L, Borah P, Chakraborty AK, Das S, Puro K, Sanjukta R, Ghatak S, Shakuntala I and Laha RG. 2018. Porcine circovirus 2 in the North Eastern region of India: Disease prevalence and genetic variation among the isolates from areas of intensive pig rearing. *Acta Trop* **182:** 166 -172.
8. Franzo G and Segalés J. 2018. Porcine circovirus 2 (PCV-2) genotype update and proposal of a new genotyping methodology. *PloS One* **13:** e0208585.
9. Tsai GT, Lin YC, Lin WH, Lin JH, Chiou MT, Liu HF and Lin CN. 2019. Phylogeographic and genetic characterization of porcine circovirus type 2 in Taiwan from 2001-2017. *Sci Rep* **9:** p.10782.
10. Anoopraj R, Rajkhowa TK, Cherian S, Arya RS, Tomar N, Gupta A, Ray PK, Somvanshi R and Saikumar G. 2015. Genetic characterisation and phylogenetic analysis of PCV2 isolates from India: indications for emergence of natural inter-genotypic recombinants. *Infect Genetics Evol* **31:** 25-32.
11. Karuppannan AK, Ramesh A, Reddy YK, Ramesh S, Mahaprabhu R, Jaisree S, Roy P, Sridhar R, Pazhanivel N, Sakthivelan SM and Sreekumar C. 2016. Emergence of porcine circovirus 2 associated reproductive failure in southern India. *Transbound Emerg Dis* **63:** 314-20.
12. Barman NN, Nath B, Kumar V, Sen A, Dutta TK, Dutta B, Rahman T and Kumar S. 2018. The emergence of porcine circovirus 2 infections in the Northeastern part of India: A retrospective study from 2011-2017. *Transbound Emerg Dis* **65:** 1959-1967.
13. John JK, Kattoor JJ, Sethi M, Tomar N, Das T and Saikumar G. 2020. Genetic diversity of Indian porcine circovirus type 2 (PCV2) isolates (2006-2018). *The Indian J Anim Sci* **90:** 842-846.
14. D'silva AL, Bharali A, Buragohain L, Pathak DC, Ramamurthy N, Batheja R, Mariappan AK, Gogoi SM, Barman NN, Dey S and Chellappa MM. 2023. Molecular characterization of porcine circovirus 2 circulating in Assam and Arunachal Pradesh of India. *Anim Biotech* **34:** 462-466.
15. Rajkumar S, Arya RS, Narnaware SD, Niceta CC and Tyween J. 2023. Pathology and Molecular Diagnosis of Respiratory Disease Outbreak due to PCV-2 in a Pig Farm in Goa, India. *Indian J Anim Res* **1:** 1-8.
16. Arenales A, Santana CH, Rolim ACR, Pereira EMMS, Nascimento E, Paixão TA and Santos RL. 2022. Histopathologic patterns and etiologic diagnosis of porcine respiratory disease complex in Brazil. *Arq Bras Med Vet Zootec* **74:** 497-508.
17. Luna LG. 1968. Manual of histologic staining methods of the Armed Forces Institute of Pathology.
18. Ellis J, Krakowka S, Lairmore M, Haines D, Bratanich A, Clark E, Allan G, Konoby C, Hassard L, Meehan B and Martin K. 1999. Reproduction of lesions of postweaning multi-systemic wasting syndrome in genotobiotic piglets. *J Vet Diagn* **11:** 3-14.
19. Aiki-Raji CO, Adebiyi AI and Oluwayelu DO. 2018. A slaughterhouse survey for porcine circovirus type 2 in commercial pigs in Ibadan, Southwest Nigeria. *Folia Vet* **62:** 30-34.
20. Al-QudahKM, Al-Majali AM and Obaidat MM. 2008. A study on pathological and microbiological conditions in goats in slaughterhouses in Jordan. *Asian J Anim Vet Adv* **3:** 269-274.
21. Alarcon P, Velasova M, Werling D, Stärk KD, Chang YM, Nevel A, Pfeiffer DU and Wieland B. 2011. Assessment and quantification of post-weaning multi-systemic wasting syndrome severity at farm level. *Prevent Vet Med* **98:** 19-28.
22. Yue W, Li Y, Zhang X, He J and Ma H. 2022. Prevalence of porcine circoviruses in slaughterhouses in central Shanxi province, China. *Front Vet Sci* **9:** 820-914.
23. Kim J, Chung HK and Chae C. 2003. Association of porcine circovirus 2 with porcine respiratory disease complex. *Vet J* **166:** 251-256.
24. Hansen MS, Pors SE, Bille-Hansen V, Kjerulff SKJ and Nielsen OL. 2010. Occurrence and tissue distribution of porcine circovirus type 2 identified by immunohistochemistry in Danish finishing pigs at slaughter. *J Comp Pathol* **142:** 109-121.
25. Thakor JC, Sahoo M, Singh KP, Singh R, Qureshi S, Kumar A, Kumar P, Patel S and Singh R. 2023. Porcine respiratory disease complex (PRDC) in Indian pigs: a slaughterhouse survey. *Vet Ital* **59:** 23-38.
26. Segalés J, Rosell C and Domingo M. 2004. Pathological findings associated with naturally acquired porcine circovirus type 2 associated disease. *Vet Microbiol* **98:** 137-149.
27. Segalés J. 2012. Porcine circovirus type 2 (PCV2) infections: Clinical signs, pathology and laboratory diagnosis. *Virus Res* **164:** 10-19.
28. Hohloch C, Reiner G, Bronnert B, Willems H and Reinacher M. 2015. Detection of porcine circovirus type 2 and its association with PMWS in wild boars and domestic pigs in Germany: A histopathological, immunohistochemical and molecular biological study. *Berl Munch tierarztli Wochenschr* **128:** 200-203.
29. Kumar R and Saikumar G. 2014. PMWS-like lesions in Preweaned Crossbred Piglets Naturally Infected with PCV2 in India. *Adv Anim Vet Sci* **2:** 26-30.
30. Stafford VV, Streltsova EB, Zaberezhny AD, Aliper TI and Gulyukin AM. 2021. Immunohistochemical Method for Detection PCV-2 Antigen in Pigs. In IOP Conference Series: Earth and Environmental Science (Vol. 666, No. 5, p: 052017). IOP Publishing.
31. Rosell C, Segale´s J, Plana-Duran J, Balasch M and Rodriguez-Arrioja GM. 1999. Pathological immunohistochemical and in-situ hybridization studies of natural cases of postweaning multisystemic wasting syndrome (PMWS) in pigs. *J Comp Pathol* **120:** 59-78.
32. Szeredi L, Dán Á, Solymosi N, Cságola A and Tuboly T. 2012. Association of porcine circovirus type 2 with vascular lesions in porcine pneumonia. *Vet Pathol* **49:** 264-270.
33. Kumar KA, Sujatha PL and Devendran P. 2023. A comprehensive analysis of circulating porcine circovirus 2 (PCV2) genotypes from 2008-2023 in India. *The Pharm Innov J* **12:** 990-996.
34. Sahoo M, Pathak M, Patel SK, Saikumar G, Upmanyu V, Thakor JC, Kumar P, Singh R and Singh K. 2022. Pathomorphology, immunohistochemical and molecular detection of an atypical porcine dermatitis and nephropathy syndrome (PDNS) due to PCV-2d-2 in naturally affected grower pigs of India. *Microb Pathog* **171:** 105-738.

Indian J. Vet. Pathol., 49(1) : 30-37, 2025: DOI: https://doi.org/10.5958/y916yk44

RESEARCH ARTICLE

Protective effects of *Spirulina* microalgal extracts on Doxorubicin-induced cardiotoxicity in rats

B.N. Laxmi, V.T. Shilpa*, B.C. Girish, N. Jaishankar[1], N.M. Rajashailesha[2], Shesharao Rathod[3] and K.R. Anjankumar

Department of Veterinary Pathology, Veterinary College, Hassan, KVAFSU, BIDAR, [1]Department of Animal Nutrition, [2]Department of Veterinary Anatomy, [3]BRIC, Dornalli, Yadgir, India

Address for Correspondence

V.T. Shilpa, Assistant Professor, Department of Veterinary Pathology, Veterinary College, Hassan, KVAFSU, BIDAR, India, E-mail: drshilpavt@gmail.com

Received: 14.8.2024; Accepted: 26.10.2024

ABSTRACT

The current study was conducted to assess the cardio protective potential of *Spirulina* microalgal extract (SME) in male Wistar rat model of doxorubicin-induced cardiotoxicity. The study consisted of sixgroups, comprising of six rats in Group I and eight rats in Groups II to VI. Group I rats received PBS orally daily for five weeks, Group II to VI rats received doxorubicin (DOX) @ 3.5 mg/kg bw intraperitoneally twice a week from 3rd to 5th week of the experiment period. In addition to DOX, Group III received vitamin E @ 200 mg/kg and Selenium @ 400 µg/kg bw orally; Group IV, V and VI rats received SME @ 250 mg/kg; 500 mg/kg and 1000 mg/kg bw orally daily for five weeks, respectively. The study revealed a significant negative variation in feed and water intake, body weight, heart weight, hematological, biochemical and pathomorphological parameters of heart in Group II, when compared to Group I. The changes caused by DOX were alleviated in SME treatment groups in a dose dependent manner. Similarly, amelioration of DOX induced cardiotoxicity was also observed in vitamin E and selenium group. Histopathologically, the SME treatment groups showed substantial improvement in toxicity lesions ofthe heart compared to Group II rats. The cardio protective efficacy of SME @ 250 mg/kg was lower than that of vitamin E and selenium, while the 500 mg/kg SME group showed slightly better protection and 1000 mg/kg SME showed highest protection, surpassing the effects of vitamin E and selenium.

Keywords: Cardiotoxicity, Doxorubicin, *Spirulina* microalgal extract

INTRODUCTION

Cardiotoxicity is a pathological condition in which damage to the electric or muscular systems of the heart results in its malfunction. As it ages, the heart weakens and becomes less effective at pumping blood. Chemotherapy and/or radiotherapy may result in cardiotoxicity[1]. Doxorubicin (DOX) is an antibiotic anthracycline that was discovered in the early 1960s from the pigment-producing bacterium *Streptomyces peucetius* and used for more than 30 years to fight cancer; however, it is currently produced chemically[2].

Dogs receiving doxorubicin treatment have shown clinically relevant cardiotoxic side effects. The most researched idea for these effects is that Doxorubicin interacts with and releases iron from storage proteins, resulting in the production of reactive superoxide molecules or oxidative free radicals[3]. The occurrence of cardiotoxicity and nephrotoxicity linked to many antineoplastic medicines currently used to treat patients is causing oncologists increasing concern, as it has been noted that such persistent adverse effects may affect the long-term results of survivors. New targeted therapies as well as unique processes linked to conventional cytotoxicities have been described[4].

Spirulina platensis is a filamentous cyanobacterium (blue-green alga) that belongs to the Oscillatoraceae family. It is rich in proteins, lipids, carbohydrates and some vital elements like zinc, magnesium, manganese, selenium. Phycocyanin, β-carotene, tocopherol, γ-linolenic acid and phenolic compounds in *Spirulina* are responsible for the antioxidant activity[5]. *Spirulina* also contains an important enzyme superoxide dismutase that acts indirectly by slowing down the rate of oxygen radical generating reactions. The antioxidant properties of *Spirulina* and its capacity to scavenge hydroxyl radicals and to inhibit lipid peroxidation have attracted the attention of many researchers[6].

A lot of antioxidant combinations have been recommended as chemo-deterrents for DOX persuaded toxicity. *Spirulina*, besides inhibiting protein oxidation and lipid peroxidation, also inhibits reactive oxygen species induced apoptosis. The present experiment is intended to delineate the protective perspective of the *Spirulina* microalgal extract against DOX-prompted cardiac injuries in Wistar rats.

How to cite this article : Laxmi, B.N., Shilpa, V.T., Girish, B.C., Jaishankar, N., Rajashailesha, N.M., Rathod, S. and Anjankumar, K.R. 2025. Protective effects of *Spirulina* microalgal extracts on Doxorubicin-induced cardiotoxicity in rats. Indian J. Vet. Pathol., 49(1) : 30-37.

MATERIALS AND METHODS

Animals

The study was conducted on 46 healthy adult male Wistar rats, weighing around 150 ± 20g, which were procured from CCSEA approved animal breeding facility, KCC BIO-LABS, Sy. No. 8/1, Tumakuru, Karnataka (Reg- 2066/PO/RcBiBt-S/Bt-L/19/ CCSEA dated 18th June 2019). All the rats were acclimatized to standard laboratory conditions at Small Animal House facility, Hassan for fifteen days prior to the initiation of the experiment and maintained at 25 ± 2^{O}C housing temperature and relative humidity of 50 to 70 per cent and to laboratory conditions of a 12-hour light/dark cycle throughout the study period and provided with regular standard pellet diet along with free access to deionized drinking water *ad libitum* throughout the course of the experiment. The animal care and handling were carried out according to the guidelines set by CCSEA. The study was approved by the Institutional Animal Ethical Committee (HVC/ IAEC/08/2023).

Preparation of drug and Mode of administration

Doxorubicin hydrochloride was procured from Khandelwal Laboratories Private Limited, Mumbai, India. It was injected intraperitoneally at 3.5 mg/kg body weight. Export grade twenty percent *Spirulina* platensis microalgal extract in liquid form was received from Department of Studies in Food Technology, Davangere University, Karnataka. It was used at the dose rates of 250, 500 and 1000 mg/kg body weightorally. Vitamin E and Selenium (Selvit-E®) were purchased from a registered chemist and administered orally at dose rate of 200 mg/kg and 400 µg/ kg, respectively, to the rats of Group III.

Experimental protocol

The study included six treatment groups comprising six rats in Group I and eight rats in each Group II to VI. Group I served as normal control and received Phospate buffered saline at 5 ml/kg/day orally throughout the experiment; Group II disease control rats received DOX at 3.5 mg/kg body weight, intraperitoneally, twice a week for three weeks (from 3rd week to end of 5th week); Group III rats along with DOX treatment received vitamin E (200 mg/kg) and Selenium (400 µg/kg) orally daily for five weeks; Group IV rats along with DOX treatment received SME at 250 mg/kg bw daily by oral gavage for five weeks; Group V rats along with DOX treatment received SME at 500 mg/kg bw daily by oral gavage for five weeks; while Group VI rats along with DOX treatment received SME at 1000 mg/kg bw daily by oral gavage for five weeks.

Parameters assessed

Body weight (g), feed (g) and water (ml) consumption were assessed every week. At the end of the study (36th day), all rats were sacrificed humanely by using overdose of Ketamine and Xylazine (as I/M injection) and subjected to detailed post-mortem examination. Blood was collected from retro-orbital plexus in EDTA and serum vitals for hematological and biochemical analysis, respectively.

Histopathological analysis

Table 1. The mean (±SE) body weight (g) and heart weight (g) values of rats of different experimental groups in the study.

Groups	Day 0	1st week	2nd week	3rd week	% change	4th week	% change	5th week	% change	Absolute weight of Heart (35th day)	% change
Group I (n = 6)	223.00±14.01^{A}	233.16±9.82^{AB}	240.33±8.93^{ABC}	253.16±9.28^{BC}		256.00±11.28^{BCb}		263.16±10.24^{Cc}		0.82±0.03^{b}	
Group II (DC, n = 8)	230.00±9.53^{A}	238.50±9.58^{A}	246.50±9.61^{A}	231.62±7.67^{AB}	-8.50	214.37±6.40^{BCa}	-16.26	197.25±5.74^{Ca}	-25.04	0.66±0.02^{a}	19.51
Group III (RC, n = 8)	229.75±8.00^{ABC}	240.62±7.67^{AB}	246.75±7.42^{A}	240.62±5.71^{A}	3.88	223.25±6.10^{BCa}	4.14	210.87±6.71^{Cab}	6.90	0.75±0.05^{ab}	13.63
Group IV (SME 250, n = 8)	232.12±7.97^{ABC}	245.00±7.62^{A}	252.00±7.04^{A}	238.62±4.99^{AB}	3.02	219.75±6.80^{BCa}	2.50	215.50±6.47^{Cab}	9.25	0.68±0.05^{ab}	3.03
Group V (SME 500, n = 8)	231.25±7.90^{ABC}	244.75±7.03^{AB}	251.50±6.90^{A}	239.62±5.18^{AC}	3.45	227.62±7.60^{BCa}	6.18	218.62±10.06^{Cab}	10.83	0.72±0.02^{ab}	9.09
Group VI (SME 1000, n = 8)	236.12±7.54^{AC}	253.87±8.35^{A}	262.62±8.05^{B}	249.62±7.57^{AC}	7.77	238.50±9.01^{ACb}	11.25	231.12±9.91^{Cb}	17.17	0.76±0.05^{ab}	15.15

Mean ± SE bearing different superscripts (abc; Within column and ABC; Between columns) are statistically significant at $p < 0.05$

Table 2. The mean (±SE) values of various hematological parameters of rats in different groups on final day (35th day) of the study.

Groups	Hb (g/dl)	% change	TEC (10^6/µl)	% change	TLC (10^3/µl)	% change	PCV (%)	% change	Platelet (10^3/µl)	% change
Group I (NC, n = 6)	13.92±0.33^c		6.21±0.60^c		8.91±0.32^b		43.94±0.29^c		541.33±53.90^b	
Group II (DC, n = 8)	8.41±0.32^a	-39.58	3.92±0.20^a	-36.87	4.08±0.47^a	-54.20	22.19±0.66^a	-49.49	292.37±22.06^a	-45.99
Group III (RC, n = 8)	10.77±0.49^b	28.06	5.11±0.31^{bc}	30.35	5.46±0.87^a	33.82	33.84±1.12^b	52.50	373.37±40.63^a	29.70
Group IV (SME 250, n = 8)	10.70±0.31^b	27.22	5.15 ±0.36^{bc}	31.37	5.75±0.42^a	40.93	33.86±1.92^b	52.59	391.62±32.01^a	33.94
Group V (SME 500, n = 8)	10.49±0.43^b	24.73	4.96±0.33^{ab}	26.53	5.22±0.70^a	27.94	30.93±1.75^b	39.38	357.5±48.15^a	22.27
Group VI (SME 1000, n = 8)	10.98±0.47^b	30.55	5.27±0.40^{bc}	34.43	5.64±0.54^a	38.23	34.11±1.54^b	53.71	351.12±41.52^a	20.09

One way ANOVA with Duncan's post hoc test (SPSS); Mean values with different superscript differ significantly at $p < 0.05$

Representative heart tissue from rats of all the groups were subjected to histopathological studies. The tissue was fixed using 10 per cent Neutral Buffered Formalin solution and sections were prepared using paraffin blocks and stained with hematoxylin and eosin, Masson'strichrome and phosphotungstic acid haematoxylin after dewaxing[7].

Histopathological scoring for heart

The heart samples were examined in random microscopic areas semi-quantitatively under high power fields and the number of changes was assessed by counting twenty non overlapped fields for the same slide of each animal. The extent of damage and the severity of lesions in the heart were assessed semi-quantitatively[8] with slight modification as follows; Score 0 - No abnormalities detected; Score 1-1 to 15% of the examined fields revealed histological alterations; Score 2 - 16 to 30% of the examined fields revealed histological alterations; Score 3 - 31 to 60% of the examined fields revealed histological alterations and Score 4 -> 60% of the examined fields revealed histological alterations.

Statistical analysis

Statistical analysis of the data collected for various parameters was done using one-way ANOVA with Duncan's multiple-range test and two-way ANOVA with Bonferroni post hoc test (p<0.05)[9].

RESULTS

General observation

Group I rats remained healthy and active throughout the period of experiment. Group II rats exhibited clinical signs such as weakness, dullness, depression, anorexia, reduced body weight and water intake, diarrhea, ruffled hairs, dehydration, arched back after 2nd dose of doxorubicin. The rats of Group III to VI manifested similar clinical signs as those of disease control rats, but with reduced intensity and frequency.

Feed and water consumption

Mean weekly feed and water consumption in Group I rats was normal to progressive. Group II rats showed statistically significant decrease (decrease of 42.1%, 71.45%, 79.17% in feed consumption and 10.63%, 43.15%, 45.96% in water consumption during 3rd, 4th and 5th week respectively) after 2nd dose of doxorubicin treatment as compared to Group I. Mean weekly feed consumption in Group V and VI rats significantly increased by 28.39%, and 31.26% than Group II rats during third week. Animals in the remaining treatment groups did not show any significant increase in mean weekly feed consumption as compared to Group II rats. Mean weekly feed consumption in Group IV, V and VI rats was significantly increased by 28.57%, 29.87% and 25.33% than Group II rats during 5th week. Though there was no significant difference in mean weekly water consumption in Group IV to VI rats during third and fourth week of experimental period, they showed slight improvement compared to Group II rats.

Body weight and organ weight

The mean body weights and heart weight in grams with standard error of mean at different time intervals of 0 day and 1st, 2nd, 3rd, 4th and 5th week of the experiment have been presented in Table 1. Group

I rats remained healthy and active throughout the period of experiment and demonstrated steady and progressive enhancement in their body weight over the course of experiment. Body weight of Group II rats decreased significantly from 4th to 5th week in comparison to normal control rats. The animals of Group VI in the present study showed reduction in the body weight from 4th to 5th week but in a slower manner as compared to Group II. Group II showed a significant decrease in absolute weight of heart in comparison to Group I rats, where as in Group IV, V, III and VI, heart weight was slightly higher from Group II.

Hematology parameters

The mean values of hematological parameters with

Table 3. The mean (±SE) values of LDH AND CK-MB in various experimental groups on final day (35th day) of the study.

Groups	LDH (U/L)	CK-MB (U/L)
Group I (NC, n=6)	278.58±28.60^{a}	631.36±53.13^{a}
Group II (DC, n=8)	881.25±51.32^{c}	915.80±41.05^{b}
Group III (RC, n=8)	562.76±46.57^{b}	706.32±34.82^{a}
Group IV (SME 250, n=8)	511.24±38.96^{b}	713.72±17.59^{a}
Group V (SME 500, n=8)	527.54±23.09^{b}	721.24±22.34^{a}
Group VI (SME 1000, n=8)	504.66±25.85^{b}	708.12±27.16^{a}

One way ANOVA with Duncan's post hoc test (SPSS); Mean values with different superscript differ significantly at $p < 0.05$

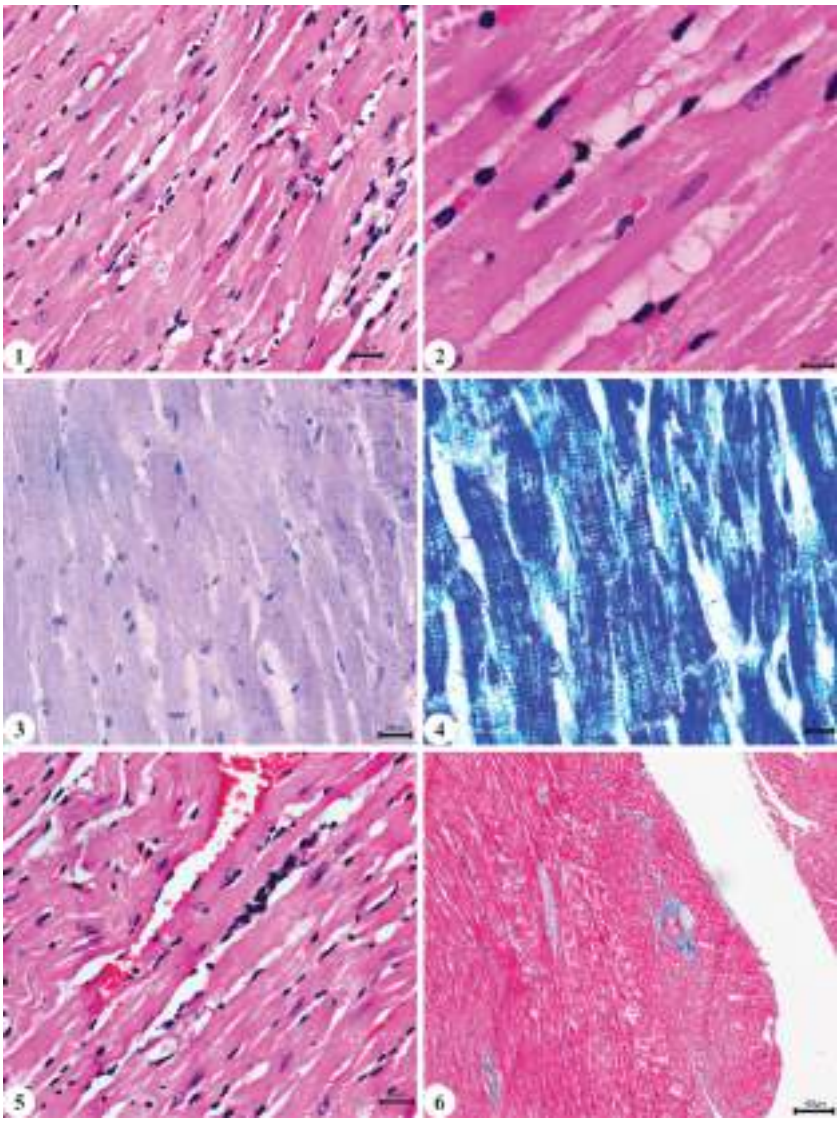

Fig. 1. Heart from disease control (Group II) rat showed increased sarcoplasmic eosinophilia with loss of cross striations along with macro-vacuolisation (H&E X400); **Fig. 2.** Higher magnification of heart from disease control (Group II) rat showing macro vacuoles separating the myocytes fiber bundle. Also absence of cross striations and nucleus in few fibers (H&E X1000); **Fig. 3.** Heart from disease control (Group II) rat showing loss of cross striations as compared to Group I rat (PTAH X400); **Fig. 4.** Heart from normal control (Group I) rat showing normal cross striations (PTAH X1000); **Fig. 5.** Heart from disease control (Group II) rat showing moderate congestion and infiltration of inflammatory cells (H&E X400); **Fig. 6.** Heart from disease control (Group II) rat showing moderate degree of interstitial and peri-vascular fibrosis (MT X100).

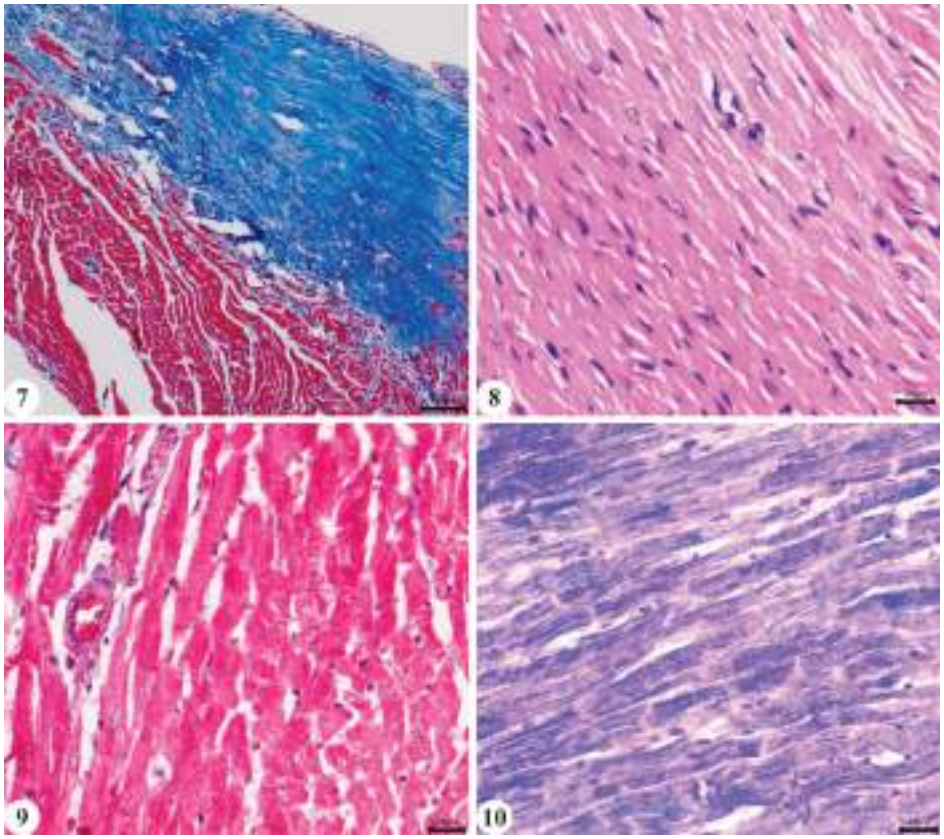

Fig. 7. Heart from disease control (Group II) rat showing thickened pericardial layer with blue staining collagen fibers (MT X100); **Fig. 8.** Heart from Group VI (SME 1000) rat showing reduced sarcoplasmic eosinophilia with normal feature of nucleus and reduced granularity as compared to Group II rats (H&E X400); **Fig. 9.** Heart from Group VI (SME 1000) rat showing reduced peri-vascular fibrosis in comparison to Group II rats (MT X400); **Fig. 10.** Heart from Group VI (SME 1000) rat showing improved appearance of cross striations in comparison to Group II rats (PTAH X400).

standard error of mean on 35th day of the experiment is presented in Table 2. The mean values of all the hematological parameters such as Total erythrocyte count (TEC), Haemoglobin (Hb), Packed Cell Volume (PCV), Total leucocyte count (TLC) and Platelets of Group II rats were significantly decreased when compared to Group I rats. The mean values of TEC in Group III, IV and VI; the mean values of Hb and PCV in Group IV to VI rats were increased significantly as compared to Group II disease control rats. The mean TEC values of Group V rats, TLC and Platelets values of Group III to VI rats though not significantly different was slightly increased as compared to Group II rat.

Serum Biochemistry

The mean values with standard error of mean on 35th day of the experiment is presented in Table 3.

Lactate dehydrogenase (LDH)

There was a significant (p<0.05) increase in serum LDH levels of Group II rats by 216.33% than Group I rats. Among the treatment groups, there was no significant difference in mean serum LDH levels. The mean values of serum LDH levels of Group III, IV, V and VI rats were significantly decreased (p<0.05) than Group II rats.

Creatine Kinase - Myocardial Band (CK-MB)

There was a significant (p<0.05) increase in serum CK-MB levels of Group II rats by 45.05% than Group I rats. The mean values of serum CK-MB levels of Group III, IV, V and VI rats were significantly decreased (p<0.05) in comparison to Group II rats and were comparable to that of Group I rat.

Gross pathology

The rats from the disease control group (Group II) showed mild degree of ascites and pleural effusion; blood mixed contents were observed in the stomach and intestine of three out of eight rats. The heart was pale and rounded and kidney appeared pale with cortico-medullary haemorrhages in comparison to Group I rat. The heart of Group III to Group VI rats did not reveal any visible gross abnormalities.

Histopathology

The heart of the disease control group (Group II) showed histopathological changes in the myocytes histology where in most of the cardiac myocytes exhibited moderate to severe disorganization and discontinuity with increased sarcoplasmic eosinophilia, wavy appearance of myofibres, loss of cross striations

Table 4. The mean (±SE) HP score of heart of rats in different groups on final day (35th day) of the study.

Groups	Swollen myocardial fibers	Granular appearance of myofiber	Pyknotic nucleoli	Macro-vacuoles formation	Haemorrhage between myofibers	Wavy myofibers
Group I	0.13±0.08^{a}	0	0	0	0.13±0.08^{a}	0.06±0.06^{a}
Group II (DC, n = 8)	3.05±0.18^{d}	3.30±0.31^{d}	3.35±0.18^{e}	3.05±0.18^{d}	3.05±0.32^{d}	2.55±0.18^{c}
Group III (RC, n = 8)	2.70±0.31^{bc}	2.90±0.31^{bc}	2.95±0.18^{d}	2.75±0.29^{bc}	2.55±0.18^{c}	1.95±0.29^{b}
Group IV (SME 250, n = 8)	2.95±0.18^{cd}	2.95±0.18^{c}	2.85±0.22^{cd}	2.95±0.18^{cd}	2.45±0.29^{c}	1.95±0.22^{b}
Group V (SME 500, n = 8)	2.60±0.42^{b}	2.85±0.22^{bc}	2.65±0.18^{cb}	2.70±0.31^{bc}	2.35±0.22^{bc}	1.95±0.29^{b}
Group VI (SME 1000, n = 8)	2.65±0.18^{bc}	2.65±0.18^{b}	2.55±0.18^{b}	2.50±0.25^{b}	2.15±0.18^{b}	1.85±0.18^{b}

One way ANOVA with Duncan's post hoc test (SPSS); Mean values with different superscript differ significantly at $p < 0.05$

with granular appearance and pyknotic nuclei. Most of the myocytes were swollen, highly eosinophilic with condensed nuclei or with absence of nucleus. In multiple areas, the myocytes bundles were widely separated with macro-vacuoles. A mild to moderate degree of interstitial mononuclear cellular infiltration, oedema, haemorrhage and congestion were noted. A mild to moderate degree of fibrosis in between myocardial fibers and periarterial fibrosis was noticed in a few areas (Fig. 1 to 7).

In the present study, the Group III revealed microscopical changes similar to that of disease control rats but with mild improvement. The heart of the treatment control group (Group IV to VI) showed mild to moderate improvement in histopathological changes in the myocytes where in very few cardiac myocytes exhibited disorganizationas compared to Group II rat with mild degree of eosinophilia, loss of cross striations and a mild degree of granular appearance of myocytes. Very few of the myocytes were slightly swollen with pyknotic nuclei. The macro vacuoles formation was reduced as compared to Group II rats. A mild degree of interstitial mononuclear cellular infiltration with mild degree of haemorrhage and congestion were noted (Fig. 8 to 10). Among the treatment group, Group VI (SME 1000) showed comparatively less histopathological alterations in cardiac muscle when compared to Group IV (SME 250) and Group V (SME 500).

Histopathological score of heart

The mean HP severity score of all sectioned heart samples was assessed for lesions like swollen myocardial fibers, granular appearance of myofiber, pyknotic nucleoli, macro-vacuoles formation, haemorrhage between myofibers and wavy myofibers. The mean HP severity score values of heart with standard error of mean have been presented in Table 4. The mean HP score of Group II disease control rats for each of the recorded lesion was significantly (p<0.05) higher than mean HP score of Group I normal control rats. The mean HP score of Group III to VI were significantly (p<0.05) lower than mean HP score of Group II disease control rats.

DISCUSSION

Doxorubicin not only has a direct impact on the heart but also an indirect influence resulting from the augmentation of hemodynamic flow changes or thrombotic events[10]. DOX induced enhanced generation of ROS may directly damage mitochondria thus altering the synthesis of proteins associated with the mitochondrial electron transport chain and *Spirulina* has antioxidant properties and have capacity to scavenge hydroxyl radicals to inhibit lipid peroxidation[6].

Doxorubicin caused severe systemic illness in the rats including anorexia, reduced body weight and water intake, diarrhea, progressive physical exhaustion after the second dose of doxorubicin, persisting until the end of the study. Our findings of doxorubicin induced reduction in heart weight are in accordance with reports of previous workers[11-13]. DOX induced cardiotoxicity related decrease in hematological parameters like TEC, Hb, PCV, TLC and Platelets were similar to those previously reported[14-15]. This was linked to various factors such as disrupted RBC production leading to anemia and leukopenia[16] and bone marrow suppression caused by doxorubicin[17]. It has been documented that myelo suppression represents the primary dose-limiting toxicity of Doxorubicin[18]. Doxorubicin notably induces marrow depression resulting in peripheral blood leukopenia (granulocytopenia), thrombocytopenia and potential anaemia[19]. Additionally, bone marrow depletion, depression, or hypoplasia have been frequently observed in rats[20] which likely may be due to the rapid division of bone marrow cells owing to their high growth fraction[21].

A significant rise in the mean values of serum LDH and CK-MB was observed. This finding aligns with previous findings[15,22-23]. It has been previously highlighted the significance of these biochemical markers in detecting cardiac injury resulting from DOX-induced cardiotoxicity[23-24]. The cardiac damage likely resulted from increased permeability or rupture of cell membranes, leading to the leakage of cytosolic enzymes into the bloodstream and subsequent elevation of their serum concentrations. The release of these markers into the bloodstream is consistently linked to DOX-induced damage to the myocardial cell membrane[25]. These results are supported by earlier studies that demonstrated DOX administration caused cardiac injury and loss of functional integrity, as seen by markedly elevated serum levels of CK-MB, ALT, AST, and LDH[26].

The examination of heart tissue from rats in the disease control group (Group II) revealed extensive damage characterized by moderate toxicity lesions affecting cardiac myocytes. The myocardial fibers displayed diverse levels of damage, from loss of striations to complete necrosis and fragmentation, appearing granular, with some exhibiting focal necrosis and eosinophilia in the cytoplasm[23]. Additionally, myocyte wavy degeneration, interstitial haemorrhages, and interfibrillar congestion were observed, along with disruption and separation of cardiac muscle fibers and infiltration of mononuclear inflammatory cells, predominantly lymphocytes. These findings were documented in earlier studies and were opined to be due to toxic metabolites of Doxorubicin[22,25,27].

In the present study, a mild to moderate degree of fibrosis in between myocardial fibers and peri-arterial fibrosis was noticed. The DOX treated rat's heart stained with Masson'strichrome stain revealed fibrotic scarring in cardiomyocytes and in the surrounding interstitial tissues. This may be attributed to an increase in pro-fibrotic factor *TGF-β1*, the extracellular matrix content collagen I and the cardiac fibrosis-associated protein α-smooth muscle actin in DOX-treated rats[28].

It's also suggested that DOX induces cardiotoxicity and myocyte damage by triggering lipid peroxidation, which is influenced by increased levels of mitochondrial iron and cellular reactive oxygen species[29]. The sarcoplasmic vacuoles observed could be attributed to enlargement of sarcoplasmic reticula and terminal cisternae leading to altered intracellular water and electrolyte distribution[30]. Edema, both perivascular and interstitial, accompanied by vascular changes like dilated blood vessels and retracted endothelial cells, observed were consistent with prior research[29-30]. It was theorized that edema results from disruptions in cardiac electrolytes, as DOX increases sodium and calcium content in the cardiac ventricle during induced cardiotoxicity in rabbits[30-31].

Improvement in treatment groups (Group IV, V, VI) may be attributed to the antioxidant and anti-inflammatory properties of *Spirulina* microalgal extracts. This restoration could be attributed to the presence of antioxidants like β-carotene and C-phycocyanin in *Spirulina*. The findings suggest that *Spirulina* may shield cardiac myocytes from oxidative stress induced by DOX. Other previous research had also demonstrated the efficacy of *Spirulina* extract in countering free radical-induced lipid peroxidation caused by lead and in offering protective effects on major organs, including the heart[32]. It is widely acknowledged that C-phycocyanin, a key biliprotein in *Spirulina,* possesses notable antioxidant and radical scavenging properties[33].

The current research showed that among the treatment groups, notably, cardiac lesions in rats from Group VI were less severe compared to those in other treatment groups and the disease control group. The cardio protective effect of *Spirulina* in the present study suggests that *Spirulina* microalgal extract (SME) can potentially be used as a therapeutic agent or as a supplement in treatment of heart ailment.However, further clinical and mechanistic investigations are needed to further validate its efficacy.

REFERENCES

1. Satliel E and McGuire W. 1983. Doxorubicin adriamycin cardiomyopathy. *Wist J Med* **139:** 332-336.
2. Carvalho C, Santos RX, Cardoso S, Correia S, Oliveira PJ, Santos MS and Moreira PI. 2009. Doxorubicin: the good, the bad and the ugly effect. *Curr Med Chem* **16:** 3267-3285.
3. Young RC, Ozols RF and Myers CE. 1981. The anthracycline antineoplastic drugs. *N Engl J Med* **305:** 139-153.
4. Oeffinger KC, Mertens AC, Sklar CA, Kawashima T, Hudson MM, Meadows AT, Friedman DL, Marina N, Hobbie W, Kadan-Lottick NS and Schwartz CL. 2006. Chronic health conditions in adult survivors of childhood cancer. *N Engl J Med* **355:** 1572-1582.
5. Chopra K and Bishnoi M. 2008. Antioxidant profile of *Spirulina*: a blue-green microalga. In: *Spirulina* in Human Nutrition and Health, Edt. Gershwin ME, Belay A, Boca Raton, CRC Press, pp. 101-118.
6. Peter C. 2008. Antioxidant potential of *Spirulina platensis* preparations. *Phytother Res* **22:** 627-633.
7. Suvarna SK, Layton C, Bancroft JD. 2019. In: Bancroft's theory and practice of histological techniques, Edn. 8th, Elsevier Publications, pp. 536.
8. Cirillo R, Sacco G, Venturella S, Brightwell J, Giachetti A and Manzini S. 2000. Comparison of doxorubicin and MEN 10755-induced long-term progressive cardiotoxicity in the rat. *J Cardiovasc Pharmacol* **35:** 100-108.
9. Snedecor GW and Cochran WG. 1994. Statistical Methods. Edn. 7th, Oxford and JBH Publications, New York, USA.
10. Albini A, Pennesi G, Donatelli F, Cammarota S and Noonan DM. 2010. Cardiotoxicity of anticancer drugs: the need for cardio-oncology and cardio-oncological prevention. *J Natl Cancer Inst* **102:** 14-25.
11. Birari L, Wagh S, Patil KR, Mahajan UB, Unger B, Belemkar S, Goyal SN, Ojha S and Patil CR. 2020. Aloin alleviates doxoru-

bicin-induced cardiotoxicity in rats by abrogating oxidative stress and pro-inflammatory cytokines. *Cancer Chem Pharmacol* **86:** 419-426.
12. Owumi SE, Lewu DO, Arunsi UO and Oyelere AK. 2021. Luteolin attenuates doxorubicin-induced derangements of liver and kidney by reducing oxidative and inflammatory stress to suppress apoptosis. *Hum Exp Toxicol* **40:** 1656-1672.
13. Espírito Santo SG, Monte MG, Polegato BF, Barbisan LF and Romualdo GR. 2023. Protective effects of Omega-3 supplementation against Doxorubicin-induced deleterious effects on the liver and kidneys of rats. *Molecul* **28:** 3004-3009.
14. Al-Harbi MM, Al-Gharably NM, Al-Shabanah OA, Al-Bekairi AM, Osman AMM and Tawfik HN. 1992. Prevention of doxorubicin-induced myocardial and haematological toxicities in rats by the iron chelator desferrioxamine. *Cancer Chem Pharmacol* **31:** 200-204.
15. Buyukokuroglu M, Taysi F and Özabacıgil F. 2007. Dantrolene: in doxorubicin toxicity. *Asian J Chem* **19:** 4035-4045.
16. Cortes-Funes H and Coronado C. 2007. Role of anthracyclines in the era of targeted therapy. *Cardiovasc Toxicol* **7:** 56-60.
17. Sindhur A, Ashok Kumar RN, Deepak C and Kumar Tiwari NP. 2019. Effect of doxorubicin on haematological and blood biochemical profile of healthy dogs. *Haryana Vet* **58:** 11-14.
18. Benjamin RS, Wiernik PH and Bachur NR. 1974. Adriamycin chemotherapy-efficacy, safety and pharmacologic basis of an intermittent single high-dosage schedule. *Cancer J* **33:** 19-27.
19. Bonadonna G, Monfardini S, De Lena M and Fossati-Bellani F. 1969. Clinical evaluation of adriamycin, a new antitumour antibiotic. *Br Med J* **3:** 503-506.
20. Duncan R, Coatsworth JK and Burtles S. 1998. Preclinical toxicology of a novel polymeric antitumour agent: HPMA copolymerd oxorubicin (PK1). *Hum Exp Toxicol* **17:** 93-104.
21. Mac Donald V. 2009. Chemotherapy: managing side effects and safe handling. *Can Vet J* **50:** 665-675.
22. Nagi MN and Mansour MA. 2000. Protective effect of thymoquinone against doxorubicin-induced cardiotoxicity in rats: A possible mechanism of protection. *Pharmacol Res* **41:** 283-289.
23. Alkreathy H, Damanhouri ZA, Ahmed N, Slevin M, Ali SS and Osman AMM. 2010. Aged garlic extract protects against doxorubicin-induced cardiotoxicity in rats. *Food Chem Toxicol* **48:** 951-956.
24. Kobayashi M, Usui F, Karasawa T, Kawashima A, Kimura H, Mizushina Y, Shirasuna K, Mizukami H, Kasahara T, Hasebe N and Takahashi M. 2016. NLRP3 deficiency reduces macrophage interleukin-10 production and enhances the susceptibility to doxorubicin-induced cardiotoxicity. *Sci Rep* **6:** 26489.
25. Khan G, Haque SE, Anwer T, Ahsan MN, Safhi MM and Alam MF. 2014. Cardioprotective effect of green tea extract on doxorubicin-induced cardiotoxicity in rats. *Acta Pol Pharm* **71:** 861-868.
26. Bilgic S, Ozgocmen M, Ozer MK and Asci H. 2020. Misoprostol ameliorates doxorubicin induced cardiac damage by decreasing oxidative stress and apoptosis in rats. *Biotech Histochem* **95:** 514-521.
27. Khan M, Shobha JC, Mohan IK, Naidu MUR, Sundaram C, Singh S, Kuppusamy P and Kutala VK. 2005. Protective effect of *Spirulina* against doxorubicin-induced cardiotoxicity. *Phytother Res* **19:** 1030-1037.
28. Lin H, Zhang J, Ni T, Lin N, Meng L, Gao F, Luo H, Liu X, Chi J and Guo H. 2019. Yellow wine polyphenolic compounds prevents doxorubicin-induced cardiotoxicity through activation of the Nrf2 signalling pathway. *J Cell Mol Med* **23:** 6034-6047.
29. Minotti G, Ronchi R, Salvatorelli E, Menna P and Cairo G. 2001. Doxorubicin irreversibly inactivates iron regulatory proteins 1 and 2 in cardiomyocytes: evidence for distinct metabolic pathways and implications for iron-mediated cardiotoxicity of antitumor therapy. *Cancer Res* **61:** 8422-8428.
30. Herman EH, Rahman A, Ferrans VJ, Vick JA and Schein PS. 1983. Prevention of chronic doxorubicin cardiotoxicity in beagles by liposomal encapsulation. *Cancer Res* **43:** 5427-5432.
31. Olson HM, Young DM, Prieur DJ, LeRoy AF and Reagan RL. 1974. Electrolyte and morphologic alterations of myocardium in adriamycin-treated rabbits. *Am J Pathol* **77:** 439-454.
32. Upasani CD, Khera A and Balararnan R. 2001. Effect of lead with vitamin E, C, or *Spirulina* on malondialdehyde, conjugated dienes and hydroperoxides in rats. *Indian J Exp Biol* **39:** 70-74.
33. Bhat VB and Madyastha KM. 2000. C-phycocyanin: a potent peroxyl radical scavenger in vivo and in vitro. *Biochem Biophys Res Comm* **275:** 20-25.

Indian J. Vet. Pathol., 49(1) : 38-48, 2025: DOI: https://doi.org/10.5958/y870gp74

RESEARCH ARTICLE

Studies on the pathomorphology of epidemics of Infectious Bursal Disease (IBD) in chicken

B.C. Girish*, K. Sujatha[1], H.D. Narayanaswamy[2], K. Nagappa[3], D. Ramesh[4] and M. Bindu[5]
Department of Veterinary Pathology, Veterinary College, Hassan, KVAFSU, Karnataka, [1]Centre for Continuing Veterinary Education and Communication, College of Veterinary Science, Tirupati, [2]Department of Veterinary Pathology, Veterinary College, Hebbal, [3]Department of Veterinary Public Health and Epidemiology, [4]Department of Veterinary Physiology and Biochemistry, [5]Affigenix Biosolutions Ltd, Hebbagodi, Bengaluru, India

Address for Correspondence
B.C. Girish, Associate Professor, Department of Veterinary Pathology, Veterinary College, Hassan, KVAFSU, Karnataka, India, E-mail: girishhouse@gmail.com

Received: 12.11.2024; Accepted: 26.12.2024

ABSTRACT

Viral pathogens induce distress in poultry and economic loss to farmers worldwide. Infectious Bursal Disease (IBD), a Birna viral immunosuppressive infection of poultry continues to affect birds including regions of Karnataka and neighbouring states; hence study on IBD was undertaken with the objective to estimate its prevalence and understand its pathology. Data from 15 IBD outbreaks from commercial broilers (11) and layers (2) as well as native birds (2) showed average morbidity of 29.3% (7.1 to 100%) and mortality of 18.4% (7.5 to 100%). Maximum number of 9 outbreaks was recorded in the age groups 1-4 weeks accounting for 60 percent of the total outbreaks and the same age group also showed highest morbidity (Average 33.1%, Range: 9-100%) and mortality (Average 22.4%, Range: 7.5-100%). Affected birds showed vascular and atrophic changes in lymphoid organs with secondary changes in liver, kidneys and skeletal muscles. Ultrastructural studies of thymus revealed severe necrosis and increased electron density in lymphocytes and hyperplasia of reticular cells. Bursa also revealed areas of lymphocytic apoptosis and engulfed phagocytic bodies in these macrophages. The cytoplasmic granules of bursal secretory dendritic cell (BSDC) had fused together, forming big, irregularly shaped, electron dense bodies. Amplification of VP2 gene using reverse transcriptase PCR showed 319 bp products having phylogenetic similarity to Indian isolates. Eight IBD outbreaks showed concurrent infection with other pathogens. The bioinformatic analysis of VP-2 protein suggested the presence of the glycine like amino acids predominant in the alpha helical secondary structure.

Keywords: Bursa of Fabricius, epidemics, PCR, RNA Virus

INTRODUCTION

A healthy immune system is vital for effective poultry production. Any factor that causes dysfunction of humoral and cellular immune system will certainly result in poor vaccination response, production and economic losses and flaring up of opportunistic pathogens. Viral pathogens can cause huge economic losses in poultry farms worldwide including immunosuppression[1-4]. The important viral agents that cause immunosuppression include Marek's disease virus (MDV), Chicken infectious anemia virus (CIAV), Infectious Bursal Disease virus (IBDV), Reovirus, Avian Leukosis virus, reticuloendotheliosis, Newcastle disease virus and Avian Influenza virus[1,5-6].

Infectious Bursal Disease (IBD) is a highly contagious and acute immunosuppressive disease of young chickens and is caused by Birna virus. The disease is characterized by severe immunosuppression leading to secondary bacterial infections and dermatitis, adenoviral infections and failure of vaccinations[7]. The immunosuppression seen in IBD is complex involving depletion of B cells by apoptosis and also inhibiting innate immune response directly[8]. Infectious Bursal Disease (IBD) targets the chicken's immune system in a very comprehensive and complex manner by destroying B lymphocytes, attracting T cells and activating macrophages[9]. It has been noted that IBDV and RNA virus has a high mutation rate and can give rise to viruses with altered antigenicity and increased virulence[10-11] and the re-emergence of IBD with antigenic variants and highly virulent strains had been the reason for significant losses and high mortality. IBD affected birds had elevated mortality rates, bursal atrophy, poorer feed conversion ratio (FCR) and reduced meat production[12].

How to cite this article : Girish, B.C., Sujatha, K., Narayanaswamy, H.D., Nagappa, K., Ramesh, D. and Bindu, M. 2025. Studies on the pathomorphology of epidemics of Infectious Bursal Disease (IBD) in chicken. Indian J. Vet. Pathol., 49(1) : 38-48.

Pathogenesis of the disease is complex involving both humoral and cellular immune responses being compromised by IBD virus; Inhibition of the humoral immunity could be attributed to the destruction of immunoglobulin-producing cells by the virus[13]. VP1 is the viral RNA dependent RNA polymerase while VP2 is the major host-protective immunogen carrying

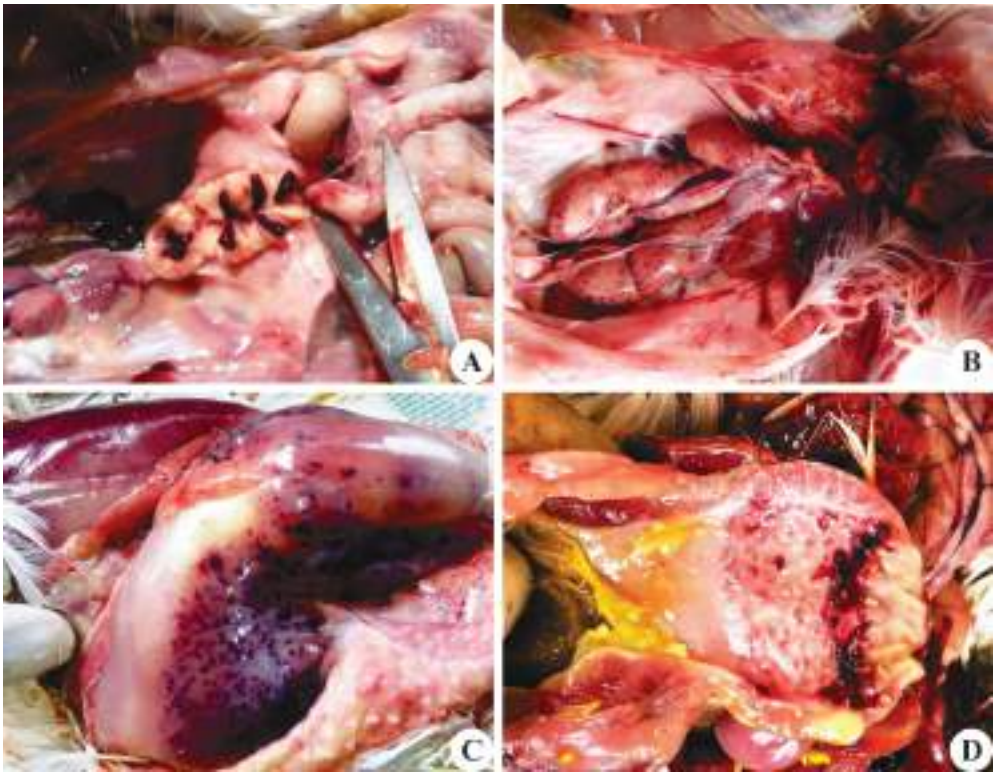

Fig. 1. Gross pathological changes in organs of chicken affected with IBDV. **A.** Bursa: Multiple extensive hemorrhages and hemorrhagic exudate. **B.** Kidney: Hemorrhages and mottled appearance in a broiler chick. **C.** Dorsal view of thigh muscles showing severe multifocal petechial to ecchymotic hemorrhages. **D.** Proventriculus: Hemorrhages prominently visible at the junction with gizzard.

all neutralizing epitopes some of which are responsible for antigenic variation[14]. It has been observed that classical and vvIBD virus induces differential host immune responses by up regulating the expression of Th1-like and pro-inflammatory cytokines such as IL-12, IFN-γ, IL-1β, IL-6, iNOS and IL-18 in bursa[11]. It is recorded that Bursa of Fabricius is the principal diagnostic organ in birds that died during the acute phase of vvIBD[7]. Various immunological and molecular diagnostic methods have been described for the confirmation of the disease[11,15-19]. Clinical presentation of the diseases varies according to the strain involved. The variant IBDV strains normally cause subclinical infection in chickens. The classical IBD viral strains can cause clinical signs of disease and moderate mortality rates whereas vvIBDV strains are known to cause high mortality rates[11-12].

The current study was carried out in Karnataka and neighbouring southern states of India with the objectives of studying prevalence and pathology of Infectious Bursal Disease (IBD) with special emphasis on lymphoid organs of chickens, characterizing the ultra-structural changes in such organs and characterizing the disease by molecular techniques.

MATERIALS AND METHODS

Sample collection

The study was carried out in the Department of Veterinary Pathology, College of Veterinary Science, Sri Venkateshwara Veterinary University, Tirupati and Department of Veterinary Pathology, Veterinary College, Hassan of Karnataka Veterinary Animal and Fisheries Sciences University between January 2017 and August 2022. Poultry farms in southern districts of Karnataka and neighbouring states including Andhra Pradesh and Tamil Nadu presenting outbreaks of IBD formed the basis of sample collection in the study.

Flock history and clinical signs

Detailed information on the farm outbreak with respect to type of birds (broiler, layer, breeder or country birds), flock strength, breed/strain details, age, source of feed and water, production performance, type of litter, vaccination details, morbidity, mortality, clinical signs, previous history of outbreak and any other necessary details were collected.

Necropsy examination and collection of biological samples

Detailed necropsy examination was undertaken. Internal examination of body cavities, visceral organs and lymphoid organs was carried out and all visible gross lesions were systematically recorded. Tissue impression smears were collected. Tissue samples from all vital organs and lymphoid organs were collected

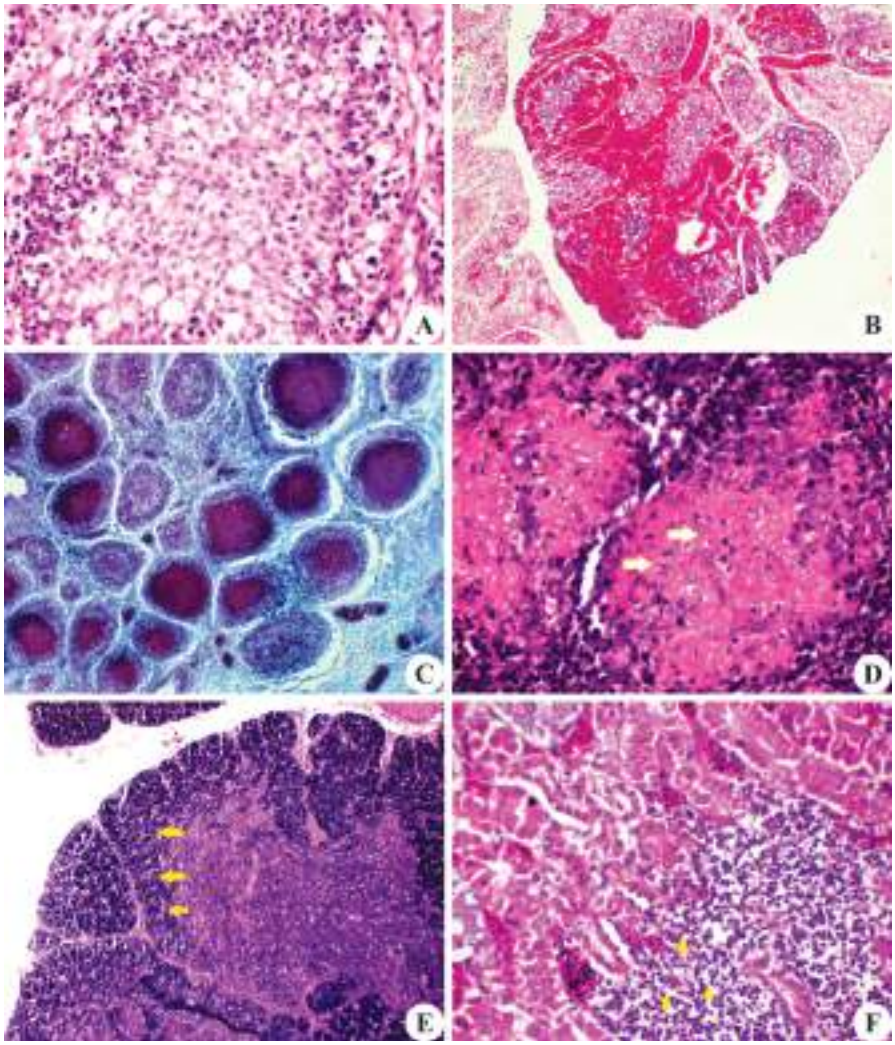

Fig. 2. Histopathological changes in organs of chicken affected with IBDV. **A.** Bursa of Fabricius: Severe depletion of lymphocytes indicated by hypocellularity and necrotic changes such as pyknosis and karyorrhexis and karyolysis of lymphocytes (H&E x400). **B.** Bursa of Fabricius: Severe hemorrhages and congestion inside and surrounding the atrophied follicles (H&E x100). **C.** Bursa of Fabricius: Extensive fibroplasia evident by proliferation of blue colored collagen fibres (Masson's x100). **D.** Spleen: Necrotic changes in the germinal follicles and the periarteriolar lymphoid sheath with proliferation of reticulo-epithelial cells (H&E x100). **E.** Thymus: Atrophy and thinning of the cortex with lymphocytolytic changes (H&E x100). **F.** Kidney: Heterophilic infiltration and nephritic area in the interstitium (H&E x400).

and preserved in 10% neutral buffered formalin for histopathological examination. The representative tissue samples were also collected for PCR in a sterilized labelled tissue sample bottles and were stored at -20^{O}C immediately.

Microbiological and histopathological examination

The samples collected aseptically during necropsy examination were used to investigate the concurrent bacterial infection as per the standard protocols. The impression smears of various vital organs during necropsy examination were air dried and fixed with absolute methanol for 5 minutes and stained with diluted Giemsa stain (1:10 V/V) for 20 minutes.

Tissue samples for histopathological examination were processed by routine paraffin embedding technique and sectioned at five micron thickness. The sections were stained with routine Hematoxylin and Eosin (H&E) method. Special stains such as Masson's Trichrome or Van Gieson (Connective tissue) and Perl's Prussian blue stain (Hemosiderin pigments) were used on need basis[20]. Tissue morphometric evaluation for measuring the diameter of the bursal follicle was done using a validated software TC Capture version 3.9 (build 5001). The average values of 5-6 bursal follicles in age matched birds was carried out for minimum of 6 birds and average was calculated for comparison.

Electron microscopy

Tissue samples from lymphoid organs were fixed in 2.5% glutaraldehyde in 0.1M Phosphate buffer (pH 7.2) for minimum of 24 hours at 4^{O}C. Further, post fixed

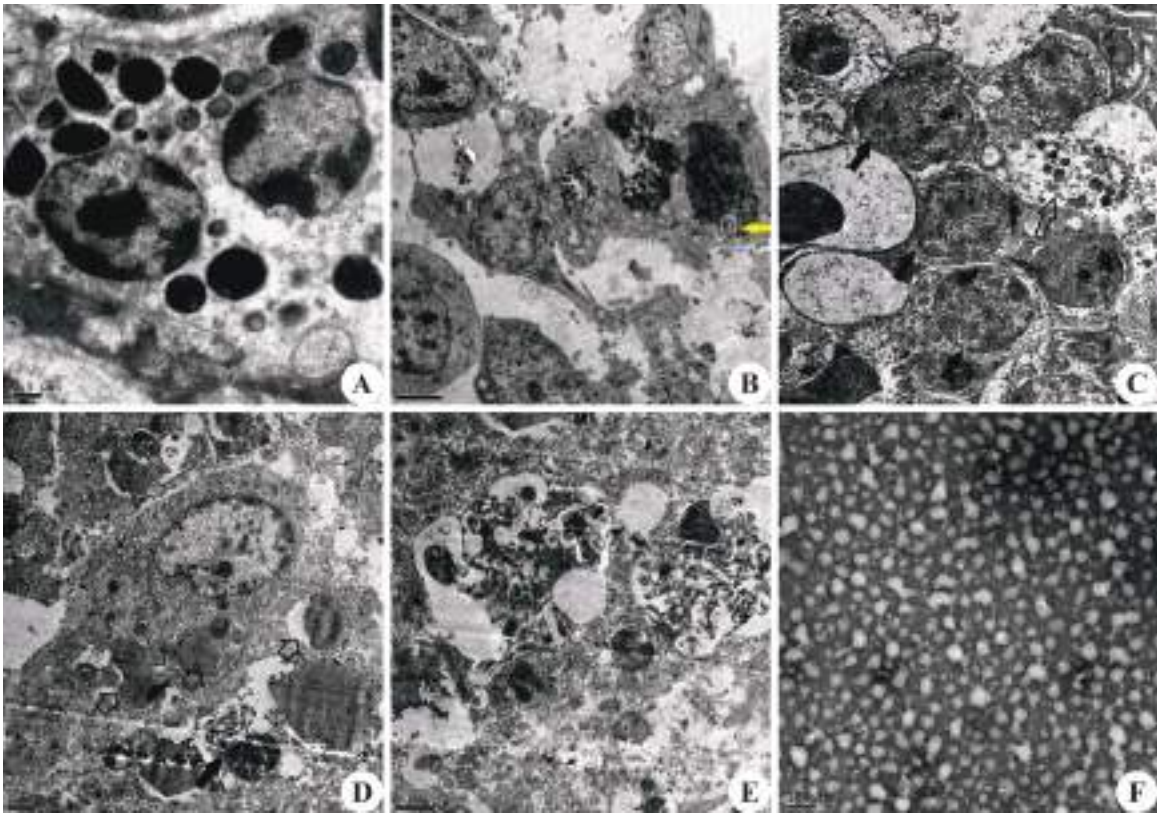

Fig. 3. Ultrastructural changes in organs of chicken affected with IBDV. **A.** Thymus: Nuclei and cytoplasm of lymphocytes showed increased electron density (Uranyl Acetate). **B.** Thymus: Lymphocytes with myelin figures (Uranyl Acetate). **C.** Thymus: Necrotic changes of the lymphocytes shown by light arrow and hyperplasia of the reticular cells indicated by dark arrow (Uranyl Acetate). **D.** Bursa of Fabricius: Note the necrotic areas with nuclear changes such as karyorhexis (Dark arrow) and karyolysed fragments (Light arrow) of lymphocytes (Uranyl Acetate). **E.** Bursa of Fabricius: Bursal secretory dendritic cell (BSDC) forming big and irregularly shaped electron dense bodies (Uranyl Acetate). **F.** Single-shelled non-enveloped IBD virions with icosahedral symmetry and a diameter of around 50 nm (Uranyl Acetate).

in aqueous osmium tetroxide for 3 hours and washed with deionized distilled water, dehydrated in series of graded alcohols, infiltrated and embedded in araldite resin. It was incubated at 80^{O}C for 72 hours for complete polymerization. Ultra-thin (60 nm) sections were made with a glass knife on ultra-microtome (Leica Ultra cut UCT-GA-D/E-1/00), mounted on copper grids and stained with saturated aqueous Uranyl acetate (UA) and counter stained with Reynolds lead citrate (LC). Viral suspension was prepared from the tissues of the affected birds. Copper grids (Carbon coated) were glow discharged for 30 seconds using polaron carbon evaporator. 5µl of sample was loaded on the glow discharged grids and allowed to dry for 10 minutes. 5µl of 2% Uranyl acetate was loaded on the grids for 30 seconds and excess was wiped off by using Whatman filter paper and allowed to dry. Samples were loaded on the TEM single tilt Holder, loaded into TEM. Further, they were finally imaged and analyzed at 120 kv[21].

Molecular characterization

RNA was extracted from the samples using Trisol (GeNei™ TRIsoln) method and cDNA was synthesized using TAKARA Kit. The temperature and time combination was 37^{O}C, 85^{O}C and 4^{O}C for 15 minute (priming), 5 seconds (Reverse transcription), for infinity (optional) respectively. cDNA synthesized thus was stored at -20^{O}C for long term storage.

Primers were designed to amplify VP2 gene which codes for VP2 protein, the major host-protective protein of IBD Virus. Primers were synthesized and procured commercially from M/s Bio Serve Biotechnologies (India) Pvt. Ltd., Hyderabad. They were reconstituted in 1x TE buffer (TE) to obtain the required concentration of 100 picomol/µL. The sequences of the primers used was 5′-ATGCTCCAGATGGGGTACTTC- 3′ (IF) and 5′-TTGGACCCGGTGTTCACG- 3′ (IVIR) to target the product size of 319 bp.

PCR cycling conditions for cDNA amplification included Initial denaturation with 95^{O}C for 3 minutes, 35 cycles of denaturation (94^{O}C for 1 minute), annealing (48^{O}C for 1 minute) and extension (72^{O}C for 2 minutes) followed by final extension (72^{O}C for 5 minutes). DNA confirmation was carried out by 1.5% Agarose gel

electrophoresis following visualization and capturing of the images by Image Lab Software (Version 5.1, Bio-Rad Laboratories Inc). Sequencing (Eurofins Genomics India Pvt. Ltd.) was done to identify the degree of homology using the final amplicons and phylogenetic tree was constructed.

Bioinformatic Analysis of IBD-VP2

The 3D structure of the VP2 with predicted protein sequence was drawn using SWISS PROT expasy platform. GMQE (Global Model Quality Estimate), a quality estimate which combines properties from the target-template alignment and the template structure was used to calculate the overall model quality measurement between 0 and 1. The QMEAN z-score in SWISS-MODEL was used to measure of how close the model is to structures of a similar size that were obtained experimentally. Structural assessment was made using Ramachandran plot.

RESULTS

Epidemiological findings

A total of 15 outbreaks were documented that included 11 outbreaks from broiler birds, 2 from non-descript birds and 2 from commercial layers. Total number of birds investigated was 298 (average of 19.87 birds per outbreak in 15 outbreaks). Out of these 15 outbreaks, maximum number of 9 outbreaks was recorded in the age groups 1-4 weeks accounting for 60 percent of the total outbreaks. In this, 7 cases (46.7%) were recorded between 3-4 weeks, making it the most susceptible age. This was followed by 5 outbreaks from age group 5-8 weeks (33.3%) and one case from age group 9-12 weeks (6.7%).

The average morbidity and mortality of 15 flocks were 29.3% (Range: 7.1 to 100%) and 18.4% (Range: 7.5 to 100%) respectively. Maximum morbidity (Average 31.4%) was seen in broilers followed by indigenous birds and layers. Highest mortality (Average 31.4%) was seen in broiler birds followed by country birds and layers. Highest morbidity was recorded in the age group 1-4 weeks (Average 33.1%, Range: 9-100%) and highest mortality was also found in the same group (Average 22.4%, Range: 7.5-100%).

Clinical signs

The affected birds initially showed trembling followed by yellowish white or greenish watery diarrhea. This was followed by dullness, depression, anorexia, ataxia, ruffled feathers, soiled vent, prostration, closed eyes, decreased water consumption and sudden death. Birds affected with IBD exhibited lateral recumbency and dyspnea before succumbing to death. Few birds also exhibited bloody discharge from cloaca. Mortality was noticed 2-3 days after appearance of first clinical sign and peaked at 4-5 days. In one flock that had concurrent infection with ND the birds exhibited severe emaciation, neurological signs and greenish diarrhea.

Gross pathology

In acute phase of disease bursa from infected birds was swollen and edematous. The enlarged bursa showed multiple hemorrhages (Fig. 1A) and necrotic foci in the follicles and presence of gelatinous inflammatory fluid surrounding the bursa. In the chronic phase the changes included greyish brown discoloration and atrophied bursa with presence of cheesy material. Spleen of few birds exhibited minimal decrease in the size due to atrophic changes with congestion and mottling. Thymus, cecal tonsils and bone marrow revealed hemorrhages, atrophy and congestion in few affected birds in acute phase of the disease. Kidneys showed nephrotic changes characterized by congestion, mottling, enlargement (Fig. 1B) and hemorrhages along with distension of ureters with whitish uric acid crystals in around 40% of the birds. Birds with kidney lesions correlated well with severe dehydrative changes. Few percentage of birds (10-15%) showed multifocal necrosis on the liver and they appeared enlarged and dark brownish. IBD affected birds also showed moderate to severe petechial and ecchymotic hemorrhages on pectoral and thigh muscles (Fig. 1C). In majority of the birds, ecchymotic hemorrhages in the mucosa of the proventriculus mainly at the junction with esophagus (Fig. 1D) and gizzard were observed. Occasionally, mucosal hemorrhages were also seen in the gizzard. Few affected birds also exhibited mucosal erosions and congestion in the small intestine.

Histopathology

Lymphoid organs: Bursa of Fabricius in acute phase of the disease showed severe depletion of lymphocytes

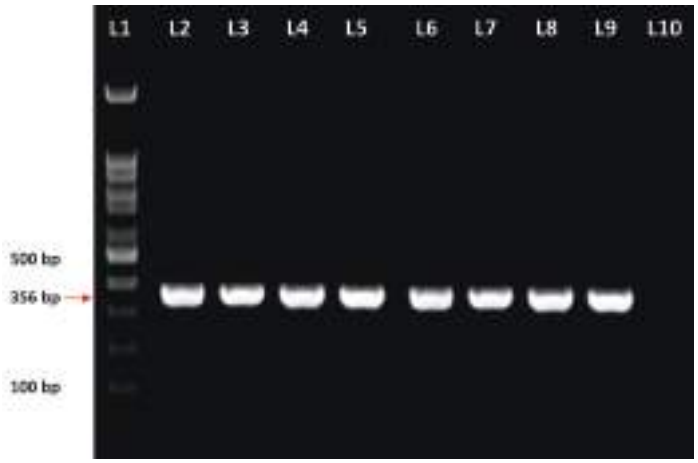

Fig. 4. Agarose gel electrophoresis image showing amplification of 319 bp PCR product in samples specific to VP2 gene of IBDV. L1: 100 bp DNA Ladder, L2: Sample ND1, L3: Sample ND2, L4: Sample ND3, L5: Sample ND4, L6: Sample ND5, L7: Sample ND6, L8: Sample ND7, L9: Sample ND8, L10: No template control.

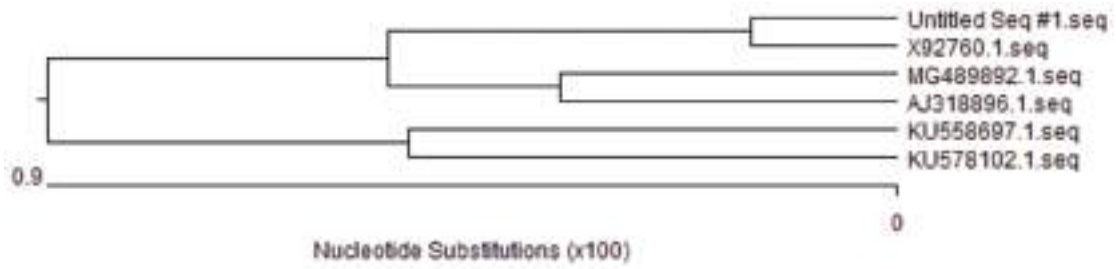

Fig. 5. Dendrogram of partial sequence of VP2 gene of IBDV showing phylogenetic relationship of field IBDV with other reported strains.

indicated by hypocellularity and multiple cystic spaces in both medulla and cortex. Many follicles in the affected birds showed necrotic tissue debris with nuclear changes involving pyknosis and karyorrhexis and karyolysis of lymphocytes (Fig. 2A). Moderate to severe hemorrhages and congestion in the follicles was also recorded more often (Fig. 2B). Birds in the post outbreak stage showed cystic cavities in the place of follicular medullary areas. There was an increase and decrease in the diameter of follicles in acute and chronic phase respectively. The mean diameter in the affected birds was 516µ in the acute phase of the disease and 214µm in the chronic phase compared to 450µ in the age matched disease free birds. Extensive fibroplasia was also evident with proliferation of collagen in the interfollicular areas (Fig. 2C). Occasionally bursal epithelial cells formed glandular appearance with mucin like material.

Spleen in acute phase of the infection showed moderate vascular changes accompanied by histiocytosis, heterophil infiltration and lymphocytolysis (Fig. 2D). In the chronic phase regenerating change was seen in the form of secondary lymphoid follicles by proliferating lymphoblasts. In the thymus, atrophy of the cortex was noticed with lymphocytolysis in small percentage of birds (Fig. 2E). This was coupled with hypertrophy of epithelial reticular cells and mild decrease in lymphocytic numbers in the medulla and increase in the number of tingible body macrophages leading to starry sky appearance of the cortex. Cecal tonsils revealed lymphoid cell necrosis leading to hypocellularity of lymphoid cells. Additionally, infiltration of heterophils and macrophages, multifocal hemorrhages, degenerative changes of reticular cells were recorded. Bone marrow revealed hypocellularity of hematopoietic cells, decrease in the number of granulocytes and agranulocytes and increased numbers of macrophages. Plasma cell population was decreased in the Harderian glands.

Non-lymphoid/Other vital organs: Cortex of the kidneys revealed moderate to severe congestion accompanied with vacuolar degeneration of the convoluted tubules. Few tubules showed eosinophilic hyaline like proteinaceous material along with infiltration of lymphocytes and mononuclear cells (Fig. 2F). Few areas of haemorrhages with heterophils infiltration and nephritic areas were also recorded in the interstitium. Livers of affected birds showed vacuolar degeneration, hyperplastic changes and perivascular infiltration of mononuclear cells and congestion of sinusoids and surrounding area of central vein and occasionally disruption of hepatic cords with lymphocytic infiltration.

Moderate to severe hemorrhages and disruption of plical architecture were noticed in the proventriculus. Similarly, mild to moderate haemorrhages in between cardiac muscles with occasional myocarditis in heart and moderate hemorrhages were recorded in skeletal muscles of thigh and pectoral area with lymphocytic infiltration. Lungs revealed congestion, haemorrhages and oedematous changes.

Ultrastructural changes

Thymus revealed severe necrosis of the lymphocytes and hyperplasia of the reticular cells. Nuclei and cytoplasm of lymphocytes showed increased electron density (Fig. 3A) and myelin figures (Fig. 3B). Reticular cells appearing dark and small with distinct cytoplasmic contents were found to be relatively increased (Fig. 3C). Lymphocyte numbers appeared decreased. Granulocytes mainly heterophils were relatively more. The normal lymphocytes, dendritic cells, macrophages, heterophils, plasma cells, endothelial cells, erythrocytes and abundant reticular cells were observed with no major pathological observations in the spleen.

Relative decrease in the number of lymphocytes and increase in macrophage like cells (mal) was observed in the Bursa of Fabricius (Fig. 3D). TEM revealed areas of lymphocytic apoptosis and engulfed phagocytic bodies within macrophages. The cytoplasmic granules of bursal secretory dendritic cell (BSDC) was fused together, forming big, irregularly shaped, electron dense bodies (Fig. 3E). A fine-flocculated discharge substance was found surrounding these cells. Few necrotic areas with nuclear changes such as karyorrhexis and karyolysis were also recorded. The virus particles single-shelled, non-enveloped virion with icosahedral symmetry and a diameter of around 50 nm were observed in negative staining preparations (Fig. 3F).

Molecular confirmation

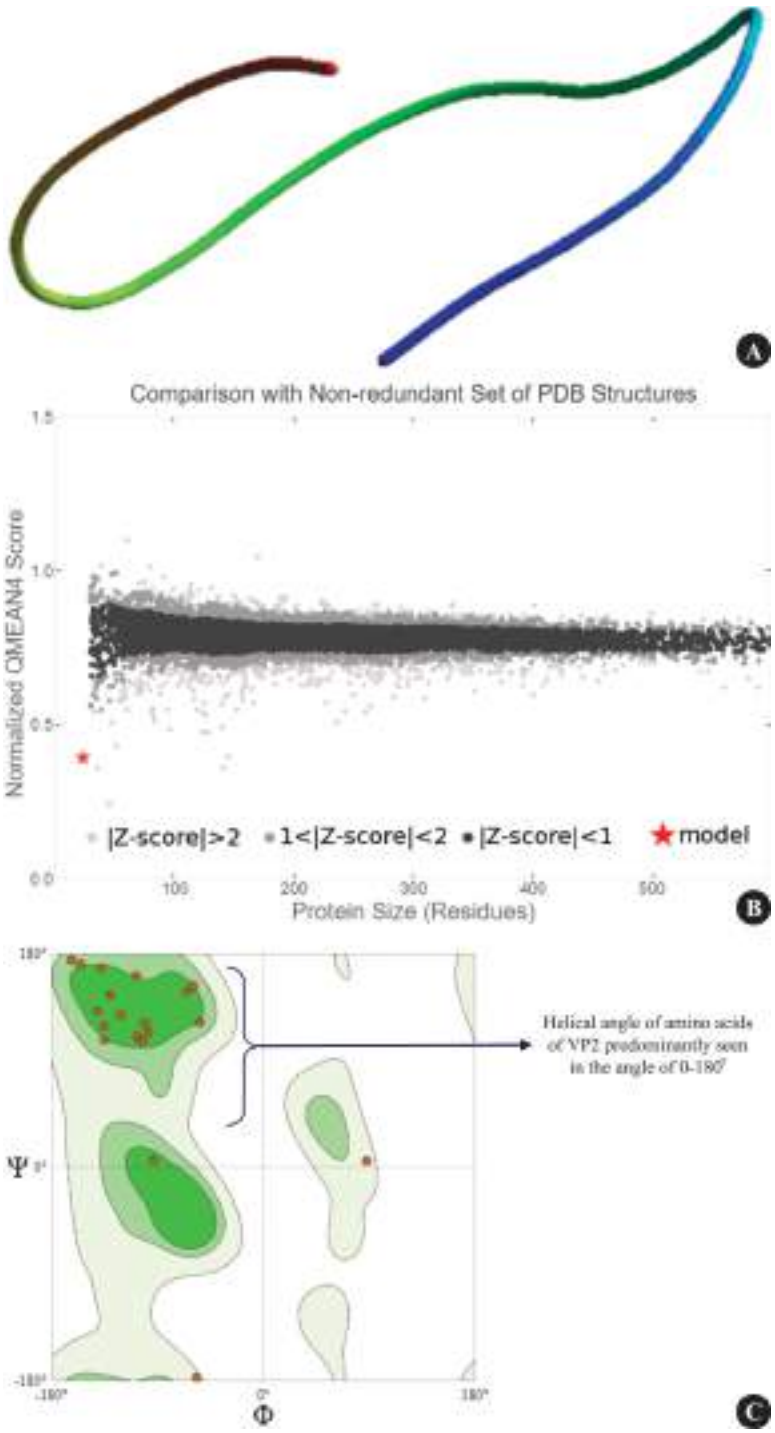

Fig. 6. Bioinformatic Analysis of IBD-VP2. **A.** 3D structure of VP2 in SWISS PROT. **B.** Normalized QMEAN score plot. **C.** Ramachandran plot showing secondary structure of VP2 protein.

Mixed tissue samples from the affected birds were subjected to RNA isolation using Trisol (GeNei™ TRIsoln) kit. The RNA obtained was used for cDNA synthesis employing TAKARA Kits. The RT-PCR was adopted for the detection of IBD antigen for the specific amplification of 319 bp product corresponding to variable region of VP2 gene of IBD virus (Fig. 4). IBD positivity was recorded in all 15 flock outbreaks.

The amplicons obtained by PCR reaction of VP2 gene from samples IBD were subjected to sequence analysis. The 319 bp product was sequenced and phylogenetic tree was drawn and similarity in terms of percentage between various isolates was presented (Fig. 5). This revealed 98 to 100% similarity of strain isolated in this study with

Infectious Bursal Disease virus gene for VP5 protein and VP2-4-3 polyprotein, genomic RNA, IBD virus gene for polyprotein, mutant IBD virus strain AvvBvv segment A and other two indian isolates.

Concurrent infection

Eight outbreaks showed concurrent infection with *E. coli* (4), Salmonellosis (1), CRD (1), Aflatoxicosis (1), Newcastle disease (1) and mixed bacterial infection leading to enteritis (1). The average morbidity and mortality in the outbreaks with concurrent infection were 27.1 and 43.5% respectively. These values in outbreaks without concurrent infection were 12.6 and 19.8% that indicated higher morbidity and mortality in the former group by 14.5 and 23.7%.

The microscopic pathological changes in concurrent infection with *E. coli*, Salmonellosis, CRD, Aflatoxicosis, ND and mixed bacterial enteritis were consistent with the usual pattern of lesions observed in these conditions and correlated well with gross observations. *E. coli* infection revealed fibrinous pericarditis and perihepatitis. The birds with Fowl cholera showed multifocal necrotic areas in the liver with heterophil infiltration and presence of bipolar gram negative organisms in the impression smears of various organs. Birds with Chronic respiratory disease (CRD) showed fibrinopurulent exudate in trachea and lungs. Mixed bacterial enteritis showed presence of many types of bacteria with multiple morphology and heterophil infiltration and concurrent aflatoxicosis was characterized by severe fatty change and multifocal necrosis in the liver.

Bioinformatic Analysis of IBD-VP2

The structural analysis of the IBD-VP2 protein using the SWISS PROT with 3D structure of VP2 and predicted protein sequence is presented in Fig. 6A. This suggested that VP2 of IBD is a manomeric protein with 99 amino acids. The GMQE score of the IBD-VP2 was 0.07. The "QMEAN" score, which is based on the linear combination of four statistical potentials of mean force, was used. Using Z-scores of four as in Fig. 6B and a total of 5 were contrasted with empirically determined structures of comparable size. Ramachandran plot (Fig. 6C) suggested the presence of the glycine like amino acid predominant in the alpha helical structure of the protein.

DISCUSSION

Viral immunosuppressive diseases are economically more important as they cause severe mortalities and loss to the farmers. Also, it makes the birds susceptible for other concurrent bacterial infections further worsening the condition[1-2].

A total of 15 outbreaks of IBD were recorded in the current study. The prevalence of this in Broilers, Layers and Non-descript/desi birds was 11, 2 and 2 respectively. Its prevalence in poultry has been described in India[22-24] and globally[6,11,25-26]. Further it is matter of concern that the re-emergence of IBD with antigenic variants and highly virulent strains that has led to significant losses to poultry farmers[26]. Maximum occurrence of 60% of IBD was recorded in the age group 1-4 weeks. In this, 7 cases (46.7%) were recorded between 3-4 weeks, making it the most susceptible age followed by 5-8 weeks that showed 33.3% similar to previous observations[23-24]. The early age susceptibility might be due to the size of the bursa in early phase of life is regarded as influencing factor for higher incidence of the disease in young chicks less than 4 weeks old[23] and broiler and breeder vaccination programs are not effective for controlling variant IBD infections[12].

The morbidity and mortality in IBD were 29.3% (Range: 7.1 to 100%) and 18.4% (Range: 7.5 to 100%) respectively. Maximum morbidity (Average 31.4%) and mortality (Average 20.5%) has been recorded in broilers. Highest morbidity was recorded in the age group 1-4 weeks in line with the previous findings[24,27,28]. Morbidity and mortality touching even 100% could also be due to culling of the entire bird stock by the farmers where birds do not show any signs of recovery in spite of attempted treatment for secondary bacterial infections. Backyard chicken flocks apart from getting clinical disease can also serve as a reservoir for these viruses and may be playing a role in their dissemination[28].

The symptomology observed in IBD was in tune with the previous findings[18,28-31]. Most of the outbreaks were of acute progressive clinical form associated with Asian/European strains and showed varying severity mostly linked to differing age, sensitivity and vaccination status[29]. The outbreaks recorded in the current study even in vaccinated flocks draw considerable support[11] who observe that vaccination though is the most important measure to control IBD, extensive usage of live vaccines is encouraging evolution of new strains resulting in outbreaks around the globe.

The gross changes in bursa and lymphoid organs might be due to the proven fact that IBDV targets the chicken's immune system in a very comprehensive and complex manner by destroying B lymphocytes, attracting T cells and activating macrophages[9]. It is also noted that the massive destruction of bursal follicles and lack of regeneration process leading to chronic immunosuppression and further complication[10]. The immunosuppressive changes in thymus and spleen have been recorded in both experimental[30,32] and natural outbreaks[24,31,33,34]. No significant change observed in the post outbreak period was probably due to reparative/ healing processes. The reason change in kidneys was probably linked to severe dehydration[35]. The concurrent infections draw significant resemblance with the observations made by previous workers[36,37]. Further, it

is stated that IBD plays a triggering role in *E. coli* and *Mycoplasma gallisepticum* induced respiratory disease complex in broilers[36]. The concurrent infections in present study might be due to immunosuppression and vaccine failure[38].

The histopathological observations in bursa of acutely affected birds were as per the previous observations made[24,27,30,33,34,39,40]. The morphometric changes in the bursal diameter might be due to vascular changes in the acute inflammation (increased) and atrophy in chronic inflammation (decreased). These changes might be due to replication of IBD virus in immature B lymphocytes that are considered as target for the virus. Hence, these changes are anticipated in bursa and other lymphoid organs. Necrotic changes noticed in the germinal follicles and the periarteriolar lymphoid sheath and proliferation in the post outbreak phase due to chronic exposure of spleen was in accordance with the earlier observation[41]. Microscopic changes noted in thymus, bone marrow and cecal tonsils were similar to previous findings[27,30,32,34,41]. It has to be noted that cecal tonsils provide protective immune response against bacterial and viral pathogens in the intestinal tract and any pathology associated with them would lead to adverse effects compromising the gut health.

It is observed most of the liver samples from IBD affected birds were normal and pathological changes may be associated with co-existing mycotoxicosis[34]. Contrary to this, in the current investigation liver changes were characteristic and consistent. Hemorrhages in proventriculus might be due to deficiency of clotting factors either linked to thrombocytopenia or related to Disseminated Intravascular Coagulopathy (DIC) or injury to blood vessel or secondary coagulation defect[42].

Ultrastructurally, thymus of IBD affected birds showed severe necrosis of the lymphocytes and hyperplasia of the reticular cells. Using SEM (Scanning Electron Microscopy) reduction in number and size of epithelial microvilli, gradual loss of the surface follicles and numerous epithelial erosions on the surface of the thymus has been recorded[43]. There are not many reports of thymic changes by previous workers. Lysosomes with remnants of necrotic lymphocytes, lipid vacuoles and myelin figure appearing as membrane bound electron dense aggregates within presumably large pale reticular cells (macrophages) is observed[44]. These cells were surrounded by degenerating lymphocytes in the early stages and pyroninophilic blast cells in the later part of the disease. Areas of lymphocytic apoptosis and engulfed phagocytic bodies within macrophages or macrophage like cells observed in the current study was indicative of high degree of apoptosis owing to viral interference. However, pyronophilic blast cells were not characteristic in the current investigation and viral particles were not detected in the lymphocytes as earlier reported[32]. In a recent study, it is explained that the granular discharge of BSDC that is predominantly glycoprotein contributes in transformation of these BSDC cells to macrophage like cells (Mal) in bursa that is experimentally infected IBD virus[45]. The virus particles single-shelled, non-enveloped virion with icosahedral symmetry and a diameter of around 50 nm were observed in negative staining preparations. These changes are in tune with the previous observations[32,44-47].

The RT-PCR was adopted for the detection of IBD antigen for amplification of 319 bp product corresponding to variable region of VP2 gene[48]. Presence of IBD virus was confirmed in 15 flock outbreaks. RT-PCR, targeting different regions of the IBD virus genome, including VP1, VP2 and VP4 genes, in concurrence with melting curve analysis is being investigated as a potential tool for molecular diagnosis of IBD[2,3,15-18]. In the recent years, the amplification of the VP2 gene has been a major focus. Amplicons of size 743 bp[16,49] and 474 bp[50] have been reported. However, recent study indicates loop-mediated isothermal amplification (LAMP) is 10 times more sensitive, specific and rapid compared to RT-PCR[11].

The amplicons obtained by PCR reaction of VP2 gene from samples IBD were subjected to sequence analysis and phylogenetic tree was drawn. Similarity in terms of percentage between various isolates was presented. This revealed 98 to 100% similarity of strain isolated in this study with Infectious Bursal Disease virus gene for VP5 protein and VP2-4-3 polyprotein, genomic RNA, IBD virus gene for polyprotein, mutant IBD virus strain AvvBvv segment A and other two Indian isolates. Also, the current isolate was distinct from various isolates of the world and formed a separate cluster with accession number X92760. Further the tree bifurcation suggested that the current isolate of the virus might have evolved phylogenetically among the X92760, MG489892 and AJ 318896 as common ancestor. The implications of the phylogenetic similarity and the impact on the strategies on disease control warrants further investigation.

Structural analysis of the IBD-VP2 protein using the SWISS PROT suggested that the VP2 of IBD was a manomeric protein with 99 amino acids. SWISS-PROT is a part of the UniProt Knowledgebase (UniProtKB), a protein sequence database that provides expert annotations on protein function, domain structure, and post-translational modifications, with very low redundancy. Of late, this has become a valuable resource for molecular biologists[51]. GMQE and QMEAND are Co global measurement that give an overall model quality measurement between 0 and 1, with higher numbers indicating higher expected quality. GMQE combines properties from the target-template alignment and the template structure. GMQE score of the IBD-VP2 was 0.07

suggesting that the optimum quality of the peptide in the current study[52]. SWISS-MODEL is a measure of how close the model was to structures of a similar size that were obtained experimentally[53,54]. Ramachandran plot results suggested the presence of the glycine like amino acids predominant in the alpha helical secondary structure of the protein[55]. The Ramachandran plot is a graphical representation used to visualize the allowed regions of amino acid residues in protein structures. Lately, it has become an essential tool for understanding protein conformation, validating structure models and also for studying secondary structure elements of proteins[56].

In the current investigation prevalence, age susceptibility, morbidity and mortality, clinical signs, gross pathology, concurrent infection, microscopic and ultrastructural Pathology and molecular confirmation by PCR and sequencing was studied in fifteen outbreaks of IBD. The gross and microscopic changes in bursa and lymphoid organs confirmed that IBDV targets the chicken's immune system in a very comprehensive and complex manner by destroying B lymphocytes and activation of macrophages. Areas of lymphocytic apoptosis and engulfed phagocytic bodies in these macrophages were observed in TEM. Phylogenetic tree for VP2 amplicons revealed 98 to 100% similarity with VP5 protein and VP2-4-3 polyprotein, genomic RNA, IBD virus gene for polyprotein, mutant IBD virus strain AvvBvv segment A and other two Indian isolates. Ramachandran plot suggested the presence of the glycine like amino acids predominant in the secondary structure of the protein.

Based on the various pathological and molecular investigations the immunosuppressive effects of IBD virus on health and in turn to the economy of poultry farming is clear and evident. Various other factors such as management, nutrition and climate change could also be involved in the expression of IBD in poultry. It is the utmost necessity to timely diagnose these conditions and control them effectively and more importantly educating the poultry farmers on timely implementation of vaccinations and biosecurity measures. Mitigating strategies involving epidemiological interventions, mechanistic studies on host immune responses, mutation based *in-silico* analysis of VP2 protein, enhanced diagnostics and making provision for better vaccines could be handy in addressing IBD in the future.

REFERENCES

1. Umar S, Munir M, U Ahsan I, Raza M, Chowdhury Z, Ahmed M and Shah. 2017. Immunosuppressive interactions of viral diseases in poultry. *World's Poult Sci J* **73:** 121-135.
2. Agnihotri AA, Awandkar SP, Kulkarni RC, Chavhan SG, Suryawanshi RD, Mohan A, Kulkarni M and Chavan VG. 2023. Isolation and molecular characterization of Infectious Bursal Disease virus circulating in western and central India. *Indian J Vet Res* **24:** 345-350.
3. Huang Y, Shu G, Huang C, Han J, Li J, Chen H and Chen Z. 2023. Characterization and pathogenicity of a novel variant Infectious Bursal Disease virus in China. *Front Microbiol*.
4. Tahir I and Alsayeqh AF. 2024. Phytochemicals: a promising approach to control infectious bursal disease. *Front Vet Sci*.
5. Gimeno IM and Schat KA. 2018. Virus-Induced Immunosuppression in Chickens. *Avian Dis* **62:** 272-285.
6. Jordan AB, Gongora V, Hartley D and Oura C. 2018. A review of eight high-priority, economically important pathogens of poultry within the Caribbean region. *J Vet Sci* **5:** 1-14.
7. Vandenberg T, Eterradossi N, Toquin D and Meulemans G. 2000. Infectious Bursal Disease (Gumboro disease). *Revue Sci Tech Office Intel Epiz* **19:** 527-543.
8. Qin Y and Zheng SJ. 2017. Infectious Bursal Disease Virus-Host Interactions: Multifunctional Viral Proteins that Perform Multiple and Differing Jobs. *Int J Mol Sci* **18:** 161-167.
9. Ingrao F, Rauw F, Lambrecht B and Vandenberg T. 2013. Infectious Bursal Disease: A complex host-pathogen interaction. *Dev Comp Immunol* **41:** 429-438.
10. Awandkar SP, Tembhurne PA, Kesharkar JA, Kurkure NV, Chaudhari SP, Bonde SW and Ingle VC. 2018. Identification and characterization of a novel Infectious Bursal Disease virus from outbreaks in Maharashtra Province of India. *Vet World* **11:** 1516-1525.
11. Dey S, Dinesh PC, Narayan R, Hemanta KM and Madhan MC. 2019. Infectious Bursal Disease virus in chickens: prevalence, impact and management strategies. *Vet Med Res Reports* **10:** 85-97.
12. Zachar T, Popowich S, Goodhope B, Knezacek T, Ojkic D, Willson P, Ahmed KA and Gomis S. 2016. A 5-year study of the incidence and economic impact of variant Infectious Bursal Disease viruses on broiler production in Saskatchewan, Canada. *Can J Vet Res* **80:** 255-261.
13. Sharma JM, Kim I, Rautenschlein S and Yeh H. 2000. Infectious Bursal Disease virus of chickens: Pathogenesis and immunosuppression. *Dev Comp Immunol* **24:** 223-235.
14. Luque D, Saugar I, Rejas MT, Carrascosa JL, Rodriguez JF and Caston JR. 2009. Infectious Bursal Disease virus: Ribonucleoprotein complexes of a Double-stranded RNA virus. *J Mol Biol* **386:** 891-901.
15. Vandenberg T, Morales D, Eterradossi N, Rivallan G, Toquin D, Raue R, Zierenberg K, Zhang M, Zhu Y and Wang C. 2004. Assessment of genetic, antigenic and pathotypic criteria for the characterization of IBDV strains. *Avian Pathol* **33:** 470-476.
16. Sreedevi B and Jackwood DJ. 2007. Real-Time Reverse Transcriptase-Polymerase Chain Reaction Detection and Sequence Analysis of the VP2 Hypervariable Region of Indian Very Virulent Infectious Bursal Disease Isolates. *Avian Dis* **51:** 750-757.
17. Wu CC, Rubinelli PA and Lin TL. 2007. Molecular detection and Differentiation of Infectious Bursal Disease Virus. *Avian Dis* **51:** 515-526.
18. Morla S, Deka P and Kumar S. 2016. Isolation of novel variants of Infectious Bursal Disease virus from different outbreaks in Northeast India. *Microb Pathog* **93:** 131-136.
19. Mendez F, Romero N, Cubas L, Laura DR, Dolores R and Rodriguez JF. 2017. Non-Lytic Egression of Infectious Bursal Disease Virus (IBDV) Particles from Infected Cells. *Plos One* **12:** 1-22.
20. Suvarna SK, Layton C and Bancroft JD. 2013. eds. Bancroft's theory and practice of histological techniques. Nottingham and Sheffield: Churchill Livingstone-Elsevier.
21. Barreto-Vieira DF and Barth OM. 2015. Eds. Microbiology in Agriculture and Human Health. Intech Open: London.

22. Karunakaran K, Thanappapilldi M and Raghavan N. 1993. Seroprevalence of Infectious Bursal Disease (IBD) in parts of Tamil Nadu, India. *Comp Immunol Microbiol Infect Dis* **16:** 241-244.
23. Farooq M, Durrani FR, Imran N, Durrani Z and Chand N. 2003. Prevalence and economic losses due to infectious Bursal diseases in broilers in Mirpur and Kotli district of Kashmir. *Int J Poult Sci* **2:** 267-270.
24. Preeti KS and Ramkaran LB. 2018. Histopathology of Bursa of Fabricius and postmortem findings in Infectious Bursal Disease affected broiler chickens in Haryana. *J Entomol Zool Stud* **6:** 876-879.
25. Mcilroy SG, Goodall EA and Mccracken RM. 1989. Economic effects of subclinical Infectious Bursal Disease on broiler production. *Avian Pathol* **18:** 465-480.
26. Zierenberg K, Nieper H, Vandenberg T, Ezeokoli C, Voss M and Muller H. 2000. The VP2 variable region of African and German isolates of Infectious Bursal Disease virus: Comparison with very virulent, classical virulent and attenuated tissue culture-adapted strains. *Arch Virol* **145:** 113-125.
27. Eterradossi N and Saif YM. 2008. Infectious Bursal Disease. In: Diseases of Poultry. Blackwell publishing, Ames, USA.
28. Linda OM, Michelle LK and Daral JJ. 2019. New introduction of a very virulent Infectious Bursal Disease virus in New York, USA. *Avian Pathol* **48:** 1-20.
29. Vandenberg TP. 2000. Acute Infectious Bursal Disease in poultry: a review. *Avian Pathol* **29:** 175-194.
30. Manjunath MT, Vijayasarathi SK, Sathyanarayana ML and Sreenivas Gowda RN. 2002. Comparative pathology of lymphoid organs in experimental Newcastle and infectious bursal disease. *Indian J Anim Sci* **72:** 1068-1071.
31. Preeti KS, Bai L, Ramkaran J, Naresh R and Gupta R. 2018. Epidemiological studies on Infectious Bursal Disease in broiler chickens in Haryana state during 2012-2015. *The Pharma Innovation J* **7:** 282-285.
32. Tanimura N, Tsukamoto K, Nakamura K, Narita M and Maeda M. 1995. Association between Pathogenicity of Infectious Bursal Disease Virus and Viral Antigen Distribution Detected by Immunohistochemistry. *Avian Dis* **39:** 9-20.
33. Sami WG and Baruah K. 1998. Pathology of Infectious Bursal Disease in broiler chickens. *Indian J Anim Sci* **68:** 1171-1172.
34. Singh J, Banga HS, Brar RS, Singh ND, Sodhi S and Leishangthem GD. 2015. Histopathological and immunohistochemical diagnosis of Infectious Bursal Disease in poultry birds. *Vet World* **8:** 1331-1339.
35. Cosgrove AS. 1962. An apparently new disease of chickens avian nephrosis. *Avian Dis* **6:** 385-389.
36. Gowthaman V, Sing SD, Dhama K, Barathidasan R and Anjaneya BP. 2012. Infectious Bursal Disease (IBD) playing a triggering role in *E. Coli* and mycoplasma induced respiratory disease complex in broilers. *Vet Pract* **13:** 223-225.
37. Devigasri C, Sankar S, Niranjana S, Rajalakshmi, Nair A and Mini M. 2018. Concurrent infection of Infectious Bursal Disease and pseudomoniasis in poultry - A Case Study. *Int J Sci Environ Technol* **7:** 1777-1781.
38. Mekibib B, Abera M, Mekuria S, Farooq UB and Abebe R. 2018. Clinicopathological Features of Concurrent Outbreak of Gumboro Disease and Aspergillosis in Chicken in Hawassa City, Ethiopia. *Asian J Poult Sci* **12:** 25-30.
39. Islam MR, Chowdhury EH, Das PM and Dewan ML. 1997. Pathology of acute Infectious Bursal Disease in chickens induced experimentally with a very virulent virus isolate. *Indian J Anim Sci* **67:** 7-9.
40. Islam NU, Saleemi MK, Khan MZ, Butt SL, Khan A, Javed I, Awan FS and Rafique S. 2013. Molecular diagnosis and pathology of chicken infectious anemia in commercial white leghorn layer flocks in Pakistan. *Vet J* **33:** 378-381.
41. Singh MP, Singh A, Grewal GS and Oberoi MS. 2002. Clinico-pathological studies of field isolates of Infectious Bursal Disease in broiler chicks. *Indian J Anim Sci* **72:** 38-41.
42. Zeryehun T, Hair-Bejo M and Rasedee A. 2012. Hemorrhagic and clotting abnormalities in Infectious Bursal Disease in specific pathogen free chick. *World Appl Sci J* **16:** 1123-1130.
43. Naqi SA and Millar DL. 1979. Morphologic changes in the Bursa of Fabricius of chickens after inoculation with Infectious Bursal Disease virus. *Am J Vet Res* **40:** 1134-1139.
44. Cheville NF. 1967. Studies on the pathogenesis of Gumboro disease in the Bursa of Fabricius, spleen and thymus of the chicken. *Am J Pathol* **51:** 527-551.
45. Felfoldi B, Bodi I, Minko K, Benyeda Z, Nagy N, Magyar A and Olah I. 2021. Infection of bursal disease virus abrogates the extracellular glycoprotein in the follicular medulla. *Poult Sci Apr* **100:** 101-000.
46. Kaufer I and Weiss E. 1976. Electron-microscope studies on the pathogenesis of Infectious Bursal Disease after intrabursal application of the causal virus. *Avian Dis* **20:** 483-95.
47. Christopher DS, Minnie M, Peter AB, Anbumani SP, Doraiswami J, Rajendran MP and Murugan M. 1997. An outbreak of acute Infectious Bursal Disease in poultry: Ultrastructural studies on bursa from clinical cases. *Indian J Anim Sci* **67:** 563-564.
48. Kong LL, Omar AR, Bejo MH, Ideris A and Tab SW. 2009. Development of SYBR green I based one-step real-time RT-PCR assay for the detection and differentiation of very virulent and classical strains of Infectious Bursal Disease virus. *J Virol Meth* **161:** 271-279.
49. Kim HR, Kwon YK, Bae YC, Oem JK and Lee OS. 2010. Genetic characteristics of virion protein 2 genes of Infectious Bursal Disease viruses isolated from commercial chickens with clinical disease in South Korea. *Poult Sci* **89:** 1642-1646.
50. Ghorashi SA, Orourke D, Ignjatovic J and Noormohammadi AH. 2011. Differentiation of Infectious Bursal Disease virus strains using real-time RT-PCR and high resolution melt curve analysis. *J Virol Methods* **171:** 264-271.
51. UniProt Consortium. 2023. UniProt: Universal Protein Knowledgebase in 2023. *Nucl Acids Res* **51:** D523-D530.
52. Mariani V, Biasini M, Barbato A and Schwede T. 2013. LDDT: a local superposition-free score for comparing protein structures and models using distance difference tests. *Bioinform* **29:** 2722-2728.
53. Studer G, Rempfer C, Waterhouse AM, Gumienny R, Haas J and Schwede T. 2020. Qmeandisco - distance constraints applied on model quality estimation. *Bioinform* **36:** 1765-1771.
54. Benkert P, Biasini M and Schwede T. 2011. Toward the estimation of the absolute quality of individual protein structure models. *Bioinform* **27:** 343-350.
55. Chenn VB, Arendall WB, Headd JJ, Keedy DA, Immormino RM, Kapral GJ, Murray LW, Richardson JS and Richardson DC. 2010. All-atom structure validation for macromolecular crystallography. *Acta Cryst D* **66:** 16-21.
56. Ramachandran GN and Sasisekharan V. 1968. Conformation of polypeptides and proteins. *Adv Protein Chem* **23:** 283-438.

Indian J. Vet. Pathol., 49(1) : 49-55, 2025: DOI: https://doi.org/10.5958/bsyfqy98

RESEARCH ARTICLE

Oxidative stress and histomorphological changes in brain and effects of supplementation of *Linumusitatissimum* (flaxseed) and *Emblica officinalis* (amla) against lead toxicity in Wistar rats

Amitava Paul[1*], Karamala Sujatha[1], Ch. Srilatha[1], N. Vinod Kumar[2] and Deep Shikha[3]

[1]Department of Veterinary Pathology, College of Veterinary Science, Sri Venkateswara Veterinary University, Tirupati -517 502, Andhra Pradesh, [2]Department of Veterinary Microbiology, College of Veterinary Science, Sri Venkateswara Veterinary University, Tirupati-517 502, Andhra Pradesh, [3]Division of Veterinary Microbiology, Sher-e-Kashmir University of Agricultural Sciences and Technology, Jammu-181 102, India

Address for Correspondence

Amitava Paul, Department of Veterinary Pathology, College of Veterinary Science, Sri Venkateswara Veterinary University, Tirupati -517 502, Andhra Pradesh, India, E-mail: amit01paul@gmail.com

Received: 13.12.2024; Accepted: 15.1.2025

ABSTRACT

Lead (Pb) is a non-biodegradable, ubiquitous, environmental contaminant and is well known for toxicity in both human and animal. This study aimed to investigate the propensity of lead to induce neurotoxicity and changes in histological and oxidative stress in Wistar rats following a 45 days oral exposure and its possible attenuation by amla and flaxseed. Rats were assigned to 6 treatment groups; Group I served as vehicle control and they received distilled water, whereas rats in Group II @ 60 mg/kg bwt. lead acetate, Group III *Emblica officinalis* @ 100 mg/rat/day, Group IV *Linumusitatissimum* @ 300 mg/kg b.wt, Group V lead acetate @ 60 mg/kg b.wt + *Emblica officinalis* @ 100 mg/rat/day, and Group VI lead acetate @ 60 mg/kg b.wt + *Linumusitatissimum* @ 300 mg/kg b. wt. were administered orally. Antioxidant enzyme activities like Catalase (CAT), Superoxide dismutase (SOD) and Glutathione peroxidase (GPx) were significantly decreased meanwhile, Thiobarbituric acid reactive substances (TBARS) were significantly increased in lead acetate-treated rats (Group-II). Upon light microscopical examination in Group II rats, severe degenerative changes were noticed in the brain. The levels of all the above parameters were significantly improved in the ameliorated group (Group V and VI). The present study revealed that the presence of amla and flaxseed could diminish the adverse effects of lead acetate as shown in the histological analysis of rat brain.

Keywords: Amla, antioxidant enzymes, brain, flaxseed, lead toxicity, wistar rats

INTRODUCTION

Lead is one of the oldest environmental contaminants and is considered to be toxic for virtually all organs of the body. Exposure to lead can occur from a multitude of sources such as soil, air, water and industrial pollutants. Inhalation (lung) and ingestion (GIT) is the major route of entry into the body. Absorbed lead mainly bind with erythrocytes in blood and from there it distributed to target organs, i.e. liver, brain, lungs, spleen, renal cortex, aorta, teeth and bones[1]. In view point of CNS toxicity, lead enters the brain and selectively deposited in the hippocampus and cortex, as well as in non-neuronal elements that are important in the maintenance of the blood brain barrier function. Studies have demonstrated that lead impairs learning, memory processes and cognitive functions both in animal models and human beings[2]. The neuropathlogical effects of lead include nervousness, anxiety and symptomatic encephalopathy. Oxidative stress induces cellular damage through production of Free radicals and inhibitions of enzymatic function are the major contributor in pathogenesis of lead induced toxicity[3].

In recent years, studies have shown the effect of several kinds of plants not only confers protection against heavy metal toxicity but it can also perform a therapeutical role against toxicity due to presence of several bioactive compound and antioxidant properties. Free radicals were generated during the pathogenesis processes induced by lead exposure, it was presumed that supplementation of antioxidants could be an alternative method for chelation therapy[4]. *Emblica officinalis* (Emblica) is also known as amla, is a rich source of tannins[5], polyphenols, flavones[6] and some bioactive substances, among them tannaoids are the active principles present in amla having vitamin C like properties which act as anti-inflammatory and potent antioxidant[7]. *Linumusitatissium* (Flaxseeds), commonly known as linseed is rich in lignan compound. The principle lignan found in flaxseed is Secoisolariciresinol di glucoside (SDG)[8]. Flaxseed also proven to have cardioprotective, chemoprotective, hepatoprotective and anti-inflamatory properties[9,10]. So this present experiment was taken to evaluate

How to cite this article : Paul, A., Sujatha, K., Srilatha, C., Kumar, N.V. and Shikha, D. 2025. Oxidative stress and histomorphological changes in brain and effects of supplementation of *Linumusitatissimum* (flaxseed) and *Emblica officinalis* (amla) against lead toxicity in Wistar rats. Indian J. Vet. Pathol., 49(1) : 49-55.

Table 1. Mean Brain TBARS values (nM of MDA / g of tissue) in rats of different experimental groups.

Weeks	GROUP I	GROUP II	GROUP III	GROUP IV	GROUP V	GROUP VI
2	602.8	1156.1	610.5	606.3	632.7	639.8
4	612.3	1185.6	584.3	594.4	625.3	632.5
6	598.4	1230.4	595.8	601.5	627.9	641.3
Mean ± SE	604.5 ± 4.1^{c}	1190.7 ± 21.59^{a}	596.86 ± 7.58^{c}	600.73 ± 3.45^{c}	628.63 ± 2.16^{bc}	637.86 ± 2.71^{b}

Mean values with different superscripts differ significantly ($P < 0.05$), ANOVA; S.E. - Standard error

the protective nature of flaxseed and amla in abating the toxic effect of lead in brain of wistar rats.

MATERIALS AND METHODS

Procurement of experimental animals, aqueous extract of *Emblica officinalis* and lead acetate

Female Wistar rats with body weight around 150 to 200 g (procured from Sri Venkateswara Agencies, Bangalore) were used for the present experiment. After one week of acclimatization the rats were grouped randomly and housed in standard polypropylene rat cages (three rats/cage) during the experimental period. They were maintained at $25^{O}C \pm 10^{O}C$ and a 12:12 hour interval light and dark cycle during the 45 days of experimental period by maintaining standard laboratory hygienic conditions with *ad libitum* supply of laboratory animal feed and water. The permission of the institutional animal ethical committee (IAEC) was obtained earlier to commencement of the experiment.

The lead acetate was procured from the Qualigens Fine Chemicals Company, product code No. 27645 with 97% purity. Aqueous extract of Amla (*Emblica officinalis*) with product code C/SVU/EMOF-01 was procured from Chemiloids Company, Vijayawada, India.

Preparation of aqueous methanolic extract of *Linumusitatissimum* (Flaxseed)

Seeds of *Linumusitatissimum* (Flax seeds) were procured from a local herbal shop. After drying in shade, seeds were ground into powder form, which then used for the preparation of aqueous methanolic extract. Flaxseed lignans was prepared as per the method of Zhang *et al*. 2007[11]. Flaxseeds (800g) were ground using a grinder to attain a fine powder form. The powder form of flaxseeds was defatted by blending with hexane (1:6 w/v, 12 h) in room temperature. The defatted flaxseed powder was air dried for around 12 hours. 200 grams of this defatted powder was again blended with 1.2 Litres complex solution of ethanol and water (7:3 v/v) for 24 hours at ambient temperature ($25^{O}C$). The extract was filtered into flask, and then filtered product was concentrated at $50^{O}C$ using a Rotary evaporator (Buch, Model 462, Germany) @ 90 rpm. Light yellow colour syrup of flaxseed lignans extract was obtained.

Experimental design

A total 108 number of female adult Wistar albino rats were assigned to 6 groups randomly with 18 rats in each group. Group I served as vehicle control and they received distilled water, whereas animals in Group II, III, IV, V and VI received lead acetate @ 60 mg/kg b.wt., *Emblica officinalis* @ 100 mg/rat/day, *Linumusitatissimum* @ 300 mg/kg b.wt, lead acetate @ 60 mg/kg b.wt + *Emblica officinalis* @ 100 mg/rat/day, lead acetate @ 60 mg/kg b.wt + *Linumusitatissimum* @ 300 mg/kg b.wt. respectively for 45 days. From each group, six rats were sacrificed at fourteen-day intervals.

Histopathology

A detailed post-mortem examination was carried out on the sacrificed rats of all the trial groups. The brain was collected and preserved in 10% NBF for histopathological studies; fixed tissues were processed by standard paraffin embedding technique. 5-6 microns thick tissue sections were cut and sections were stained with Haematoxylin and Eosin stain (H&E)[12].

Lipid peroxidation (TBARS) assay and Antioxidant profile

For oxidative stress brain was collected and stored at $-20^{O}C$ until use. Small tissue pieces of brain tissue were minced in separate containers and homogenized in 0.05 M ice cold phosphate buffer (pH 7.4) and make 10% homogenate by using a virtis homogenizer. 0.2 ml of

Table 2. Mean brain catalase activity (nM of H_2O_2 decomposed/min/mg of protein) in rats of different experimental groups.

Weeks	GROUP I	GROUP II	GROUP III	GROUP IV	GROUP V	GROUP VI
2	0.33	0.17	0.32	0.29	0.26	0.25
4	0.30	0.15	0.29	0.30	0.27	0.24
6	0.31	0.11	0.31	0.32	0.30	0.28
Mean ± SE	0.31 ± 0.008^{a}	0.14 ± 0.01^{c}	0.30 ± 0.008^{a}	0.30 ± 0.008^{a}	0.27 ± 0.01^{ab}	0.25 ± 0.01^{b}

Mean values with different superscripts differ significantly ($P < 0.05$), ANOVA; S.E. - Standard error

Table 3. Mean brain SOD activity (U/min/mg of protein) in rats of different experimental groups.

Weeks	GROUP I	GROUP II	GROUP III	GROUP IV	GROUP V	GROUP VI
2	15.2	7.2	15.1	15.3	14.7	14.4
4	15.7	6.7	15.4	15.2	14.9	14.5
6	15.5	5.9	15.6	15.5	15	14.8
Mean ± SE	15.46 ± 0.14^{a}	6.6 ± 0.37^{c}	15.36 ± 0.14^{a}	15.33 ± 0.08^{a}	14.86 ± 0.88^{ab}	14.56 ± 0.12^{b}

Mean values with different superscripts differ significantly ($P < 0.05$), ANOVA; S.E. - Standard error

the 10% homogenate was utilized for lipid peroxidation assay[13]. The residual part of homogenate then mixed with 10% trichloroacetic acid in 1:1 ratio, then centrifuged @ 5000 g at 4^{O}C for 10 min and the supernatant was collected and was used for valuation of reduced glutathione[14]. The residual portion of the homogenate was centrifuged for 60 min. at 15,000 g at 4^{O}C and the supernatant attained was used for the valuation of superoxide dismutase[15], catalase[16] and glutathione peroxidase[17] in brain of all rats in all groups.

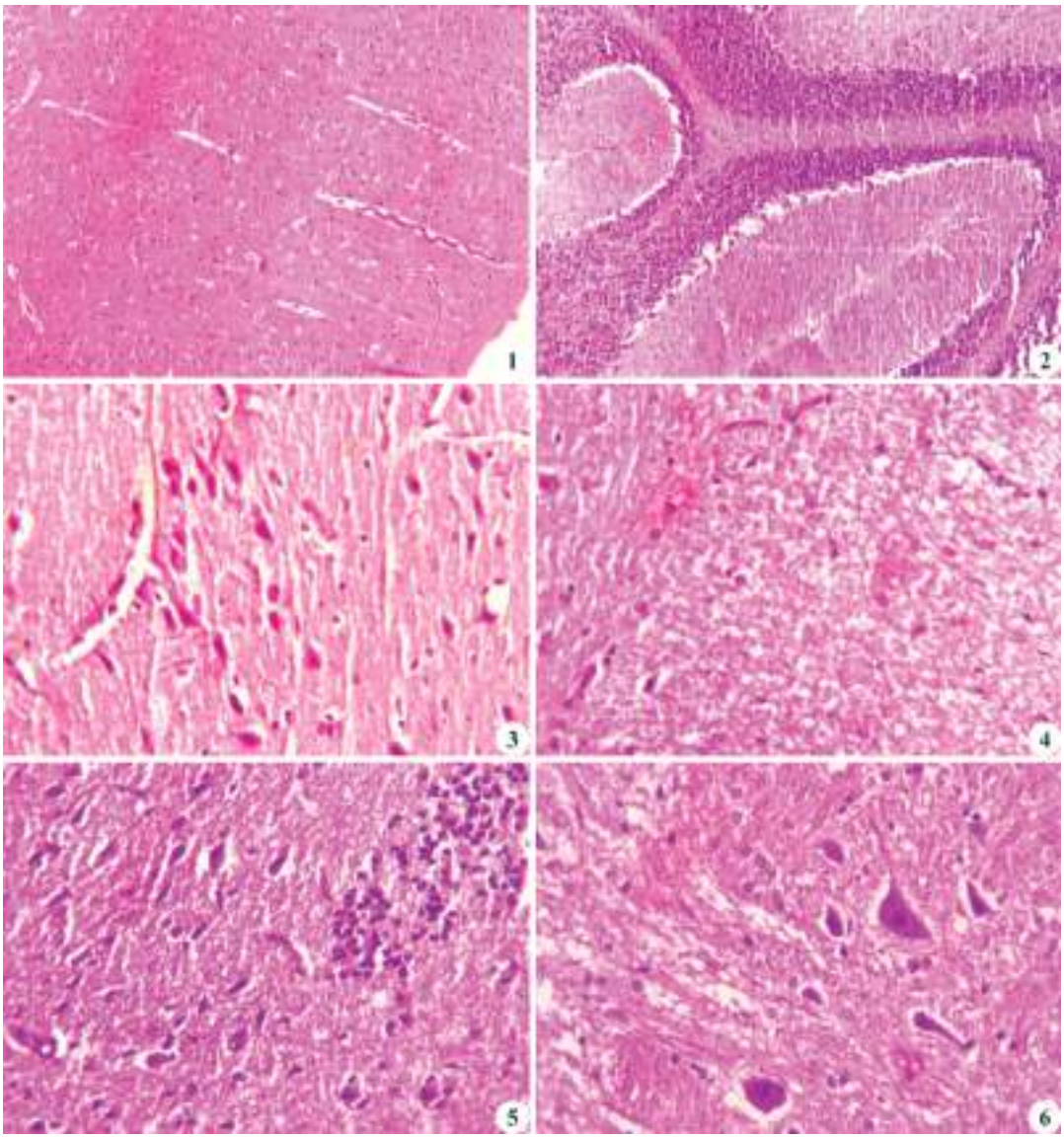

Fig. 1. Cerebrum: Group II: Section showing capillary proliferation (H&E X40); **Fig. 2.** Cerebellum: Group II: Section showing loss of a few Purkinje cells in Purkinje cell layer (H&E X100); **Fig. 3.** Cerebrum: Group II: Section showing shrinkage of neurons and capillary proliferation (H&E X400); **Fig. 4.** Cerebrum: Group II: Section showing demyelinating changes (H&E X400); **Fig. 5.** Brain: Group II: Section showing gliosis and shrinkage of nerve cells in cerebral cortex (H&E X400); **Fig. 6.** Cerebellum: Group II: Section showing nerve cell with central chromatolysis (H&E X400).

Table 4. Mean brain glutathione peroxidase activity (μ of glutathione utilized/min/mg of protein) in rats of different experimental groups.

Weeks	GROUP I	GROUP II	GROUP III	GROUP IV	GROUP V	GROUP VI
2	25.63	18.28	24.85	24.95	21.26	20.69
4	24.92	13.42	25.37	25.12	21.64	20.91
6	25.47	7.34	26.12	25.53	22.19	21.29
Mean ± SE	25.34 ± 0.21[a]	13.01 ± 3.1[c]	25.44 ± 0.36[a]	25.20 ± 0.17[a]	21.69 ± 0.26[ab]	20.96 ± 0.17[b]

Mean values with different superscripts differ significantly (P < 0.05), ANOVA; S.E. - Standard error

Statistical analysis

The results were analysed statistically by performing one-way ANOVA[18].

Ethical approval

The ethics governing the use and conduct of experiments on laboratory animals were strictly observed and the experimental protocol was approved by the Institutional Animal Ethical Committee (IAEC), Sri Venkateswara Veterinary University, Tirupati, Andhra Pradesh, India (Reference Number 281/go/ReBi/S/2000/CPCSEA/CVSC/TPTY/018/VPP/2016-17). Institutional Animal Ethical Committee (IAEC), Sri Venkateswara Veterinary University, Tirupati, Andhra Pradesh, is affiliated under The Committee for the Purpose of Control and Supervision of Experiments on Animal (CPCSEA, India) with the Registration Number-281/go/ReBi/S/2000/CPCSEA.

RESULTS

Lipid peroxidation - Thiobarbituric acid reactive substances (TBARS)

Statistically significant (P< 0.05) increase in mean brain TBARS levels was noticed in lead acetate-treated rats (Group II) when compared to the control rats (Group I). The mean brain TBARS values from Group I to VI were 604.5, 1190.7, 596.86, 600.73, 628.63 and 637.86 (nM of MDA/g of tissue) respectively and are shown in Table 1. A significant decrease was observed in mean brain TBARS levels in Emblica ameliorated rats (Group V) and Flaxseed ameliorated rats (Group VI) when compared to the lead acetate-treated rats (Group II). There was no significant alteration in lipid peroxidation levels in

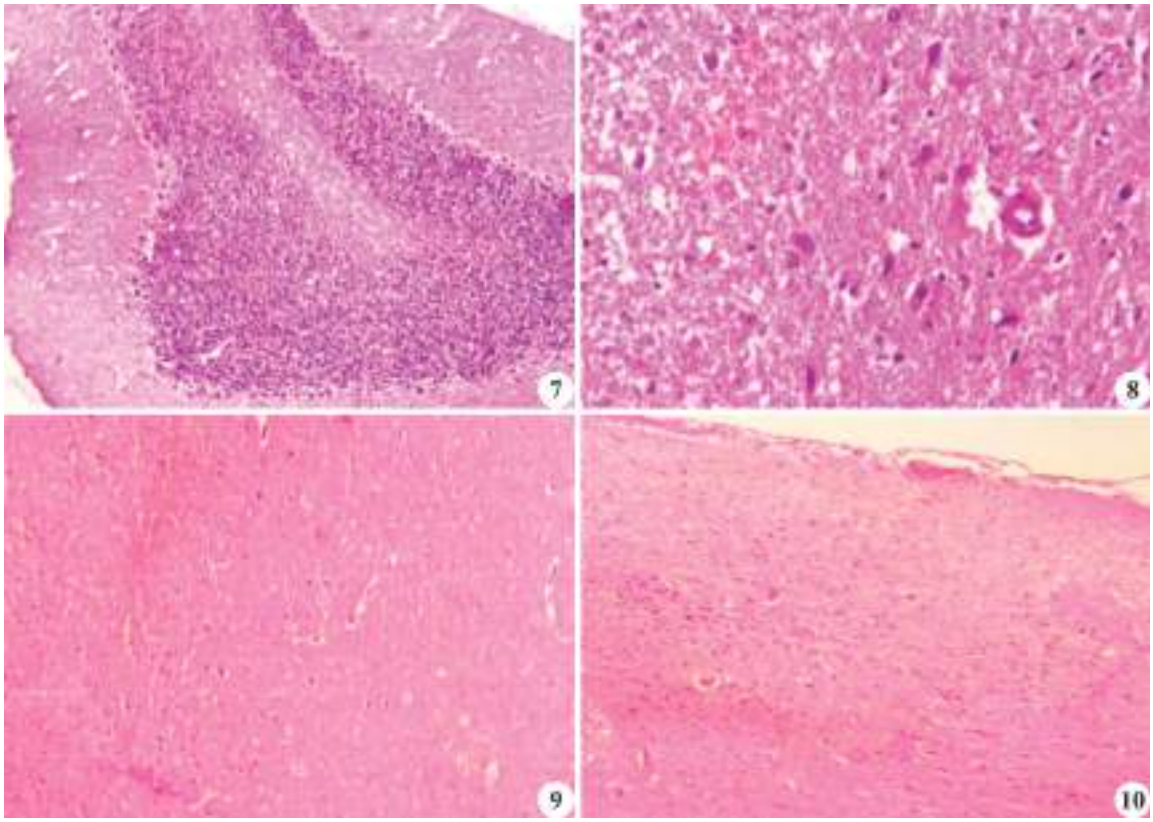

Fig. 7. Cerebellum: Group V: Section showing normal Purkinje cell layer (H&E x100); **Fig. 8.** Cerebrum: Group V: Section showing mild demyelinating changes (H&E x400); **Fig. 9.** Cerebrum: Group VI: Section showing mild capillary proliferation (H&E x40); **Fig. 10.** Cerebrum: Group VI: Section showing mild demyelinating changes and congested sub meningeal blood vessels (H&E x40).

brain of Emblica (Group III) and Flaxseed (Group IV) treated rats.

Antioxidant Profile

Catalase (CAT)

There was a significant ($P < 0.05$) decrease in mean brain catalase activity in lead acetate-treated rats (Group II) when compared to the control rats (Group I). The mean brain catalase activity in Group I to VI were 0.31, 0.14, 0.30, 0.30, 0.27 and 0.25 (nM of H_2O_2 decomposed/min/mg of protein) respectively and are shown in Table 2. Statistically significant improvement was noticed in mean brain catalase activity in Emblica ameliorated rats (Group V) and Flaxseed ameliorated rats (Group VI) when compared to the lead acetate treated rats (Group II).

Superoxide dismutase (SOD)

In the present study statistically significant ($P<0.05$) decrease in mean brain SOD activity was noticed in lead acetate treated rats (Group II) when compared to the control rats (Group I). The mean brain SOD activity from Group I to VI were 15.46, 6.6, 15.36, 15.33, 14.86 and 14.56 (U/min/mg of protein) respectively and are shown in Table 3. A significant improvement was observed in mean brain SOD activity in Emblica ameliorated rats (Group V) and Flaxseed ameliorated rats (Group VI) when compared to the lead acetate treated rats (Group II).

Glutathione peroxidase (GPx)

There was a significant ($P < 0.05$) decrease in mean brain GP_X activity in lead acetate-treated rats (Group II) when compared to the control rats (Group I). The mean brain GP_X activity in Group I to VI were 25.34, 13.01, 25.44, 25.20, 21.69 and 20.96 (μ of glutathione utilized/min/mg protein) respectively and presented in Table 4. Statistically significant improvement was noticed in mean brain GP_X activity in emblica ameliorated rats (Group V) and Flaxseed ameliorated rats (Group VI) when compared to the lead acetate treated rats (Group II).

There was no significant alteration in CAT, SOD and GPx level in brains of Emblica (Group III) and Flaxseed (Group IV) treated rats was observed when compared to control rats (Group I).

Histopathology

Light microscopic examination of the brain of lead-treated rats (Group II) revealed mild to moderate capillary proliferation (Fig. 1), and shrinkage of neurons in the cerebral cortex (Fig. 2). In the cerebellum, rounding, degeneration of Purkinje cells and loss of a few Purkinje cells (Fig. 3) were observed by the end of 2nd week. Later stages of experiment (4th week) in addition to the above changes, moderate capillary proliferation with shrinkage of neurons, demyelinating changes and spongiosis (Fig. 4) in cerebral cortex and gliosis were evident. By the end of 6th week, degenerative changes such as thickening of meninges with infiltration of cells, severe congestion of cerebral blood vessels and choroid plexus, severe demyelinating and spongiosis, gliosis and shrinkage of neuron in cerebral cortex (Fig. 5), Severe neuronal degeneration with central chromatolysis (Fig. 6) neurophagia and severe capillary proliferation in cerebral cortex and formation of nodule like structure along with MNCs infiltration in cerebral cortex were conspicuous.In Group V (*Emblica* ameliorated rats) histopathologically, brains revealed, similar lesions like Group II up to 4th week. Later the changes were gradually reduced in intensity like mild capillary proliferation, normal Purkinje cell layer (Fig. 7), mild degenerative changes (Fig. 8) and by the end of 6th week brain regained almost it normal structure. Flaxseed ameliorated rats (Group VI) similar lesions as described in Group II were noticed up to 4th weeks and later stages the changes were gradually reduced in its severity with mild capillary proliferation (Fig. 9), mild demyelinating changes in cerebral cortex and congestion of submeningeal blood vessels (Fig. 10) and almost near to normal appearance of cerebellum with all the three layers having normal arrangement were observed by the end of 6th week of experiment. There was no significant gross and microscopic alteration was observed in brain of *Emblica* (Group III) and Flaxseed (Group IV) treated rats compared to control group (I).

DISCUSSION

In the present study, significant increases in lipid peroxidation values in brain were noticed in lead acetate treated rats (Group II) compared to control rats (Group I). Similar observations were reported by earlier authors[19,20] and the possible explanation in increased lipid peroxidation level may be related to the role of GSH (Glutathione) which helps in the active excretion of lead through bile by binding to the thiol group of GSH, decrease in GSH levels lead to increase tissue burden of lead (Pb), which in turn results in lead induced oxidative stress and a consequent increase in lipid peroxidation[21]. Moreover, lead induces direct depletion of antioxidant enzymes[19]. These antioxidant enzymes like SOD, GPx and CAT take part in maintaining GSH homeostatis in tissues, so depletion of these antioxidant enzymes may contribute to the explanation of the mechanisms responsible for decrease in GSH concentration in tissues due to the exposure to this heavy metal[22]. Emblica ameliorated group (Group V) showed a significant decrease in lipid peroxidation activity and might be due to its antioxidant defence activity and lipid peroxidation inhibition activity of the ascorbic acid content of the Emblica[23]. Similarly, Flaxseed ameliorated rats (Group VI) also showed significant ($P<0.05$) decreased in lipid peroxidation activity when compared to lead treated groups and this might be due to action of lipid lowering effect and reduction of tissue lipid peroxide (MDA) of

flaxseed[24,25,26].

Significant decrease in the SOD, CAT and GPX levels was recorded in brains of lead acetate-treated rats (Group II) compared to control rats (Group I). These findings were in agreement with previous researchers[27,28,29] and the decrease in levels of antioxidant enzymes might be due to lead-induced generation of reactive oxygen species (ROS) (or) by reducing the antioxidant cell defense system by depleting glutathione (or) by inhibiting sulfhydryl dependent enzymes or by interfering with some essential metals like copper needed for antioxidant enzyme activities[30]. Emblica ameliorated group (Group V) showed significant increase in SOD, GPx and CAT levels and this might be due to antioxidant property of the tannoid rich fraction of Emblica includes Emblican in A and B[31]. Significant increase in SOD, GPx and CAT levels were noticed in Flaxseed treated rats (Group VI) and this might be due to presence of Omega-3 fatty acid and SDG in flaxseed which exhibit antioxidant properties and may help in maintaining the normal antioxidant enzymes levels by preventing lead induced cell damage[32].

Microscopically, brain revealed sub meningeal haemorrhages, mild to moderate capillary proliferation in cerebral cortex, rounding and loss of Purkinje cells in the cerebellum, severe congestion of cerebral blood vessels and choroid plexuses, shrinkage of neurons, demyelinating changes and spongiosis and focal loss of cerebral cortex with gliosis, severe neuronal degeneration with central chromatolysis, neurophagia, formation of nodule like structure along with MNCs infiltration in cerebral cortex throughout the experiment. These results were in accordance with[32,33] and the changes in present study might be due to neurotoxic effect of lead by altering certain membrane bound enzymes and might have led to oxidative stress as lead crosses the blood brain barrier quite readily[34,35]. The changes noticed in Emblica ameliorated group (Group V) were mild in intensity when compared to lead treated rats (Group II) and this might be associated with ascorbic acid content of Emblica that promotes elimination of reactive oxygen species (ROS), thereby helping to reduce oxidative stress generated by lead toxicity[30&36]. Microscopically, similar lesions were observed in brain of Flaxseed ameliorated groups (Group VI) but in mild form the reason might be due to the presence of Omega-3 fatty acid and SDG in flaxseed which exhibit antioxidant properties and helps in scavenging the reactive oxygen species (ROS) produced during lead exposure. Thus prevent the oxidative stress induced cell death in brain and explain the less severe degenerative changes in brain tissue of flaxseed ameliorated rats (Group VI)[31,32].

In conclusion, the findings from the present study indicate that lead (Pb) is having deleterious effect on brain and causes various degenerative changes and these changes were aggravated by increase in lipid peroxidation and decrease in antioxidant enzymes levels in brain. Co-administration of flaxseed oramla with lead found to be beneficial against lead induced toxicity as it is evident by improvement in various pathological manifestations in flaxseed and amla ameliorated group. So it can be assumed that supplementation of antioxidant agents like amla and flaxseed in veterinary and human medicine can be useful in heavy metal toxicity as a supportive therapy to minimize the harmful and toxic effects of different heavy metals like lead.

ACKNOWLEDGEMENTS

The authors are thankful to Dean, College of Veterinary Science, Tirupati, India for providing various facilities during the research period.

REFERENCES

1. Skerfving S, Nilsson U, Schutz A and Gerhardsson L. 1993. Biological monitoring of inorganic lead. *Scand J Work Environ Health* **19:** 59-64.
2. Canfield R, Henderson C, Cory-Slechta D, Cox C, Jusko T and Lanphear B. 2003. Intellectual Impairment in Children with Blood lead concentration below 10 microgram per decilitre. *N Engl J Med* **348:** 1517-1526.
3. Guilarte TR, Toscano CD, McGlothan JL and Weaver SA. 2003. Environmental enrichment reverses cognitive and molecular deficits induced by developmental lead exposure. *Ann Neurol* **53:** 50-56.
4. Flora S, Pande M and Mehta A. 2003. Beneficial effects of combined administration of some naturally occurring antioxidants (vitamins) and thiol chelators in the treatment of chronic lead intoxication. *Chem Biol Interact* **145:** 267-280.
5. Zhang Y, Abe T, Uang C and Kouno I. 2001. Phyllanemblinins A-F, New ellagitannins from *Phyllanthus emblica*. *J Nat Prod* **64:** 1527-153.
6. Anila L and Vijayalakshmi NR. 2002. Flavinoids from *Emblica officinalis* and *Mangiferaindica* effectiveness for dyslipidemia. *J Ethano Pharmacol* **79:** 81-87.
7. Ghosal S, Tripathi VK and Chauhan S. 1996. Active constituents of *Emblica officinalis*: Part I - The chemistry and antioxidant effects of two new hydrolysable tannins, Emblicanin - A and B. *Indian J Chem* **35:** 941-948.
8. Rhee Y and Brunt A. 2011. Flaxseeds supplementation improved insulin resistance in obese glucose intolerant people: a randomized crossover design. *Nut J* **10:** 44.
9. Zanwar AA, Hedge MV and Bodhankar SL. 2011. Cardioprotective activity of flax lignan concentrate extracted from seeds of *Linumusitatissiumum* in isoprenalin induced myocardial necrosis in rats. *Inter Toxicol* **4:** 90-97.
10. Troina AA, Figueriedo MS, Moura EG, Boaventura GT, Soares LL and Cardozo LF. 2010. Maternal flaxseed diet during lactation alters milk composition and programs the offspring body composition, lipid profile and sexual function. *Food Chem Toxicol* **48:** 697-703.
11. Zhang Z, Li D, Wang L, Ozkan N, Chen XD, Mao Z and Yang H. 2007. Optimization of ethanol-water extraction of lignans from flaxseed. *Sep Purif Technol* **57:** 17-24.
12. Culling CFA. 1974. eds. Hand Book of Histopathological and Histochemical Techniques (Including Museum Techniques). Butterworth-Heinemann-London.

13. Yagi K. 1976. Simple fluorimetric assay for lipid peroxides in blood plasma. *Biochem Med* **15:** 212-216.
14. Moron MS, Depierre JW and Mannervik B. 1979. Levels of glutathione, glutathione reductase and glutathione-S-transferase activities in rat lung and liver. *Acta Biochem Biophys* **582:** 67-78.
15. Marklund SL and Marklund G. 1974. Involvement of superoxide anion radical in the autoxidation of pyrogallol and a convenient assay for superoxide dismutase. *Eur J Biochem* **47:** 496-474.
16. Caliborne AL. 1985. eds. In Handbook of Oxygen Radical Research. Florida: CRC Press, Baco-Raton.
17. Rotruck JD, Pope AL, Ganther HE, Swanson AB, Hafeman DG and Hekstra. 1973. Selenium, biochemical role as a component of glutathione peroxidase and assay. *Science* **179:** 588-590.
18. Snedecor WG and Cochran GW. 1994. Statistical Methods, New Delhi: Oxford and IBH Publishing Company.
19. Upasani CD, Khera A and Balaraman R. 2001. Effect of lead with Vitamin E, C or Spirulina on malondialdehyde, conjugated dienes and hydroperoxides in rats. *Indian J Exp Biol* **39:** 70-74.
20. Wang J, Zhu H, Yang Z and Liu Z. 2013. Antioxidative effects of hesperetin against lead acetate-induced oxidative stress in rats. *Indian J Pharmacol* **45:** 395-8.
21. El-Nekeety AA, El-Kady AA, Soliman MS, Hassan NS and Abdel-Wahhab MA. 2009. Protective effect of Aquilegiavulgaris (L.) against lead acetate-induced oxidative stress in rats. *Food Chem Toxicol* **47:** 2209-2215.
22. Ponce-Canchihuaman JC, P´erez-M´endez O, Hern´andez-Mu˜noz PV, Torres-Dur´an K and Ju´arez-Oropeza MA. 2010. Protective effects of Spirulina maxima on hyperlipidemia and oxidative-stress induced by lead acetate in the liver and kidney. *Lipids Health Dis* **9:** 35-38.
23. Paul A, Sujatha K, Srilatha CH and Kumar NV. 2021. Amelioration of Lead induced toxicity on rat ovary with *Linumusitatissimum* (flaxseed) and *Emblica officinalis* (Amla). *J Pharm Innov* **10:** 1124-1130.
24. Prasad K. 2000. Antioxidant activity of secoisolariciresinol di glucoside-derived metabolites, secoisolariciresinol, enterodiol, and enterolactone. *Int J Angiol* **9:** 220-225.
25. Lee P and Prasad K. 2003. Effects of flaxseed oil on serum lipids and atherosclerosis in hypercholesterolemic rabbits. *J Card Pharmacol Ther* **8:** 227-235.
26. Khan MW, Privamvada S, Khan SA, Naqshbandi A, Khan S and Yusufi AN. 2012. Protective effect of 3 polyunsaturated fatty acids (PUFAs) on sodium nitroprusside-induced nephrotoxicity and oxidative damage in rat kidney. *Hum Exp Toxicol* **31:** 1035-1049.
27. Wang C, Liang J, Zhang C, Bi Y and Shi S. 2007. Effect of Ascorbic Acid and Thiamine Supplementation at Different Concentrations on Lead Toxicity in Liver. *Ann Occup Hyg* **51:** 563-569.
28. Wang J, Wu J and Zhang Z. 2006. Oxidative Stress in Mouse Brain Exposed to Lead. *Ann Occup Hyg* **50:** 405-409.
29. Paul A, Sujatha K, Srilatha CH and Kumar NV. 2022. Effect of Lead toxicity on liver and kidney in Wistar rats and its amelioration with *Linumusitatissimum* (flaxseed) and *Emblica officinalis* (amla). *Indian J Vet Pathol* **46:** 49-58.
30. Alghazal MA, Lenartova V, Holovska K, Sobekova A, Falis M and Legath J. 2008. Activities of Anti-oxidant and detoxifying enzymes in rats after lead exposure. *Acta Vet Brno* **77:** 347-354.
31. Paul A, Sujatha K, Srilatha CH and Kumar NV. 2022. Haematobiochemical study on effect of *Linumusitatissimum* (flaxseed) and *Emblica officinalis* (amla) against lead toxicity in Wistar rats. *Indian J Vet Pathol* **46:** 141-149.
32. Sekine S, Sasanuki S, Murana Y, Aoyama T and Takeuchi H. 2008. Alpha-linolenicacidrich flaxseed oil ingestion increases plasma adiponectin level in rats. *Int J Vitam Nut Res* **78:** 223-229.
33. Christian RG and Tryphonas LC. 1971. Lead poisoning in Cattle: Brain lesions and Haematological changes. *Am J Vet Res* **32:** 203-216.
34. Wells GA, Howell JMC and Gopinath C. 2008. Experimental Lead Encephalopathy of calves. Histological observations on the nature and distribution of the lesions. *Neuropathol Appl Neurobiol* **21:** 175-190.
35. Reddy GR, Devi BC and Chetty CS. 2006. Developmental lead neurotoxicity: Alterations in brain cholinergic system. *Neurotoxicol* **30:** 568-574.
36. Shalini B and Sharma JD. 2014. Mitigation of fluoride toxicity through emblica officinalis in rats. *Int J Innov Res Tecnol Sci* **2:** 5-10.

Indian J. Vet. Pathol., 49(1) : 56-63, 2025: DOI: https://doi.org/10.5958/px9q4t80

RESEARCH ARTICLE

Ameliorative effects of microalgal *Spirulina* protein fortified with leaf powder of *Moringa* and finger millet on glucocorticoid induced osteoporosis in rats

Vijay Kumar, V.T. Shilpa*, B.C. Girish, G.B. Manjunatha Reddy[1], S.P. Satheesha[2], N.M. Rajashailesha[3], K.R. Anjan Kumar, P. Ravikumar[4] and S.N. Pramod[5]

Department of Veterinary Pathology, Veterinary College, Hassan, KVAFSU, Bidar, [1]NIVEDI-ICAR, Bengaluru, India, [2]Department of Veterinary Public Health and Epidemiology, [3]Department of Veterinary Anatomy, [4]Department of Veterinary Pathology, Veterinary College, Shivamogga, India, [5]Department of Studies in Biochemistry and Food Technology, Davangere University, Shivagangotri, Davanagere, India

Address for Correspondence

V.T. Shilpa, Assistant Professor, Department of Veterinary Pathology, Veterinary College, Hassan, KVAFSU, Bidar, India, E-mail: drshilpavt@gmail.com

Received: 4.1.2025; Accepted: 21.1.2025

ABSTRACT

The current investigation was conducted to assess the anti-osteoporotic potential of microalgal *Spirulina* protein fortified with leaf powder of *Moringa* and Finger millet (MSMF) in female Wistar rat model of Methylprednisolone induced osteoporosis. The study included six groups of six rats each. Group I (normal control) rats, received distilled water orally daily for seven weeks, Group II (disease control) to VI rats received Methylprednisolone @ 40 mg/kg bw subcutaneously thrice a week for six weeks from 2nd to 7th week of the experimental period. Additionally, Group III (reference control) rats received Alendronate at 40 µg/kg body weight subcutaneously three times a week for the same duration. Group IV, V and VI rats received MSMF @ 500, 1000 and 2000 mg/kg bw respectively, daily orally for seven weeks, along with Methylprednisolone. Group II rats showed significant decrease in feed intake, body weight, femur weight, haemato-biochemical parameters, radiological and histopathological parameters of the femur. The changes caused by Methylprednisolone were alleviated in Alendronate group and MSMF treatment groups in a dose dependent manner. Histopathologically, the MSMF treatment groups showed substantial improvement in trabecular thickness, cortex thickness, osteocyte number, reduction in resorption cavities and erosion of cartilage. The anti-osteoporotic efficacy of MSMF @ 500 mg/kg was lower than that of Alendronate, while the MSMF @ 1000 mg/kg and 2000 mg/kg bw showed better efficacy than MSMF @ 500 mg/kg and equivalent to the effects of Alendronate.

Keywords: Finger millet, methylprednisolone, microalgal *Spirulina* protein, *moringa*, Osteoporosis

INTRODUCTION

Osteoporosis is a systemic condition associated with aging that typically affects mammals, primarily humans. It is a condition marked by reduced bone density and the weakening of bone structure, which results in increased fragility and vulnerability to fractures[1]. About one in three women and one in five men over 50 years will suffer a fracture due to osteoporosis[2]. These numbers emphasize the importance of awareness, early detection and proactive measures to prevent osteoporotic fractures.

Osteoporosis arises through either primary or secondary causes. Primary osteoporosis is due to rapid bone loss following menopause due to oestrogen decline and gradual age-related bone loss in older individuals, affecting both men and women[3]. Secondary osteoporosis arises due to many causes including hypogonadism, endocrine disorders, gastrointestinal diseases, transplantation, genetic disorders and drugs such as anticoagulants, glucocorticoids, anti-convulsants etc. Among drug-induced osteoporosis cases, glucocorticoids are the most frequent cause. Glucocorticoids, directly and indirectly impact the skeleton, mainly affecting osteoblasts and osteocytes. They promote the formation of osteoclasts, leading to increased bone breakdown[4].

Glucocorticoids are widely used as the standard treatment for alleviating inflammation and to promote immunosuppression in conditions such as asthma, allergic reactions, rheumatoid diseases, dermatological issues, collagen and vascular disorders, inflammatory bowel disease, other systemic illnesses and ocular inflammatory diseases. However, use of glucocorticoids with higher doses and for prolonged periods may increase the likelihood of osteonecrosis and osteoporosis[5].

How to cite this article : Kumar, V., Shilpa, V.T., Girish, B.C., Reddy, G.B.M., Satheesha, S.P., Rajashailesha, N.M., Kumar, K.R.A., Ravikumar, P. and Pramod, S.N. 2025. Ameliorative effects of microalgal *Spirulina* protein fortified with leaf powder of *Moringa* and finger millet on glucocorticoid induced osteoporosis in rats. Indian J. Vet. Pathol., 49(1) : 56-63.

Table 1. The mean (± SE) body weight (g) values of rats of different experimental groups in the study at weekly interval.

Groups	Day 0	1st Week	2nd Week	3rd Week	4th Week	5th Week	6th Week	7th Week
Group I (NC)	227.0 ± 5.63^{A}	231.0 ± 5.63^{A}	232.7 ± 4.65^{A}	254.0 ± 3.13^{Ba}	263.5 ± 1.23^{BCa}	268.2 ± 2.41^{Ca}	271.3 ± 3.65^{Ca}	275.5 ± 3.60^{Ca}
Group II (DC)	226.8 ± 5.27^{A}	230.8 ± 5.27^{A}	229.2 ± 4.83^{A}	210.0 ± 4.13^{Bb}	208.8 ± 5.11^{Bb}	218.2 ± 3.02^{ABb}	225.0 ± 7.76^{Ab}	228.5 ± 4.11^{Ab}
Group III (RC)	227.2 ± 6.21^{A}	231.2 ± 6.21^{A}	230.8 ± 3.76^{A}	237.7 ± 3.02^{ABc}	251.0 ± 3.71^{BCa}	258.8 ± 2.84^{Ca}	262.2 ± 2.04^{Ca}	263.7 ± 4.77^{Ca}
Group IV (MSMF @ 500)	227.5 ± 6.71^{A}	231.5 ± 6.71^{A}	236.5 ± 4.58^{AB}	247.0 ± 4.85^{BCac}	253.0 ± 4.11^{CDa}	260.0 ± 3.40^{CDa}	262.7 ± 3.87^{Da}	264.5 ± 4.94^{Da}
Group V (MSMF @ 1000)	227.7 ± 7.64^{A}	231.7 ± 7.64^{A}	235.7 ± 5.39^{AB}	248.3 ± 4.59^{BCac}	257.5 ± 3.06^{CDa}	260.7 ± 2.68^{CDa}	261.5 ± 2.58^{CDa}	265.8 ± 5.57^{Da}
Group VI (MSMF @ 2000)	227.8 ± 7.20^{A}	231.8 ± 7.20^{A}	238.3 ± 4.98^{AB}	248.7 ± 5.47^{BCac}	256.5 ± 4.73^{CDa}	264.0 ± 3.44^{Da}	264.0 ± 2.74^{Da}	266.5 ± 4.97^{Da}

Mean ± SE bearing different superscripts (abcd; within column and ABCD; between columns) are statistically significant at $p < 0.05$ (n = 6)

Various drugs targeting bone resorption or formation have been developed to address bone loss, but they are often ineffective for primary and secondary osteoporosis and may cause adverse side effects. As a result, herbal remedies are used as alternatives as they are widely accepted, accessible, affordable and believed to have fewer side effects[6].

Spirulina platensis is a type of blue-green microalgae which has been recognized for its potential as a calcium source. Since, *Spirulina* is rich in protein and minerals, it has garnered attention for its ability to boost mineral absorption by influencing intestinal microflora[7]. *Moringa Oleifera* leaves are rich in minerals like calcium, potassium, zinc, magnesium, iron and copper. Additionally, they contain abundant phytosterols such as stigmasterol, sitosterol and kampesterol, serves as precursors for oestrogen production which can have positive effect on bone[8]. Finger millet has all the quantitative and qualitative attributes needed to be a prototype for calcium bio fortification. It notably emerges as the most abundant source of calcium among all cereal grains contributing to bone strength[9].

To avoid osteopenia and osteoporosis, it's necessary to take calcium and vitamin D supplements. *Spirulina, Moringa oleifera* leaves and Finger millet have good amounts of calcium and phytochemicals which prevents bone loss. The present research work was undertaken to investigate the protective effects of microalgal *Spirulina* protein fortified with leaf powder of *Moringa* and Finger millet (MSMF) on glucocorticoid induced osteoporosis in female rats.

MATERIALS AND METHODS

Animals

The study was conducted on 36 adult female Wistar rats, of six month age, weighing around 200 to 250g, procured from Spring Labs, Vasanthanarasapura, Tumkur, Karnataka (Reg. No. 2259/PORcbiVt/S/23/CCSEA). All the rats were acclimatized to standard laboratory conditions for seven days prior initiation of the experiment and maintained at 22±3^{O}C temperature, humidity of 30 to 70% and 12-hour light/dark cycle throughout the study period. Rats provided with regular standard pellet diet along with free access to deionized drinking water *ad libitum* throughout the course of the experiment. The animals were handled as per CCSEA guidelines and study was approved by the Institutional Animal Ethical Committee (HVC/IAEC/08/2024).

Preparation and administration of drug

Methylprednisolone sodium succinate (MP) was procured from NEON Laboratories Limited, Mumbai, India. It was diluted in distilled water and injected subcutaneously at 40 mg/kg bw. The MSMF, which was extracted, purified and having composition of 55 g of brown ragi, 20 g of *Moringa* powder, 15 g of *Spirulina* and 10 g of jaggery powder per 100 g was obtained from the Department of Food Technology, Davangere University, Shivagangotri, Davangere. It was used at the dose rate of 500, 1000 and 2000 mg/kg bw orally. Alendronate was procured from Sigma Aldrich Corporation, St. Louis, USA and was injected subcutaneously at the rate of 40 µg/kg bw in distilled water.

Experimental design

The study included six treatment groups comprising of six rats in each group. Group I served as normal control (NC) and received distilled water orally throughout the experiment and subcutaneously from 2nd week to end of 7th week; Group II disease control (DC) rats

Fig. 1. Dorso-ventral radiograph of femur of control Group I rat showing normal cortex thickness and radiodensity; **Fig. 2.** Dorso-ventral radiograph of femur of disease control Group II rat showing reduction in cortex thickness and reduced radiodensity; **Fig. 3.** Dorso-ventral radiograph of femur of Group VI rat showing improved cortex thickness and radiodensity.

received MP at 40 mg/kg bw, subcutaneously, thrice a week for six weeks (from 2nd to 7th week) and distilled water orally throughout the experiment; Group III (RC) rats along with MP treatment received Alendronate subcutaneously thrice a week (from 2nd to 7th week); Group IV rats along with MP treatment received MSMF at 500 mg/kg bw daily from 1st week to 7th week; Group V rats along with MP treatment received MSMF at 1000 mg/kg bw daily from 1st week to 7th week; while Group VI rats along with MP treatment received MSMF at 2000 mg/kg bw daily from 1st week to 7th week.

Parameters studied

Body weight (g) and feed (g) consumption were assessed every week. At the end of the study (49th day), all rats were anaesthetized by using Ketamine and Xylazine (as I/M injection) to take lateral and anterio-posterior radiographs of femurs of animals. The radiographic images were acquired using 63 kVp, 8 mA and exposure time of 0.06 s with focal distance of 30 mm. Radio density of bones was used for evaluation of osteoporosis in long bones of rats. Blood was collected from retro-orbital plexus in EDTA and serum vials for hematological and biochemical analysis, respectively. All animals were sacrificed humanely and were subjected for detailed post-mortem examination. The mean femur weight in grams at the end of the study were recorded.

Histopathology

Representative femur samples from rats of all the groups were subjected to histopathological studies. The tissue was fixed using 10% Neutral Buffered Formalin solution and decalcified by formic acid (90%) sodium citrate method. Sections were prepared using paraffin blocks and stained with hematoxylin and eosin (H&E) and Masson's trichrome (MT) after dewaxing[10].

Histopathological scoring

The femur samples were examined in random microscopic areas and the changes were assessed by counting 20 different non overlapped fields for the same slide of each animal[11]. Cortical bone thickness (µm) was measured under low power field from the periosteum to endosteum at three different points in each section; osteocyte lacunae with or without nuclei were counted in oil immersion to know the severity of osteoporosis.

Statistical analysis

Statistical analysis of the data collected for various parameters was done using one-way ANOVA with Tukey's test and two-way ANOVA with Duncan's post hoc test[12].

RESULTS

General observations

Group I rats remained active throughout the period

Table 2. The mean (±SE) values of various haematological parameters of rats in different groups on day 49th of the study.

Groups	TEC (10^6/µl)	TLC (10^3/µl)	Hb (g/dl)	Platelet (10^3/µl)	PCV (%)
Group I (NC)	5.04 ± 0.10^{a}	8.43 ± 0.12^{a}	13.02 ± 0.52^{a}	494.0 ± 18.65^{a}	40.50 ± 1.68^{a}
Group II (DC)	3.77 ± 0.15^{d}	4.48 ± 0.11^{d}	9.68 ± 0.38^{b}	299.7 ± 10.64^{b}	32.47 ± 1.06^{b}
Group III (RC)	4.02 ± 0.17^{cd}	5.43 ± 0.12^{c}	11.82 ± 0.45^{a}	360.0 ± 9.52^{b}	34.75 ± 0.76^{bc}
Group IV (MSMF @ 500)	4.16 ± 0.09^{bd}	6.93 ± 0.08^{b}	12.17 ± 0.29^{a}	435.2 ± 15.94^{a}	36.88 ± 1.64^{ab}
Group V (MSMF @ 1000)	4.56 ± 0.09^{abc}	7.12 ± 0.11^{b}	12.37 ± 0.32^{a}	463.2 ± 14.01^{a}	36.58 ± 1.19^{ab}
Group VI (MSMF @ 2000)	4.67 ± 0.16^{ab}	7.10 ± 0.08^{b}	12.73 ± 0.27^{a}	450.5 ± 14.62^{a}	38.55 ± 1.27^{ac}

Mean ± SE values with different superscript differ significantly at $p < 0.05$ (n = 6)

of experiment. Group II rats exhibited clinical signs such as reduced feed intake, dullness, reduced body weight, arched back, ruffled fur, looked restless and were difficult to handle. The rats of Group III to VI manifested similar clinical signs as that of disease control rats, but with reduced intensity and frequency.

Feed consumption

Mean weekly feed consumption in Group I rats were normal and progressive. Group II rats showed significant decrease in

Table 3. The mean (±SE) values of various serum biochemical parameters of rats in different groups on day 49th of the study.

Groups	Calcium (mg/dl)	Phosphorous (mg/dl)	ALP (IU/L)
Group I (NC)	9.93 ± 0.28^{a}	4.92 ± 0.17^{a}	76.33 ± 3.32^{a}
Group II (DC)	8.12 ± 0.21^{b}	4.07 ± 0.28^{b}	44.50 ± 1.78^{c}
Group III (RC)	9.37 ± 0.40^{ab}	4.63 ± 0.12^{ab}	75.00 ± 2.38^{a}
Group IV (MSMF @ 500)	8.75 ± 0.26^{ab}	4.45 ± 0.11^{ab}	58.33 ± 1.87^{b}
Group V (MSMF @ 1000)	9.08 ± 0.35^{ab}	4.33 ± 0.18^{ab}	64.67 ± 1.84^{b}
Group VI (MSMF @ 2000)	9.22 ± 0.42^{ab}	4.55 ± 0.19^{ab}	67.17 ± 1.81^{ab}

Mean values with different superscript differ significantly at $p < 0.05$ (n = 6)

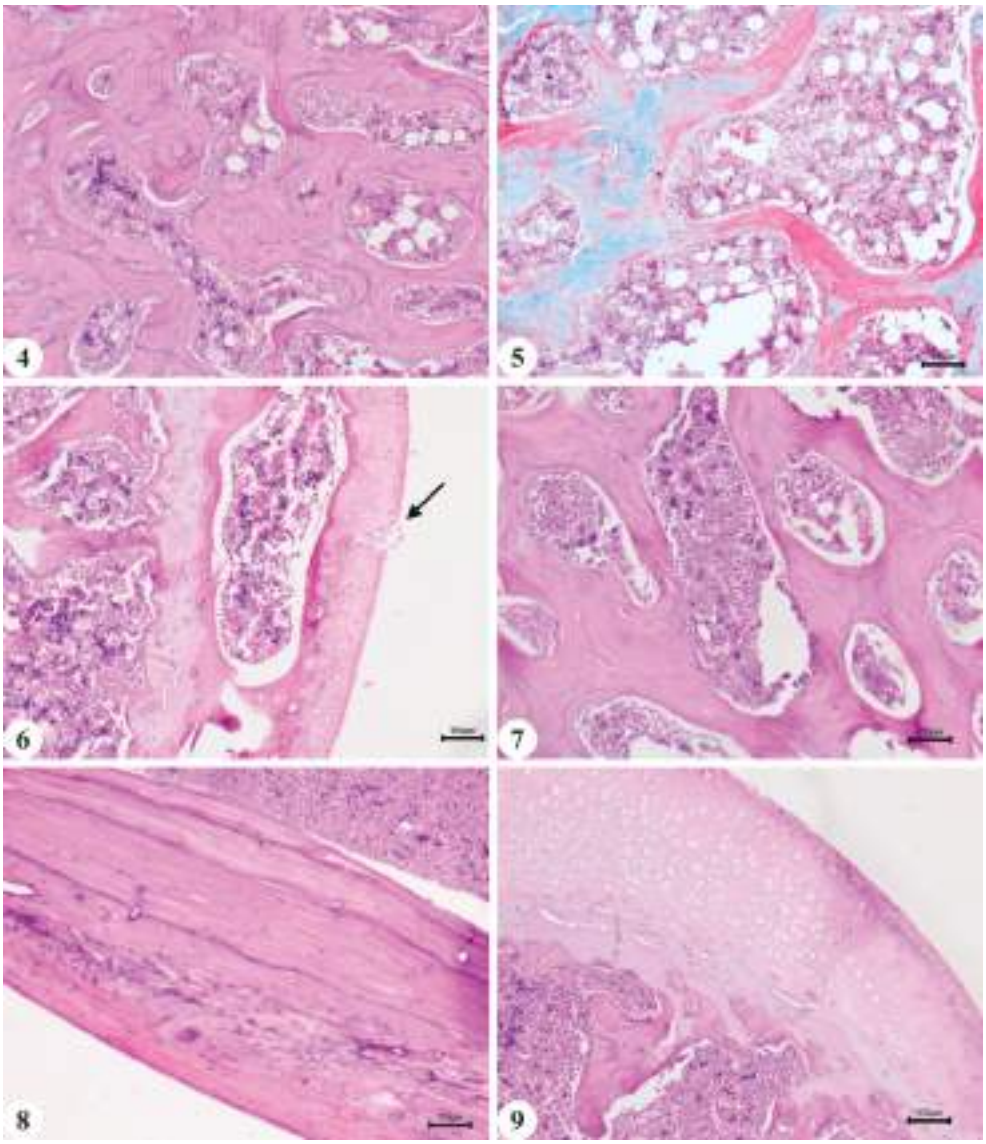

Fig. 4. Femur head from Group I rat showing normal architecture of trabecular bone with thick network of trabeculae and regular bone marrow spaces (H&E X100); **Fig. 5.** Femur bone from Group II rat showing thinning of trabeculae with reduced collagen and wider bone marrow spaces (MT X100); **Fig. 6.** Femur bone from Group II rat showing reduced cartilage thickness and with erosion (arrow) (H&E X100); **Fig. 7.** Femur head from Group VI rat showing moderate improvement in the thickness of trabeculae with increased collagen and reduced widening of bone marrow spaces (H&E X100); **Fig. 8.** Femur bone from Group IV rat showing improvement in the cortical thickness of compact bone and increased cellularity (H&E X100); **Fig. 9.** Femur head from Group VI rat showing moderate improvement in cartilage thickness with reduced break in between cartilage (H&E X100).

feed consumption of about 5.29%, 10.99%, 11.23%, 8.49%, 7.72% and 8.40% during 2nd, 3rd, 4th, 5th, 6th and 7th week, respectively as compared to Group I. During first two weeks, Group V rats showed a significantly ($p < 0.05$) higher feed intake compared to other groups. From 3rd to 7th week, all the treatment groups showed a significant increase in weekly feed consumption compared to Group II rats.

Body weight

The mean±SE body weights at different time intervals of 0 day and 1st, 2nd, 3rd, 4th, 5th, 6th and 7th week of experiment are presented in Table 1. Group I rats remained healthy throughout the period of experiment and showed progressive enhancement in their body weight over the course of experiment. Body weight of Group II rats decreased significantly from 3rd to 7th week compared to Group I. The animals of Group IV to VI showed significant improvement in the body weight from 3rd to 7th week when compared to Group II.

Radiography

Radiographic images of femur and tibia of Group II rats revealed decreased radio density (bone density) with thinning of cortical bone and increased medullary cavity. Also, diaphyseal fracture of tibia was seen in one rat in Group II. In the treatment groups (Group IV to VI), the radiographic images of femur and tibia showed no significant difference in radio density, cortex thickness and were comparable to that of control rats. Also, the treatment groups showed significant improvement in bone density and cortex thickness of femur and tibia when compared to Group II with no evidence of fractures (Fig. 1 to 3).

Organ weight

Group II showed significant ($p < 0.05$) decrease in absolute weight of femur in comparison to Group I, where as in Group III, IV, V and VI, femur weights were significantly ($p < 0.05$) higher than Group II.

Haematology parameters

The mean±SE values of hematological parameters on 49th day of the experiment are presented in Table 2. The mean values of Total erythrocyte count (TEC), total leucocyte count (TLC), haemoglobin (Hb), platelets (PLT) and packed cell volume (PCV) of Group II rats were significantly ($p < 0.05$) decreased when compared to Group I rats. The TEC in Group V and VI; the TLC, Hb and PLT in Group IV to VI rats; the PCV in Group VI were increased significantly ($p < 0.05$) as compared to Group II rats. The TEC values of Group V rats and PCV values of Group V and VI rats were slightly increased as compared to Group II rats.

Serum biochemistry

The mean±SE values on 49th day of the experiment are presented in Table 3.

Serum calcium

There was a significant ($p < 0.05$) decrease in serum calcium levels of Group II rats by 18.22% than Group I rats. Among the treatment groups, there was no significant difference in mean serum calcium levels. The mean values of serum calcium levels of Group III, IV, V and VI rats were improved than Group II rats.

Serum phosphorous

There was a significant ($p < 0.05$) decrease in serum phosphorous levels of Group II rats by 17.28% than Group I rats. Among the treatment groups, there was no significant difference in mean serum phosphorous levels. The mean values of serum phosphorous levels of Group III, IV, V and VI rats were improved than Group II rats.

Alkaline phosphatase (ALP)

There was a significant ($p < 0.05$) decrease in serum ALP levels of Group II rats by 41.70% than Group I rats. Among the treatment groups (Group IV to VI), there was no significant difference in mean serum ALP levels. The mean values of serum ALP levels of Group III, IV, V and VI rats were significantly ($p < 0.05$) improved than Group II rats.

Gross pathology

The rats from Group II showed reduction in the femur length and reduction in the size of lymph node in four out of six rats. The rats from Group III to VI did not reveal any visible gross abnormalities.

Histopathology

Table 4. The mean (±SE) values of femur cortex thickness (μm), osteocyte number and number of empty lacunae (per field in oil immersion) of rats in different groups on final day (49th day) of the study.

Groups	Femur cortex thickness	Osteocyte number	Number of empty lacunae
Group I (NC)	682.3 ± 10.89^{a}	10.50 ± 0.56^{a}	2.45 ± 0.25^{a}
Group II (DC)	461.9 ± 11.31^{b}	6.60 ± 0.41^{b}	5.30 ± 0.33^{b}
Group III (RC)	621.9 ± 9.59^{c}	10.00 ± 0.47^{a}	2.95 ± 0.28^{a}
Group IV (MSMF @ 500)	482.7 ± 12.70^{b}	9.30 ± 0.42^{a}	4.15 ± 0.23^{c}
Group V (MSMF @ 1000)	580.7 ± 8.21^{c}	9.75 ± 0.45^{a}	3.35 ± 0.23^{ac}
Group VI (MSMF @ 2000)	596.6 ± 6.75^{c}	9.85 ± 0.55^{a}	3.25 ± 0.30^{ac}

Mean values with different superscript differ significantly at $p < 0.05$ (n = 6)

The femur of the Group II rats showed decreased cortical thickness of compact bone, reduced osteocyte and osteoblast numbers, increased number of empty lacunae without osteocytes, erosion of periosteal and endosteal layers. The cortical bones showed cracks and fissures with few abnormal osteocytes and haversian canals. There was loss of normal architecture of inner cancellous bone trabeculae with thinning of trabeculae thickness, wider bone marrow spaces filled with increased number of adipocytes and discontinuous bony ossicles. Further, the cartilage thickness was reduced along with break in between or incomplete cartilage when compared to control Group I rats (Fig. 4 to 6). Group III rats revealed microscopical changes similar to that of Group II rats but with mild improvement. The femur of Group IV to VI rats showed mild to moderate improvement in the cortical thickness of compact bone, minimal to moderate increase in cellularity, decreased empty lacunae and increased mineralisation when compared to Group II rats. There was mild improvement in the endosteal surface with reduced erosion. The cracks and fissures of cortical bones were reduced. There was mild improvement in the loss of normal architecture of inner cancellous bone trabeculae with minimal improvement in trabeculae thickness and reduced bone marrow spaces. The thickness of cartilage was improved with reduced break in between when compared to Group II rats (Fig. 7 to 9).

Histopathological score of femur

The HP score of all sectioned femur samples assessed for parameters like femur cortex thickness and osteocyte lacunae with or without nuclei are presented in the Table 4. Group II rats showed significant ($p < 0.05$) decrease in mean femur cortical thickness and mean number of osteocyte lacunae with nuclei and significant ($p < 0.05$) increase in mean number of osteocyte lacunae without nuclei when compared to Group I rats. The mean femur cortex thickness was significantly ($p < 0.05$) higher in Group III, V and VI but non-significantly higher in Group IV rats in comparison to Group II rats. The mean osteocyte lacunae with nuclei was significantly ($p < 0.05$) higher in Group III to VI in comparison to Group II rats. The mean osteocyte lacunae without nuclei were significantly ($p < 0.05$) lower in Group III to VI in comparison to Group II rats.

DISCUSSION

Glucocorticoid induced reduction in femur weight were in accordance with the reports of previous findings[13,14]. MP induced decrease in haematological parameters like TEC, TLC, Hb, PLT and PCV values were similar to those previously reported[14]. Decline in blood parameters could be associated with the negative effects of glucocorticoids on bone marrow and intravascular lysis and decreased release of immune cells from the bone marrow[15].

The TEC, TLC, PLT and Hb values in all the MSMF treated groups (Groups IV to VI) were improved significantly compared to Group II rats. Studies on animal models documented that phycocyanin of *Spirulina* induces the expression of bcl-2 in haematopoietic cells that may inhibit apoptosis. There is also evidence that c-phycocyanin and polysaccharides of *Spirulina* enhance white blood cell production[16]. It plays a role in improves immune system efficiency, as well as playing an important part in stimulation of the erythropoiesis[17]. It was opined that increased haematological values in *Moringa* leaves administration was related to the components such as protein amino acids, vitamins B, E and iron[18]. Finger millet has good amounts of thiamine, riboflavin, iron, methionine, isoleucine, leucine, phenylalanine, essential amino acids and polyphenols[19] which may enhance the production of haematological parameters.

A significant decrease in the mean values of serum calcium, phosphorous and alkaline phosphatase was observed in the disease control rats[13,20]. It has been previously highlighted the significance of these biochemical markers in detecting osteoporosis resulting from Glucocorticoid administration[13,15]. Glucocorticoid usage may cause decrease in calcium and phosphorous absorption in the intestine and decreased renal reabsorption of calcium and phosphorus[21]. The reduction in ALP is due to inhibition of osteoblastogenesis and apoptotic effects of glucocorticoids on both osteoblasts and osteocytes[22].

The improved serum calcium, phosphorous and ALP levels in MSMF treated groups may be attributed due to presence of rich minerals, vitamins in *Spirulina* and improved mineral absorption in intestine by positive effect on intestinal microflora by *Spirulina*[23], due to *Moringa* leaf which are rich in flavonoids, phytoestrogens and phytochemicals like kaempferol and quercetin which has osteoblastic potential and prevents osteoclastic resorption[24].

MP administration also caused a significant reduction in radio density (bone density) of femur and tibia with thinning of cortical bone and increased medullary cavity. Further, diaphyseal fracture of tibia was seen in one out of six rats. These findings were previously reported earlier[14,21] and they opined that long term use of glucocorticoids causes bone resorption and decreased bone mineral density.

The histopathological examination of femur from rats in the disease control group revealed decreased cortical thickness of femur, reduced osteocyte and osteoblast numbers, increased number of empty lacunae without osteocytes[11]. The endosteal surface was irregular[25], cortex showed cracks and fissures with few abnormal

osteocytes and haversian canals. The intercellular substance consisted of non-homogenous ground matrix with several resorption cavities within the matrix when compared to normal control group rats. The lamellae of the compact bone were reduced in thickness[11] when compared to normal control rats. Further, there was loss of normal architecture of inner cancellous bone trabeculae with thinning of trabeculae thickness, discontinuous bony ossicles and wider bone marrow spaces filled with increased number of adipocytes[23,26]. Histological changes in disease control rats may be due to use of glucocorticoids. Glucocorticoids inhibit expression of genes important for bone formation including those responsible for the production of collagen A1 TGF-β, fibronectin and IGF-1. They, also increase production of receptor activator of NF-kB ligand (RANKL) and reduced production of osteoprotegerin, resulting in increased osteoclast recruitment and survival[4,22]. Glucocorticoids induce apoptosis in osteoblasts and osteocytes by activating GSK-3 and caspase-3[27]. They lower IGF-1 gene transcription in osteoblasts leading to decrease production of type 1 collagen[4]. When glucocorticoids cause osteocyte apoptosis, this network may be disrupted, impairing the repair process and leading to micro damage accumulation and increased bone fragility[22].

Improvement in the treatment groups (Group IV, V and VI) may be attributed to the synergistic antiosteoporotic effects of *Spirulina*, *Moringa* leaves powder and Finger millet. *Spirulina* have been shown to reduce osteoclast formation by decreasing the number of TRAcP and RANKL-positive cells[28]. *Moringa* is abundant in flavonoids and phytoestrogens, which stimulate osteoblasts by acting through the estrogen receptor signalling and by reducing the RANKL-mediated osteoclastogenesis[13]. Further, ragi is rich source of calcium may be attributed to the improved microarchitecture and bone mineral density.

The current research showed that among the treatment groups, notably, histological changes of femur in rats from Group V and VI were less severe compared to those in Group IV and Group II rats. The anti-osteoporotic effect of MSMF in the present study suggests that *Spirulina* microalgae, leaf powder of *Moringa* and Finger millet can be used in combination as a potential preventive agent or as a supplement in treatment of osteoporosis. However, the underlying mechanisms that may play a therapeutic role in the prevention and control of osteoporosis by MSMF warrant further mechanistic studies to elucidate the mechanism of action.

REFERENCES

1. Karasik D. 2008. Osteoporosis: an evolutionary perspective. *Hum Genet* **124:** 349-356.
2. Akarirmak U. 2018. Osteoporosis: a major problem - worldwide. *Arch Sports Med* **2:** 106-108.
3. Hannan MT, Felson DT, Dawson-Hughes B, Tucker KL, Cupples LA, Wilson PW and Kiel DP. 2000. Risk factors for longitudinal bone loss in elderly men and women: the Framingham Osteoporosis Study. *J Bone Miner Res* **15:** 710-720.
4. Canalis E, Mazziotti G, Giustina A and Bilezikian JP. 2007. Glucocorticoid-induced osteoporosis: Pathophysiology and therapy. *Osteoporos Intl* **18:** 1319-1328.
5. Oray M, Abu Samra K, Ebrahimiadib N, Meese H and Foster CS. 2016. Long-term side effects of glucocorticoids. *Expert Opin Drug Saf* **15:** 457-465.
6. Che CT, Wong MS and Lam CWK. 2016. Natural products from Chinese medicines with potential benefits to bone health. *Molecul* **21:** 239-242.
7. Ishimi Y, Sugiyama F, Ezaki J, Fujioka M and Wu J. 2006. Effects of *Spirulina*, a blue-green alga, on bone metabolism in ovariectomized rats and hind limb-unloaded mice. *Biosci Biotech Biochem* **70:** 363-368.
8. Gopalakrishnan L, Doriya K and Kumar DS. 2016. *Moringa oleifera*: A review on nutritive importance and its medicinal application. *Food Sci Human Wellness* **5:** 49-56.
9. Dube S, Varade S and Choudhari V. 2024. Utility of Finger millet (ragi) in post-menopausal osteoporosis: A Review. *World J Pharm Res* **13:** 272-279.
10. Suvarna KS, Layton C and Bancroft JD. 2018. In: Bancroft's Theory and Practice of Histological Techniques, Edt. Kim Suvarna, Christopher Layton, John Bancroft. Edn. 8th, Elsevier Health Sciences Publication. Churchill Livingstone, pp. 174-190.
11. Kasem MA, Abdel-Aleem AM, Said AS and Khedr ESG. 2016. Histological effect of bisphosphonate, vitamin D and olive oil on glucocorticoid induced osteoporosis (GIO) in Albino Rat. *Egypt J Hosp Med* **65:** 699-708.
12. Snedecor GW and Cochran WG. 1994. Statistical Methods. Edn. 7th, Oxford and JBH Publications, New York, USA.
13. Elbahnasawy AS, Valeeva ER, El-Sayed EM and Stepanova NV. 2019. Protective effect of dietary oils containing omega-3 fatty acids against glucocorticoid-induced osteoporosis. *J Nutr Health* **52:** 323-331.
14. Rawat P, Ahmad AH, Pant D, Verma MK and Bisht P. 2020. Evaluation of anti-osteoporotic potential of *Moringa olifera* leaves in rats. *J Vet Pharma Toxicol* **19:** 25-28.
15. El-Sawy AESF, El-Maddawy ZK and Ashoura NR. 2018. Role of Silymarin in restoring the deleterious effects induced by dexamethasone in male rats. *Alex J Vet Sci* **59:** 32-46.
16. Khan Z, Bhadouria P and Bisen PS. 2005. Nutritional and therapeutic potential of *Spirulina*. *Curr Pharm Biotechnol* **6:** 373 -379.
17. Ali SK and Arabi MS. 2012. *Spirulina* - An overview. *Int J Pharm Pharm Sci* **4:** 9-15.
18. Nurhayati T, Fathoni MI, Fatimah SN, Tarawan VM, Goenawan H and Dwiwina RG. 2023. Effect of *Moringa oleifera* leaf powder on hematological profile of male wistar rats. *J Blood Med* **14:** 477-485.
19. Pandey V and Dahiya OS. 2018. Finger Millet: Secure food for future. *Indian Farmer* **5:** 1007-1013.
20. Elshal MF, Almalki AL, Hussein HK and Khan JA. 2013. Synergistic antiosteoporotic effect of *Lepidium sativum* and alendronate in glucocorticoid-induced osteoporosis in Wistar rats. *Afr J Tradit Complement Altern Med* **10:** 267-273.
21. Sousa LHT, Moura EV, Queiroz AL, Val D, Chaves H, Lisboa M, Furlaneto F, Brito GA and Goes P. 2017. Effects of glucocorticoid-induced osteoporosis on bone tissue of rats with experimental periodontitis. *Arch Oral Biol* **77:** 55-61.

22. Weinstein RS, Jilka RL, Parfitt AM and Manolagas SC. 1998. Inhibition of osteoblastogenesis and promotion of apoptosis of osteoblasts and osteocytes by glucocorticoids. Potential mechanisms of their deleterious effects on bone. *J Clin Invest* **102:** 274-282.
23. Siddiqui SA, Srikanth SP, Wu YS, Kalita T, Ambartsumov TG, Tseng W, Kumar AP, Ahmad A and Michalek JE. 2024. Different types of algae beneficial for bone health in animals and in humans-A review. *Algal Res* **88:** 103-593.
24. Guo AJ, Choi RC, Zheng KY, Chen VP, Dong TT, Wang ZT, Vollmer G, Lau DT and Tsim KWK. 2012. Kaempferol as a flavonoid induces osteoblastic differentiation via oestrogen receptor signalling. *Chinese Med* **7:** 1-7.
25. Moghazy HM, Mahmoud AA, Gebril SM, Foad AM, Refaei RA and Fadeil MR. 2023. Impact of exercise-induced irisin on bones of osteoporotic male rat model. *Gene Reports* **33:** 101-804.
26. Soliman T, Ali Z, Zayed M, Sabry D and AbuBakr N. 2021. The anti-osteoporotic effect of Moringa oleifera leaves extract on glucocorticoids-induced jawbone osteoporosis in Albino rats. *Braz Dent Sci* **24:** 1-9.
27. Yun SI, Yoon HY, Jeong SY and Chung YS. 2009. Glucocorticoid induces apoptosis of osteoblast cells through the activation of glycogen synthase kinase 3β. *J Bone Min Met* **27:** 140-148.
28. Yang Y, Yang H, Feng X, Song Q, Cui J, Hou Y, Fu X and Pei Y. 2024. Selenium containing protein from selenium-enriched *Spirulina platensis* relieves osteoporosis by inhibiting inflammatory response, osteoblast inactivation and osteoclastogenesis. *J Food Biochem* **16:** 1-11.

Indian J. Vet. Pathol., 49(1) : 64-67, 2025: DOI: https://doi.org/10.5958/x4ft9d66

SHORT COMMUNICATION

Atypical pathological presentation of *S. Suis* serotype 2 induced cerebral abscess in a naturally infected buffalo calf

Sourabh Babu, Dinesh Murali, Sagar Patel, Jigarji Chaturji Thakor, Rajendra Singh, Mamata Pasayat[1], Ramakant Acharya[1], Jagannath Prasad Tripathy[1], Prabin Kumar Sahoo[1], Nihar Ranjan Sahoo[1] and Monalisa Sahoo[1*]

Division of Pathology, ICAR-Indian Veterinary Research Institute (IVRI), Izatnagar, India, [1]ICAR-National Institute on Foot and Mouth Disease (NIFMD), Arugul, Jatni, Bhubaneswar, Odisha, India

Address for Correspondence

Monalisa Sahoo, Scientist, ICAR-National Institute on Foot and Mouth Disease (NIFMD), Arugul, Jatni, Bhubaneswar, Odisha, India, E-mail: vety.lisa@gmail.com

Received: 20.8.2024; Accepted: 27.9.2024

ABSTRACT

The present study reports a rare case of cerebral abscess in a 10 month old male crossbred buffalo calf showing the clinical signs of lateral recumbency, torticollis, stiffness of neck, muscle twitching, paddling movement and opisthotunus. Grossly, the brain showed a large abscess in anterior part of the right cerebral hemisphere. Histopathologically, purulent meningitis was observed showing marked infiltration of inflammatory cells in the leptomeningeal space. The brain parenchyma showed purulent exudates lined by thick connective tissue capsule, marked perivascular cuffing, multi-focal areas of gliosis, vasculitis and neuronal degenerations. The DNA from the affected brain tissue showed the presence of *S. suis* by PCR targeting *gdh* gene and further confirmed as serotype 2 by multiplex PCR amplifying 498 bp base pair fragment of the capsular gene. Immunohistochemically, the inflammatory cells infiltrating the brain parenchyma and glial cells showed the abundant immunoreactivity for SS2 antigens confirming the etiology. The histopathological, immunohistochemical and molecular findings support the diagnosis of rare case of *S. suis* serotype 2 induced cerebral abscess in a buffalo calf.

Keywords: Buffalo calf, cerebral abscess, immunohistochemistry, neuropathology, PCR

Streptococcus suis is an emerging bacterial swine zoonotic pathogen responsible for causing huge economic loss to the pig production specially in intensive pig production systems[1]. Recent report showed the average cost of *S. suis* per pig (summed across all production phases) was estimated to be 1.30 euros, 0.96 euros and 0.60 euros in Germany, Netherland and Spain respectively[2]. This pathogen is frequently reported to be associated with various diseases such as meningitis, endocarditis, pneumonia, arthritis and septic shock in pigs and human[1,2]. The prevalence of *S. suis* has been reported in Indian pigs[3,4]. *S. suis* is among the pathogens for which scientific interest has increased faster in recent years, and it is currently included among the top ten swine pathogens worldwide. Besides pigs and humans, cross species transmission of *S. suis* infection in different species showing broad host range has been reported in previous reports[5,6]. Among the different species reported, it has been isolated frequently from cattle showing diverse pathological cases of meningitis, bronchopneumonia and multifocal acute necrotizing hepatitis[7,8]. Out of identified thirty-eight capsular serotypes of *S. suis* based on the co-agglutination and DNA sequencing methods, serotype 2 is the most common and virulent serotype frequently recovered from diseased swine and humans and predominant in Asia, North and South America[1]. In the present investigation, we confirmed a rare case of *S. suis* infection in a buffalo calf showing the clinical signs of neurological manifestation.

A 10-month-old crossbred dead male buffalo calf was received to Postmortem Facility, IVRI, Izatnagar from experimental animal shed of Animal Nutrition division with the history of high fever, paddling movement, tremor, stiffness of neck, dysphasia, clonic convulsion and opistotonus. The animal was under treatment after the immediate onset of clinical signs with an antibiotic (cefazolin), neurobion and steroids. However, even with treatment, the calf died after undergoing treatment for 7 days.

How to cite this article : Babu, S., Murali, D., Patel, S., Thakor, J.C., Singh, R., Pasayat, M., Acharya, R., Tripathy, J.P., Sahoo, P.K., Sahoo, N.R. and Sahoo, M. 2025. Atypical pathological presentation of *S. Suis* serotype 2 induced cerebral abscess in a naturally infected buffalo calf. Indian J. Vet. Pathol., 49(1) : 64-67.

The systemic necropsy was performed and thin representative tissues from the brain, lungs, heart, spleen, liver, kidneys and intestine were fixed in 10% neutral buffered formalin for pathological investigation. Fixed tissues were embedded in paraffin wax, sectioned at a thickness of approximately 5 µm and stained with routine hematoxylin and eosin (H&E). The immunolocalization of *S. suis*

Fig. 1. Cerebral abscess in a buffalo calf. Note the opened pus cavity at the anterior part of right cerebrum.

type 2 antigen was done on the paraffin embedded (FFPE) tissue sections of brain and lungs using commercially available polyclonal anti-rabbit *S. suis* type antibody (Cat orb7028, biorbyt). Another set of same tissues were kept in -20^{O}C for molecular investigation. For the molecular detection, DNA was isolated from the affected brain, lungs and spleen tissues using DNAeasy blood and tissue kit (Qiagen, India) and screened for the probable bacterial agents such as *Listeria monocytogenes*[9], *Streptococcus suis*[10], *Pasteurella multocida*[11] and viral pathogens bovine Herpes virus[12] and Bovine viral diarrhoea virus[13] were ruled out in complementary DNA (cDNA) prepared from brain tissue using published primers. For the serotype identification of *S. suis*, multiplex PCR was used as per previous report[14].

The neurological signs exhibited by the buffalo calf in the present study are consistent with those attributed to *S. suis* induced meningitis[15,16]. Grossly, the brain showed abscess of 5.5 cm diameter raised firm abscess at the anterior part of right cerebral hemisphere (Fig. 1). The meningeal vessels covering the brain surface were markedly congested. On cutting the pus pocket, 20-30 ml of thick purulent creamy exudates oozed out. Besides brain, the remaining visceral organs did not show any appreciable gross lesions. Microscopically, the brain showed significant histopathological lesions. The leptomeningeal space was widened and filled with inflammatory cellular exudates along with congestion and oedema (Fig. 2a). The cerebrum and medulla showed predominant histopathological lesions as compared to cerebellum. The brain parenchyma showed marked presence of purulent exudates surrounded by thick connective capsule (Fig. 2b), perivascular cuffing (Fig. 2c), vasculitis (Fig. 2d), extensive areas of congestion, haemorrhages, oedema, multifocal areas of gliosis, increased microglial proliferation, astrocytosis, neuronophagia, swollen endothelial cells in capillaries, neuronal necrosis and degeneration. The purkinje neurons of cerebellum showed neuronal loss and neuronal degeneration with mild perivascular cuffing. The brain stem showed status spongiosus, gliosis, vasculitis, neuronal necrosis with severe perivascular cuffing. The neuropathological lesions observed in the present study

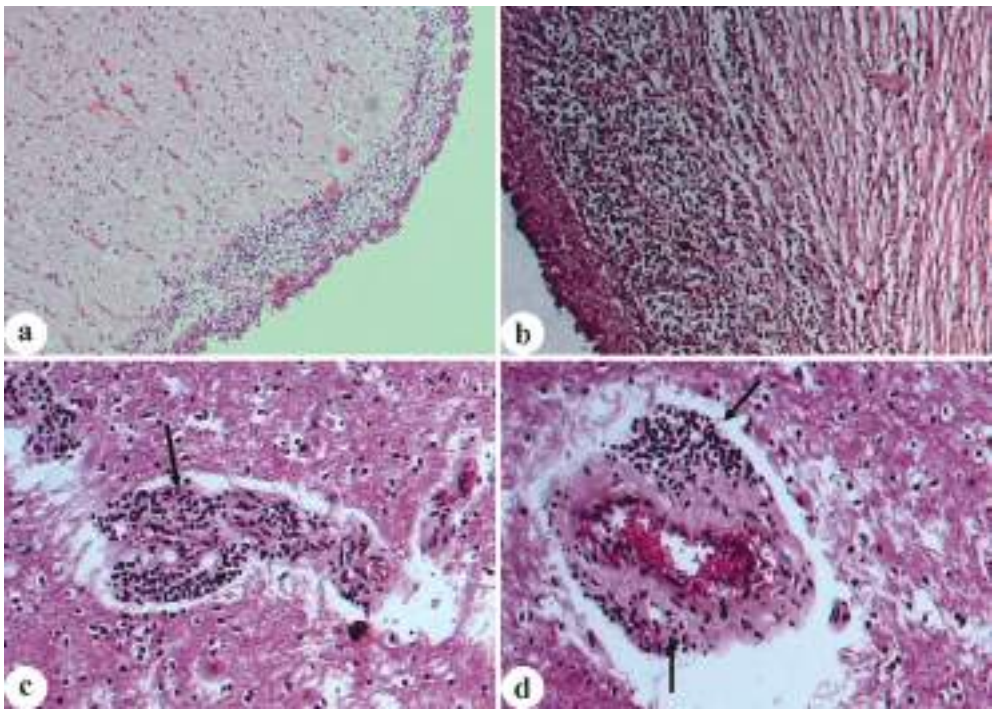

Fig. 2. Histopathological sections of brain of naturally infected buffalo calf showing **a.** Leptomeningitis (H&E X100); **b.** Purulent exudates lined by thick connective tissue capsule (H&E X100); **c.** Perivascular cuffing (H&E X200); **d.** Vasculitis (H&E X200).

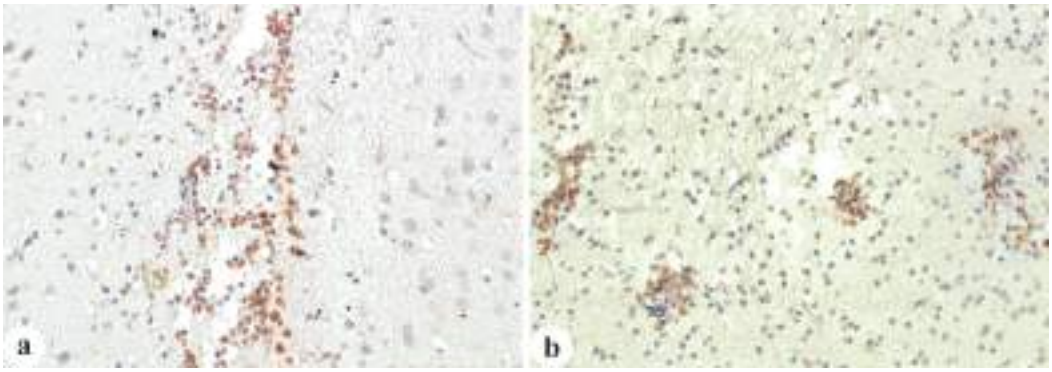

Fig. 3. Immunohistochemical stained sections of brain showing immunoreactivity **a.** Inflammatory cells, neocortex; **b.** Glial cells (IHC X200).

corroborated with the earlier findings of *S. suis* type 2 induced meningoencephalitis in natural and experimental cases[17,18]. The microscopic lesions of meningoencephalitis with well encapsulated fibrous tissue was documented in a previous report[19]. The neuropathological lesions might be due to destruction of blood brain barrier by the actions of suilysin protein and other virulence factors of *S. suis*[19]. The immunohistochemical stained brain section showed the abundant immunoreactivity for *S. suis* type 2 antigen in the inflammatory cells infiltrating the brain parenchyma (Fig. 3a) and glial cells (Fig. 3b) correlating with neuropathological lesions. The similar findings were reported in previous reports[17,18]. Besides brain, the visceral organs failed to show any appreciable gross or histopathological lesions. The absence of any systemic lesions in the present case ruled out the possibility of vascular dissemination from extraneural organs. The extensive lesions of meningoencephalitis with close proximity to right ear suggest the possibility of getting transient the infection from otitis interna[19]. Moreover, the colonization of *S. suis* within the nasal cavity with transient rhinitis might lead to the subsequent dissemination of bacterial pathogens to the brain via cribiform plate might result in neuropathological lesion due to bacteraemia[19]. Earlier report showed the endocarditis associated brain lesion in slaughtered pigs[20]. Further, brain lesions associated with endocarditis were mostly focal and disseminated to various organs. On contrary, in our case, neither endocarditis nor any other systemic disseminated lesions were recorded. Moreover, the distribution of the brain lesions were extensive rather than focal in the brain parenchyma. The pure involvement of brain without showing any systemic microscopic lesions was congruent with an earlier report describing *S. suis* type 2 induced cerebral abscess in a pig[19]. The genomic DNA isolated from the brain showed amplification for *S. suis* targeting partial fragment of *gdh* gene yielding 566 bp product (Fig. 4a) whereas other organs failed to show any amplification. Further, brain showed the amplification for partial fragment of capsular polysaccharide gene (cps) gene yielding 498 bp confirming the association of *S. suis* type 2 (Fig. 4b).

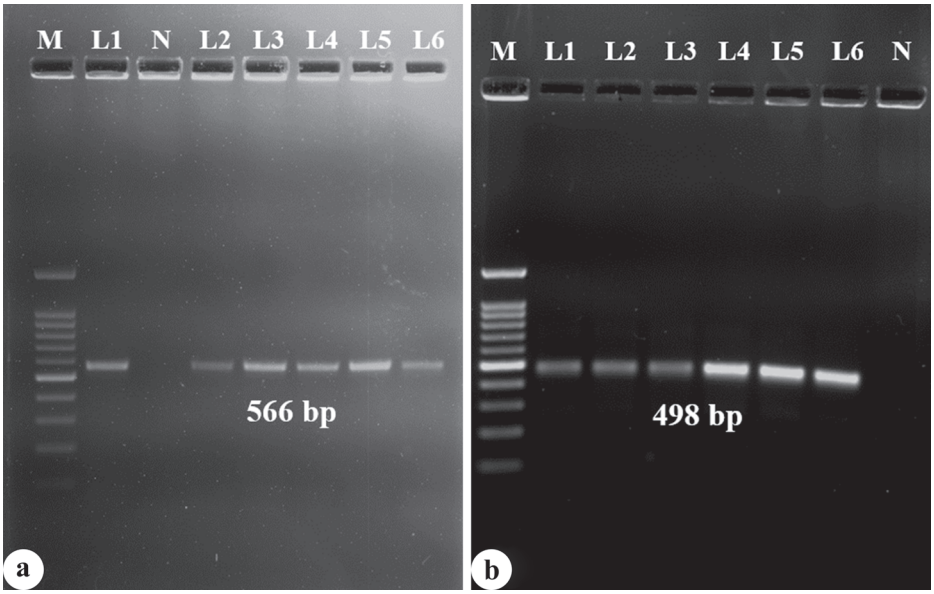

Fig. 4. Molecular detection of *S. suis* and its serotype in the brain showing **a.** M-100 bp marker, L1: Positive control, N: Negative control, L2-L6: Brain tissues positive for *S. suis* yielding 566 bp; **b.** M-Marker (100 bp), L1-L6: Positive for *S. suis* type 2 yielding 498 bp.

The brain failed to show amplification for other bacterial and viral pathogens. The detection of *S. suis* serotype 2 in the brain suggest the neurotropism of this pathogen. *S. suis* type 2 is reported worldwide associated with meninoencephalitis in pigs and human[16].

Based on histopathological, immunohistochemical and molecular findings, the present case is confirmed to be a rare case of *S. suis* induced cerebral abscess in a buffalo calf. Therefore, the presence of *S. suis* has to be taken into consideration while dealing with cases of buffalo showing neurological manifestations.

ACKNOWLEDGEMENTS

The authors would like to acknowledge the financial support extended by the Director, Indian Veterinary Research Institute (IVRI), Izatnagar and Indian Council for Agricultural Research (ICAR), New Delhi are gratefully acknowledged.

REFERENCES

1. Goyette Desjardins G, Auger JP, Xu J, Segura M and Gottschalk M. 2014. *Streptococcus suis*, an important pig pathogen and emerging zoonotic agent-an update on the worldwide distribution based on serotyping and sequence typing. *Emerg Microb Infect* **3:** 1-20.
2. Neila-Ibáñez C, Casal J, Hennig-Pauka I, Stockhofe-Zurwieden N, Gottschalk M, Migura-García L, Pailler-García L and Napp S. 2021. Stochastic assessment of the economic impact of *Streptococcus suis* associated disease in German, Dutch and Spanish swine farms. *Front Vet Sci* **8:** p.676002.
3. Dinesh M, Thakor JC, Singh KP, Singh R, Anbazhagan S, Chauhan R, Qureshi S, Sahoo NR and Sahoo M. 2022. Patho-epidemiological study of *Streptococcus suis* infections in slaughtered pigs from North and North-Eastern Region, India. *Indian J Vet Pathol* **46:** 26-32.
4. Dinesh M, Thakor JC, Patel S, Roopa N, Singh R, Qureshi S, Singh KP, Kalaiselvan E, Manikandan R and Sahoo M. 2023. Seroprevalence of *Streptococcus suis* in live and slaughtered pigs of India. *Indian J Vet Pathol* **47:** 158-161.
5. Hommez J, Wullepit J, Cassimon P, Castryck F, Ceyssens K and Devriese LA. 1988. *Streptococcus suis* and other streptococcal species as a cause of extramammary infection in ruminants. *Vet Rec* **123:** 626-627.
6. Muckle A, Giles J, Lund L, Stewart T and Gottschalk M. 2010. Isolation of *Streptococcus suis* from the urine of a clinically ill dog. *Can Vet J* **51:** 773.
7. Okwumabua O, Peterson H, Hsu HM, Bochsler P and Behr M. 2017. Isolation and partial characterization of *Streptococcus suis* from clinical cases in cattle. *J Vet Diagn Invest* **29:** 160-168.
8. Komatsu T, Watando E, Inaba N, Sugie K, Okura M and Shibahara T. 2018. Bovine vegetative endocarditis caused by *Streptococcus suis*. *J Vet Med Sci* **80:** 1567-71.
9. Rosa-Zariñana AE, Crosby-Galván MM, Ramírez-Guzmán ME, Hernández-Sánchez D and Mata-Espinosa MA. 2018. Standardization of PCR technique for detecting *Listeria monocytogenes* in chicken, beef and pork. *Ecosistemasy Recursosagropecuarios* **5:** 25-34.
10. Okwumabua O, O'Connor M and Shull E. 2003. A polymerase chain reaction (PCR) assay specific for *Streptococcus suis* based on the gene encoding the glutamate dehydrogenase. *FEMS Microbiol Lett* **218:** 79-84.
11. Townsend KM, Frost AJ, Lee CW, Papadimitriou JM and Dawkins HJ. 1998. Development of PCR assays for species-and type-specific identification of *Pasteurella multocida* isolates. *J Clinic Microbiol* **36:** 1096-100.
12. Fuchs M, Hübert P, Detterer J and Rziha HJ. 1999. Detection of bovine herpesvirus type 1 in blood from naturally infected cattle by using a sensitive PCR that discriminates between wild type virus and virus lacking glycoprotein E. *J Clinic Microbiol* **37:** 2498-507.
13. Behera SP, Mishra N, Vilcek S, Rajukumar K, Nema RK, Prakash A, Kalaiyarasu S and Dubey SC. 2011. Genetic and antigenic characterization of bovine viral diarrhoea virus type 2 isolated from cattle in India. *Comp Immunol Microbiol Infect Dis* **34:** 189-96.
14. Kerdsin A, Akeda Y, Hatrongjit R, Detchawna U, Sekizaki T, Hamada S, Gottschalk M and Oishi K. 2014. *Streptococcus suis* serotyping by a new multiplex PCR. *J Med Microbiol* **63:** 824-30.
15. Reams RY, Glickman LT, Harrington DD, Thacker HL and Bowersock TL. 1994. *Streptococcus suis* infection in swine: a retrospective study of 256 cases. Part II: Clinical signs, gross and microscopic lesions and coexisting microorganisms. *J Vet Diagn Invest* **6:** 326-34.
16. Hlebowicz M, Jakubowski P and Smiatacz T. 2019. *Streptococcus suis* meningitis: epidemiology, clinical presentation and treatment. *Vector Borne Zoonotic Dis* **19:** 557-62.
17. Berthelot Herault F, Cariolet R, Labbe A, Gottschalk M, Cardinal JY and Kobisch M. 2001. Experimental infection of specific pathogen free piglets with French strains of *Streptococcus suis* capsular type 2. *Can J Vet Res* **65:** 196.
18. Zheng P, Zhao YX, Zhang AD, Kang C, Chen HC and Jin ML. 2009. Pathologic analysis of the brain from *Streptococcus suis* type 2 experimentally infected pigs. *Vet Pathol* **46:** 531-535.
19. Headley SA, Silva LC and Okano W. 2012. Cerebral abscesses in a pig: atypical manifestations of *Streptococcus suis* serotype 2-induced meningoencephalitis. *J Swine Hlth Prod* **20:** 179-183.
20. Karstrup CC, Jensen HE, Aalbæk B, Leifsson PS, Boye M and Agerholm JS. 2011. Endocarditis associated brain lesions in slaughter pigs. *J Comp Pathol* **144:** 289-95.

Indian J. Vet. Pathol., 49(1) : 68-72, 2025: DOI: https://doi.org/10.5958/6r4gn257

SHORT COMMUNICATION

Effect of foot and mouth disease virus infection on hematobiochemical profile in goats under natural conditions

Jasmine Pamia, Rajeev Ranjan[1*], Madhurendu Kumar Gupta, Jitendra K. Biswal[1], Smrutirekha Mallick[1], Praggaya Priya Lakra and Sanjit Kumar[2]

Department of Veterinary Pathology, College of Veterinary Science and Animal Husbandry, Birsa Agricultural University, Kanke-834 006, Jharkhand, [1]ICAR-National Institute on Foot and Mouth Disease, Bhubaneswar-752 050, Odisha, India, [2]Krishi Vigyan Kendra, Bihar Agricultural University, Sabour-813 210, Bihar, India

Address for Correspondence

Rajeev Ranjan, Senior Scientist, ICAR-National Institute on Foot and Mouth Disease, Bhubaneswar-752 050, Odisha, India, E-mail: drrajraj@gmail.com

Received: 3.12.2024; Accepted: 13.12.2024

ABSTRACT

Foot and mouth disease (FMD) is a contagious viral disease that has a high economic impact on livestock industry affecting large and small ruminant. Most research works are carried out on hematobiochemical alteration due to FMD virus (FMDV) in bovine but there is a paucity of literature and a dearth of research on how FMDV affects the hematobiochemical profiles of goats. This study was aimed to investigate the impact of FMDV on hematobiochemical profile of goats. Forty two whole blood samples were collected from FMDV-infected (n=32) and apparently healthy (n=10) goats to estimate hematobiochemical profile alteration. There was a significant ($p<01$) decrease in values of hematobiochemical parameters *viz.* haemoglobin (6.45±0.55 g%), total erythrocytes (4.22±0.27x10^6/µl), packed cell volume (21.35±1.66%), mean corpuscular volume (50.49±0.65 fl), mean corpuscular haemoglobin (15.24±0.32 pg), mean corpuscular haemoglobin concentration (30.19±0.25 gm/dl), glucose (20.42±4.24 mg/dL), alanine transaminase (29.26±3.74 U/L), blood urea nitrogen (39.57±4.46 mg/dL), serum creatinine (0.7±0.12 mg/dL), sodium ion (143.73±1.33 mEq/L), total protein (7.57±0.55 g/dL), albumin (3.15±0.31 g/dL), globulin (4.425±0.37 g/dL). There was a significant ($p<01$) increase of aspartate transaminase (86.36±11.41 U/L), albumin: globulin ratio (0.715±0.08) as well as cholesterol (104.77±0.86 mg/dL) and no significant changes were observed in alkaline phosphatase (267.76±236.52 U/L), potassium ion (5.21±0.36 mEq/L), neutrophils, monocytes, lymphocytes, eosinophils in FMDV infected goats than the apparently healthy goat. Hematobiochemical parameters alter significantly in goat during the active phase of FMDV infection under natural condition and these findings would be useful for developing a therapeutic or preventive measure to avoid the biotic stress and negative effect of FMD virus infection in convalescent goat.

Keywords: Biochemical profile, foot and mouth disease virus, goat, hematological profile

In rural economies, goats have been regarded as poor man's cow due to its immense contribution to the poor man's economy. A few infectious diseases that are frequently encountered in goats includes mastitis, bluetongue, haemonchosis, enterotoxaemia, paste-des-petits ruminants, foot and mouth disease (FMD) etc.

The FMD virus (FMDV) is highly contagious in cloven-footed animals, most prevalent in cattle and buffaloes followed by sheep and goats, whereas pigs act as amplifiers. The causative agent of FMD is classified into seven serotypes, O, A, C, Asia-1, SAT-1, SAT-2 and SAT-3 which are serologically and immunologically distinct[2]. Disease is mainly characterised by fever, anorexia, ropy and foamy salivation, reluctant to walk in cattle whereas lameness, depression and anorexia is usually the first indication of FMD in sheep and goats[3]. Vesicles develop in the interdigital cleft, on the heel bulb and on the coronary band. In sheep vesicles also form in the mouth on dental pad, hard palate, lips and gums but they rupture easily[4]. The disease in goat is generally overlooked due to absence of frank clinical signs and symptoms. During the viraemic phase of FMDV infection haematological and serum biochemical parameters alteration may pose stress on animals which leads to production losses.

However, majority of works published are on hematological and biochemical alteration due to FMDV infection in cattle and buffaloes[5,6,7,8] but there are paucity of literatures dealing with FMDV infection and dearth of research on how FMDV affects the haematological and serum biochemical profiles of goats. Based on this, the present study was conducted to understand the hematological and serum biochemical profile alteration in goat infected with foot and mouth disease virus under natural condition. As per the author's knowledge, this was the first kind of work carried in goat under natural condition and findings of the present study

How to cite this article : Pamia, J., Ranjan, R., Gupta, M.K., Biswal, J.K., Mallick, S., Lakra, P.P. and Kumar, S. 2025. Effect of foot and mouth disease virus infection on hemato biochemical profile in goats under natural conditions. Indian J. Vet. Pathol., 49(1) : 68-72.

Table 1. Haematological and biochemical profile (Mean ± SE) in FMDV affected and apparently healthy goats under natural condition.

Parameters	FMD affected (n=32) (Mean ± SE)	Apparently healthy (n=10) (Mean ± SE)	p value
TLC	11962.5 ± 1605.58	10780 ± 1877.82	0.058
Neutrophils (%)	36.75 ± 13.85	40 ± 8.27	0.488
Lymphocytes (%)	53.25 ± 14.03	49.3 ± 8.69	0.408
Eosinophils (%)	5.37 ± 2.82	4.5 ± 2.71	0.394
Monocytes (%)	4.62 ± 2.43	4 ± 1.63	0.453
N/L	0.84 ± 0.64	0.86 ± 0.31	0.932
Haemoglobin (g%)	6.45 ± 0.55	8.46 ± 0.32	< 0.01
PCV (%)	21.35 ± 1.66	27.38 ± 0.98	< 0.01
TEC (million/ul)	4.22 ± 0.27	5.23 ± 0.16	< 0.01
MCV (fl)	50.49 ± 0.65	52.345 ± 0.24	< 0.01
MCH (pg)	15.24 ± 0.32	16.173 ± 0.12	< 0.01
MCHC (gm/dl)	30.19 ± 0.25	30.896 ± 0.08	< 0.01
Glucose (mg/dL)	20.42 ± 4.24	50.7 ± 10.35	< 0.01
AST (U/L)	86.36 ± 11.41	33.92 ± 3.12	< 0.01
ALT (U/L)	29.26 ± 3.74	95.73 ± 9.82	< 0.01
ALP (U/L)	267.76 ± 236.52	138.5 ± 80.46	0.1
BUN (mg/dL)	39.57 ± 4.46	55.1 ± 7.37	< 0.01
Creatinine (mg/dL)	0.7 ± 0.12	1.19 ± 0.16	< 0.01
Na^+ (mEq/L)	143.73 ± 1.33	148.59 ± 1.56	< 0.01
K^+ (mEq/L)	5.21 ± 0.36	5.286 ± 0.49	0.603
TP (g/dL)	7.57 ± 0.55	9.61 ± 0.46	< 0.01
Albumin (g/dL)	3.15 ± 0.31	3.58 ± 0.32	< 0.01
Globulin (g/dL)	4.425 ± 0.37	6.03 ± 0.61	< 0.01
A/G ratio	0.715 ± 0.08	0.603 ± 0.11	< 0.01
Cholesterol (mg/dL)	104.77 ± 0.86	62.1 ± 13.34	< 0.01

P ≤ 0.05 and P ≤ 0.01 were taken as the significance level; TLC - Total leukocyte count, TEC - Total erythrocyte count, PCV - Packed cell volume, MCV - Mean corpuscular volume, MCHC - Mean corpuscular haemoglobin concentration, AST - Aspartate transaminase, ALT - Alanine transaminase, ALP - Alkaline phosphatase, BUN - Blood urea nitrogen, Na^+ - Sodium ion, K^+ - Potassium ion, TP - Total protein

would be useful for the development of a therapeutic or preventive measure to avoid the biotic stress and negative effect of FMDV infection in convalescent goat.

Cross sectional study was conducted in field under natural condition where all the animals were reared in same geographical climatic and environmental condition. Animals were divided into two groups, group (Gr) 1, FMDV infected [tested positive for FMD viral genome using FMDV specific primers (reverse primer: 5'-GACATGTCCTCCTGCATCTG-3; Forward primer: serotype 'O'- 5'- GTGACTGAACTGCTTTACCGCAT- 3', serotype 'A'- 5'- CAACGGGACGARCAAGTACTC- 3', serotype 'Asia 1'- 5'- GACCTGGAGGTYGCGCTTGT-3')] and Gr 2, apparently healthy (tested negative for FMD viral genome). Gr1 consisted 32 goats (n=32) whereas Gr 2 consists of 10 goats. This research protocol was approved by the Institute Animal Ethics Committee of Ranchi Veterinary College, Birsa Agricultural University, Kanke, Ranchi, Jharkhand followed by the committee for control and supervision of experiments on animals (CCSEA), Government of India vide letter no. V-11011(13)/12/2022-CPCSEA-DADF.

Whole blood samples were collected aseptically from all FMDV infected (n=32) and apparently healthy goats (10) through jugular vein. Two mL blood was collected in a heparinised vacutainer tube (BD, Franklin, USA) for estimation of hematological parameters while 10 mL blood was collected in a vacutainer tube containing clot activators (BD, Franklin, USA) to estimate the serum biochemical profile. Serum samples were separated by centrifugation of blood at 3000 rpm for 20 min and stored at -80^{O}C till estimation.

The haematological parameters *viz.*, haemoglobin (Hb), total erythrocyte count (TEC), packed cell volume (PCV), and total leukocytes count (TLC), mean corpuscular volume (MCV), mean corpuscular haemoglobin concentration (MCHC) were estimated

using haematology analyser (Transasia, Sysmex, XN-550). Moreover, differential leukocyte count (DLC) was carried out manually on blood smear stained with Giemsa stain[9].

Biochemical parameters *viz.*, glucose, aspartate transaminase (AST), alanine transaminase (ALT), serum alkaline phosphatase (ALP), urea, creatinine, Sodium ion (Na^+), Potassium ion (K^+), Total protein (TP), albumin: globulin, A/G ratio and cholesterol were performed on each serum samples. These serum biochemical parameters were estimated using commercial kits (Tulip diagnostics (P) Ltd) in autoanalyzer (Tulip semi-automated analyzer).

All values were presented as means ± standard error (SE). T-test was used to statistically analyze the significant difference between the group means. The value of $P \leq 0.05$ and $P \leq 0.01$ was taken as statistically significant[10].

The values of various haematological and serum biochemical profiles (mean ± SE) in FMDV infected and apparently healthy goats are depicted in Table 1.

Haematological parameters of FMDV infected and apparently healthy goats are shown in Table 1. There was a significant ($p<0.01$) decrease in the values of hematological parameters *viz.* haemoglobin, total erythrocytes, PCV, MCV, MCH, MCHC in FMDV infected goats than those of the apparently healthy goat (Table 1). Although, there was an absolute increase in the counts of total leukocyte, lymphocytes, monocytes, eosinophils whereas reduction in absolute count of neutrophils and neutrophils: lymphocyte ratio but all these changes were statistically non-significant.

Serum biochemical parameters of FMDV infected and apparently healthy goats are shown in Table 1. There was a significant ($p<01$) decrease in values of serum biochemical parameters *viz.* glucose, ALT, blood urea nitrogen, creatinine, sodium ion, total protein, albumin, globulin while significant ($p<0.01$) increase in the value of AST (86.36±11.41), albumin : globulin ratio and cholesterol and there was no significant changes were observed in value of ALP, potassium ion, neutrophils, monocytes, lymphocytes, Eosinophils in FMDV infected goats than those of the apparently healthy goat.

Initial replication of FMDV took place at primary site followed by viraemia and then reaches up to secondary site. At secondary site it replicated and produce vesicle followed by rupture of vesicle and leads to different types of wounds. During the viraemic phase of infection FMDV affects the hematological and biochemical profile of animals which disturb the harmony of general status of health and followed by production loss especially in cattle and buffalo but it was not studied in goat. Therefore, the present study was conducted to understand the hematological and serum biochemical profile alteration in goat infected with FMD virus under natural condition to develop therapeutic or preventive measures for avoiding the biotic stress and negative effect of the FMDV infection in goat.

There was a significant decrease in Hb in FMDV infected goats as compared to apparently healthy goat and this condition could be attributed to endocrinopathy effect occurring secondary to the viral infection[11]. Similar findings were also reported by the earlier workers[8,12,13] in cattle. FMDV infected goats has a significant reduction in TEC/RBC in compared to the apparently healthy goat and it could be due to the reduction in the process of erythropoiesis[14] and this report is in line with preceding published reports in cattle[6,11,12,13]. The PCV content of FMDV affected goats decreased significantly which could be due to reduction in RBC/TEC and it is comparable with the previous findings as demonstrated in cattle[12,13] but same time it contrary to the report published by Mousa and Galal[7]. MCV, MCH and MCHC values in the Gr1 (FMDV affected group) are significantly lower than Gr 2 (apparently healthy goat). In contrary to the present report, MCV and MCH values were shown to be considerably higher in the FMDV infected animals[7,11]. Few reports said that there is a non-significant change in these value[8,13]. In present study, TLC in Gr1 was higher than that of Gr 2 but it has not been differ significantly between the Gr 1 and Gr 2 and it has also been mentioned in the previous report[8,14]. In FMDV infected groups of goats the count of neutrophils and neutrophils: lymphocyte ratios were decreased whereas the count of lymphocytes, monocytes and eosinophils increased but these changes are non-significant in nature as compare to the apparently healthy group and similar finding were also recorded in published reports[6,15]. Lymphocytosis is the phenomenon of virus infection as it has also been observed in FMDV infected group under natural condition[16,17] during active phase of infection in the present study but few report said that there is a significant decrease in TLC, lymphocytes after 7-14 days post FMDV infection[18].

There was significant decrease in the concentration of glucose in FMDV affected goats than the apparently healthy goats. This contrasts with a significant increase of glucose in diseased cattle and buffaloes compared to healthy animal in the previous study[12,14,19]. Possible mechanisms leading to hypoglycaemia include impaired glycogenolysis and gluconeogenesis in the liver or increased catabolism of glucose by the animal[20]. A reduction of blood sugar levels during infection is a well-regulated process that is a part of the body's natural antiviral response. Significant increase in the concentration of AST in FMDV affected group than the apparently healthy group and it could be due to involvement of liver, muscular or cardiac damages

occurs[14,21] and this finding coincide with the earlier report indicating hypoglycaemia due to FMDV infection[12,13,15]. A change in the amount of AST in the blood serum is one of the most distinctive indicators of the disruption of the integrity of the liver tissue[22]. As activity of AST reflects the functional state of liver that means FMDV also affects liver function during acute phase of infection. A significant decrease in the concentration of ALT was observed in FMDV affected group than the apparently healthy group of animals which concurred with the findings of earlier report[8]. This contrasts with no significant change observed in ALT in the previous study[12]. Enzyme activities of ALP were increased in FMDV affected group of animals in comparison to apparently healthy group of animals but there was no significant difference as reported in previous report[13]. Serum biochemical analysis showed significant reduction in total protein, albumin, globulin in FMDV affected group in the present study and similar finding were also reported by previous worker[7,13,15,23]. This is contrary to non-significant changes in serum total protein, albumin and A:G ratio was observed under experimental FMDV infection[18]. Low albumin and protein concentration may also be due to alteration in pancreatic β-cell function that might have developed during the clinical course of FMDV[24] and it could also be due to liver and kidney damage[25]. The hypoproteinemia might be attributed to hypoalbuminemia and hypoglobulinemia in present study and it could be due to anorexia, reduced feed intake, malnutrition, mal absorption, enteropathy, and transudation of plasma from ulcers due to FMDV infection[8,15,25]. Due to FMDV infection there is impairment in the function of thyroid gland[3]. Thyroid hormone increases both the rate of cholesterol synthesis and the rate of its catabolism by the liver. In hypothyroidism condition, lipids and cholesterol catabolism are decreased to a lesser degree than the synthesis of the cholesterol. The effect of these changes, results in an increase in serum cholesterol[26] due to this reason there was a significant increase in the cholesterol level in FMDV affected goat in present study. Significant reduction in the concentration of blood urea nitrogen (BUN) and creatinine has been observed in FMDV infected goats than the apparently healthy goats and this coincide with the finding of earlier worker and it could be due to hypoproteinemia[14]. This contrasts with non-significant changes observed in BUN and serum creatinine (sCRT) in the previous study[12]. BUN and sCRT are the commonly used biomarkers to know the intensity of renal failure since it is released in to the plasma at relatively constant rate in healthy state, which are freely filtered by the glomerulus and neither metabolized nor released by the kidney. By preventing or promoting renal tubular secretion, glomerular filtration rate or both, the real sCRT can be altered independently of variations in the glomerular filtration rate[27]. Significant reduction in the concentration of sodium ion was observed in FMDV affected group than apparently healthy goats[15]. The recorded hyponatremia may be attributed to sodium loss through exudation from erosions, excessive salivation and/or decreased sodium intake due to starvation resulted from fever in cattle[6,15]. No significant difference was observed in the serum potassium in both the infected and apparently healthy goats. There were significant changes in the parameters like AST, ALT, albumin, globulin, BUN, sCRT etc indicating that FMD virus has negative effect on liver and kidneys. Changes in the haematological parameters due to FMDV infection indicates that it affects the major organs like liver, kidneys etc and effect of these changes has been visible by significant changes in liver and kidneys function test parameters. Therefore, during the acute phase of FMDV infection liver and kidney protectant may be advisable to reduce the further health associated risk.

CONCLUSION

It would be concluded that during the viraemic phase of foot and mouth disease virus infection hematobiochemical parameters showed significant variations in FMDV affected goat than apparently healthy goat. Hematological parameters which significantly decrease in FMDV affected goats are haemoglobin, total erythrocyte, PCV, MCV, MCH and MCHC values. Biochemical parameters which significantly decrease in FMDV affected goats are glucose, ALT, urea, creatinine, sodium, total protein, albumin, globulin, A/G ratio while significant increase in AST and cholesterol. Changes in the haematological parameters due to FMDV infection indicates that it affects the major organs like liver, kidneys etc. and effect of these changes has been visible by significant changes in liver and kidney functions test. Present findings would be useful in developing therapeutic or preventive measures to reduce the health associated risk due to FMDV infection in goat to enhance productivity as these are not included in vaccination in most of the countries pursuing FMD control.

ACKNOWLEDGEMENTS

The author would like to thank the Dean of the College of Veterinary Science and Animal Husbandry at BAU in Kanke, Jharkhand, India for providing the necessary facilities for this research. State field veterinarians and animal owners were also recognized for their unwavering support throughout the study.

REFERENCES

1. Knowles NJ and Samuel AR. 2003. Molecular epidemiology of foot-and-mouth disease virus. *Virus Res* **91:** 65-80.
2. Robson KJ, Harris TJ and Brown F. 1977. An assessment by

competition hybridization of the sequence homology between the RNAs of the seven serotypes of FMDV. *J Gen Virol* **37:** 271-6.
3. Alexandersen S, Zhang Z, Donaldson AI and Garland AJ. 2003. The pathogenesis and diagnosis of foot-and-mouth disease. *J Comp Pathol* **129:** 1-36.
4. Gattani A, Gupta KK, Joshi G and Gupta SR. 2011. Metabolic profile of foot and mouth disease stressed sheep in semi-arid region. *J Stress Physiol Biochem* **7:** 148-153.
5. Mohan MS, Gajendragad MR, Subodh K, Gopalakrishna S and Nem S. 2008. Experimental foot-and-mouth disease in cattle and buffalo: Haematological changes. *Indian J Vet Pathol* **32:** 56-58.
6. Ghanem MM and Abdel-Hamid OM. 2010. Clinical, haematological and biochemical alterations in heat intolerance (panting) syndrome in Egyptian Cattle following natural foot-and-mouth disease (FMD). *Trop Anim Health Prod* **42:** 1167-1173.
7. Mousa SA and Galal MK. 2013. Alteration in clinical and hemobiochemical and oxidative stress parameters in Egyptian cattle infected with foot and mouth disease. *J Anim Sci Adv* **3:** 485-491.
8. Khan D, Sheikh IS, Ullah A, Kasi KK, Mustafa MZ, Din ZU, Anwar I, Kakar N and Waheed A. 2024. Circulation of foot-and-mouth disease serotypes, risk factors and their effect on hematological and biochemical profiles among cattle and buffalo in Quetta, Balochistan, Pakistan. *Vet World* **17:** 329-336.
9. Feldman BF, Zinki JG and Jain VC. 2000. Schalm's Veterinary Hematology, 5th Ed., Lippincott Williams and Wilkins, Canada.
10. Tamhane A and Dunlop D. 2000. Statistics and Data Analysis: From Elementary to Intermediate. 2nd Eds Prentice-Hall. 1-722.
11. Gökçe G, Gökce Hİ, Güneş V, Erdoğan HM and Çitil M. 2004. Alterations in Some Haematological and Biochemical Parameters in Cattle Suffering from Foot-and-Mouth Disease. *Turk J Vet Anim Sci* **28:** 723-727.
12. EI-Mandrawy SAM and Farag GK. 2017. Molecular characterization, haematological and biochemical studies on foot and mouth disease virus serotype O in buffaloes and cows in Dakahlia Governorate, Egypt. *Zagazig Vet J* **45:** 65-73.
13. Hashem MA, Shefaa AME, Iman EE and Alaa AAE. 2018. Molecular diagnosis of foot and mouth disease virus in cattle with reference to hematological and biochemical changes. *Zagazig Vet J* **46:** 105-116.
14. Barkakati J, Sarma S and Kalita DJ. 2015. Effect of foot and mouth disease on haematological and biochemical profile of cattle. *Indian J Anim Res* **49:** 713-716.
15. Nasr EI-Deen NAM, Neamat-Allah ANF, Rizk LG and Fareed RSG. 2017. Serological, hematological, biochemical and oxidative markers during foot and mouth disease serotype 'O' Infection, Egypt. *Bulletin UASVM Vet Med* **74:** 218-226.
16. Weiss DJ and Wardrop KJ. 2010. Schalm's Veterinary Hematology, 6th Ed, Ames, Wiley-182, Blackwell.
17. Dawood AA and Alsaad KM. 2018. Clinical and diagnostic studies of myocarditis result from FMD In lambs. *IOSR J Agric Vet Sci* **11:** 1-10.
18. Saravanan S, Umapathi V, Priyanka M, Hosamani M, Sreenivasa BP, Patel BHM, Narayanan K, Sanyal A and Basagoudanavar SH. 2020. Hematological and serum biochemical profile in cattle experimentally infected with foot-and-mouth disease virus. *Vet World* **13:** 426-432.
19. Mohapatra APK, Kundu AK, Bisoi PC and Prusty BM. 2005. Haematological and biochemical changes in crossbred cattle affected with foot and mouth disease. *Indian Vet J* **82:** 141-144.
20. Klein KA, Clark C and Allen AL. 2002. Hypoglycemia in sick and moribund farmed elk calves. *Can Vet J* **43:** 778-781.
21. Hoffmann WE and Solter PF. 2008. Diagnostic enzymology of domestic animals. In Clinical Biochemistry of Domestic Animals. Pp. 351-378.
22. TopchiyevaSh A. 2018. Change in the Enzymatic Activity of Aspartate Amino transferase in the Blood of Goats Related to the State of Animal Health. *J Med Res Biol Stud* **1:** 102.
23. Faruk AZ, Das SK, Abdul Awal M and Das D. 2021. Hematological and biochemical alterations at different stages in cattle affected with foot-and-mouth disease in Bangladesh. *J Sci Tech Res* **37:** 29202-29207.
24. Barboni E, Mannocchio I and Asdrubali G. 1966. The development of diabetes mellitus in cattle experimentally infected with virus of foot and mouth disease. *Vet Ital* **17:** 339.
25. Roussel AJ, Whitney MS and Cole DJ. 1997. Interpreting a bovine serum chemistry profile: Part 1. *Vet Med* **92:** 553-558.
26. Kaneko JJ, Harvey JW and Bruss M. 1997. Clinical biochemistry of Domestic Animals. 5th ed. Academic press California, US, pp. 661-668.
27. Mishra A, Chatterjee US and Mandal TK. 2013. Induction of chronic renal failure in goats using Cisplatin: A new animal model. *Toxicol Int* **20:** 56-60.

Indian J. Vet. Pathol., 49(1) : 73-77, 2025: DOI: https://doi.org/10.5958/58k9j928

SHORT COMMUNICATION

Pathology of concurrent pasteurellosis, fasciolopsiasis and sarcocystosis in a non-descript grower pig

T. Das*, H.B. Vidyarani[1], M. Pathak[2], M. Sethi[3], M. Sahoo, J.K. John[4], N.K. Das[5] and G. Saikumar[1]
ICAR-National Institute of Foot and Mouth Disease, Arugul, Bhubaneswar, India, [1]ICAR-IVRI, Izatnagar, [2]CAU, Imphal, India, [3]BHU, Varanasi, UP, [4]COVAS, SVPUAT, Meerut, UP, India, [5]FARD, Govt. of Odisha, India

Address for Correspondence
T. Das, Scientist, ICAR-National Institute of Foot and Mouth Disease, Arugul, Bhubaneswar, India, E-mail: tarenisahoo@gmail.com

Received: 9.12.2024; Accepted: 16.1.2025

ABSTRACT

A three months old nondescript female pig carcass was submitted to postmortem facility, division of pathology, ICAR-IVRI, Izatnagar, Uttar Pradesh, India. Concurrent infections with *F. buski*, *Pasteurella* and *Sarcocystis* were detected based on cultural examination, Gram staining of bacteria and morphology of parasites. On necropsy examination, gross lesions observed were hydrothorax and hydroperitoneum, frothy exudate in trachea, severe congestion, consolidation and edema of lungs, lymphadenitis, hepatitis with whitish necrotic foci and prominent lobular pattern, congestion of kidneys, meningeal and mesenteric blood vessels and serosa of small intestine. Histologically, acute fibrino-suppurative bronchopneumonia, myocarditis with sarcocysts, enteritis, hepatic necrosis with thickened capsule and interlobular septa, perivascular cuffing, perivascular and perineuronal oedema in brain, lymphoid necrosis and depletion were observed. The case was diagnosed as acute fibrino-suppurative bronchopneumonia and septicaemia caused by *Pasteurella* spp. associated with cardiac sarcocystosis and intestinal fasciolopsiasis.

Keywords: *F. buski*, *Pasteurella*, pathology, *Sarcocystis*

Pig is one of the important domesticated livestock having significant role in food security and socioeconomic improvement. Pig industry is facing various challenges due to many infectious and non-infectious diseases. Concurrent infection of single host by different pathogens (macroparasites like helminths and microparasite like bacteria) is a very common phenomenon. They may guard or exacerbate infection risk and shifts disease severity[1]. Pasteurellosis is an important bacterial disease of pigs worldwide causing great economic losses. It is caused by gram negative coccobacillary bipolar organism, *Pasteurella multocida.* Based on antigenicity of its polysaccharide capsule, there are five different serogroups of *P. multocida* such as A, B, D, E or F[2]. *P. multocida type* A and *P. multocida* type D cause bronchopneumonia, pleuritis and atrophic rhinitis in pigs and *P. multocida* type B is associated with septicemic pasteurellosis in pigs in India[3-5]. It is the common inhabitant in the respiratory tract of healthy animals. It was considered as secondary pathogen associated with pig pneumonia. Recently, it is considered as primary agent associated with swine pneumonia and septicemia[6]. It is also mostly prevalent zoonotic pathogen associated with human infection. Fasciolopsiasis is an important food borne infection caused by giant intestinal digenetic fluke *Fasciolopsis buski* in pigs causing significant economic losses in pig farms. The pathology is due to traumatic, obstructive and toxic effect of adult parasite in duodenum and jejunum of pigs and humans. Hemorrhage, inflammation, small bowl stricture, ulceration, micro abscesses etc. occur at the attachment sites of the adult parasite in the intestine.

Pigs act as intermediate host for three different *Sarcocyst* species like *S. porcifelis, S. suihominis* and *S. miescheriana.* Later two parasitic species are pathogenic to pigs. Pigs get infected after ingesting sporocysts excreted in the definite host faeces. In the endothelial cells of capillaries and arterioles of internal organs, the parasites undergo merogonic reproduction and in the skeletal muscles, they produce tissue cysts containing banana shaped bradyzoites. Morphologically, the cyst wall of *S. miescheriana* has radial perpendicular papillomatous striations and *S. suihominis* has hair like villar protrusions[7].

How to cite this article : Das, T., Vidyarani, H.B., Pathak, M., Sethi, M., Sahoo, M., John, J.K., Das, N.K. and Saikumar, G. 2025. Pathology of concurrent pasteurellosis, fasciolopsiasis and sarcocystosis in a nondescript grower pig. Indian J. Vet. Pathol., 49(1) : 73-77.

To the best of our knowledge, there are no published literature on pathology of concurrent infection of swine *with F. buski, Pasteurella* and *Sarcocystis*. Therefore, the aim of the present study is to describe pathological changes in a non-descript grower pig associated with natural concurrent infection with *F. buski, Pasteurella* and *Sarcocystis*.

A three months old non-descript female pig carcass was submitted to postmortem facility, division of pathology, ICAR-IVRI, Izatnagar, Uttar Pradesh, India. Detailed necropsy was conducted and gross pathological findings of different organs were recorded. Representative tissue specimens from different organs were collected and preserved in 10% percent buffered formalin

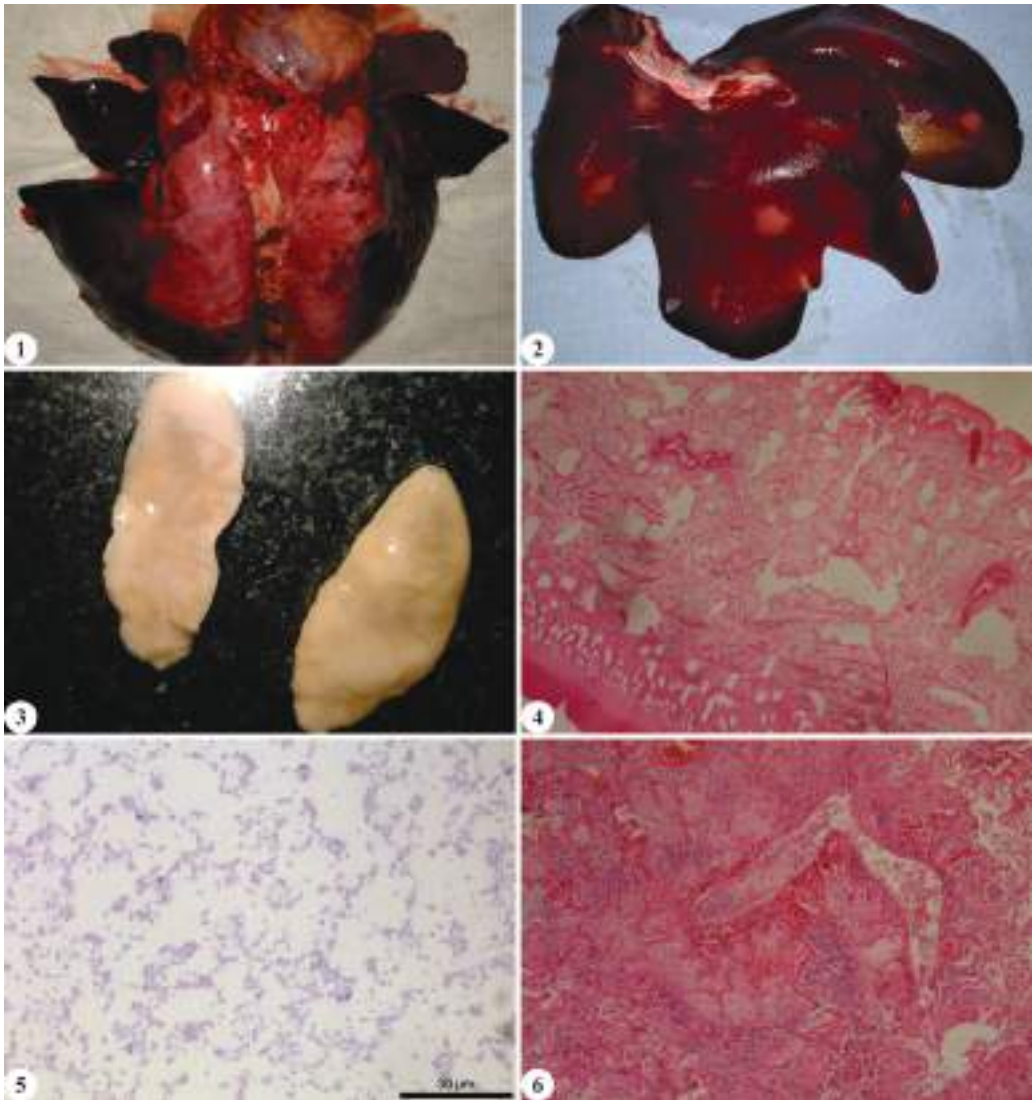

Fig. 1. Lung showing consolidations, haemorrhage and oedema; **Fig. 2.** Firm and enlarged liver with whitish necrotic foci and prominent lobular pattern; **Fig. 3.** Adult *Fasciolopsis buski* parasites; **Fig. 4.** Histological section of *F. Buski* parasite on H&E staining (x40); **Fig. 5.** Gram negative non-spore forming coccobacillary showing bipolarity on Gram stain (x1000); **Fig. 6.** Lung showing acute fibrino-suppurative bronchopneumonia on H&E staining (x40).

for histopathological processing. After fixation, tissue samples were dehydrated in serially ascending grades of alcohol, then cleared in xylene, embedded in paraffin wax and sectioned at 4 µm thickness and stained with hematoxylin and eosin routine stain. The slides were examined under light microscope. For bacteriological examination, heart blood sample was aseptically collected in a sterile syringe and stored at - 4^{O}C for further cultural examination. The blood sample was streaked on 5% sheep blood agar for bacterial isolation and incubated at 37^{O}C for 24-48 hours. The bacteria were identified based on colony morphology, hemolytic pattern on blood agar and microscopic examination of Gram-stained slide smear of culture. Adult *F. buski* and tissue cyst of *Sarcocystis* were identified based on their morphology[7,8].

The gross examination revealed moderate hydrothorax and hydroperitoneum, frothy exudate in trachea, severe congestion, consolidations and oedema of ventral parts of both left and right lung (Fig. 1), thickened pericardium of heart, congested and enlarged bronchial lymph nodes, firm and enlarged liver with whitish necrotic foci and prominent lobular pattern (Fig. 2), moderately enlarged and congested spleen, congested kidney and meningeal blood vessel congestion, congestion of mesenteric blood vessels and serosa of small intestine. Similar gross lesions were also reported earlier with natural outbreak of swine pasteurellosis[9]. Small intestine showed heavy infestation of adult *Fasciolopsis buski* parasites (Fig. 3 and Fig. 4). The parasites were of different sizes and dorsoventrally flattened, characterized by blunt anterior end with presence of large

ventral sucker and absence of cephalic cone[10]. Infection of human and pigs with zoonotic intestinal parasite *F. buski* has been reported in different parts of India[11-13]. In West Bengal, North-East India and Rajasthan 27.93%, 20.55% and 4.46% prevalence of *F. buski* were recorded in pigs[11-13]. Bacteriological culture of heart blood produced small greyish non hemolytic colonies in blood agar and gram staining of impression smear from lung revealed gram negative bipolarcocco bacillary organism indicating *Pasteurella* spp.[14-15] (Fig. 5). The characteristic colony morphology and Gram staining are useful methods for initial diagnosis of pasteurellosis.

Histopathological examination of lung revealed thickening of pleura with fibrin and sub pleural haemorrhages in lungs, thickening of interlobular septae with congested capillary, fibrin and inflammatory cells, severe hemorrhage, edema with fibrin strands and severe infiltration of PMNCs and MNCs in alveolar lumen, severe hemorrhage and cellular infiltration in and around the bronchi and bronchiolar wall and presence of RBCs, desquamated lining epithelial cells,

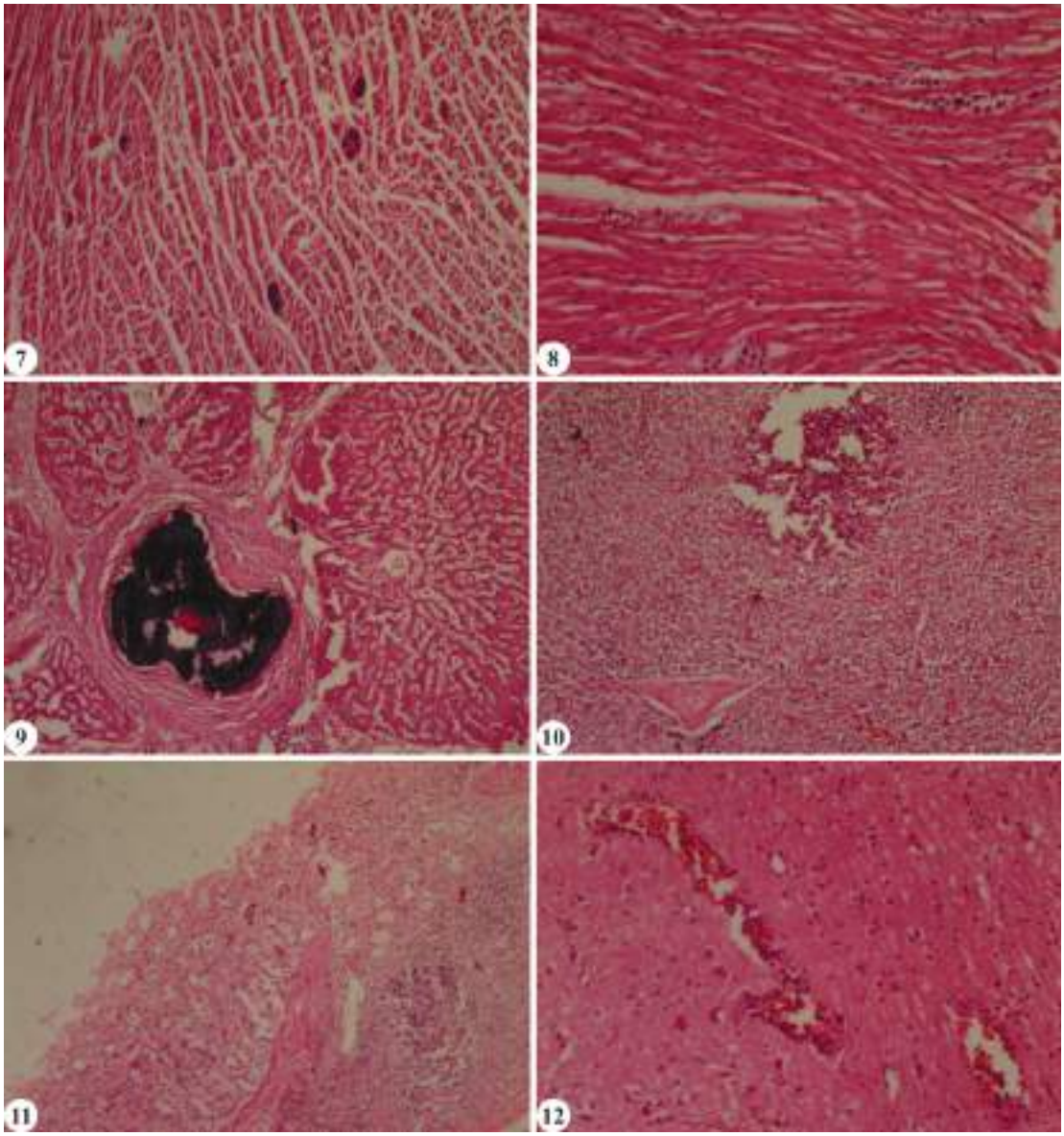

Fig. 7. Several sarcocysts with banana shaped bradyzoites in the myocardium of heart (X40); **Fig. 8.** Myocardium showing capillary congestion, haemorrhage, cellular infiltration and degeneration (X40); **Fig. 9.** Liver showing thickened interlobular septae, hepatocyte necrosis, atrophy of hepatic lobules, old granuloma with bluish stained calcified central mass surrounded by fibrous capsule and inflammatory cells in the periportal area on H&E staining (X40); **Fig. 10.** Lymphocyte necrosis and depletion, capillary congestion in lymphnode on H&E staining (X40); **Fig. 11.** Intestine showing necrosis of lining epithelial cells with infiltration of inflammatory cells in lamina propria on H&E staining (X40); **Fig. 12.** Brain showing perivascular cuffing, congestion, margination of leucocytes in blood vessels, perivascular and perineuronal oedema on H&E staining (X100).

inflammatory cells and fibrin strands in the lumen, presence of bacterial colonies in the lungs (Fig. 6). Lesions like thickening of pleura and septae with fibrin, fibrinous bronchopneumonia and filling of alveoli with fibrin, PMNCs and RBCs were described in previous studies[15, 16]. Heart revealed thickening of epicardium with fibrin and inflammatory cells; capillary congestion, neutrophil and eosinophil infiltration, hemorrhages and oedema with fibrin strands, degeneration and presence of many sarcocysts with banana shaped bradyzoites in the myocardium of heart (Fig. 7 and Fig. 8). The pathological changes in the myocardium might be due to combined effect of bacteria *Pasteurella* and parasite *Sarcocystis*. Severe non-suppurative myocarditis was described in a naturally infected sarcocystosis in a pig breeding stock[17]. However, natural Sarcocystis infections in pigs are unobvious due to development of immunity to usual low dose infections[17]. However, in highly organized farm where natural immunity to sarcocystis is diminishing due to high biosecurity measures, clinical signs may become severe after infection[17]. In a previous study, lesions like degenerative myocytolysis, inflammatory reactions, fibroblast proliferation and arterial hyperplasia were reported in naturally infected sheep with Sarcocyst species[18]. Liver revealed thickened Glisson's capsule and interlobular septae with fibrin and with accumulation of neutrophils, fibrin mass in the blood vessels with margination of neutrophils, sinusoidal congestion, haemosiderin laden macrophages, hepatocyte necrosis, atrophy of hepatic lobules, old calcified granuloma with bluish stained calcified central mass surrounded by fibrous capsule and inflammatory cells in the periportal area (Fig. 9). There are reports on severe hepatic pathology associated *Pasteurella* spp. in different animal species[19,20]. Lymphocyte necrosis and depletion, capillary congestion, haemorrhage and neutrophilic infiltration were observed in bronchial and mediastinal lymphnodes (Fig. 10) and spleen. Necrosis and desquamation of lining epithelial cells were noticed in stomach. Presence of inflammatory cells, RBCs, necrosed and desquamated lining epithelial cells in the lumen of intestine and capillary congestion and infiltration of inflammatory cells including eosinophils and plasma cells were observed in lamina propria of intestine (Fig. 11). Haemorrhage, ulceration and denudation of intestinal lining epithelial cells with infiltration of mononuclear cells and eosinophils in the intestinal tissue was reported in pigs infected with *F. buski*[11,21]. Helminths infection induces Th-2 cytokines and down regulates Th-1 cytokines inhibiting intracellular microparasite control and may cause exacerbation of concomitant infections those were controlled by Th-1 response[22]. The pathological changes in the intestine might be due to combined effect of bacteria and parasite. In kidney, thickened capsule, inflammatory cells in the interstitium, capillary congestion and tubular epithelial degeneration were observed microscopically. In our study, perivascular cuffing, congestion and margination of leucocytes in blood vessels, perivascular oedema, neuronal degeneration and perineuronal oedema were observed in the brain (Fig. 12). Cerebral lesions like perineuronal and perivascular oedema, encephalomalacia and fibrinous meningitis were reported in goat kid infected with *P. multocida*[23].

Concurrent infection alters disease progression in many instances. Concurrent parasitic infection may aggravate or ameliorate the pathological effect. The increased incidence of pneumonia due to increased gastro intestinal parasitism in Nigerian Goats was reported[24]. Impediment of pulmonary defense mechanism and aggravating pneumonia in Nigerian goats due to other bacterial and viral pathogens could be due to pulmonary oedema associated with parasitic protein loosing enteropathy[24]. In another study in different species, the direct and indirect effects of invasive parasite on disease outbreak were studied. It was demonstrated that infection of blue mussels with parasitic copepod *Mytiicolla intestinalis* increased the rate of secondary *Vibrio* infection as compared to mussels not exposed to parasitic copepod infection due to decreased efficiency of cellular immunity and not due to direct serious pathological effect[25]. Co-infection of cattle with *Fasciola gigantic* and tuberculosis was reported to increase the risk of developing TB lesions due to lower INF-γ Level[26]. In other instances, parasitic co-infection resulted in increased mortality of the host due to increased bacterial loads in different organs as a result of facilitation of bacterial invasion owing to more damage to the epithelium or by disturbing metabolic profile of GI tract or by increasing level of cortisol causing immunosuppression or by increasing blood β-hydroxybutyrate level and damaging mammary cellular immunity or by causing significant lymphopenia in co-infected host[27]. Therefore, in the present study, the parasitic infection (*F. buski* and *Sarcocystis* spp.) might have enhanced the pathological effect of *Pasteurella* infection directly or indirectly in pig resulting in fatal outcome. Further future studies are required at cellular and molecular level for better understanding of complex mechanism of interaction among above three pathogens and for future development of therapeutics and control measures.

CONCLUSION

Based on pathological, bacteriological and parasitological examination, the case was diagnosed as acute fibrino-suppurative bronchopneumonia and septicaemia caused by *Pasteurella* spp. associated with cardiac sarcocystosis and intestinal fasciolopsiasis. This is the first documented report on pathology of natural concurrent bacterial and parasitic infection in swine.

In field conditions, it is suggested to consider parasitic concurrent infection before initiating any treatment or vaccination against other pathogens. Due to one health significance of the above pathogens, coordinated multidisciplinary effort is essential to develop new strategies for effective diagnosis, treatment, prevention and control of the above pathogens.

ACKNOWLEDGEMENT

The authors wish to acknowledge Director, ICAR-IVRI for providing necessary facility to carry out this research work.

REFERENCES

1. Risco D, Serrano E, Fernández-Llario P, Cuesta JM, Gonçalves P, Garcia-Jimenez WL, Martinez R, Cerrato R, Velarde R, Gómez L and Segales J. 2014. Severity of bovine tuberculosis is associated with co-infection with common pathogens in wild boar. *PLoS One* **9:** e110123.
2. Rhoades KR and Rimler RB. 1987. Capsular groups of Pasteurella multocida isolated from avian hosts. *Avian Dis* **31:** 895-898.
3. John JK, Das T, Kumar S, Sethi M, Vamadeavan B, Tomar N and Saikumar G. 2017. Polyserositis associated with *Pasturella multocida* Type A in a crossbred pig. *Int J Livest Res* **7:** 268-74.
4. Sethi M, Kumar S, Tomar N, John JK, Das T, Agarwal RK and Saikumar G. 2017. Molecular diagnosis and antibiogram of *Pasteurella multocida* type B associated with septicemic pasteurellosis in pigs. *Indian J Anim Sci* **87:** 1488-1491.
5. Vu-Khac H, Trinh TTH, Nguyen TTG, Nguyen XT and Nguyen TT. 2020. Prevalence of virulence factor, antibiotic resistance, and serotype genes of *Pasteurella multocida* strains isolated from pigs in Vietnam. *Vet World* **13:** 896-904.
6. Piva MM, Schwertz CI, Bianchi RM, Henker LC, Morés MA, Rebelatto R, Kemper RT, Goslar MS, Nagae RY and Pavarini SP. 2023. Pasteurella multocida polyserositis in growing-finishing pigs. *J Comp Pathol* **202:** 16-22.
7. Saleque A and Bhatia BB. 1991. Prevalence of Sarcocystis in domestic pigs in India. *Vet Parasitol* **40:** 151-153.
8. Ranjan S, Saurabh K and Prasad RR. 2017. Gastrointestinal manifestations of Fasciolopsis buski associated polyparasitism in patients of an endemic area: a hospital-based study. *Int J Community Med Public Health* **4:** 1898-900.
9. Choudhary M, Choudhary BK and Ghosh RC. 2020. Pathological changes associated with natural outbreak of swine pasteurellosis. In Pests, Weeds and Diseases in Agricultural Crop and Animal Husbandry Production. Intech Open.
10. Liu LX and Harinasuta KT. 1996. Liver and intestinal flukes. *Clin Gastroenterol* **25:** 627-636.
11. Datta S, Sasmal NK, Mukherjee GS, Ghosh JD, Basak DK, Mukhopadhayay SK and Singh KS. 2004. Prevalence of gastro-intestinal parasites with special reference to pathology of Fasciolopsis Buski infection in local pigs of West Bengal. *Indian J Vet Pathol* **28:** 18-20.
12. Patra G, Al-Abodi HR, Sahara A, Ghosh S, Borthakur SK, Polley S, Behera P and Deka A. 2020. Prevalence of parasitic fauna of pigs in North-Eastern region of India. *Biol Rhythm Res* **51:** 1298-1315.
13. Yadav S, Gupta A, Choudhary P, Pilania PK and Joshi SP. 2021. Prevalence of gastrointestinal helminths and assessment of associated risk factors in pigs from Rajasthan districts, India. *J Entomol Zool Stud* **9:** 1418-1423.
14. Bartholomew JW and Mittwer T. 1952. The gram stain. *Bacteriol Rev* **16:** 1-29.
15. Tigga M, Ghosh RC, Malik P, Choudhary BK, Tigga P and Nagar DK. 2014. Isolation, characterization, antibiogram and pathology of Pasteurella multocida isolated from pigs. *Vet World* **7:** 363-368.
16. Bhat P, Singh ND, Leishangthem GD, Kaur A, Mahajan V, Banga HS and Brar RS. 2016. Histopathological and immunohistochemical approaches for the diagnosis of Pasteurellosis in swine population of Punjab. *Vet World* **9:** 989.
17. Caspari K, Grimm F, Kühn N, Caspari NC and Basso W. 2011. First report of naturally acquired clinical sarcocystosis in a pig breeding stock. *Vet Parasitol* **177:** 175-8.
18. Farhangpazhouh F, Yakhchali M, Farshid AA and Rezaei H. 2020. Prevalence and pathologic changes due to Sarcocystis species in naturally infected sheep in Urmia city. *Iran J Zoonotic Dis* **4:** 54-60.
19. Cheville NF, Rimler RB and Thurston JR. 1988. A Toxin from Pasteurella multocida Type D Causes Acute Hepatic Necrosis in Pigs. *Vet Pathol* **25:** 518-520.
20. Cheville NF and Rimler RB. 1989. A protein toxin from Pasteurella multocida type D causes acute and chronic hepatic toxicity in rats. *Vet Pathol* **26:** 148-157.
21. Haque M and Siddiqi AH. 1978. Histopathology of gastrointestinal trematode parasites of pig and man. *Indian J Parasitol* **2:** 97-99.
22. Graham AL, Cattadori IM, Lloyd-Smith JO, Ferrari MJ and Bjørnstad ON. 2007. Transmission consequences of coinfection: cytokines writ large. *Trends Parasitol* **23:** 284-291.
23. Abdelsalam EB and Mohamed Ebrahim SS. 2023. Pasteurella multocida-induced cerebral lesions in experimentally infected Nubian goat kids: A Brief communication. *J New Medi Inn Res* **4**.
24. Adeyemi MT, Morenikeji OA, Emikpe BO and Jarikre TA. 2017. Interactions between gastrointestinal parasitism and pneumonia in Nigerian goats. *J Parasit Dis* **41:** 726-733.
25. Demann F and Wegner KM. 2019. Infection by invasive parasites increases susceptibility of native hosts to secondary infection via modulation of cellular immunity. *J Anim Ecol* **88:** 427-438.
26. Kelly RF, Callaby R, Egbe NF, Williams DJ, Victor NN, Tanya VN, Sander M, Ndip L, Ngandolo R, Morgan KL and Handel IG. 2018. Association of Fasciol agigantica co-infection with bovine tuberculosis infection and diagnosis in a naturally infected cattle population in Africa. *Front Vet Sci* **6:** 214.
27. Hananeh WM, Radhi A, Mukbel RM and Ismail ZB. 2022. Effects of parasites coinfection with other pathogens on animal host: A literature review. *Vet World* **15:** 2414-2424.

Indian J. Vet. Pathol., 49(1) : 78-81, 2025: DOI: https://doi.org/10.5958/wsv7jq89

SHORT COMMUNICATION

Clinico-pathological studies on granulosa cell tumor in a Shitzu dog

V. Sarachandra[1], A. Nasreen[*], A. Anand Kumar[1], N. Dhanalakshmi, V. Vaikunta Rao, K. Rajesh and M. Raghunath

Department of Veterinary Clinical Complex, College of Veterinary Science, Sri Venkateswara Veterinary University, Tirupati, Andhra Pradesh, India, [1]Department of Veterinary Pathology

Address for Correspondence

A. Nasreen, Assistant Professor, Department of Veterinary Clinical Complex, College of Veterinary Science, Sri Venkateswara Veterinary University, Tirupati, Andhra Pradesh, India, E-mail: nashreen7@gmail.com

Received: 13.12.2024; Accepted: 2.1.2025

ABSTRACT

A six years old Shih Tzu breed intact female dog was presented to department of veterinary clinical complex, with history of abdominal distension, exercise intolerance and normal food intake. On ultra sound examination, intestines appeared floating due to fibrinous fluid in abdomen and pleural effusions were also noticed upon x-ray examination. Cytology of ascitic fluid revealed activated mesothelial cells with clusters of cells showing anaplasia. Exploratory laparotomy was conducted upon which bilateral ovarian masses appearing soft, nodular and hyperaemic within ovarian bursa were retrieved. Impression smears showed 'Call-Exner' bodies pattern. Histopathological examination revealed neoplastic polyhedral to fusiform epithelial cells with abundant vacuolated eosinophilic cytoplasm, clustered in solid and acinar pattern supported by varying amount of fibrous connective tissue. Immunohistochemistry showed strong positivity for inhibin-α. The case was confirmed as granulosa cell tumor based on gross, cytological, histopathological and immunohistochemical examinations.

Keywords: Ascites, call-exner bodies, granulosa cell tumor, inhibin-α

How to cite this article : Sarachandra, V., Nasreen, A., Kumar, A.A., Dhanalakshmi, N., Rao, V.V., Rajesh, K. and Raghunath, M. 2025. Clinico-pathological studies on granulosa cell tumor in a Shitzu dog. Indian J. Vet. Pathol., 49(1) : 78-81.

Canine ovarian neoplasms are generally classified into three primary categories: germ cell tumors, epithelial tumors and sex cord-stromal tumors. The prevalence of these histological types differs across various studies[1]. Epithelial neoplasms are prevalent in certain studies while sex cord-stromal tumors are more frequently observed in others[1,2]. Granulosa cell tumors (GCT) are rare ovarian neoplasms in dogs and have been documented only sporadically[1]. Granulosa cell tumors (GCT) are regarded as rare low-grade malignant neoplasms in both humans and canines, with a low likelihood of metastasis. Granulosa cell tumors in felines and bovines are considered to be more aggressive compared to those found in canines[3]. GCTs are most frequently observed in middle-aged to older female dogs. A GCT falls under the category of sex cord-stromal tumors, originating from sex cords or primitive cortical lobules, as well as the specialized stroma or mesenchyme of the developing gonad. These tumors may have the capacity to synthesize estrogen and progesterone, leading to clinical manifestations associated with the reproductive system[4].

A female intact shih tzu dog of 6 years age was presented to department of teaching clinical complex with a history of abdominal distension for 10 days, exercise intolerance, normal feeding and voiding. On physical examination, temperature was recorded as 102.7^{O}F and conjunctival mucous membrane appeared pink. On ultrasonography, ascitic fluid was noticed in abdomen. Remaining visceral organs appeared normal. X-ray examination revealed ascitic fluid in ventral abdomen displacing intestines dorsally. Whole blood and serum samples were collected for hematological and serological studies. Ascitic fluid was collected and analysed for cytopathology and biochemical alterations. The case was advised to undergo exploratory laparotomy.

By performing exploratory laparotomy, ovarian mass was identified within ovarian bursa bilaterally and tumor mass was incised along with ovariohysterectomy. Cytological impression smears were obtained upon incising the ovarian mass and stained. Tumor sample was fixed in 10% neutral buffered formalin for histopathological examination. The tissues were stained using haematoxylin and eosin method after the standard tissue preparation using paraffin embedding procedure[5]. Immunohistochemistry was conducted using inhibin alpha marker procured from Biogenex Bangalore.

A six-year-old unspayed female shit tzu dog was presented to the department of veterinary clinical complex with a history of exercise tolerance with abdomen distension since 10 days with normal feeding history (Fig. 1). The animal had undergone regular deworming and vaccination. On clinical examination, the animal was seen active with pink conjunctival

Table 1. Haematology of GCT dog.

Haematology	Hb (g%)	TEC (mill/μL)	TLC (1000/μL)	PLT (1000/ml)	N (%)	L (%)	E (%)	M (%)
GCT	10	3.4	27	155	76	23	-	1

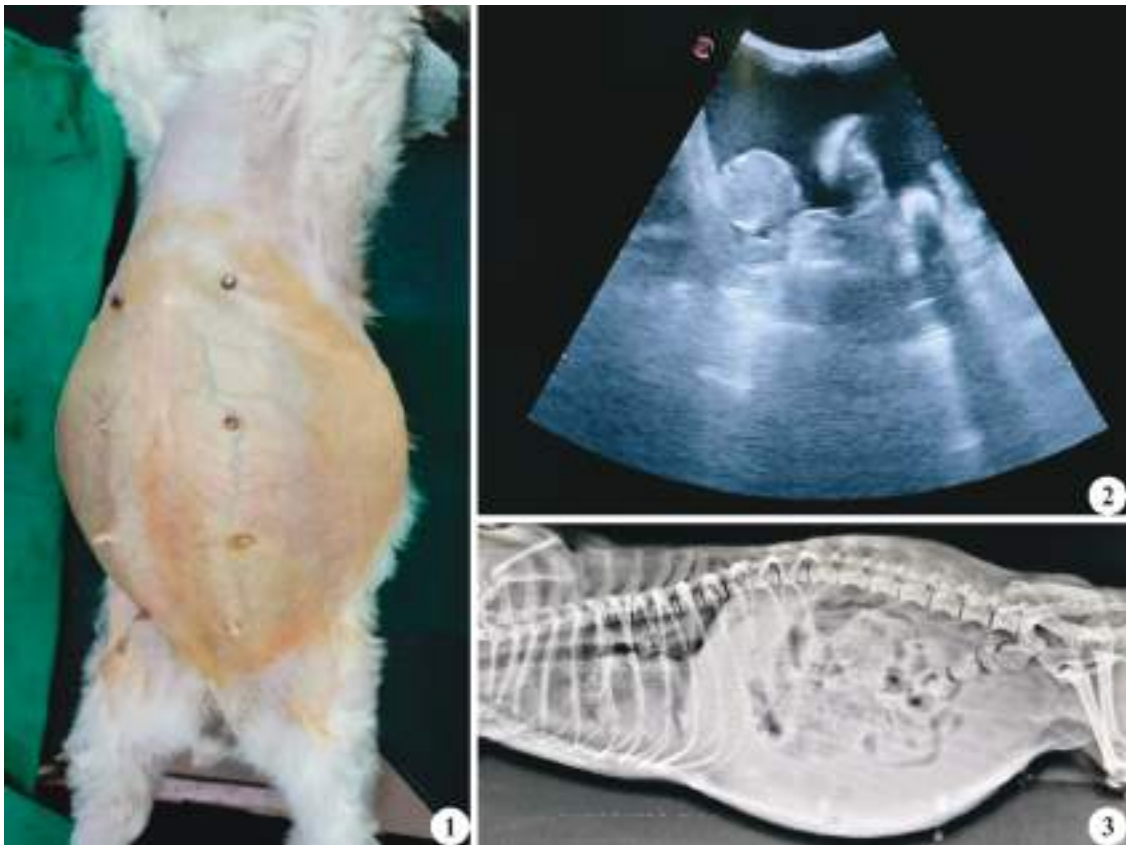

Fig. 1. Dog showing distended abdomen; **Fig. 2.** Ultrasound image showing effusion in abdomen; **Fig. 3.** X-ray showing distended abdomen due to effusion with intestines floating.

mucous membrane, buthada temperature of 102.7^{O}F and distended abdomen. On palpation of the abdomen, fluid thrill was noticed. Canine ovarian tumors that remain asymptomatic for extended durations pose a significant risk for clinical diagnosis. In certain instances of non-functional germ cell tumors, the absence of reproductive symptoms or misdiagnosis can lead to delays in imparting the necessary treatment. Delays in diagnosing large, non-functioning GCTs and reports of incidental findings have been recorded[6]. Heamatology and biochemical analysis of the dog revealed anemia, leucocytosis, hypoalbuminemia and hyper globulinema which were a few of the paraneoplastic syndromes observed in many canine tumors[7] (Table 1 & 2). Abdominal ultrasonography revealed hypoechoic ascitic fluid with normal visceral organs (Fig. 2). X-ray of lateral abdomen revealed ascitic fluid in ventral abdomen displacing intestines dorsally (Fig. 3). Pleural effusions in cranial lung lobe could be observed. In instances where abdominal effusion is present, cytological evaluations along with transabdominal ultrasonography prove to be valuable diagnostic tools for identifying these tumors[8].

Ascitic fluid analysis showed a specific gravity of 1.030, total protein was 5 g/dl, albumin was 2.9 g/dl, A/G ratio was 1:1, fluid creatinine was 1.5 mg/dl, fluid glucose was 20 mg/dl, fluid bilirubin was 0.5 mg/dl, fluid cholesterol was 213 mg/dl and fluid triglyceride was 22 mg/dl. Cytological examination of ascitic fluid revealed activated polyhedral to oval shaped pleomorphic

Table 2. Serum biochemistry of GCT dog.

Biochemistry	ALT (U/L)	AST (U/L)	TP (g/dL)	Albumin (g/dL)	Globulin (g/dL)	Creatinine (mg/dL)	BUN (mg/dL)	Glucose (mg/dL)	Calcium (mg/dL)	GGT (U/L)
GCT	28	58	8.8	3.6	5.2	1.54	25	89	10.1	18

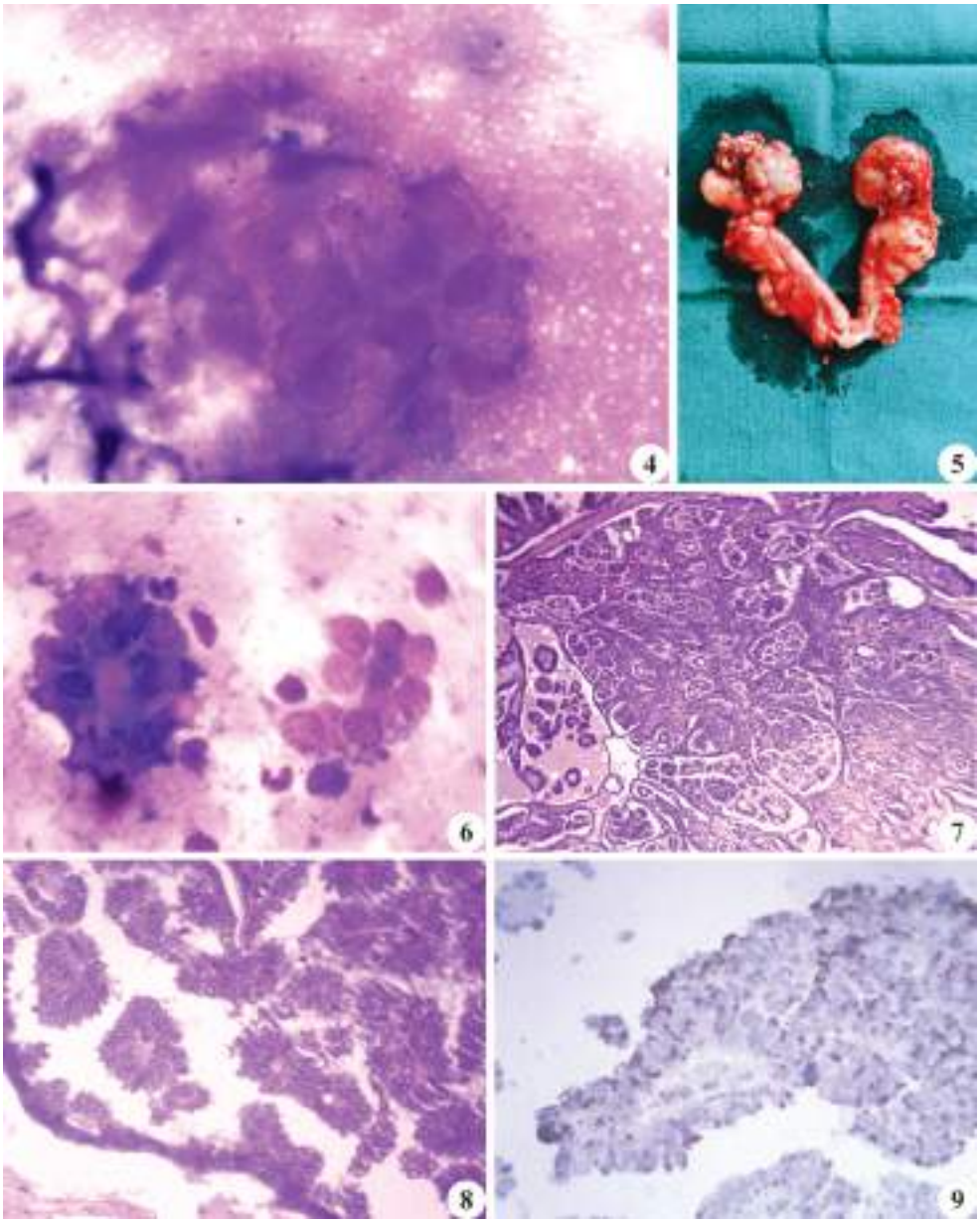

Fig. 4. Ascitic fluid cytology - Clusters of cells showing anaplasia (Fields Stain X1000); **Fig. 5.** Bilateral enlargement of ovaries with nodular surface; **Fig. 6.** Ovary impression smear - Cells arranged in rosette pattern with central eosinophilic call exner body (Fields Stain X1000); **Fig. 7.** Ovary - Diffuse proliferation of granulosa cells forming rosettes (H&E X100); **Fig. 8.** Ovary - Granulosa cells in rosette pattern with central eosinophilic call exner body (H&E X400); **Fig. 9.** Ovary - Brown precipitate in the cytoplasm of granulosa cells (Inhibin-alpha X400).

mesothelial cells with prominent nucleoli (Fig. 4). Exploratory laparotomy was conducted by a team of expert surgeons under inhalant general anaesthesia. Fluid was drained and ovarian mass were observed by palpating the ovarian bursa and metastasis was noticed in abdomen with intestinal mesentery showing few greyish white nodules and spleen having nodular mass. GCT has been linked to metastases in various organs including the mesentery, omentum, liver, kidneys, bladder, diaphragm, uterus and lymph nodes. Additionally, there has been one reported case of metastasis to the myocardium and lungs[9]. Ovariohysterectomy was conducted and ovaries along with uterus were incised and removed from abdomen.

Grossly, both the ovarian masses appeared nodular with soft consistency and haemorrhagic areas (Fig. 5). On cut section, mass appeared haemorrhagic with mild oozing of fluid. Impression smears showed clusters of polyhedral to oval granulosa cells arranged in rosette manner forming pink eosinophilic Call-Exner bodies in the centre (Fig. 6). Histopathology of both ovarian masses showed haemorrhages, engorged blood vessels and neoplastic cells arranged in solid and tubular to

acinar pattern, supported by fibrous connective tissue. Some areas showed serous eosinophilic fluid. The cells were cuboidal to columnar type with centrally placed vesicular nuclei containing single to multiple nucleoli and surrounded by moderate quantity of pale foamy cytoplasm. In focal areas of acinar structures, clusters of cells were arranged in rosettes around protein droplets, suggesting the formation of 'Call-Exner' bodies (Fig. 7 & 8). Mild lymphocytic infiltration was observed. GCTs are defined by the significant presence of cells exhibiting morphological characteristics typical of granulosa cells. Additionally, cells that resemble theca externa, theca interna, and collagen-producing fibroblasts are often found and may exceed the number of granulosa cells. The existence of stromal components, such as theca cells, may indicate a non-neoplastic reaction of the ovarian stroma to the proliferation of granulosa cells, rather than representing neoplastic activity in certain instances[12]. Bilateral ovarian granulosa tumor was reported in mares[10]. Immunohistochemical evaluation of inhibin alpha revealed positive staining in the granulosa cells as brown amorphous precipitate in cytoplasm (Fig. 9). Positive immunostaining for inhibin is a distinctive characteristic of both normal and neoplastic granulosa cells, associated with sex-cord differentiation. Therefore, inhibin can be considered as ahistogenetic marker for granulosa cell tumors and thecomas, while acting as a negative marker for non-stromal ovarian neoplasms[11].

REFERENCES

1. Patnaik AK and Greenlee PG. 1987. Canine ovarian neoplasms: a clinicopathologic study of 71 cases, including histology of 12 granulosa cell tumors. *Vet Pathol* **24:** 509-514.
2. Norris HJ, Garner FM and Taylor HB. 1970. Comparative pathology of ovarian neoplasms IV. Gonadal stromal tumors of canine species. *J Comp Pathol* **80:** 399-405.
3. Gelberg HB and McEntee K. 1985. Feline ovarian neoplasms. *Vet Pathol* **22:** 572-576.
4. Klein MK. 1996. Tumors of the female reproductive system. In: Withrow SJ, MacEwen EG, editors. Small Animal Clinical Oncology. 2nd edn. Saunders, Philadelphia, 347-355.
5. Bancroft DJ and Cook CH. 1994. Fundamentals of normal histology and histopathology. Manual of histopathological techniques and their diagnostic application, 2nd edition, Churchill Livingstone, Edinburgh.
6. Pragathi A, Chowdary CSR, Samatha V, Subhashini N, Devi VR and Vardhan MS. 2024. Histomorphological and immunohistochemical studies on Canine ovarian tumours. *Indian J Vet Pathol* **48:** 231-235.
7. Allen HL and Franklin GA. 1975. Malignant granulosa cell tumor in a bitch. *J Am Vet Med Assoc* **166:** 447-448.
8. Anikwue C, Dawood MY and Kramer E. 1978. Granulosa and theca cell tumors. *Obstets Gynecol* **51:** 214-220.
9. Cotchin E. 1961. Canine ovarian neoplasms. *Res Vet Sci* **2:** 133-142.
10. Chesnutt RK. 1980. Granulosa cell tumor in a Golden Retiever. *Vet Med Small Anim Clin* **75:** 444-445.
11. Van Niekerk CC, Ramaekers FC and Hanselaar AGJM. 1993. Changes in expression of differentiation markers between normal ovarian cells and derived tumors. *Am J Pathol* **142:** 157-177.

Indian J. Vet. Pathol., 49(1) : 82-84, 2025: DOI: https://doi.org/10.5958/7zgtf226

SHORT COMMUNICATION

Pathomorphological study of Notoedric Mange in rabbit

N.D. Singh*, A. Verma, R. Sood and H. Singh[1]
Department of Veterinary Pathology, College of Veterinary Science, GADVASU, Ludhiana, Punjab-141 004, India,
[1]Department of Veterinary Parasitology

Address for Correspondence
N.D. Singh, Professor, Department of Veterinary Pathology, College of Veterinary Science, GADVASU, Ludhiana, Punjab-141 004, India, E-mail: nitindevsingh@gadvasu.in

Received: 28.10.2024; Accepted: 2.12.2024

ABSTRACT

In order to identify the cause of death, a carcass of an 8-month-old *Soviet chinchilla* was presented to Department of Veterinary Pathology, GADVASU, Ludhiana with the history of emaciation and dermatitis. A detailed investigation of the carcass revealed crusty lesions in ears and alopecic patches around eyes and lips. The parasitological investigation of skin scrapings revealed the presence of *Notoedres cati*, which very rarely infests rabbits. Histopathology revealed multiple mite burrows in skin along with hyperkeratosis and lymphoeosinophilic infiltration. Based on the gross lesions, morphology and histopathology, a very rare case of Notoedric mange in soviet chinchilla is documented.

Keywords: Mites, notoedric mange, skin, *soviet chinchilla*

Oryctolagus cuniculus are the domesticated rabbit and can be reared in varying conditions and acts as a source good quality protein, fiber, animal model for various research and company[1,2]. Mange in rabbits is an emerging and highly transmissible disease brought about by numerous burrowing and non-burrowing mite species and creates a significant threat to the sustainability of rabbit husbandry practices[3]. The borrowing mite *Notoedres cati* is a cause a of highly infectious skin infestation referred as notoedric mange, also Feline scabies and head mange, is one of least reported cause of acariotic mange in rabbits[4]. *N. cati* is classified under the family Sarcoptidae which also includes other borrowing mites *viz. Sarcoptes* and *Trixacarus*. The adult female borrows into epidermis and cause varying degree of dermatitis along with erythema, pruritis, hair loss, scaling and dermal encrustation characteristic of mange, persistent infestation can lead severe cachexia[5,6] as well as vestibular disease and meningitis[7] and also predisposes their skin to other complications like secondary bacterial infections[8]. The mites typically feed off stratum granulosum and serum of the host[9].

An 8-month-old male *Soviet chinchilla* was presented for necropsy examination at the Department of Veterinary Pathology, GADAVASU, Ludhiana with a history of long-standing dermatitis and subsequent debilitation. A thorough necropsy examination was conducted at the departmental necropsy hall. All the gross lesions were recorded and photographed. Representative tissues were taken in 10% neutral buffered formalin. Collected tissues were processed and stained using hematoxylin and eosin (H&E)[10]. Furthermore, ear scrapping was taken in 10% KOH solution and heated at 75^{O}C and observed under microscope[11].

On gross examination, the dehydrated rabbit carcass exhibited emaciation partially dried and crusted scab over both ears and areas of alopecia and eczema of skin around eyes and lips (Figs. 1 and 2). Adult *Notoedres cati* parasites were characterized by circular rings on the dorsal surface, lack of scales and prominent dorsal anus in rabbit skin scrapings (Fig. 3).

On histological examination, lesions on skin were characterized by hyperkeratosis with both para and orthokeratosis along with rete pegs invading into underlying dermis (Fig. 4). Cross sections of mites were also seen in burrows in the epidermis mainly in stratum corneum (Fig. 5) and also in overlying scab. Some keratin cysts were also observed. Under affected epidermis there was infiltration of mainly lymphocytes as well as eosinophils (Fig. 6). Epidermal micro abscesses were also observed.

How to cite this article : Singh, N.D., Verma, A., Sood, R. and Singh, H. 2025. Pathomorphological study of Notoedric Mange in rabbit. Indian J. Vet. Pathol., 49(1) : 82-84.

N. cati infestation have been rarely described in rabbits. Transmission is generally through intimate contact within a host species[12] and also from one animal to another via direct contact or via interaction with the environment[13,14]. One epidemiological study conducted in Egypt revealed only a 2.5% prevalence of Notoedric mange in lagomorphs[15].Concurrent infestation of *Notoedres* with Sarcoptic and/or Psoropti cacariosis in rabbits have also been described in various studies[4,14,16]. Clinically *N. cati* infestations in rabbits can cause scales, scabs,

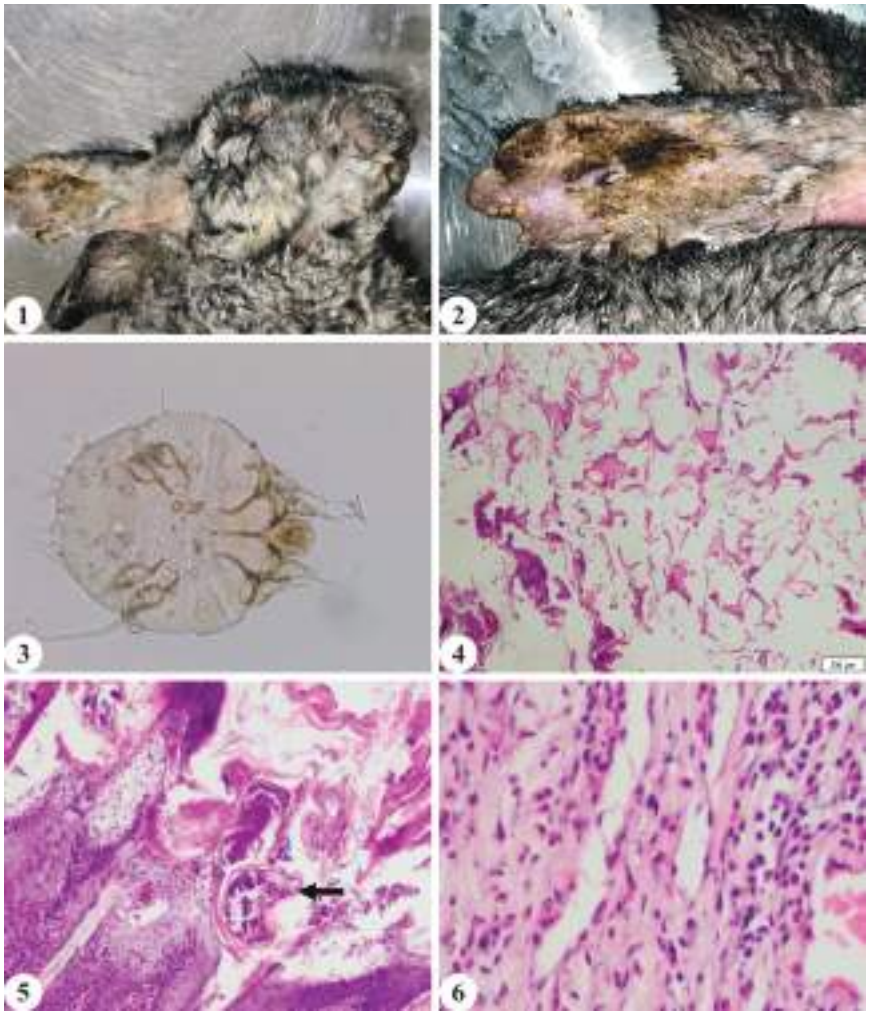

Fig. 1. Eczemia and alopecaon skin around eyes and lips; **Fig. 2.** Thick crusted scab over ear; **Fig. 3.** Photomicrograph of the notoedric mite (400x); **Fig. 4.** Skin: Low power image revealing massive hyperkeratosis with numerous mites (H&E 40x); **Fig. 5.** A section of skin exposes mites (arrow) in burrows in the epidermis, as well as rete papillae development in the epithelium along with serocellular and eosinophilic crust (H&E 100x); **Fig. 6.** Mononuclear inflammatory cells infiltration along with heterophils in the underlying dermis (H&E 400x).

and irritation on the pinnae, ear canal, lips, nose and face as well as other body areas such as the neck, legs and genitalia[13]. *Notoedres* sp. create pathogenic effects by tunneling behavior and physical damage produced by the mites during excavations, irritating action of their secretions and excretions, allergic responses to certain of their extracellular products and mainly the production of interlukin-1[17,18]. The pathological finding in current study were in concordance with earlier literature which described similar lesions[4,19]. The primary way to identify *N. cati* is by deep skin scrapings. The most widely used acaricides are organophosphorus chemicals (diazinon), synthesized pyrethroids and macrolactones. Ivermectin, either orally or parenterally is proven to be an efficient acaricide for disease treatment[14,20].

The gross, histopathology and parasitological findings in current case confirmed notoedric mange infestation in rabbit. This report highlights the pathological alterations during the *N. cati* infestation in rabbits which is seldomly reported. Although treatment with several acaricidals have been proven affective none the less preventing it is crucial, since it is highly contagious may cause significant economic losses for rabbit herds.

REFERENCES

1. Rafay J and Parkányi V. 2016. The rabbit as a model and farm animal at the Research Institute for Animal Production Nitra: A review. *Slovak J Anim Sci* **49:** 141-146.
2. Bharathy N, Sivakumar K, Vasanthakumar P and Sakthivadivu R. 2022. Rabbit Farming in India: An Overview. *Agri Rev* **43:** 223-228.
3. Abd El-Ghany WA. 2022. Mange in Rabbits: An Ectoparasitic Disease with a Zoonotic Potential. *Vet Med Int* 5506272.
4. Darzi MM, Mir MS, Shahardar RA and Pandit B. 2007. Clinico-pathological, histochemical and therapeutic studies on concurrent sarcoptic and notoedric acariosis in rabbits *(Oryc-*

tolagus cuniculus). Vet Arh **77:** 167-175.
5. Choe S, Kim S, Na KJ, Nath TC, Ndosi BA, Kang Y, Bia MM, Lee D, Park H, Eamudomkarn C and Jeon HK. 2020. First Infestation Case of Sarcoptic Mange from a Pet Rabbit *Oryctolagus Cuniculus* in Republic of Korea. *Korean J Parasitol* **3:** 315-319.
6. Mullen GR and O Connor BM. 2019. Chapter 26 - Mites (Acari). In: Mullen GR, Durden LA, editors. Medical and Veterinary Entomology (Third Edition). Academic Press. pp. 533-602.
7. Ulutas B, Voyvoda H, Bayramli G and Karagenc T. 2005. Efficacy of topical administration of eprinomectin for treatment of ear mite infestation in six rabbits. *Vet Dermatol* **16:** 334-337.
8. Swe PM, Zakrzewski M, Kelly A, Krause L and Fischer K. 2014. Scabies Mites Alter the Skin Microbiome and Promote Growth of Opportunistic Pathogens in a Porcine Model. *PLOS Neglected Trop Dis* **8:** e2897.
9. McCarthy JS, Kemp DJ, Walton SF and Currie BJ. 2004. Scabies: more than just an irritation. *Postgrad Med J* **80:** 382-387.
10. Luna LG. 1968. Manual of Histological Staining Methods of the Armed Forces Institute of Pathology. 3rd Edn. McGraw Hill Book Co. New York. pp. 230.
11. Soulsby EJL. 1982. Helminths, Arthropods and Protozoa of Domesticated Animals, 7th Paris, France: ELBS. Baillers Tindall. pp. 764-765.
12. Sivajothi S, Sudhakara Reddy B, Rayulu VC and Sreedevi C. 2015. *Notoedrescati* in cats and its management. *J Parasit Dis* **39:** 303-305.
13. Borkataki S, Islam S and Goswami P. 2018. Efficacy of ivermectin against *Notoedrescati*var cuniculi in New Zealand white rabbits. *Vet Pract* **19:** 29-30.
14. Panigrahi PN, Mohanty BN, Gupta AR, Patra RC and Dey S. 2016. Concurrent infestation of Notoedres, Sarcoptic and Psoropticacariosis in rabbit and its management. *J Parasit Dis* **40:** 1091-1093.
15. Elshahawy I, El-Goniemy A and Ali E. 2016. Epidemiological survey on mange mite of rabbits in the Southern region of Egypt. *Sains Malaysiana* **45:** 745-751.
16. Ravindran R and Subramanian H. 2000. Effect of seasonal and climatic variations on the prevalence of mite infestation in rabbits. *IVJ* **77:** 991-992.
17. Wall R and Shearer D. 1997. Veterinary Entomology. London: Chapman and Hall; Pp. 43-83.
18. RA McPherson MR and Pincus. 2017. Henry's Clinical Diagnosis and Management by Laboratory Methods, 23rd edn. St. Louis, Missouri: Elsevier, Pp. 1276-1283.
19. Schoeb TR, Cartner SC, Baker RA and Gerrity LG. 2007. Parasites of rabbits. In: Baker, DG (Ed), Flynn's Parasites of Laboratory Animals. Blackwell Publishing, Ames, pp. 451-500.
20. Eraslan G, Kanbur M, Liman BC, Çam Y, Karabacak M and Altınordulu Ş. 2010. Comparative pharmaco kinetics of some injectable preparations containing ivermectin in dogs. *Food-Chem Toxicol* **48:** 2181-2185.

Indian J. Vet. Pathol., 49(1) : 85-89, 2025: DOI: https://doi.org/10.5958/ehyqc013

SHORT COMMUNICATION

Pathology of *Aeromonas hydrophila* infection in rainbow trout (*Oncorhynchus mykiss*) of Himachal Pradesh

Rajendra Damu Patil*, Ekta Bisht, Abhishek Verma, Rinku Sharma[1] and Rajesh Kumar Asrani
Department of Veterinary Pathology, Dr G.C. Negi College of Veterinary and Animal Sciences, CSK Himachal Pradesh Krishi Vishvavidyalaya, Palampur-176 062, Himachal Pradesh, [1]Disease Investigation Laboratory, ICAR-Indian Veterinary Research Institute, Regional Station, Palampur-176 061, Himachal Pradesh, India

Address for Correspondence
Rajendra Damu Patil, Associate Professor, Department of Veterinary Pathology, Dr G.C. Negi College of Veterinary and Animal Sciences, CSK Himachal Pradesh Krishi Vishvavidyalaya, Palampur-176 062, Himachal Pradesh, E-mail: rdpatil02@gmail.com

Received: 10.10.2024; Accepted: 22.1.2025

ABSTRACT

Trout fish farming is playing an important role in providing livelihood and nutritional security to the people of hilly state like Himachal Pradesh. The present investigation was conducted during a natural outbreak of *Aeromonas hydrophila* infection in rainbow trout *(Oncorhynchus mykiss)* in a commercial trout fish farm located in the Mandi district of Himachal Pradesh, India. The overall mortality was 30%. A total of twenty-one moribund rainbow trout of around 5 months age were investigated. The clinical signs exhibited by the fish before death were lethargy, slow movement and gasping. The gross lesions at necropsy were distended abdomen (dropsy), cutaneous haemorrhages and/or ulcerative lesions at the base of fins and anal area, ascites and mild to severe degree of congestion and haemorrhage in the visceral organs. The samples collected at necropsy included swabs from the skin lesions, liver and kidney for bacteriological studies and representative tissues for histopathological evaluation. Bacteriological studies revealed the presence of *Aeromonas hydrophila* in the samples of moribund trout. Microscopically, gills, liver, kidneys and skeletal muscles revealed predominant vascular changes such as congestion, haemorrhage and oedema, vacuolar or Zenker's degeneration, necrosis and an inflammatory reaction. In addition, decreased haematopoiesis in the anterior kidney and melano-macrophage center infiltration in the liver and kidney were also observed. In conclusion, the outbreak was diagnosed as acute severe septicaemic *Aeromonas hydrophila* infection associated with significant mortality in rainbow trout leading to economic losses.

Keywords: *Aeromonas hydrophila, Oncorhynchus mykiss,* pathology, trout fish

How to cite this article : Patil, R.D., Bisht, E., Verma, A., Sharma, R. and Asrani, R.K. 2025. Pathology of *Aeromonas hydrophila* infection in rainbow trout *(Oncorhynchus mykiss)* of Himachal Pradesh. Indian J. Vet. Pathol., 49(1) : 85-89.

Aquaculture production is nowadays gaining popularity in meeting the nutritional requirements of humans due to increasing population[1]. Rainbow trout *(Oncorhynchus mykiss)* is a cold-water fish belonging to *Salmonid* family and is highly valued for its nutritional potential. Himachal Pradesh is one of the leading states in rainbow trout farming and seed production in India with a total production of 849.7 tonnes in the recent past[2]. The rich water resources of Himachal Pradesh offer a great potential for trout fish farming, providing livelihoods to the native population and ensuring food security.

Aeromonas hydrophila is a ubiquitous bacterial pathogen in marine and freshwater habitats but can emerge as a primary or opportunistic pathogen if it encounters favourable conditions, affecting fish farming on a large scale and causing significant economic losses[3]. *A. hydrophila* is facultatively anaerobic, motile, Gram-negative bacterium that optimally grows at 22-32^{O}C, with a few strains surviving even at low temperature, affecting and causing diseases in all classes of vertebrates including fishes[4,5]. It is a non-spore forming, rod-shaped bacterium belonging to *Aeromonadaceae* family of the class, *Gammaproteo bacteria*. The biochemical characteristics are positive for catalase, oxidase and indole tests[6]. Many studies have demonstrated freshwater bodies to be the reservoirs of *A. hydrophila* which is the etiological agent involved in causing disease conditions such as motile aeromonas septicemia (MAS), hemorrhagic and ulcerative diseases in fishes including rainbow trout, catfish, carp and salmon[1,6,7].

Fish farmers are greatly impacted by acute *A. hydrophila* outbreaks in which mortality rates can reach up to 100 percent[8]. Food, animals, groundwater and wastewater are some of the other sources of this pathogen contributing to its zoonotic potential and hence raising public health concerns[1,9]. Overcrowding, increased organic content, trauma, change in temperature, unhygienic handling, contaminated feed, pollution and deficit of dissolved oxygen are some of the stressors that may contribute in the development of the infection in fishes[10]. The natural infection of *A. hydrophila* in fish depends on the species affected, season and environmental conditions[11].

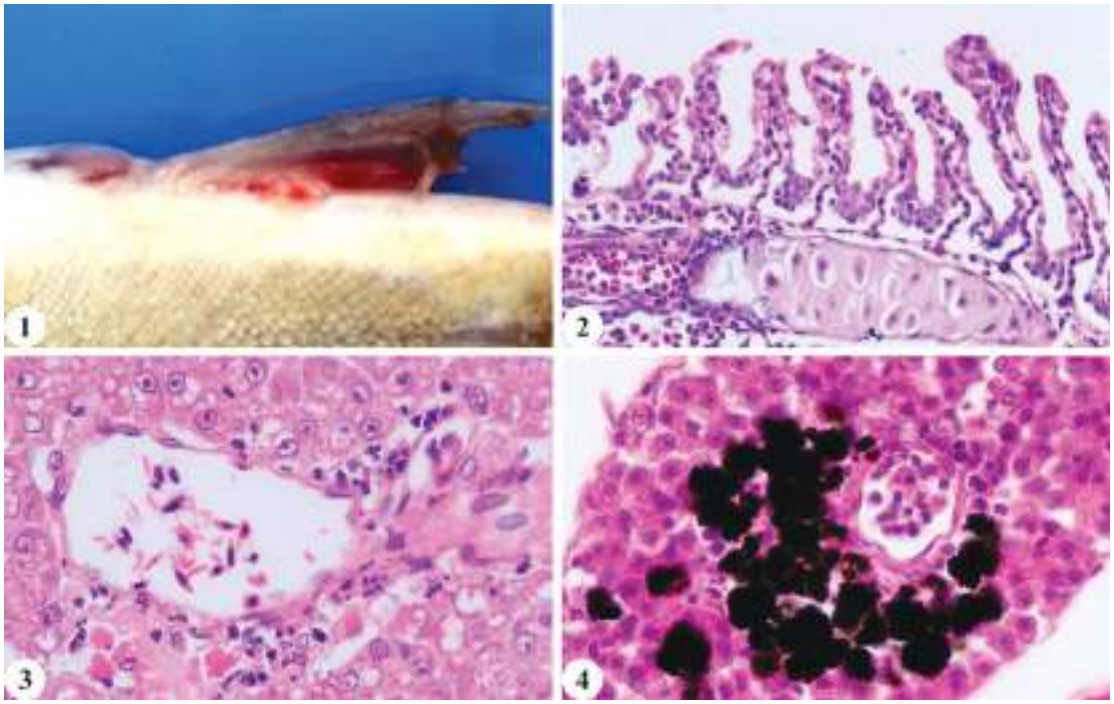

Fig. 1. Hemorrhages at the base of anal fin of rainbow trout *(Oncorhynchus mykiss)*; **Fig. 2. Gills:** Engorged and dilated vasculature, short and thickened primary and secondary lamellae and mild lymphocytic infiltration in gill lamellae (H&E x200); **Fig. 3. Liver:** Congestion, vacuolar degeneration and necrosis of a few hepatocytes in the centrilobular region (H&E x400); **Fig. 4. Liver:** Melano-macrophage center (MMC) aggregation around the central vein (H&E x400).

The present investigation was conducted during a natural outbreak of *A. hydrophila* infection in rainbow trout *(O. mykiss)* in a commercial farm with a total stock of 4000 fish located in the Mandi district of Himachal Pradesh, India. The disease outbreak was recorded in the month of July, 2023. A total of twenty-one moribund rainbow trout aged 5 months and of either sex were investigated in the Department of Veterinary Pathology, Dr G.C. Negi College of Veterinary and Animal Sciences, CSK Himachal Pradesh Krishi Vishvavidyalaya, Palampur, Himachal Pradesh. The body weights of the affected fish ranged from 110 to 150 g and the body lengths varied from 13 to 18 cm. A thorough post-mortem examination was performed and gross pathological lesions were recorded. Simultaneously, swabs were collected aseptically from the lesions on the skin and visceral organs including liver and kidney for microbiological analysis. For isolation and identification of bacteria, the swabs were streaked onto tryptic soy agar (TSA) plates and incubated at 22^{O}C for 48 hrs. The subculturing was performed to obtain pure colonies and the biochemical characterization of the bacterial isolates was performed as per the standard procedure[12]. Various biochemical tests including catalase, oxidase, indole, methyl red, citrate, Voges-Proskauer, gelatin liquefaction and motility tests were employed for species level identification of *Aeromonas* spp.

Representative tissue samples were collected at necropsy and fixed in 10% neutral buffered formalin. Thereafter, the tissue samples were processed and embedded in paraffin blocks[13]. Haematoxylin and eosin-stained sections (3-4 µm) were then examined under the light microscope.

In the present investigation, overall 30% mortality was recorded in rainbow trout. Prior to death, the affected moribund fishes exhibited clinical signs including lethargy, slow movement, gasping and distended abdomen (dropsy). At necropsy, external examination revealed eroded scales along with focally extensive areas of well-demarcated, ulcerative lesions with or without haemorrhagic borders on the skin, base of dorsal, pectoral, caudal and anal fins and anal region (Fig. 1). Internal examination showed ascitic fluid accumulation and mild to severe degree of congestion and/or haemorrhages in almost all the internal organs suggestive of septicaemia.

Histopathological examination of the tissues revealed lesions in gills, liver, kidneys and skeletal muscles. Microscopically, gills revealed severe congestion, foci of haemorrhages, short, curled to thickened primary and secondary lamellae and infiltration of lymphocytes in both primary and secondary lamellae (Fig. 2). Liver sections revealed vascular and sinusoidal congestion, areas of haemorrhage, vacuolar degeneration and necrosis of hepatocytes and infiltration of mononuclear cells, predominantly, lymphocytes (Fig. 3). Hepatic

parenchyma also revealed the presence of melano-macrophage center (MMC) aggregation in a few foci (Fig. 4). Histologically, anterior kidney exhibited decreased haematopoiesis and presence of bacterial colonies (Fig. 5). However, posterior kidney exhibited congestion, areas of haemorrhages, degeneration and necrosis of tubular epithelium, epithelial cast formation and multifocal areas of MMC aggregation in the interstitium (Fig. 6). Histopathology of the skeletal muscles revealed necrotizing myositis characterized by extensive exudation between the muscle bundles, Zenker's degeneration and necrosis of muscle fibers with loss of striations and infiltration of mononuclear inflammatory cells mainly lymphocytes (Fig. 7).

The bacterial isolates obtained from the skin lesions, liver and kidney showed yellowish opaque, round, convex, smooth-edged colonies of *A. hydrophila* on TSA media (Fig. 8). The Gram staining of the isolates revealed Gram-negative, bacilli present singly, in pairs and a few in short chains. Confirmatory diagnosis of *A. hydrophila* was made on the basis of biochemical characterization of the isolates that included positive reactions for catalase, oxidase, indole, methyl red, citrate, Voges-Proskauer, gelatin liquefaction and motility tests.

Aeromonas hydrophila is an emerging aquatic pathogen, widely distributed in the environment. It can cause disease in fish, humans and in other animals. The clinical signs including lethargy, slow movement, gasping and distended abdomen were more or less similar to those described earlier in *A. hydrophila* infected rainbow trout[14].

Aeromonas infection in fish causes world economic problems because of the high number of fish mortalities. The mortality rate of *A. hydrophila* in fish can vary (up to 100%) depending on the strain of the bacteria and the type of fish infected[8]. In the present outbreak, overall 30% mortality was recorded in rainbow trout. The susceptibility of rainbow trout to *A. hydrophila*, may be related to the environment of trout fish, which lives on clear running water, that is less exposed and less resistant to this pathogenic bacterium. Besides this, *A. hydrophila* bacteria multiplies at faster rate, colonize and cause mortality quickly in comparison to other pathogenic bacteria in fish. Additionally, the bacteria can directly cause death and co-infect with viruses, fungi, and other bacteria and synergistically aggravate the disease severity or mortality in fish[15]. Interestingly, the present disease outbreak occurred in the rainy season i.e. in the month of July, when water temperature is relatively higher than the other months of the year.

The gross findings such as eroded scales, dermal haemorrhages, ulcerations, ascitic fluid accumulation, congestion and/or haemorrhages in the internal organs are more or less similar to those reported by Zepeda-Velázquez and co-workers during the natural infection of *Aeromonas* species in rainbow trout[14]. The gross and

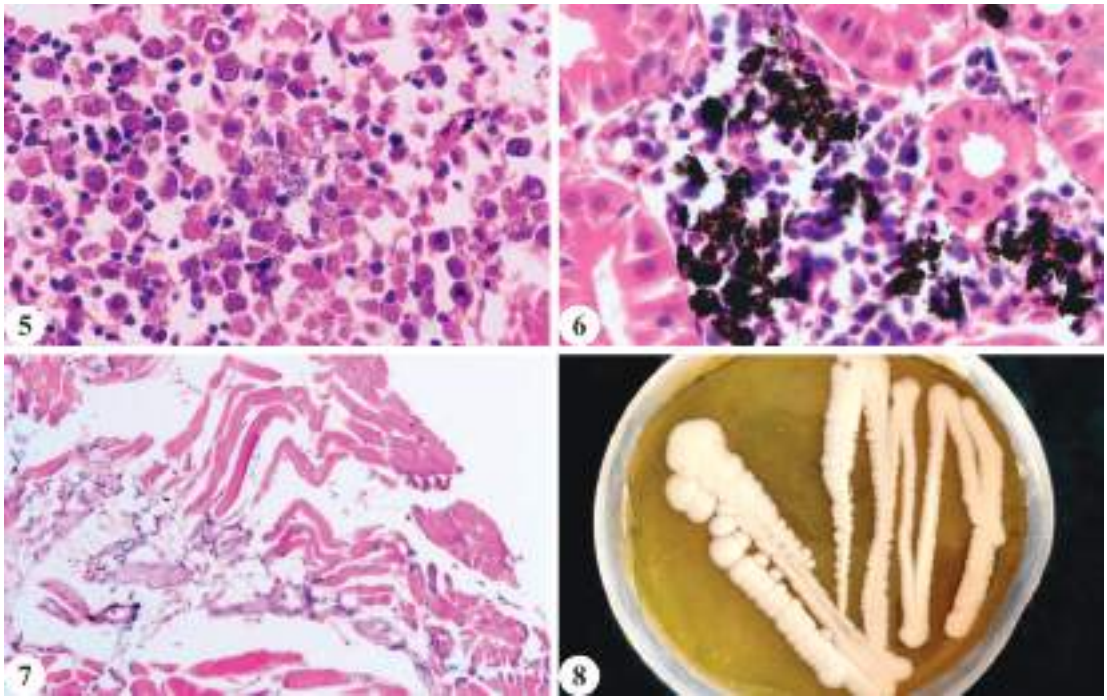

Fig. 5. Anterior kidney: Decreased hematopoietic activity and presence of bacilli (arrow) along with infiltration of lymphocytes (H&E x400); **Fig. 6. Posterior kidney:** Degeneration and necrosis of tubular epithelium and MMC aggregation in the interstitium (H&E x400); **Fig. 7. Skeletal muscles:** Severely disrupted muscle bundles showing extensive necrosis of muscle fibers and infiltration of lymphocytes (H&E x40); **Fig. 8.** Yellowish opaque, round, convex smooth-edged colonies of *A. hydrophila* on TSA media.

histopathological findings of this study confirmed that *A. hydrophila* is pathogenic to rainbow trout. The microscopic lesions such as vascular changes, degeneration and/or necrosis, inflammatory response, presence of bacterial colonies and/or MMC aggregates in the internal organs or tissues are more or less consistent with those reported during experimental studies in infected fishes[14,16]. In fishes, kidney is one of the target organs of an acute septicemia caused by aeromonads and this organ is apparently attacked by bacterial toxins and loses its structural integrity as also observed in the present study. The MMC or macrophage aggregates, are the distinctive groupings of pigment-containing phagocytic cells within the tissues of fish and it plays an important role in the humoral adaptive immune response to foreign materials, including infectious agents[17].

A. hydrophila has a natural habitat in water and can thrive at temperatures ranging from 0 to 45^{O}C with an optimum temperature of 22 to 32^{O}C. In addition, environmental and stress conditions such as overcrowding, low dissolved oxygen, poor water quality, higher organic content, physical injuries, temperature fluctuation, factory pollution, unhygienic handling, contaminated feed and poor nutrition may influence *A. hydrophila* infection in fish[6,10].

Isolation, identification and confirmation of fish pathogenic bacteria are important in the accurate diagnosis of suspected disease[18]. The conventional bacteriological and biochemical methods used for the present investigation have proven effective for identification of *A. hydrophila*[10]. The morphology of the Gram-negative motile bacterium, colony characteristics on TSA media and the biochemical properties of *A. hydrophila* isolates recovered in this study are consistent with those in other reports[18-20].

A. hydrophila is also considered the most important zoonotic pathogen of concern. Fish play a fundamental role in *Aeromonas* transmission to humans[21]. In humans, it may transmit through ingestion of contaminated fish flesh and may lead to various intestinal and extra-intestinal diseases. The diseases in humans include gastroenteritis, traveler's diarrhoea, septic arthritis, skin and wound infections, blood-borne infections, pneumonia, meningitis and fulminating septicaemia[22,23]. Fever, abdominal pain and signs of respiratory distress are commonly exhibited by patients infected with *A. hydrophila*[23]. *A. hydrophila* isolated from fish and humans showed several virulence factors and exhibit a wide range of antibiotic resistance which also considered as a public health hazard[22]. Moreover, the occurrence of *Aeromonas* septicemia is reported to be 32 to 45% in immunocompromised patients and the risk of mortality during the infection increases with the number of comorbidities in human patients[23]. *A. hydrophila* is a widespread, emerging food pathogen and frequently isolated from different environmental or clinical samples as well as from retail foods including fish, seafood, raw milk, poultry and red meats[10,24]. Hence, investigation of *Aeromonas* outbreaks in table fish like rainbow trout must be carried out with due precaution due to its seemingly high zoonotic potential to consumers.

In conclusion, the study reports a natural outbreak of acute *A. hydrophila* infection associated with septicemia and dermal lesions in rainbow trout of Himachal Pradesh resulting in significant mortality among trout fish with a significant economic impact on the cold water fisheries of the state.

ACKNOWLEDGEMENTS

The authors are grateful to CSK Himachal Pradesh Krishi Vishvavidyalaya, Palampur, Himachal Pradesh for providing the facilities to conduct the research work.

REFERENCES

1. Abdella B, Abozahra NA, Shokrak NM, Mohamed RA and El-Helow ER. 2023. Whole spectrum of *Aeromonas hydrophila* virulence determinants and the identification of novel SNPs using comparative pathogenomics. *Sci Rep* **13:** 7712.
2. Zahoor S, Jan A and Husain N. 2024. Current status of rainbow trout *(Oncorhynchus mykiss)* production in India and global world. *Int Creat Res Thoughts* **12:** 2402232.
3. Pauzi NA, Mohamad N, Azzam-Sayuti M, Yasin ISM, Saad MZ, Nasruddin NS and Azmai MNA. 2020. Antibiotic susceptibility and pathogenicity of *Aeromonas hydrophila* isolated from red hybrid tilapia *(Oreochromis niloticus* × *Oreochromis mossambicus)* in Malaysia. *Vet World* **13:** 2166-2171.
4. Rasmussen-Ivey CR, Figueras MJ, McGarey D and Liles MR. 2016. Virulence factors of *Aeromonas hydrophila*: In the wake of reclassification. *Front Microbiol* **7:** 217-548.
5. Daskalov H. 2006. The importance of *Aeromonas hydrophila* in food safety. *Food Control* **17:** 474-483.
6. Semwal A, Kumar A and Kumar N. 2023. A review on pathogenicity of *Aeromonas hydrophila* and their mitigation through medicinal herbs in aquaculture. *Heliyon* **9:** e14088.
7. Shahi N, Mallik SK, Sahoo M and Das P. 2013. Biological characteristics and pathogenicity of a virulent *Aeromonas hydrophila* associated with ulcerative syndrome in farmed rainbow trout, *Oncorhynchus mykiss* (Walbaum) in *India. Isr J Aquac* **65:** 926-936.
8. Kusdarwati R, Kurniawan H and Prayogi YT. 2017. Isolation and identification of *Aeromonas hydrophila* and *Saprolegnia* spp. on catfish *(Clarias gariepinus)* in floating cages in Bozem Moro Krembangan Surabaya. *IOP Conf Series: Earth & Env Sci* **55:** 012-038.
9. Awan F, Dong Y, Wang N, Liu J, Ma K and Liu Y. 2018. The fight for invincibility: Environmental stress response mechanisms and *Aeromonas hydrophila*. *Microb Pathog* **116:** 135-145.
10. Moya-Salazar J, Diaz CR, Cañari B, Badillo RX, Verano-Zelada M, Chicoma-Flores K and Contreras-Pulache H. 2022. Detection of pathogenic *Aeromonas hydrophila* from two rainbow trout *(Oncorhynchus mykiss)* farms in Peru. *Braz J Vet Med* **44:** e000922.
11. Yardimci B and Aydin Y. 2011. Pathological findings of experimental *Aeromonas hydrophila* infection in Nile tilapia *(Oreochromis niloticus)*. *Ankara Univ Vet Fak Derg* **58:** 47-54.

12. Carter GR and Cole Jr JR. 1990. Diagnostic Procedure in Veterinary Bacteriology and Mycology. 5th ed. Academic Press, San Diego, USA.
13. Luna LG. 1968. Manual of Histologic Staining Methods of the Armed Forces Institute of Pathology. 3rd ed., Mc-Graw-Hill Book, New York.
14. Zepeda-Velazquez AP, Vega-Sanchez V, Salgado-Miranda C and Soriano-Vargas E. 2015. Histopathological findings in farmed rainbow trout *(Oncorhynchus mykiss)* naturally infected with 3 different Aeromonas species. *Can J Vet Res* **79:** 250-254.
15. Nicholson P, Monon N, Jaemwimol P, Tattiyapong P and Surachetpong W. 2020. Coinfection of tilapia lake virus and *Aeromonas hydrophila* synergistically increased mortality and worsened the disease severity in tilapia (Oreochromis spp.). *Aquac* **520:** 734-746.
16. Marinho-Neto FA, Claudiano GS, Yunis-Aguinaga J, Cueva-Quiroz VA, Kobashigawa KK, Cruz NR, Moraes FR and Moraes JR. 2019. Morphological, microbiological and ultrastructural aspects of sepsis by *Aeromonas hydrophila* in Piaractus mesopotamicus. *PLoS One* **14:** e0222626.
17. Agius C and Roberts RJ. 2003. Melano-macrophage centres and their role in fish pathology. *J Fish Dis* **26:** 499-509.
18. Yazdanpanah-Goharrizi L, Rokhbakhsh-Zamin F, Zorriehzahra MJ, Kazemipour N and Kheirkhah B. 2020. Isolation, biochemical and molecular detection of *Aeromonas hydrophila* from cultured *Oncorhynchus mykiss*. *Iran J Fish Sci* **19:** 2422-2436.
19. Bakiyev S, Smekenov I, Zharkova I, Kobegenova S, Sergaliyev N, Absatirov G and Bissenbaev A. 2022. Isolation, identification and characterization of pathogenic *Aeromonas hydrophila* from critically endangered *Acipenser baerii*. *Aquac Rep* **26:** 101-293.
20. Das R, Sarma K, Hazarika G, Choudhury H and Sarma D. 2023. Identification and characterisation of emerging fish pathogens *Aeromonas veronii* and *Aeromonas hydrophila* isolated from naturally infected *Channa punctata*. *ALJMAO* **28:** 117.
21. Abd-El-Malek A. 2017. Incidence and virulence characteristics of Aeromonas spp. in fish. *Vet World* **10:** 34-37.
22. Ahmed HA, Mohamed ME, Rezk MM, Gharieb RM and Abdel-Maksoud SA. 2018. *Aeromonas hydrophila* in fish and humans, prevalence, virulotyping and antimicrobial resistance. *Slov Vet Res* **55:** 113-124.
23. Kaki R. 2023. A retrospective study of *Aeromonas hydrophila* infections at a university tertiary hospital in Saudi Arabia. *BMC Infect Dis* **23:** 671.
24. Tahoun AB, Ahmed HA, Abou Elez RM, El-Gedawy AA, Elsohaby I and Abd El-Ghafar AE. 2016. Molecular characterisation, genotyping and survival of *Aeromonas hydrophila* isolated from milk, dairy products and humans in Egypt. *Int Dairy J* **63:** 52-58.

Indian J. Vet. Pathol., 49(1) : 90-92, 2025: DOI: https://doi.org/10.5958/7byed083

CASE REPORT

Pathology and molecular diagnosis of Jaagsiekte in Goat - Case report

J.G. Patel*, P.B. Rathod[1], A.I. Dadawala[2], P.P. Joshi and Y.H. Nayi
Department of Veterinary Pathology, College of Veterinary Science and Animal Husbandry, Kamdhenu University, Rajpur (Nava), Himmatnagar, Gujarat, India, [1]Polytechnic in Animal Husbandry, Rajpur (Nava), Himmatnagar, [2]Department of Veterinary Microbiology, Polytechnic in Animal Husbandry Rajpur (Nava), Himmatnagar

Address for Correspondence
J.G. Patel, Associate Professor, Department of Veterinary Pathology, College of Veterinary Science and Animal Husbandry, Kamdhenu University, Rajpur (Nava), Himmatnagar, Gujarat, India, E-mail: jasmi0102@gmail.com

Received: 24.9.2024; Accepted: 26.10.2024

ABSTRACT

A two-years-old goat with anorexia, progressive emaciation and weak body condition were received for post mortem examination in the Department of Veterinary Pathology, College of Veterinary Science and Animal Husbandry, Himmatnagar from Teaching Veterinary Clinical Complex, CVS & AH, Himmatnagar, Gujarat. Grossly, diffuse pale oedematous lungs were found. Mediastinal lymph nodes revealed mild congestion and oedema. Further, PCR was used for molecular detection of jaagsiekte sheep retrovirus (JSRV). The presence of jaagsiekte was confirmed by PCR results with anticipated sizes of 229 bp and 176 bp for the gag gene and U3 region of the JSRV genome, respectively.

Keywords: Goat, Jaagsiekte, pathology, PCR

Jaggsiekte is a contagious lung tumor mainly of sheep and it is rarely seen in goats. It is also known as ovine pulmonary adenocarcinoma (OPA) or ovine pulmonary adenomatosis[1]. The natural occurrence rate is low in goats, but experimentally OPA has been transmitted in goats[2]. Jaagsiekte sheep retro virus (JSRV) is the virus that is causative agent for the OPA[3] and is a Beta retrovirus which belongs to the family Retroviridae. In goat, incidence of neoplastic conditions are very few, and it is reported that neoplasms in goats range from 0.8 to 7.6% of total recorded tumors of domestic animals[4]. Transmission of this virus mainly occur through inhalation of infected respiratory secretions and it may also be transmitted by colostrum and milk to nursing animals[5]. Jaggsiekte is an Africans term that means driving sickness, jagmeans chase and siekte means sickness to describe the respiratory distress observed in an animal from being chased especially when the animals are stressed through exercise such as herding[6].

Clinical diagnosis of the disease usually possible at later stage, when animal start to show the clinical signs and symptoms due to longer incubation period of virus. Mainly, JSRV infected animals does not show any clinical signs during their lifespan[6] but once clinical signs become evident it show progressive respiratory distress particularly after exercise and there is accumulation of frothy fluid within the respiratory tract which drains from the nostrils when animal lower down its head. Coughing, fever and inappetence are not common but weight loss is progressive and the disease is terminal within weeks or months. Death may occur due to secondary bacterial pneumonia. It is very difficult to identify JSRV infection in live animals because there is no reliable laboratory method for the ante mortem diagnosis of OPA in individual animals[7] and production of antibody to JSRV due to poor immune response. This virus cannot yet be propagated *in vitro*, therefore routine diagnostic methods such as virus isolation are not available for diagnosis. Farm history, clinical signs and post mortem lesions are the primary method for the diagnosis of disease and other than these histopathology, immunohistochemistry and PCR are also useful methods for confirmatory diagnosis[7].

During necropsy finding, OPA lesions in most cases are confined to the lungs although intra and extrathoracic metastasis to lymph nodes and other tissues may occur[1]. In typical case, affected lungs are enlarged and heavier than normal and there is presence of frothy fluid in respiratory passages. Tumors are solid, grey or light purple with a glossy translucent sheen. By PCR, viral DNA or RNA can be detected in tumor, draining lymph nodes, blood, milk or nasal swabs. Histologically, the lesions are characterized by neoplastic proliferation of the type 2 pneumocytes, a secretory epithelial cell of alveoli and clara cells of bronchioles. Prominent feature is the accumulation of large numbers of alveolar macrophages in the alveoli adjacent to the neoplastic lesions[1].

In the present case, a two-years-old goat with anorexia, progressive emaciation and weak body condition were received

How to cite this article : Patel, J.G., Rathod, P.B., Dadawala, A.I., Joshi, P.P. and Nayi, Y.H. 2025. Pathology and molecular diagnosis of Jaagsiekte in Goat - Case report. Indian J. Vet. Pathol., 49(1) : 90-92.

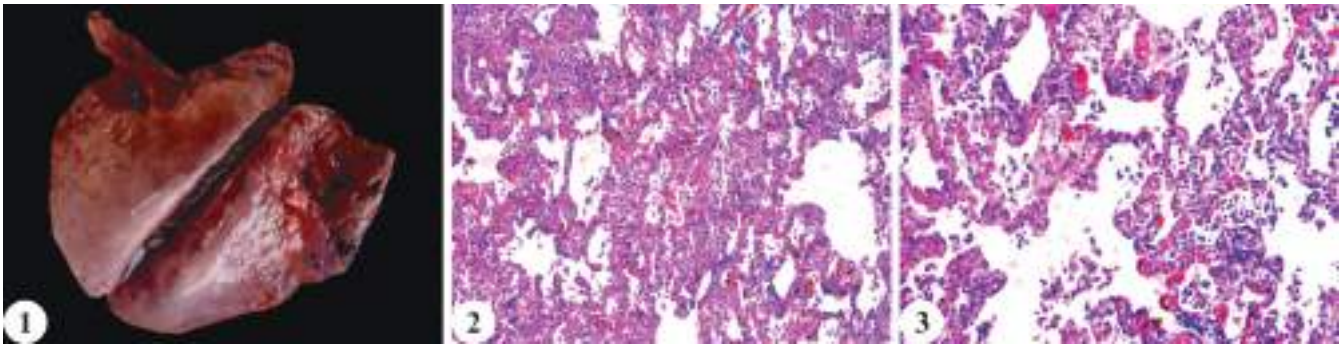

Fig. 1. Goat lungs showing greyish to purple coloured, enlargement, heavy, diffusely oedematous and consolidation; **Fig. 2.** Microscopic sections of lungs showing diffuse marked intra-alveolar septa thickened with infiltration of chronic inflammatory cells and erythrocytes along with mild oedema (H&E X200); **Fig. 3.** Microscopic sections of lungs showing diffuse thickening of intraalveolar septa with infiltration of macrophages and erythrocytes (H&E X400).

for post mortem examination in the Department of Veterinary Pathology, CVS & AH, Himmatnagar, Gujarat from Teaching Veterinary Clinical Complex, CVS & AH, Himmatnagar, Gujarat. Necropsy was performed and the lung samples from different lobes were collected in 10% neutral buffered formalin for histopathological investigation and lung tissue was also collected and stored at -20^{O}C for PCR. For histopathological processing, the tissue samples were rehydrated in tap water, dehydrated in increasing grades of alcohol, cleared in xylene and embedded in paraffin. From paraffin embedded tissue blocks, 4-5µm thick tissue sections were cut on clean, grease free glass slides and haematoxylin and eosin staining was done by routine standard protocol[8]. Then sections were examined under the light microscope for histopathological evaluation of tissue.

To confirm the presence of OPA, PCR was performed. The genomic proviral DNA was extracted from the frozen lung samples by using phenol chloroform extraction method and the extracted genomic DNA was used as a template and the primer of forward 5' TGGGAGCTCTTIGGCAAAAGCC 3', reverse 5' CACCGGATTITTACACAATCACCGG 3' flanking a region of 176 bp region of U3-LTR gene as described earlier[9] and primer of forward 5'GCTGCTTTGAGACCITATCGAAA3', reverse 5'ATACTGCAGCTCGATGGCCAG 3' for a product size 229 bp region of gag gene published by researchers[10] (1µM of each primer/PCR reaction, for both reactions) with the thermal cycle conditions as follows: initial denaturation at 94^{O}C for 3 min; 35 cycles of denaturation at 94^{O}C for 30 s for U3 or 60 s for gag, annealing at 54^{O}C for U3 or at 52^{O}C for gag, for 90 sec and extension at 72^{O}C for 1 min and final extension at 72^{O}C for 4 min. PCR products were electrophoresed in 1.5% agarose gel and examined in Gel Documentation system.

Grossly, goat lung was enlarged, heavy, diffusely edematous and consolidated during necropsy (Fig. 1). Mediastinal lymph nodes were also slightly enlarged and edematous. Histopathological examination of lung tissue showing diffuse marked intra alveolar septa thickened (Fig. 2) with infiltration of chronic inflammatory cells and erythrocytes along with mild oedema (Fig. 3). In PCR, an expected size of amplified DNA product of 176 bp for U3-LTR (Fig. 4A) and 229 bp for gag primer (Fig. 4B) was found. There was no amplification in negative control. Hence, based on history, clinical signs, necropsy findings, histopathology and PCR it can be concluded

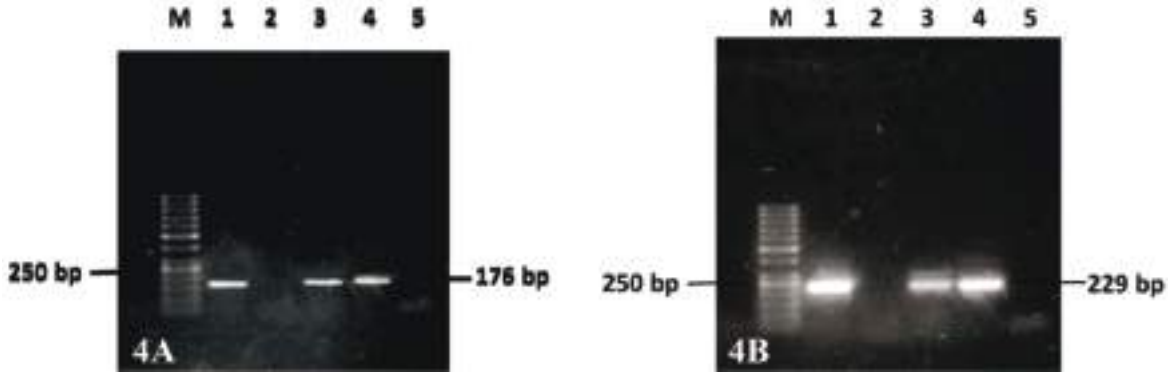

Fig. 4. Detection of JSRV proviral DNA in pneumonic lung tissue: **A.** PCR for U3-LTR gene: Lanes 3 and 4 are positive samples (176 bp); Lanes 2 are negative; Lane 1 as positive control and Lane 5 as negative control and M-50 bp ladder. **B.** PCR for gag gene: Lanes 3 and 4 are positive samples (229 bp); Lanes 2 are negative; Lane 1 as positive control and Lane 5 as negative control and M-50 bp ladder.

that goat is susceptible to JSRV infection, although reports of OPA in goat are very rare. The susceptibility of goats to JSRV infection may be due to rearing of goats mostly along with sheep[4].

Based on gross and histopathological analysis, the lungs examined in this study exhibited a greyish to purple coloration, a swollen and moist surface, and signs of edema with consolidation, which are in concurrence with the classical presentation of OPA (Garcia-Goti *et al*. 2000)[10]. In typical cases, tumours are solid, grey or light purple and have a glossy translucent sheen in the diaphragmatic lobe, accompanied by several smaller nodules in the main lobes. These nodules usually present a hard, pearly white appearance with a dry cut surface, as reported by previous studies[9,12]. However, such features were not observed in the current investigation.

In the present study, U3 LTR and gag-specific PCR products confirmed the presence of JSRV proviral DNA in the lung samples of infected goats. The use of PCR to detect OPA-causing proviruses in lung samples from abattoir cases has proven valuable technique for identifying infected sheep and goats. This method has been effectively applied in multiple studies for OPA diagnosis and it can greatly support control and eradication activities[11].

ACKNOWLEDGEMENTS

The authors are thankful to the Principal, College of Veterinary Science and Animal Husbandry, Kamdhenu University, Rajpur (Nava), Himmatnagar, Gujarat, India for providing the necessary facilities to carry out this work.

REFERENCES

1. WOAH terrestrial manual. 2021. Ovine pulmonary adenocarcinoma (adenomatosis).
2. Tustin RC, York DF, Williamson AL and Verwoerd DW. 1988. Experimental transmission of jaagsiekte (ovine pulmonary adenomatosis) to goats. *Onderstepoort J Vet Res* **55:** 27-32.
3. Cousens C, Bishop JV, Philbey AW, Gill CA, Palmarini M, Carlson JO, DeMartini JC and Sharp JM. 2004. Analysis of integration sites of jaagsiekte sheep retrovirus in ovine pulmonary adenocarcinoma. *J Virol* **78:** 8506-8512.
4. Mishra S, Kumar P, Dar JA, Singh V, Pandit K and Mahanta D. 2018. A rare case of pulmonary adenocarcinoma in goat. *J Entomol Zoo Stud* **6:** 981-982.
5. Mishra S, Kumar P, Dar JA, George N, Singh R, Singh V and Singh R. 2020. Detection and prevalence of small ruminant lentiviral (SRLV) infections in indian sheep and goats. *Indian J Vet Pathol* **44:** 207-211.
6. Griffiths DJ, Martineau HM and Cousens C. 2010. Pathology and pathogenesis of ovine pulmonary adenocarcinoma. *J Comp Pathol* **142:** 260-283.
7. Sonawane GG, Tripathi BN, Kumar R and Kumar J. 2016. Diagnosis and prevalence of ovine pulmonary adenocarcinoma in lung tissues of naturally infected farm sheep. *Vet World* **9:** 365.
8. Luna LG. 1968. Manual of Histologic Staining Method of Armed Forces Institute of Pathology (3rd Edn), McGraw Hill book Co, London, Pp. 124-125.
9. Palmarini M, Holland MJ, Cousens C, Dalziel RG and Sharp JM. 1996. Jaagsiekte retrovirus establishes a disseminated infection of the lymphoid tissues of sheep affected by pulmonary adenomatosis. *J Gen Virol* **77:** 2991-2998.
10. Rosati S, Pittau M, Alberti A, Pozzi S, York DF, Sharp JM and Palmarini M. 2000. An accessory open reading frame (orf-x) of jaagsiekte sheep retrovirus is conserved between different virus isolates. *Vir Res* **66:** 109-116.
11. Garcia GM, Gonzalez L, Cousens C, Cortabarria N, Extramiana AB, Minguijon E, Ortin A, De lasHeras M and Sharp JM. 2000. Sheep pulmonary adenomatosis: Characterization of two pathological forms associated with jaagsiekte retrovirus. *J Comp Pathol* **122:** 55-65.
12. Devi VR, Yadav EJ, Rao TS, Satheesh K, Suresh P and Manasa BB. 2014. Nucleotide sequencing and phylogenetic analysis using PCR amplicons of U3 gene of Jaagsiekte sheep retrovirus (JSRV) detected in natural cases of ovine pulmonary adenocarcinoma in India. *Open J Vet Med* **4:** 267.

Indian J. Vet. Pathol., 49(1) : 93-95, 2025: DOI: https://doi.org/10.5958/ahsg0w78

CASE REPORT

Pathology of mycotic rumenitis and reticulitis in sheep - A case report

Dharanesha N. Krishnegowda[1*], Saritha N. Sannegowda[1], Mamta Pathak, Javeed A. Dar, Rhushikesh S. Khetmalis, Stephanie S. Pradhan, Pawan Kumar, Prathviraj R. Hanamshetty[2] and Rajendra Singh

Division of Pathology, ICAR-Indian Veterinary Research Institute, Izatnagar, Bareilly, Uttar Pradesh-243 122, India, [1]Central Animal Disease Diagnostic Laboratory/Forensic Science Laboratory/Foot and Mouth Disease Laboratory, Institute of Animal Health & Veterinary Biologicals, Karnataka Veterinary Animal and Fisheries Sciences University, Hebbal, Bangalore-560 024, [2]Department of Veterinary Physiology and Biochemistry, Veterinary College, Bidar, Karnataka Veterinary Animal and Fisheries Sciences University, Nandinagar-585 226, India

Address for Correspondence

Dharanesha N. Krishnegowda, Assistant Professor, Central Animal Disease Diagnostic Laboratory/Forensic Science Laboratory/ Foot and Mouth Disease Laboratory, Institute of Animal Health & Veterinary Biologicals, Karnataka Veterinary Animal and Fisheries Sciences University, Hebbal, Bangalore-560 024, India, E-mail: drdharanivet@kvafsul.edu.in

Received: 23.8.2024; Accepted: 13.9.2024

ABSTRACT

The current case report describes the pathology of mycotic rumenitis and reticulitis in sheep. A carcass of female adult sheep with a history of abortion (a few weeks before) was presented for necropsy at the post-mortem facility, Division of Pathology, IVRI. Post-mortem examination revealed focal to widespread, irregular, hemorrhagic, necrotic and transmural lesions on serosal and mucosal surfaces in the rumen and reticulum. The mucosal surface of the reticulum showed erosive, ulcerative and necrotic lesions with loss of honeycomb structure and characterized by whitish necrotic deposits. The reticulum at one side was firmly adhered to the diaphragm. The heart showed gelatinized epicardial fat. Histopathological examination of tissue samples showed the presence of numerous fungal hyphae in homogenous eosinophilic necrotic mucosa and infiltration of mononuclear cells in the submucosa and muscularis of the reticulum. The swabs from lesions of rumen and reticulum were found negative for *Fusobacterium* spp. and *Clostridium* spp. Further, PAS staining revealed the presence of magenta-colored numerous branching and septate hyphae and free chlamydospores in the reticulum.

Keywords: Fungal hyphae, PAS, Reticulitis, Rumenitis

Mycotic rumenitis and reticulitis in sheep, commonly referred to as fungal infections of the forestomach, represent a significant health concern in small ruminants. These conditions are primarily caused by fungal species such as *Aspergillus* spp., *Candida* spp., and *Mucor* spp., which opportunistically invade the rumen and reticulum, leading to inflammation and tissue damage[1,2]. Mycotic rumenitis can be caused by initial ruminal acidosis, excess grain consumption and traumatic or chemically induced mucosal injury and this significant mucosal injury allows invasion and proliferation of fungi[3]. The pathology of mycotic rumenitis and reticulitis typically involves fungal colonization of the mucosa, which triggers an inflammatory response characterized by edema, hyperemia, and necrosis of the affected tissues[4]. Fungi can penetrate the epithelial layer, leading to ulceration and subsequent abscess formation within the rumen and reticulum. Clinically, affected sheep may present with signs of anorexia, weight loss, depression, rumen atony, abdominal discomfort, profuse diarrhoea, foul-smelling feces and decreased milk production[5]. Acidosis causes elevated cardiac and respiratory rates. A change in osmotic pressure will cause fluid to migrate from the circulation into the rumen, resulting in hypovolemia. Diagnosis often involves a combination of clinical signs, histopathology, Immunohistochemistry, immunofluorescence, enzyme immunocomplex and microbiological culture of rumen contents or tissue samples[2]. Management strategies include antifungal therapy, supportive care to alleviate clinical signs and improvement of environmental conditions to minimize fungal exposure[4,5]. The prognosis varies according to the severity of the illness and the timing of intervention. This case describes the pathology of mycotic rumenitis and reticulitis in sheep.

How to cite this article : Krishnegowda, D.N., Sannegowda, S.N., Pathak, M., Dar, J.A., Khetmalis, R.S., Pradhan, S.S., Kumar, P., Hanamshetty, P.R. and Singh, R. 2025. Pathology of mycotic rumenitis and reticulitis in sheep - A case report. Indian J. Vet. Pathol., 49(1) : 93-95.

A carcass of female adult sheep with a history of abortion (a few weeks before) was presented for necropsy at the post-mortem facility, Division of Pathology, IVRI. The physical examination of the carcass revealed pale conjunctival mucous membranes, rigor mortis in hind limbs, rough hair coat and maggot wound with soiled wool at the perineal region. The carcass was opened systematically and all the internal organs and cavities were examined for the presence of gross lesions. The representative samples from the rumen and reticulum showing gross lesions, were collected and fixed in 10%

Fig. 1. Reticulum showing focal hemorrhagic and necrotic lesions on the serosal surface with a portion of reticulum firmly adhered to the diaphragm; **Fig. 2.** Rumen showing transmural rumenitis and numerous focal to diffuse irregular hemorrhagic, necrotic lesions on the serosal surface; **Fig. 3.** Reticulum showing erosive, ulcerative, necro-suppurative lesions with loss of honeycomb structure, characterized by whitish necrotic deposits.

neutral buffered formalin for histopathological studies and processed routinely and stained with hematoxylin and eosin[6]. Tissue sections were also processed for PAS staining[7,8]. The swabs from lesions of rumen and reticulum were collected in a sterile container for bacteriological examination.

On gross pathological examination, the reticulum on one side was firmly adhered to the diaphragm (Fig. 1). Numerous focal to widespread, irregular, hemorrhagic, necrotic and transmural lesions were present on the serosal and mucosal surfaces of the rumen and reticulum, similar to the case described by the previous author[9] (Fig. 2). The lesions on the mucosal surface of the reticulum included erosive, ulcerative, and necrotic lesions with loss of honeycomb structure and characterized by whitish necrotic deposits, which were comparable to previous studies[10] (Fig. 3). Histopathological examination revealed the marked infiltration of mononuclear cells (MNC) in the submucosa and tunica muscularis of the reticulum (Figs. 4-5) and the presence of numerous fungal hyphae in homogenous eosinophilic necrotic mucosa and infiltration of mononuclear cells in the submucosa and muscularis of the reticulum and is in accordance with the previous reports[11-13] (Fig. 6). The bacteriological culture examination found negative for *Fusobacterium* spp. and *Clostridium* spp. Further, PAS staining revealed the presence of magenta-colored numerous branching and septate hyphae and free chlamydospores in the reticulum

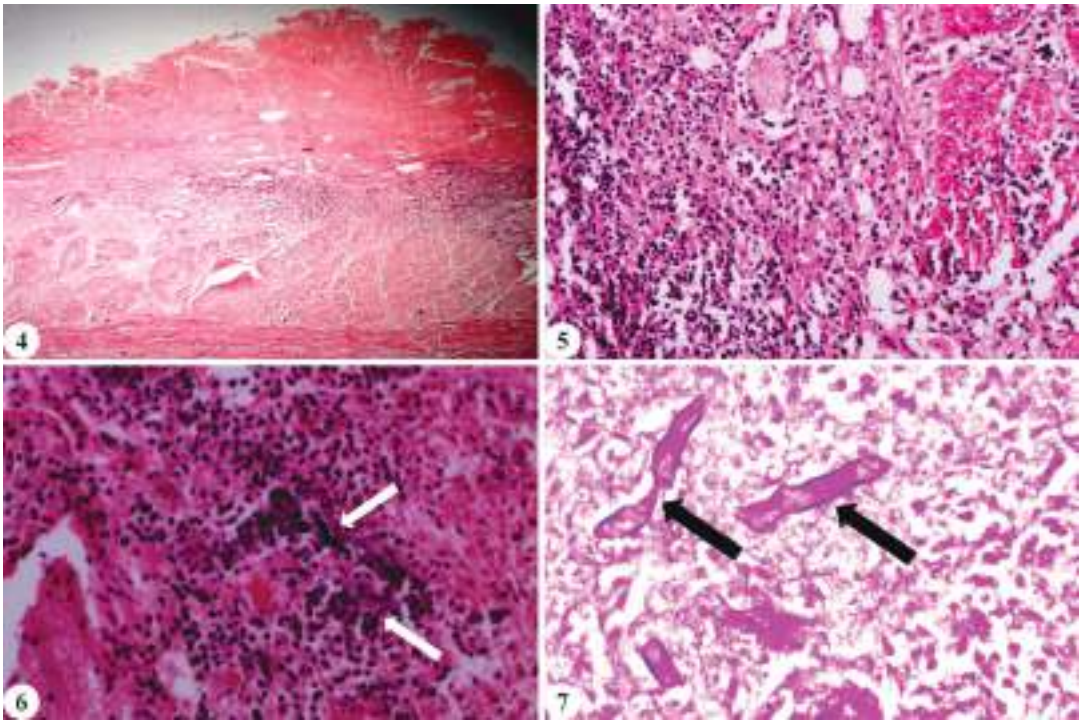

Fig. 4. Reticulum showing necrosis of mucosa, marked infiltration of MNC in submucosa and muscularis (H&E x40); **Fig. 5.** Reticulum showing marked MNC infiltration in submucosa and tunica muscularis (H&E x200); **Fig. 6.** Reticulum showing fungal hyphae (arrow) surrounded by MNC infiltration in submucosa and lamina propria (H&E x200); **Fig. 7.** Reticulum showing magenta-colored fungal hyphae (arrow) (PAS x400).

(Fig. 7).

This report briefly detailed the gross and microscopic lesions associated with mycotic rumenitis and reticulitis in sheep. This case was diagnosed as mycotic rumenitis and reticulitis due to the presence of fungal hyphae in the ruminal and reticulum tissue, as well as distinctive gross necrotic lesions.

REFERENCES

1. Smith BP. 2020. *Large Animal Internal Medicine* (6th ed.). Elsevier.
2. Jones TC, Hunt RD and King NW. 2018. *Vet Pathol* (7th ed.). Wiley-Blackwell.
3. Njaa BL, Panciera RJ, Clark EG and Lamm CG. 2012. Gross lesions of alimentary disease in adult cattle. *Vet Clin North Am Food Anim Pract* **28:** 483-513.
4. Brown C. 2019. *Clin Pathol Farm Anim* (4th ed.). Wiley-Blackwell.
5. Roberts SJ and Ellis A. 2017. *Manual Sheep Dis* (2nd ed.). Wiley-Blackwell.
6. Luna LG. 1968. Manual of histologic staining methods of the Armed Forces Institute of Pathology. New York, USA: Mc Graw Hill.
7. McManus JFA. 1961. General cytochemical methods. *JF Danielli Ed 2:* p.171.
8. Frickmann H, Loderstaedt U, Racz P, Tenner-Racz K, Eggert P, Haeupler A, Bialek R and Hagen RM. 2015. Detection of tropical fungi in formalin-fixed, paraffin-embedded tissue: still an indication for microscopy in times of sequence-based diagnosis. *Biomed Res Int* 938-721.
9. Headley SA, Müller MC, de Oliveira TES, Duarte CABG, Pereira PFV, Vieira MV, Cunha CW, Flores EF, Lisbôa JAN and Pretto-Giordano LG. 2020. Diphtheric aspergillosis tracheitis with gastrointestinal dissemination secondary to viral infections in a dairy calf. *Microb Pathol* **149:** 104-497.
10. Jensen HE, Olsena SN and Aalbek B. 1994. Gastrointestinal aspergillosis and zygomycosis of cattle. *Vet Pathol* **31:** 28-36.
11. Ates MB, Ortatatli M, Hatipoglu F, Ciftci MK, Ozdemir O and Terzi F. 2016. Mycotic gastritis and enteric cryptosporidiosis in a Holstein calf. Second international conference on science, ecology and technology.
12. Dyer NW and Newell TK. 2002. Mycotic rumenitis in American bison *(Bison bison)*. *J Vet Diagn Invest* **14:** 414-416.
13. Chihayak Y, Matsukawa K, Mizushima S and Matsui Y. 1988. Ruminant forestomach and abomasalmucormycosis under rumen acidosis. *Vet Pathol* **251:** 119-123.

Indian J. Vet. Pathol., 49(1) : 96-98, 2025: DOI: https://doi.org/10.5958/tdxw2641

CASE REPORT

Trichoblastoma in a dog: A case report

M. Mani Bharathi*, S. Ramesh, G.V. Sudhakar Rao[1], G. Vijayakumar[2], N. Pazhanivel[1], S. Hemalatha[1] and M. Sandhya Bhavani

Centralised Clinical Laboratory, Madras Veterinary College, TANUVAS, Chennai, [1]Department of Veterinary Pathology, Madras Veterinary College, TANUVAS, Chennai, [2]Department of Clinics, Madras Veterinary College, TANUVAS, Chennai, India

Address for Correspondence

M. Mani Bharathi, Centralised Clinical Laboratory, Madras Veterinary College, TANUVAS, Chennai, India, E-mail: drmanibharathi16@gmail.com

Received: 8.10.2024; Accepted: 28.10.2024

ABSTRACT

A five-year-old male Labrador with a mass in the ear pinna was brought to the Madras Veterinary College Teaching Hospital, Chennai. On clinical examination, the mass appeared pale pink in colour, firm in consistency with discrete lobulation and measured 3 cm in diameter. Haemato-biochemical studies and imaging assessments revealed no abnormalities while cytological findings of the mass showed basal epithelial cells arranged in a row which was suggestive of trichoblastoma. Histopathological examination revealed cuboidal to elongated neoplastic cells with pale eosinophilic cytoplasm arranged in ribbon pattern, supported by fibrovascular stroma which was confirmative of trichoblastoma. Immunohistochemical studies also confirmed the tumour by showing positive expression of cytokeratin. Based on the laboratory findings, the tumour was identified as trichoblastoma.

Keywords: Cytokeratin, labrador, ribbon pattern, trichoblastoma

How to cite this article : Bharathi, M.M., Ramesh, S., Rao, G.V.S., Vijayakumar, G., Pazhanivel, N., Hemalatha, S and Bhavani, M.S. 2025. Tricho-blastoma in a dog: A case report. Indian J. Vet. Pathol., 49(1) : 96-98.

Trichoblastoma is a rare skin neoplasm derived from the primitive hair follicles, having epithelial and mesenchymal components. It is more prevalent in dogs and cats when compared to other species[1]. They are dome-shaped, polypoid, solitary or multinodular tumours, usually smaller having a diameter of 1-2 centimetres and sometimes larger having a diameter of more than 30 centimetres[2]. Clinical signs noticed include alopecia with or without ulcerated lesions. Ulcerations at the centre of the tumours are often the most common findings in large-sized tumours[3].

Lesions usually affect the head, neck and especially the base of the ear. Pigmented lesions on the skin might have a grey or blue appearance[2]. Four histological subtypes of canine trichoblastoma are recognized namely ribbon, trabecular, granular and spindle cell type. A combination of these patterns characterizes the majority of cases, with ribbon epithelial aggregates predominating and being encircled by fibrous stroma[4,5].

Among various breeds of dogs affected, Poodles and Cocker Spaniels are more likely to develop trichoblastoma and Basal cell carcinomas. Nevertheless, the additional significant breed predispositions are found in Siberian Huskies, Cockapoos, Kerry Blue Terriers, Bichon Frises and Shetland Sheep dogs[4]. With regard to the age affected, it is more common in the age group of 4 to 9 years[5]. However, no sex predilections were recorded[6]. Cytological examination revealed small clusters of basal epithelial cells which were suggestive of basal cell carcinoma due to their high nucleus-cytoplasm ratio, monomorphic nuclei and strongly basophilic and pigmented cytoplasm[7].

A five year old male labrador dog with a history of swelling in the medial aspect of the ear pinna region was brought to the Madras Veterinary College Teaching Hospital for clinical diagnosis and treatment. The dog's tutor reported that the primary issue was a gradual rise in the area of the dog's ear, accompanied by itching and touch sensitivity for the past two months. Blood samples were collected for routine haematological and biochemical studies using autoanalyser's (Mindray - BC-2800 and A15 Biosystems) and the animal was subjected to various imaging techniques namely radiography and ultrasound imaging. In addition, fine needle aspiration procedure was performed on the lump for cytological studies. The aspiration smears were air dried and stained with Leishman and Giemsa cocktail stain as described[8]. Excisional biopsy was performed and the mass was removed. The tissue samples were collected in 10% formalin, processed by routine paraffin embedding method, stained by haematoxylin and eosin and subjected to histopathological studies. For immunohistochemical studies, the tissue samples were processed by routine paraffin embedding method and the cut sections were treated with specific marker namely cytokeratin.

On clinical examination, a

Table 1. Hematology

Parameters	Values	Reference Values	Differential Count	Values	Reference Values
Haemoglobin	11.9 g/dl	11.9-18.9 g/dl	Neutrophils	75	60-75%
PCV	42%	37-55%	Lymphocytes	20	12-30%
RBC	4.89 m/cmm	4.95-7.87 m/cmm	Monocytes	5	3-9%
WBC	12000/cmm	6000-11000/cmm	Eosinophils	0	2-10%
Platelets	297000/cmm	2-9/cmm	Basophils	0	0%
Blood Picture	NAD		Parasite	Nil	

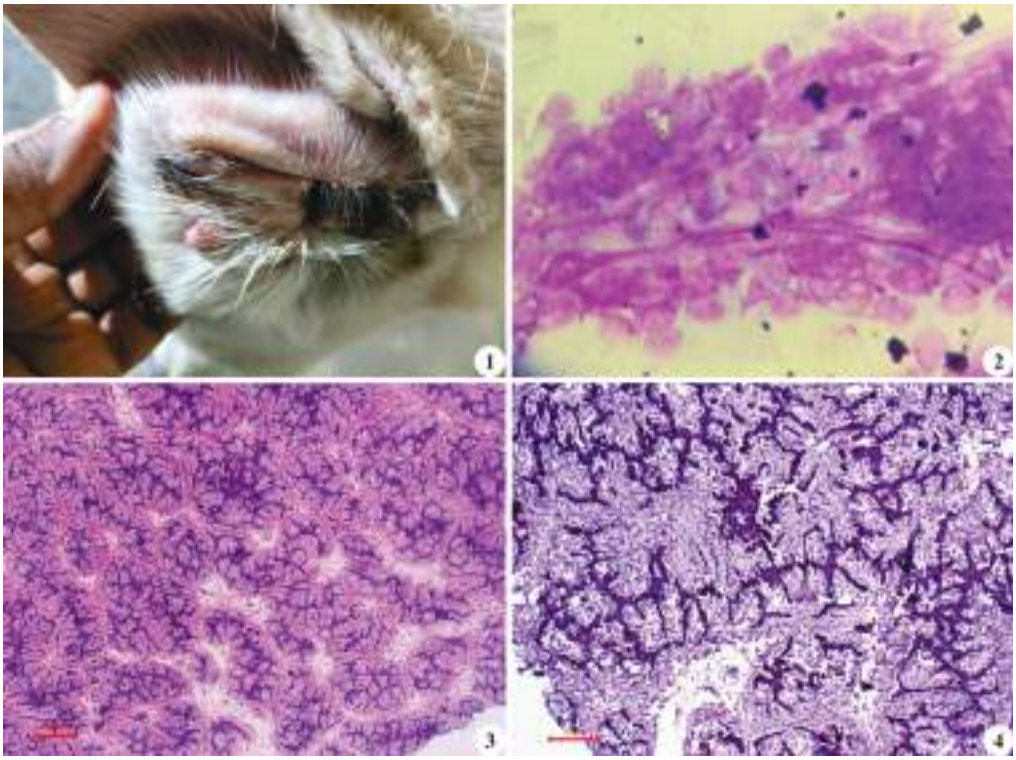

Fig. 1. Trichoblastoma - Raised, oval, alopecic, solitary, hard nodule in ear; **Fig. 2.** Trichoblastoma - Small clusters of basal epithelial cells arranged in a typical row (LG Stain 5 μm); **Fig. 3.** Trichoblastoma - HP cells are arranged in ribbon like pattern, cells have scanty cytoplasm and uniform (H&E 100 μm); **Fig. 4.** Trichoblastoma - IHC - Cytokeratin has moderately expressed (H&E x100).

well-defined, mass of 3 cm in diameter and localized alopecia were found in the ear pinna region (Fig. 1). The tumour mass measured 3.0 x 3.0 x 4.0 cm in size, appeared pale pink in colour and firm in consistency with discrete lobulation. The haematobiochemical findings recorded in the present study are shown in Table 1 and 2. No abnormal findings were recorded either in hemato-biochemical studies or imaging tests except fine needle aspiration cytology. Cytological studies revealed small clusters of basal epithelial cells arranged in a typical row (Fig. 2). Histopathological studies revealed numerous small cuboidal to elongated cells with a pale, sparse eosinophilic cytoplasm containing round to oval nucleus with loose chromatin and little discernible nucleolus. Neoplastic cells were grouped into islands, palisades, or strings (ribbon type) with the fibrovascular stroma separating them (Fig. 3). Immunohistochemical studies revealed positive expression of cytokeratin in basal

Table 2. Serum Biochemistry

Parameters	Values	Reference Values	Parameters	Values	Reference Values
BUN	13 mg/dl	10-28 mg/dl	ALP	98 U/L	1-114 U/L
Creatinine	0.8 mg/dl	0.7-1.4 mg/dl	Calcium	9.86 mg/dl	9.1-11.7 mg/dl
Total Protein	7.2 g/dl	6.1-7.8 g/dl	Phosphorus	3.43 mg/dl	2.9-5.3 mg/dl
Albumin	3.4 g/dl	3.1-4 g/dl	Glucose	78 md/dl	76-119 md/dl
ALT	20 U/L	10-109 U/L			

epithelial cells (Fig. 4). Based on the present laboratory findings, the tumour was identified as trichoblastoma.

The diagnosis of trichoblastoma was confirmed by the clinical study of the case in conjunction with the cytological and histological investigation of the tumour, which made physical and cellular changes visible[2]. The present cytological findings were small, grouped basal epithelial cells, characterized by a high nucleus-cytoplasm ratio, monomorphic nuclei and intensely basophilic and pigmented cytoplasm in a dog affected with trichoblastoma[7]. The present histological lesions, the presence of neoplastic trichoblasts with scanty, pale eosinophilic cytoplasm containing ovoid, euchromatic nuclei and small nucleoli were noticed[3,4]. Immunohistochemical lesions described in the present study observed the positive staining of neoplastic epithelial cells for cytokeratin[4,10,11].

ACKNOWLEDGEMENT

The authors acknowledge TANUVAS for providing the facilities to carryout the work.

REFERENCES

1. Mauldin EA and Peters-Kennedy J. 2016. Integumentary system. Jubb, Kennedy & Palmer's Pathology of Domestic Animals: Volume 1: 509.
2. Haydardedeoğlu AE, Ergin İ, Alıhosseını H, Çolakoğlu EC and Baydın A. 2015. Atypical localised benign adnexal Tumour (Trichoblastoma) in a dog. *Kocatepe Vet J* **8:** 93-95.
3. Gross TL, Ihrke PJ, Walder EJ and Affolter VK. 2008. Skin diseases of the dog and cat: Clinical and histopathologic diagnosis. John Wiley & Sons.
4. Campos AG, Coglıatı B, Guerra JM and Matera JM. 2014 Multiple Trichoblastomas in a dog. *Vet Dermatol* **25:** 48-e19.
5. Goldschmidt MH and Goldschmidt KH. 2017. Epithelial and melanocytic tumours of the skin. In Tumours in Domestic Animals. Meuten DJ (Ed), Fifth edition. Wiley Blackwell, Danvers 88-141.
6. Raval SH, Joshi DV, Patel BJ, Patel JG, Prajwalita S, Panchal HM and Patel PG. 2015. Hair follicle tumours in dogs: A report of two cases. *Indian J Vet Pathol* **39:** 84-86.
7. Machado de Souza, VF Pereira, ZS Carneiro I deO, Gomes Júnior DC, Frade MTS, Alves da Silva and Vieira LC. 2020. "Trichoblastoma in a Dog: A Clinical, Diagnostic and Therapeutic Analysis". *Acta Sci Vet* **48**.
8. Garbayl RS, Agarwal N and Kumar P. 2006. Leishman-Giemsa Cocktail, An Effective Romanowsky stain for air dried cytologic smears. *Acta Cytol* **50:** 403-406.
9. Kumar S, Sakshi V and Kumar V. 2024. Trichoblastoma in an Indian Dog: A clinical and diagnostic investigation. *Indian Journal Anim Health* **63:** 141-142.
10. Yoon JS and Park J. 2014. Immunohistochemical characterisation of a canine case of granular cell type trichoblastoma: a case report.
11. Sakuma A, Nishiyama S, Yasuno K, Ohmuro T, Kamiie J and Shirota K. 2010. A case of canine cutaneous clear cell adnexal carcinoma with prominent expression of smooth muscle actin. *J Toxicol Pathol* **23:** 265-269.

Indian J. Vet. Pathol., 49(1) : 99-101, 2025: DOI: https://doi.org/10.5958/10k8zh08

CASE REPORT

Corneal dermoid in a dog

N. Umeshwori Devi*, Deepshikha Singh and Geeta Devi Leishangthem[1]
Department of Veterinary Surgery and Radiology, College of Veterinary Science, Guru Angad Dev Veterinary and Animal Science University, Ludhiana-141 004, India, [1]Department of Veterinary Pathology

Address for Correspondence
N. Umeshwori Devi, Assistant Professor, Department of Veterinary Surgery and Radiology, College of Veterinary Science, Guru Angad Dev Veterinary and Animal Science University, Ludhiana-141 004, E-mail: umeshwori.nameirakpam@gmail.com

Received: 10.10.2024; Accepted: 8.11.2024

ABSTRACT

A 1 year old Shih Tzu dog weighing 5 kg was presented with a complaint of abnormal hair growth in the right eye. Ophthalmic examination revealed a round black coloured hairy lesion on the surface of cornea and bulbar conjunctiva, measuring around 5 mm in diameter in the superior temporal quadrant of the right eye. Superficial keratectomy of the corneal lesion was performed under general anaesthesia. Microscopically, the histopathology of the tissue revealed the presence of an outer stratified squamous epithelium lining and numerous sebaceous glands along with hair follicles and sudoriparous gland within the connective tissue stroma. Based on the histopathological features, the growth was diagnosed as dermoidcyst.

Keywords: Cornea, dermoid, dogs

A dermoid is a benign congenital choriostoma characterized by the unusual presence of heterotropic cutaneous tissue formed at an inappropriate location[1]. These are most often unilateral and may affect conjunctiva (bulbar and palpebral), cornea, rarely the nictitating membrane and eyelids[2]. Dermoids are composed of dermis-like connective tissue including the epidermis, dermis, sebaceous glands, fat and hair follicles[3]. Hair from the lesion causes severe irritation to the eye which leads to chronic epiphora, keratitis, corneal ulceration and blepharopasm[4]. Surgical excision of ocular dermoid is one of the best treatment options which ensures complete elimination of signs and minimum scarring of the cornea[2,3].

A 1 year old Shih Tzu dog weighing 5 kg was presented to the Small Animal Clinic, Department of Veterinary Surgery and Radiology, College of Veterinary Science, GADVASU, Ludhiana (Punjab) with a complaint of abnormal hair growth in the right eye since last two months. A round black color lesion slightly elevated from the surface of the cornea and bulbar conjunctiva, measuring around 5 mm in diameter with a tuft of hair over the surface was grossly visible in the superior temporal quadrant of the right eye (Fig. 1). Ocular discharge, hyperaemia and mild corneal opacity were observed upon ophthalmic examination of the affected eye. The animal was active with normal feeding pattern. The rectal temperature, heart rate and respiratory rate were within normal limits.

Superficial keratectomy was performed to excise the corneo-conjunctival dermoid under general anaesthesia. The dog was pre-medicated intramuscularly with a mixture of Inj. Butorphanol (Inj. Butrum®, Aristo, New Delhi) @ 0.2 mg/kg BW (I/M), Inj. Acepromazine (Inj. Ilium-Acepril®-10, Troy Laboratories Pvt. Ltd. Australia) @ 0.05 mg/kg BW (I/M) and Inj. Atropine sulphate @ 0.01 mg/kg BW (I/M) prior to surgery. The anaesthesia was induced with Inj. propofol (1%) (Inj. Neorof®, Neon Laboratories Ltd. India) @ 4 mg/kg BW (I/V) and was maintained with 1-2% isoflurane in oxygen by cuffed endotracheal tube attached to the circle system of the small animal anaesthetic unit.

The patient was positioned on the operating table in left lateral recumbency with the affected right eye facing upwards. The eye was thoroughly cleaned and draped to maintain asepsis. The globe was fixed by placing Lieberman eye speculum and the dermoid was removed gradually by incising the peripheral margins in a circum ferential manner using micro-surgical ophthalmic instruments (Fig. 2).

How to cite this article : Devi, N.U., Singh, D. and Leishangthem, G.D. 2025. Corneal dermoid in a dog. Indian J. Vet. Pathol., 49(1) : 99-101.

The excised dermoid tissue was processed and paraffin tissue blocks were prepared using the standard method[5]. The tissue sections (5 µm) were stained with hematoxylin and eosin stain for routine histopathology. Histopathologically, the tissue revealed the presence of an outer stratified squamous epithelium lining. The inner area revealed connective tissue stroma with numerous sebaceous glands, hair follicles and sudoriparous gland (sweat gland) along with few lymphocytes' infiltration were observed (Fig. 3). Post-operative care and management included topical installation of eye drop. Gatiquin (Gatifloxacin 0.3% w/v, Cipla) for a period of one week along with parenteral antibiotic administration of Inj. Cefotaxime @ 20-25 mg/kg BW twice daily for 5 days and Inj. Meloxicam (Inj.

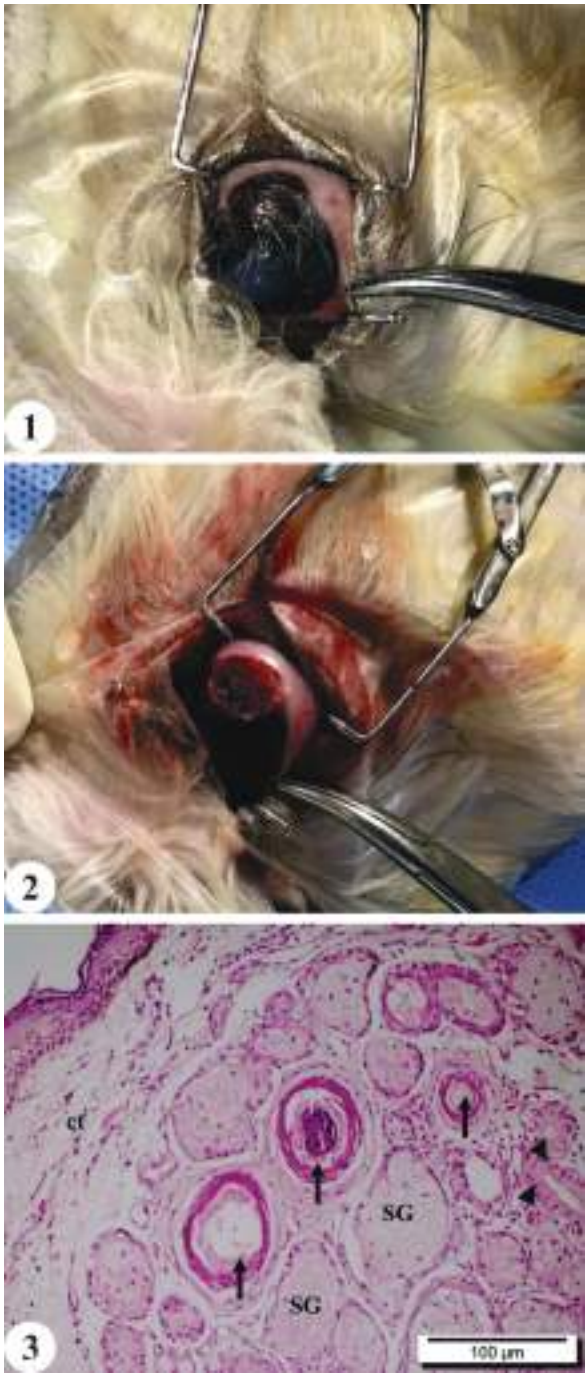

Fig. 1. Dermoid in the right eye: Presence of tissue and hair on the surface of the cornea, limbus and bulbar conjunctiva; **Fig. 2.** Appearance of eye after surgical resection of the dermoid; **Fig. 3.** Histopathology of the dermoid cyst showing the presence of an outer stratified squamous epithelium lining and numerous sebaceous glands (SG) along with hair follicles (arrow) and sudoriparous gland (arrow head) within the connective tissue stroma (ct) (H&E, Bar = 100 µm).

Melonex®, Intas Pharmaceuticals Ltd., Ahmedabad) @ 0.2 mg/kg once daily for 3 days. The owner was advised to apply an Elizabethan collar for 10 days.

The physiopathological mechanism for a choristoma formation is unknown, however most likely hypothesis is that a dermoid is developed by abnormal differentiation of ectoderm at an aberrant location maintaining the histological characterstics of skin[6]. The presence of dermoid has been reported at different sites which may vary with species and even breeds[7]. Corneal dermoid causes discomfort to the patient due to continuous irritation, pain and ocular discharge, warranting appropriate medical or surgical management[3]. Dermoids have been reported in canine and rarely in feline patients. Certain breed predisposition has been documented in dogs with development of cutaneous dermoid cysts seen in Rhodesian ridgeback, Shih-Tzu, Siberian Husky, Beagle, Welsh Corgi and Dachshund breeds[8,9]. It is believed that dermoids are congenital and not hereditary, however, cases have been reported linked to genetic factors[10].

A dermoid cystis usually composed of sebaceous, sweat glands along with hair follicles and can be differentially diagnosed with other cysts such as epidermoid cyst. In the present study, the diagnosis was made on the basis of histopathological features containing the hair follicles, sebaceous and sweat gland as corneal dermoid. In a retrospective study, ocular dermoid were divided as limbal, eyelid, corneal and conjunctival. They also showed that surgical removal of ocular dermoids was curative[7]. Superficial keratectomy is considered as a successful treatment for corneal dermoid. Some degree of recurrence can be expected if complete removal of dermoid is not carried out and manual epilation of hair is a temporary relief to the patient as the hair may grow again[2]. Moreover, surgical excision should be performed at an early age to restore functional development of the eye and prevent visual impairment[11]. In the present case, the dermoid was excised completely and the corneal wound healed uneventfully without any signs of corneal opacity/scarring or visual impairment. There was no recurrence of dermoid up to one year following resection.

REFERENCES

1. Erdikmen DO, Aydin D, Saroglu M, Guzel O, Hasimbegovic H, Ekici A, Gurel A and Ozturk GY. 2012. Surgical correction of ocular dermoids in dogs: 22 Cases. *Kafkas Univ Vet Fak Derg* **19:** 41-47.
2. Lee J, Kim M, Kim I, Kim Y and Kim M. 2005. Surgical correction of corneal dermoid in a dog. *J Vet Sci* **4:** 369-3706.
3. Rajput A, Malik V, Vijay R, Gangwar H and Pandey RP. 2018. Surgical correction of ocular dermoid in a Labrador dog. *J Entomol Zool Stud* **6:** 59-61.
4. Choudhary M and Kalita D. 2016. Surgical management of sclero-corneal dermoid in a dog. *Intas Polivet* **17:** 478-479.
5. Al-Sabawy HB, Rahawy AM and Al-mahmood SS. 2021. Standard techniques for formalin fixed paraffin embedded tissue: A pathologist perspective. *Iraq J Vet Sci* **35:** 127-135.
6. Balland O, Raymond I, Matheison I, Isard PF, Videmont-Drevon E and Dulaurent T. 2015. Canine bilateral conjuncti-

vo-palpebral dermoid: Description of two clinical cases and discussion of the relevance of the terminology. *Case Rep Vet Med* 1-6.
7. Zachary B and Eric L. 2019. Ocular dermoids in dogs: A retrospective study. *Vet Ophthalmol* **22:** 760-766.
8. Abu-seida AM. 2014. Corneal dermoid in dogs and cats: a case series and review of literature. *Glob Vet* **13:** 184-188.
9. Alam MM and Rahman MM. 2012. A three years retrospective study on the nature and cause of ocular dermoids in cross-bred calves. *Open Vet J* **2:** 10-14.
10. Horikri K, Ozaki K, Maeba H and Narama I. 1994. Corneal dermoid in two laboratory beagle dogs. *Exp Anim* **43:** 417-4204.
11. Assefa A. 2018. Surgical management of congenital ocular dermoid cyst: a review. *J Glob Sci* **6:** 207-2018.

Title of Thesis	:	Pathomorphological studies on mortality of Kamrupa variety of chicken with special reference to respiratory tract infection
Name of the Student	:	**Mandhadi Sravan Kumar Reddy**
Name of the Advisor	:	Dr Nayanjyoti Pathak
Degree/Year	:	MVSc/2023
Name of the University	:	Assam Agricultural University, Jorhat -785 013, Assam

Kamrupa variety is a new improved variety of chicken developed by crossing indigenous birds of Assam with a broiler parent PB-2 and a layer parent Dahlem Red. In the present study a total 784 unhatched eggs were examined and 320 Kamrupa carcasses were necropsied to study the factors associated with dead-in-shell embryos in embryonated eggs and pathomorphology of mortality in Kamarupa variety of chicken, respectively.

Among unhatched eggs 444 (56.63%) and 340 (43.37%) were dead-in-shell embryos and infertile eggs, respectively. Of the 444 dead-in-shell embryos examined, 2.47% showed adhesions, 2.70% stunted growth, 2.70% embryo with excess yolk retention, 5.40% malformations, 7.88% dehydration, 20.27% malpositions, 20.94% dead-in-shell embryos suspected of infectious reasons, 4.09% decomposed eggs were recorded with 33.55% cases showing no definite abnormalities or died of undiagnosed causes.

Different malpositions were recorded as head towards the left (48.89%), feet over the head and face (20%), beak above the right wing (15.56%), head in between the thighs (13.33%) and cases with upward orientation of the beak towards aircell with twisted neck (2.22%). Different malformations recorded in the present study include crossed beak (37.50%), monsters (25%), short lower beak (brachygnathia) (16.67%), short upper beak (16.67%) and vitelline rupture conditions (4.16%). In the present study 20.94% dead-in-shell embryos were suspected for infection from which 89 isolates of *Escherichia spp.*, *Staphylococcus spp.*, *Proteus spp.*, *Klebsiella spp.* and *Bacillus spp.* could be isolated.

In 320 necropsied carcasses 15% Newcastle disease, 13.75% Marek's disease, 7.5% infectious bronchitis, 13.44% colibacillosis (7.5% colisepticaemia, 3.75% oophoritis and salpingitis, 1.56% egg peritonitis and 0.63% egg bound condition), 9.38% coccidiosis, 3.75% ascardiasis, 4.38% visceral gout, 3.75% fatty liver haemorrhagic syndrome and 20.31% miscellaneous condition which includes 10.93% trauma, 4.06% hepatic dysfunction, 4.06% haemorrhagic enteritis and 1.25% pneumonia were recorded. Along with above mentioned diseases 8.75% carcasses were autolysed or putrified in which any pathological conditions could not be diagnosed. In the present study highest mortality was due to Newcastle disease.

Age wise the highest mortality (40.63%) was recorded in chicks (0-8 weeks old), followed by 30.31% in adults (>20 weeks) and 29.06% in growers (9-20 weeks). Season wise highest mortality (38.44%) was recorded during winter followed by 26.56% in post-monsoon, 24.69% in monsoon and 10.31% in pre-monsoon.

Fifteen (15) and two (2) oro-pharyngeal swabs out of 118 swabs sample collected from live birds found positive for ND and IB through RT-PCR. Other important respiratory diseases such as ILT and CRD were found negative through PCR. Among the carcasses 48 cases of Newcastle disease and 24 cases of Infectious bronchitis were molecularly diagnosed using RT-PCR targeting F gene and N gene, respectively. Similarly 44 cases of Marek's disease was also moleculary confirmed by PCR targeting pp38 gene.

Title of Thesis	:	Pathomorphological studies on canine tumors with special reference to paraneoplastic syndrome
Name of the Student	:	**V. Sarachandra**
Name of the Advisor	:	Dr A. Nasreen
Degree/Year	:	MVSc/2025
Name of the University	:	Sri Venkateswara Veterinary University, Tirupati, Andhra Pradesh

The study aimed to establish the paraneoplastic syndrome in veterinary medicine, evaluating blood and serum alterations, gross pathology and associated cytological, histopathological and immunohistochemical changes in various canine tumors. According to the study, there were 55 cases of different kinds of cancer, such as round cell tumors (20%), mammary tumors (18.18%), mesenchymal tumors (23.64%), epithelial tumors (21.82%) and other tumors (16.36%).

With papilloma (7.3%), squamous cell carcinoma (3.63%), individual cases (1.82%) of infundibular keratinizing acanthoma, hepatoid gland adenoma, sebaceous carcinoma, apocrine gland adenocarcinoma, basosquamous carcinoma and basal cell carcinoma as the most prevalent tumors, epithelial tumors (21.82%) ranked second in the study. Mild to severe anaemia, leucocytosis, hypoglycemia, hypocalcemia and occasionally higher levels of alanine aminotransferase, aspartate aminotransferase, gamma glutaryltransferase and alkaline phosphatase were hemato-biochemical alterations.

With fibromyxoleiomyoma (3.63%), leiomyxofibroma (3.63%), cavernous hemangioma (3.63%), individual cases (1.82%) of lipoma, liposarcoma, lipofibroma, chondroma, fibroma, myxofibroma and hemangiopericytoma, mesenchymal tumors were the most prevalent (23.64%). Moderate anemia, leucocytosis with lymphocytosis and eosinophilia were among the hematological alterations. Hypoproteinemia, hypoglycemia, hypocalcemia and occasionally elevated levels of AST, GGT, ALP and BUN were among the biochemical alterations.

Simple cystic-papillary carcinoma (3.63%), individual cases (1.82%) of simple tubulopapillary carcinoma, mixed cystic-papillary carcinoma, microacinar adenocarcinoma, chondrosarcoma with adenocarcinoma, capillary hemangioma, fibrosarcoma, mixed cystic chondrolipo fibroma and cystic hemangiochondro fibrolipoma was the most common type of mammary gland tumors reported (18.18%). Moderate anemia, neutrophilic leucocytosis, lymphocytosis, monocytosis, thrombocytopenia, hypoproteinemia, hypoalbuminemia, hypoglycemia, hypocalcemia, elevated levels of AST, ALT, ALP and BUN were all found by hemato-biochemical analysis.

Histiocytic sarcoma (1.82%), histiocytoma (1.82%), mast cell tumor (5.4%), transmissible venereal tumor (9.1%) and lymphoma (1.82%) were the next most common tumors in dogs, after round cell tumors. Haematology showed leucocytosis, eosinophilia, mild to moderate anemia, and occasionally monocytosis. Hyper and hypoproteinemia, hypoalbuminemia, hypergamma globulinemia, hypoglycemia, hypocalcemia, and occasionally depleted AST and elevated AST and ALP levels were found by serum biochemical analysis.

Seminoma (3.63%), sertoli cell tumor (3.63%), individual cases (1.82%) of granulosa cell tumor, luteoma, clear cell hepatocellular carcinoma, malignant melanoma and melanoma were the least common tumors, accounting for 16.36% of all tumors. Haematology revealed eosinophilia, neutrophilic leucocytosis, mild to moderate anemia and occasionally monocytosis. Hyperproteinemia, hyperalbuminemia, hypergamma globulinemia, hypoglycemia, hypocalcemia and in certain instances, elevated ALP levels in biochemical analysis.

Vangies on showed red collagen in papilloma, fibromyxoleiomyoma, leiomyxofibroma, lipofibroma, myxofibroma and certain mammary tumors, while toluidine blue staining showed purple metachromatic granules in mast cell tumors. Antinuclear antibodies (ANA) were not a reliable indicator of tumor progression due to their lower values than reference in many tumors.

Strong vimentin expression was found in TVT and MCT by immunohistochemical analysis, with focal positivity in tumors of the mammary gland and sertoli cell. While cytokeratin expression was focal in clear cell hepatocellular carcinoma, it was strong and diffuse in poorly differentiated SQCC, papillary adenocarcinoma type mammary tumors and apocrine gland adenocarcinoma. Papillary type mammary gland tumors showed positive expression of the estrogen receptor and progesterone receptor. In MCT, CD117 expression was highly positive. Granulosa cell tumors had focally positive inhibin-α.

Title of Thesis	:	Toxic effects of co-exposure of dibutyl phthalate and cadmium chloride on ovary and brain of adult zebrafish
Name of the Student	:	**Badi Mohamadmusaraf Ibrahim**
Name of the Advisor	:	Bhavesh Trangadia
Degree/Year	:	MVSc/2025
Name of the University	:	College of Veterinary Science and Animal Husbandry, Kamdhenu University, Junagadh-362 001, Gujarat

Dibutyl phthalate (DBP) and cadmium chloride ($CdCl_2$) are environmental contaminants with significant endocrine disrupting properties. Both compounds exhibit toxicity through disrupting reproductive and neurological functions in aquatic organisms and posing serious ecological and health risks. A total of 450 adult female zebrafish, aged above 3 months were used to evaluate the toxicological effects of DBP and $CdCl_2$ in ovary and brain after daily exposure for 28 days. The study carried out in two phases under standard laboratory conditions. In phase-I, 30 zebrafish were equally divided in 5 groups *viz.*, control (RO water), vehicle control (0.01% ethanol) and remaining groups were co-exposed to DBP and $CdCl_2$ at concentration of TP1 (0.25 mg/L of water + 0.25 mg/L of water), TP2 (0.5 mg/L of water + 0.5 mg/L of water), TP3 (1 mg/L of water + 1 mg/L of water). Mortality or any symptoms of toxicity were not observed during the phase-I of the study. Histopathological evaluation was carried out during phase-I. Microscopic examination of ovary revealed yolk granule depletion (DYG) in zebrafish of TP1 and TP2 groups; while DYG and degenerated mature oocyte (DMO) along with comparatively increased number of peri-nuclear oocytes (PO) were evident in ovary of zebrafish from TP3 group. Histopathological examination of the brain did not reveal any appreciable microscopic changes in any of the treatment groups. Based on phase-I results, dose for the phase-II study was selected at 1 mg/L of water of each compound. In phase-II, 420 fish divided equally in 5 groups *viz.*, control (RO water), vehicle control (0.01% ethanol), T1: DBP (1 mg/L of water), T2: $CdCl_2$ (1 mg/L of water), T3: DBP+$CdCl_2$ (each at 1 mg/L of water). Behavioral parameters, oxidative stress parameters, histopathological changes and mRNA expression profile of *sod, cat* and *nrf2* genes in ovary and brain were carried out during this phase. Anxiety like behaviour and social behaviour evaluated on day 14 and 28 of the experiment using novel tank, light-dark preference, social preference and social recognition tests. Group T3 showed anxiety-like behavior and alterations in social behaviour on day 14 and 28 of the experiment. Grossly, ovary and brain of zebrafish from all treatment groups were apparently normal. Histopathological examination of ovary revealed DYG in mature oocytes and DMO along with a significantly increased number of PO was observed in T1 group; while DYG in mature oocytes along with DMO evident in ovary of zebrafish from T2 group. In T3 group, DYG, DMO and a comparatively increased number of PO were observed. Superoxide dismutase (SOD) activity and total antioxidant capacity (TAC) levels in the ovary of all treatment groups, and catalase (CAT) activity in T1 and T3 groups, were significantly lower, whereas malondialdehyde (MDA) was significantly higher in the T3 group as compared to control group. In brain, SOD activity and TAC level were significantly lower in T3 group; Significantly CAT activity and significantly higher MDA level reported in all treatment groups as compared to the control group. In the ovary, mRNA expression of *sod* genes was down-regulated in T1 and T3 groups, *cat* in the T3 group and *nrf2* in all treatment groups as compared to the control group. In the brain, *cat* and *nrf2* expression levels were significantly down-regulated in the T3 group as compared to the control group.

Title of Thesis	:	Pathology of porcine circovirus associated with respiratory disease complex in pig
Name of the Student	:	**Thesni M. Thomas**
Name of the Advisor	:	Dr Chandrakanta Jana
Degree/Year	:	MVSc/2024
Name of the University	:	ICAR-Indian Veterinary Research Institute, Izatnagar, UP

Porcine circovirus (PCV) causes a diverse range of diseases in pigs, which incurs huge economic losses to swine industry globally. PCV2 is a significant pathogen contributing to PRDC outcome. Recently, PCV3 was also detected in pigs showing respiratory disease. The present study was performed to study the occurrence and pathology of porcine circoviral infections associated with respiratory disease complex in pigs and further characterise the circovirus. Representative tissue samples were collected from PM facility, ICAR-IVRI, Izatnagar and slaughter houses in Bareilly. Following systematic necropsy and pathological investigation, the samples were subjected to PCR to detect PCV2 and PCV3. Other methodologies like immunohistochemistry and TUNEL assay were also performed. The present study revealed a high occurrence of PCV2 as 36.15% (47/130) of animals were infected with PCV2. Nursery piglets (52.94%) were the most affected group in the particular study. Out of 47 positive PCV2 infections, 7 (14.89%) cases were coinfected with *Haemophilus parasuis* and *Streptococcus suis*. The clinical form of PCV2 was associated with PCV2-SD with respiratory organ as the major target. PCV3 was not detected in any of the samples. The most consistent gross lesions observed in PCV2 associated respiratory disease was in lungs and lymph node. The salient gross findings in lungs involved uncollapsed and edematous lungs with varying degree of consolidation and congestion. Lymphadenopathy with severe congestion and haemorrhage were the salient gross lesions in lymph node. The important histopathological findings in lungs were interstitial, bronchointerstitial and bronchopneumonia. The major type of pneumonia caused by PCV2 in the present study was bronchointerstitial (53.19%) and interstitial pneumonia (31.91%). Bronchopneumonia was associated with coinfections of PCV2 with *Streptococcus suis* and *Haemophilus parasuis*. Moderate to severe lymphoid depletion were observed in lymphoid organs like lymph nodes, tonsil, spleen and Peyer patches of ileum. Amphophilic to basophilic intracytoplasmic inclusion bodies were observed in bronchial epithelial cells of lungs and macrophages of lymph node. PCR detected a fragment of ORF2 gene specific for PCV2 from lungs and lymph nodes. PCV2 antigen was demonstrated in formalin fixed, paraffin embedded tissue sections by IHC. IHC against PCV2 revealed immunoreactivity in degenerating bronchiolar epithelial cells, macrophages and intravascular leukocytes of alveolar interstitium. PCV2 antigen was detected in the lymphocytes of lymphoid follicles of tonsil, mononuclear cells of lymphoid follicles in lymph nodes and mononuclear cells infiltrating the branch of splenic artery and in the lymphocytes of PALS indicating immunosuppression. TUNEL assay was performed in tissue sections of lymph nodes and tonsils. TUNEL assay of PCV2 affected lymph nodes and tonsils, revealed positive staining in lymphocytes. Phylogenetic analysis based on ORF2 genome sequences of PCV2, revealed that the circulating virus in the present study sharing close homology with PCV2d genotypes. One of the important etiology of PRDC in pigs is PCV2 causing mainly bronchointerstitial and interstitial pneumonia, lymphoid depletion in lymphoid organs, mainly affected nursery piglets and the circulating virus in affected pigs belongs to PCV2d genotype.

Title of Thesis : Characterization of Foot and Mouth Disease virus isolated from outbreaks in farm ruminants and localization of viral antigen in goat tissues

Name of the Student : **Shrinivas Janardhan Wattamwar**

Name of the Advisor : Dr Chandrakanta Jana

Degree/Year : MVSc/2023

Name of the University : ICAR-Indian Veterinary Research Institute, Izatnagar, UP

Foot and Mouth Disease (FMD) a contagious and economically devastating viral disease of cloven-footed animals and is caused by FMD virus (FMDV) of the genus *Aphthovirus* family *Picornaviridae*. India has undertaken a holistic FMD control measures through vaccination, disease surveillance and sero-monitoring in view of serious disease consequences and significant economic losses. Still, the sporadic disease outbreaks have been noticed in different parts of the country. Thus, an active and continuous surveillance through outbreak investigation, regular monitoring of antigenicity and genomic framework of FMDV strains is necessary in endemic setting. The present study was carriedout with the objectives a) to isolate and characterize FMD virus from farm ruminants in field outbreaks b) to study the localization of FMD virus antigen in goat tissues. Detailed history, farming practices and clinical observations were recorded from representative outbreaks (n=6) at Maharashtra, Uttarakhand and Uttar Pradesh in the year 2021. The clinical samples like vesicular fluid/ vesicular epithelium/hoof scrapping/other (n=79) and serum (n=141) were subjected for diagnosis by in-house serotyping ELISA, DIVA-ELISA and RT-mPCR. Histopathological and immunohistochemical studies of necropsy samples from milching cattle (n=2) and adult goat (n=1) were also performed. The outbreaks were noticed to be affected cattle, buffalo and goats. The multiple species rearing practice, access of common grazing land and water bodies, use of common milking machine and common milking man were found to be major risk factors in the disease transmission. Characteristic clinical signs and lesions were observed in cattle and buffalo, whereas goats showed mild and subtle clinical lesions. Grossly, typical lesions of disease were found in cattle like ulceration of tongue, gingival and ruminal pillar, lung emphysema and tigeroid heart. In goat, gross lesions included ulcerations on gums and dental pad, congestion in thyroid gland, pulmonary congestion, emphysema and oedema in lung lobes. Goat heart ventricles appeared flabby. Microscpically, cattle tongue tissues showed ballooning degeneration and lysis of stratum spinosum and subsequent formation of fluid filled vesicles in cornified epithelium. Lung section showed interstitial pneumonia and thickening of interstitium. Heart section showed hyalinization and extensive dissolution of cardiac muscles fibres. Tongue section of goat showed severe ballooning degeneration and necrosis of the epidermal cells accompanied with inflammatory cells infiltration. There were congested blood vessels and moderate to large size follicles having vacuolations in thyroid gland. Similar pulmonary and cardiac lesions in goats were evident. FMDV antigen was immune-detected in heart and lung tissue of cattle, whereas in goat, it was detected only in lung tissue. The laboratory tests confirmed five outbreaks as FMDV serotype O while one outbreak as FMDV serotype A. Three field virus isolates were identified as FMDV serotype O and vaccine matching exercise showed antigenic homology with currently used vaccine strain (r1 value > 0.3). In conclusion, the present study investigates risk factors, pathological features and antigenic characters of virus isolates of representative FMD outbreaks. The findings suggest disease outbreaks were caused by two FMDV serotypes and serotype O was found to be more predominantly circulating. The virus affected either irregularly vaccinated or unvaccinated farm ruminants and caused mortality in calves and adult animals also. The preparedness towards identified risk factors needs to be undertaken by the local animal health authorities to minimize the spread of disease and losses.

Proceedings of Executive Committee (EC) / General Body (GB) Meeting of XLI Annual Conference of Indian Association of Veterinary Pathologists and XV Annual Meeting of Indian College of Veterinary Pathologists and National Symposium on "Exploring Veterinary Pathology and Diagnostic Innovations in Animal and Poultry Diseases Amidst Climatic Challenge" held w.e.f. 28-30 November, 2024 at Sher-e-Kashmir University of Agricultural Sciences & Technology - Jammu, Union Territory of Jammu & Kashmir, India

The Executive Committee / General Body Meetings were held under the Chairmanship of Dr B.N. Tripathi, President, IAVP on 27th and 29th November, 2024 at SKAUST - Jammu, respectively. The meeting was attended by Vice Presidents, the Secretary General, Web Manager, Zonal Secretaries, EC Members and Life Members. Dr G.A. Balasubramaniam, Secretary General, IAVP welcomed all office bearers and EC/GB members. Dr B.N. Tripathi, President, IAVP & Vice Chancellor, Sher-e-Kashmir University of Agricultural Sciences & Technology - Jammu, Union Territory of Jammu & Kashmir, India gave opening remarks and appreciated the efforts of office bearers for advancement of IAVP/IVCP:

1. He emphasized that the sincere efforts should be made to improve the rating of the Indian Journal of Veterinary Pathology.
2. Members should be encouraged to submit plenty number of quality research papers to improve the standard of the Indian Journal of Veterinary Pathologists.
3. He also reiterated that the Heads of the Department of Veterinary Pathology should encourage their students to submit their MVSc and PhD thesis abstracts to the journal for publication without fail.

Agenda No. 1: Approval of the minutes of the Proceedings of last Executive Committee / General Body meeting held at ICAR-Indian Veterinary Research Institute, Izatnagar, Bareilly, Uttar Pradesh

1. The Secretary General informed the members about the action taken report (ATR) based on the Proceedings of 40th IAVP Conference, 2023 held at ICAR-IVRI, Bareilly.
2. The Proceedings have been circulated among the EC members and all the members agreed with the same.
3. The approval of minutes of the 40th Proceedings of IAVP held at Bareilly was proposed by Dr S.K. Panda, Zonal Secretary (East) and seconded by Dr R.V.S. Pawaiya, Secretary, ICVP. The minutes were approved by EC/GB members, respectively.

Agenda No. 2: Report by the Secretary General

1. **Request of Dr R.C. Ghosh to utilise the unspent balance money of IAVPCON 2016 held at Durg:** Dr R.C. Ghosh had requested for permission to utilise the unspent balance amount (Rs 2,58,855) of the conference. He organised in 2016 at Durg to purchase microscopes and repair works of equipment for teaching and research work of students of Department of Veterinary Pathology. Necessary permission was accorded to utilise the amount for the purpose requested with the condition that due acknowledgement should be given to the society.
2. **Zonal Activities:** West Zonal Conference and "Brain storming session on emerging diseases of livestock and poultry" and National Workshop of ICVP were conducted by the Department of Veterinary Pathology on 3rd & 4th June 2024 at Krantisinh Nana Patil College of Veterinary Science, MAFSU, Shirwal. South Zone Conference and National Symposium on "Recent advances in diagnosis of infectious, non-infectious and zoonotic diseases of domestic and wild animals" were organized by the Department of Veterinary Pathology on 26th & 27th of September 2024 in Veterinary College at Shivamogga, KVAFSU, Karnataka. While appreciating the organisers of both zonal conferences, the President of IAVP entreated all the Zonal Secretaries should come forward to organize at least one event each year Conference/Symposium/Workshop in their respective zone in order to motivate the youngsters. Zonal Secretaries were directed to undertake some activities and cooperate for strengthening of the society.
3. **New Life Members:** A total of 58 new Veterinary Pathologists had been enrolled as Life Member of IAVP in 2024. As on date, there are around 1597 members in the society. HoDs were requested to enrol their PG students compulsorily as Life Members of the society.
4. **Database Updating:** Updating of the addresses of Life Members of the IAVP was discussed and the Zonal Secretaries were requested to expedite the process and complete the work at the earliest.

Agenda No. 3: Report of the Chief Editor

Dr A. Anand Kumar, Chief Editor, IJVP, could not turn up for the EC/GB meeting due to personal reasons and expressed inability to attend the same in advance. On his behalf, Secretary General briefed the house about the IJVP report and informed that:

1. A total of 46 research articles and 3 thesis abstracts were received for publication in the IJVP.
2. All four issues of IJVP of 2024 were published well in time and uploaded in IAVP Website.
3. The acceptance and rejection rate of the articles were 91.31% and 8.69%, respectively.
4. A wide discussion was held to switch over the Indian Journal of Veterinary Pathology from IndianJournals.com to Indian Council of Agricultural Research, Directorate of Knowledge Management in Agriculture (ICAR-DKMA), e-Journal publication system for publication of the journal both online and offline w.e.f. 2025. Finally as per the directions and approval of Dr B.N. Tripathi, Honourable Vice Chancellor, SKUAST, Jammu and President (IAVP) it was decided to discontinue the publication system of IJVP with IndianJournals.com and to transfer the ownership of the IJVP to ICAR-DKMA to improve the NAAS rating and Citation Index. The purpose of the incorporating our journal in ICAR e-Journal publication system is to have wider reach and higher usage among the academicians, scientists and research scholars. The Chief editor and his team were requested to expedite the process.
5. The Chief Editor and Editors were requested to collect detailed reports of citations, downloads etc. of IJVP.
6. The President requested Secretary General to write a letter to all the HODs to send the PG thesis abstracts to IJVP for publication.

Agenda No. 4: Non-return of the advance/seed amount (Rs 50,000/-) received by Dr M. Lakshman, Organizing Secretary of XXXIX Annual Conference of IAVP during 17-20 November, 2022 held at Department of Veterinary Pathology, College of Veterinary and Animal Science, Rajendranagar, PVNRTVU, Hyderabad, Telangana

The matter was elaborately discussed. Secretary General explained in detail about the action taken so far in this regard. A letter was sent to Dr M. Lakshman requesting to refund the long pending issue of seed money (Rs 50,000/-) and the 20% of the registration fee of the Conference. He organised in PVNRTVU, Hyderabad in 2022. In response, Dr M. Lakshman has requested the society for exemption from the return of the seed money and 20% of the registration fee as the expenditure had exceeded his original estimate during the conference. Subsequently another letter was sent by the Secretary General to him mentioning that there is no any possibility for exemption and insisted him to return the money. Still he has not returned the amount. After a long deliberation on the issue, the EC/GB members are in view that Dr M. Lakshman should refund the seed money (Rs 50,000/-) without fail. After the receipt of the seed money (Rs 50,000/-) from him, the possibility for exemption for the 20% of the registration fee may be considered.

Agenda No. 5: Treasurer Report

Dr Pawan Kumar, Treasurer could not turn up for the EC/GB meeting due to his personal reason. Instead, Dr K.P. Singh, Vice President presented the Audit Report of the income and expenses of the IAVP for the year 2023-24. He informed the house:

Opening Balance for the year 2022-23	Rs 2,55,298.00
Income during the year	Rs 6,29,421.00

(Subscription fee, membership fee, publication charges, financial assistance from ICAR, interest earned from FDR, Award processing fee etc.)

Expenditure during year	Rs 9,57,269.00

(Printing IJVP charges, remunerations and salary, website maintenance, postal stamps, zonal conferences, audit fee, etc.)

Excess Expenditure	Rs 3,03,748.00
Total Balance	Rs 2,97,961.00
Cash in Hand	Rs 5,787.00
Fixed deposit in SBI	Rs 43,10,757.00

Treasurer's Report was accepted by EC/GB members.

1. Treasurer is constantly observing and narrating that in the recent past years income of IAVP is reduced and expenditure is increased which resulting in breaking of fixed deposit certificates annually to meet out expenditures. This was matter of great concerned. One of important reason of over expenditure is payment of salary of Rs 3,60,000/- (Rs 15,000/- X 2 = Rs 30,000/- X 12 = Rs 3,60,000/-) for two contractual staff one at with Chief Editor at Tirupati and another at with Managing Editor at Izatnagar. The matter was discussed in great detail and following decision was taken:
2. The Chief Editor is requested to restrict the wages of contractual labour within Rs 10,000/- in view of financial constraints.
3. At Izatnagar, full time contractual worker with monthly salary of Rs 10,000/- should be kept instead of Rs 15,000/-

Concerned IAVP office bearer should make attempt to enhance income of by making new LMs, sale of journal and other measures.

Agenda No. 6: Web Manager Report

1. Dr R. Somvanshi, Web Manager informed that IAVP website (https://www.iavp.org) is regularly updated and functioning smoothly.
2. He also informed that The Lesion, 2024 was published and circulated to life members and also uploaded in IAVP website.

Agenda No. 7: Venue of the next IAVP conferences

1. The venue of the next IAVP Conference was discussed in detail. The Department of Veterinary Pathology, Faculty of Veterinary Science & Animal Husbandry, Birsa Agricultural University, Ranchi, Jharkhand was proposed as the venue for the Veterinary Pathology Conference, 2025. Dr M.K. Gupta, Professor & Head was proposed to be the Organizing Secretary of the Conference.
2. Department of Veterinary Pathology, College of Veterinary Sciences & Animal Husbandry, DUVASU, Mathura, Uttar Pradesh was proposed as the venue for the Veterinary Pathology Conference, 2026. Dr Desh Deepak Singh, Professor and Head was proposed to be the Organizing Secretary of the Conference.

Agenda No. 8: Miscellaneous

1. The most of IAVP Patrons *viz.* Drs P.K.R. Iyer, R.R. Shukla, D.D. Heranjal, D.L. Paikne, Mrs. Shanta Sinha, T.L. Som, N.C. Jain and Mrs. Shanti Vyas are either aged and no-active or passed away in due course. As such Eminent Veterinary Pathologists and Ex. President IAVP viz. Drs J.L.Vegad (Jabalpur), G.C. Mohanty (Bhubaneswar), R.N.S. Gowda (Bengaluru), Lal Krishna (New Delhi) and B. Muralimanohar (Chennai) who build IAVP should be inducted as Patron.
2. The non or poorly sponsored and uneconomic IAVP Awards which, are not on the names of Veterinary Pathologists should be discontinued. As such matter was discussed in detail following decisions were taken to modify/ discontinue following three IAVP Awards:

   IAVP-Savithree Jibachch Sinha Third Best-Poster Presentation Award - To be discontinued

   IAVP-Gang-Mana Sharma Award for Best Article/Case Report on Pack Animals - To be discontinued

   IAVP-Dr Ram Raksha-Kiran Shukla Award for Second Best MVSc Thesis - To be modified as IAVP-Award for Second Best MVSc Thesis

3. **Proposal of New Awards:**

   A. Dr Supriya Shukla, Mhow, MP proposed to institute a new award in honor of Dr J.L. Vegad. She consented to donate Rs 1.00 lakh to IAVP. The matter was discussed and it was decided that one of currently existing award may be named after Dr Vegad *viz.* IAVP-Dr J.L.Vegad-Best PhD Thesis Award.

   B. Dr M.K. Gupta, Ranchi proposed to institute a new award in honor of Dr H.V.S. Chauhan. He consented to donate Rs 1.00 lakh to IAVP. The matter was discussed and it was decided that one of currently existing award may be named after Dr Chauhan *viz.* IAVP-Dr H.V.S. Chauhan-Best Poultry Pathologist Award.

Agenda No. 9: Condolence on Deceased IAVP Members

1. The house was informed that two Veterinary Pathologists viz. Dr U.K. Sharma (17.11.2024), Pantnagar and Dr A. Prakash (21.08.2024) Tamil Nadu have passed away.
2. Dr Uma Kant Sharma (95) born on November 11th of 1931 completed his under graduation and Post graduation

in Veterinary College, Mathura and IVRI, Mukteshwar, respectively. Subsequently, he had undergone the study of M.S. in Illinois in 1964 and later pursued his PhD, program in Indian Veterinary Research Institute, Izatnagar in 1976 under the guidance of Dr C.M. Singh, Director of the Institute. He was the recipient of gold and silver medals for his outstanding excellence in academics. He was having total professional service of 38 years with working in different capacities in various laboratories within country and abroad. He had served for more than 20 years as a faculty in Veterinary College, Pantnagar and about 8 years as Professor and Head, Department of Veterinary Pathology & Hygiene. He had contributed considerably for research, extension and disease diagnosis during his career. Dr Sharma was Patron of IAVP and he donated Rs 50,000/- to IAVP. He passed away on 17th November, 2024.

3. Dr A. Prakash, alumni of Veterinary College and Research Institute, Namakkal was Wildlife Veterinary Pathologist, Tamil Nadu working with the Forest Department for the past 14 years and since last 8 years as Wildlife Veterinary Surgeon. Dr Prakash had involved in several elephant captures and other wildlife rescue operations. He was conferred with 'Anna Award' by the state government in recognition of his bravery during such rescue operations. The elephant calf Raghu, featured in the Oscar winning film, "The Elephant Whisperers", was rescued and treated by him. He has also published several scientific papers and articles in reputed journals. He passed away on 21st August, 2024.
4. The house appreciated the contributions and services of the both individuals to the profession and IAVP and a silence of 2 minutes was observed for peace of departed souls.

Agenda No. 10: Vote of Thanks

Dr G.A. Balasubramaniam, Secretary General proposed the vote of thanks to all the members of the EC/GB for their contributions in fruitful discussion in the meeting.

RESULTS OF IAVP AWARDS - 2024

The Indian Association of Veterinary Pathologists has instituted a number of awards. Awards are distributed to Veterinary Pathologists who have excelled in professional competence as assessed by appropriate criteria. The IAVP administers more than 6 groups of awards where an application is required, the last date for receiving award application is one month before the opening day of Annual Conference. The awards results for IAVP, 2024 are listed below:

I. IAVP-Young Scientists Awards

1. IAVP-Dr Balwant Singh Memorial Young Scientist Award for Best Oral Presentation

Title: Patho-epidemiology of canine distemper virus and characterisation of SLAM/CD150 receptor in Indian wild carnivores

Authors: Deekshita V., Karikalan M., Sharma G.K., Sharma K., Sai Balaji K.G., Chatla A., Thilakeshwaran S. and Pawde A.M.

Affiliation: Centre for Wildlife, ICAR-Indian Veterinary Research Institute, Izatnagar, Bareilly, Uttar Pradesh

2. IAVP-Dr S.K. Nigam Memorial Young Scientist Award for Second Best Oral Presentation

Title: Therapeutic evaluation of quercetin-loaded chitosan nanoparticles in diabetic cutaneous wound healing in Wistar rats

Authors: Saharan M., Sharma M., Jangir B.L., Kant V., Joshi V.G., Saini P. and Lather D.

Affiliation: College of Veterinary Sciences, LUVAS, Hisar, Haryana

3. IAVP-Prof S. Ramachandran Memorial Best Molecular Oncologist Presentation Award

Title: Role of exosomes and its cargo in the diagnosis and progression of spontaneous canine mammary tumours and chemically induced mammary tumours in rat model

Authors: Neha, Yadav H.S., Kumar S.D.V., Manohar S., Sree Lakshmi P., Singh C.P., Srivastav A., Singh V., Pawaiya R.V.S., Pawde A.M., Kumar R. and Kumar P.

Affiliation: ICAR-IVRI, Izatnagar, Bareilly, Uttar Pradesh

4. IAVP-Prof C. Balachandran Molecular Pathology Award

Title: Attenuation of recombinant EHV1 through deletion of glycoprotein I and its pathological and immunological study in murine model for selection of an improved vaccine candidate

Authors: Supriya K., Bera B.C., Madhwal A., Pradhan S.S., Balena V., Khetmalis R.S., Pavulraj S., Anand T., Tripathi B.N. and Virmani N.

Affiliation: ICAR-NRC on Equines, Hisar, Haryana

II. (A) IAVP-Poster Presentation Awards

1. IAVP-Best Poster Presentation Award

Title: Assessment of immunohistochemical expression of phenotypic biomarkers of epithelial mesenchymal transition in canine mammary tumors

Authors: Bhate Y.A., Srivastav A., Gangwar K., Prabhu S.N., Gangwar N.K., Singh A.P., Chaudhary J.K., Singh R. and Singh D.D.

Affiliation: CVS & AH, DUVASU, Mathura, Uttar Pradesh

2. IAVP-Organizing Secretary Second Best Poster Presentation Award

Title: Retrospective analysis of tumors and tumor like lesions in equines in Punjab

Authors: Sood R., Omer K. Baba, Geeta Devi L., Amarjit Singh, Kuldip Gupta, N.D. Singh, S. Deshmukh, A.P.S. Brar, Vishal Mahajan, Jagmeet Kaur, Sonam S. Bal, A. Verma and Vanshika

Affiliation: Guru Angad Dev Veterinary and Animal Sciences University, Ludhiana, Punjab

3. IAVP-Savithree Jibachch Sinha Third Best Poster Presentation Award

Title: Molecular detection of canine Bocavirus infection in a pup - A first report from India

Authors: Jayappa K., Rajkhowa T.K. and Khithie J.B.

Affiliation: CVSc & AH, Central Agricultural University, Selesih, Aizawl, Mizoram

II. (B) Sessional IAVP Poster Presentation Awards

Session: Molecular Pathology and Oncology

1. **Title:** Clinico-pathological investigation of nasal adenocarcinoma in the sheep of semi-arid Rajasthan
   Authors: Sonawane G.G., Sharma D.K., Pandian S.J., Sharma S.R., Kumar J., Jain A.K. and Swarnkar C.P.
   Affiliation: ICAR-Central Sheep and Wool Research Institute, Avikanagar, Rajasthan
2. **Title:** Studies on different stages of bovine ocular squamous cell carcinoma (BOSCC) and identification of Bovine papilloma virus-1 (BPV-1) by polymerase chain reaction in OSCC in cattle
   Authors: Nithya P., Balasubramaniam G.A., Arulmozhi A., Gopalakrishnamurthy T.R. and Kathirvel S.
   Affiliation: Veterinary College and Research Institute, Namakkal, TANUVAS, Chennai, Tamil Nadu

Session: Pet/Companion Animals and Avian Pathology

1. **Title:** Prevalence and molecular characterization of Hydropericardium Hepatitis Syndrome - Inclusion Body Hepatitis in broiler chickens in the Jammu region
   Authors: Naveen B., Rahman S., Abrol R., Nashiruddullah N., Goswami P., Sood S., Farhan S. and Andrabi S.A.
   Affiliation: FVC & AH, Sher-e-Kashmir University of Agricultural Sciences, Jammu
2. **Title:** Clinicopathological diagnosis and application of Convolutional Neural Network (CNN) model for identifying *Babesia* infection in canines
   Authors: Sharma M., Kumar T., Agnihotri D., Sharma A., Sindhu N., Saharan S., Chauhan S. and Singh G.
   Affiliation: College of Veterinary Sciences, Lala Lajpat Rai University of Veterinary and Animal Sciences (LUVAS), Hisar

Session: Laboratory, Wild Animals and Forensic Pathology

1. **Title:** Assessment of anticarcinogenic effect of *Annona squamosa* (Custard Apple) seed extract in the experimentally induced mammary tumor of Sprague-Dawley rats
   Authors: Behera B., Vairamuthu S., Pazhanivel N., Sureshkannan S. and Senthil Kumar T.M.A.
   Affiliation: Madras Veterinary College, TANUVAS, Chennai, Tamil Nadu
2. **Title:** Amelioration of indomethacin induced gastric ulceration by quercetin loaded chitosan nanoparticles via modulation of COX-2 pathway: A novel therapeutic approach
   Authors: Saharan M., Sharma M., Jangir B.L., Kant V., Saini P., Jadhav M.N. and Nehra V.
   Affiliation: College of Veterinary Sciences, LUVAS, Hisar, Haryana

Session: Farm Animals Pathology

1. **Title:** Chronic cholangitis due to fascioliasis in a goat
   Authors: Sethi M., Kumar S., Suvaneeth P., Kadam R.G. and Gupta A.R.
   Affiliation: Faculty of Veterinary and Animal Sciences, Banaras Hindu University, Varanasi, Uttar Pradesh
2. **Title:** Cytopathological and molecular approaches of anthrax outbreaks in small ruminants
   Authors: Kumar V., Thangathurai R., Rajagunalan S., Madhesh E. and Ponnarasi S.
   Affiliation: Veterinary College and Research Institute, Tirunelveli, TANUVAS, Tamil Nadu

Session: Toxicopathology and Aquatic Animals Pathology

1. **Title:** Acute (fixed dose) and sub-acute (repeated dose) oral toxicity evaluation of polyherbal formulation in BALB/c mice
   Authors: Bharathi R., Prasanna K.S., Dhanush Krishna B., Bibu John Kariyil, Krithiga K., Dinesh C.N., Udhayakumar C., Pazhanivel N. and Venkataramanan R.
   Affiliation: College of Veterinary and Animal Sciences, Mannuthy, KVASU, Kerala
2. **Title:** Incidence of anisakiasis in grey mullet, *Mugil cephalus* from Kovalam coast of Tamil Nadu
   Authors: Ananda Raja R., Dixit A. and Sathish Kumar T.
   Affiliation: ICAR-Central Institute of Brackishwater Aquaculture, Chennai, Tamil Nadu

III. Journal Awards, 2023

1. IAVP-Dr C.M. Singh Award for Best Full Research Article (Non-Pack Animals)

Title: Emergence of a novel Canine Parvovirus 2c strain in India

Authors: J. Kiran and Tridib Kumar Rajkhowa

Issue: *Indian J. Vet. Pathol., 47(1): 39-46, 2023: DOI:10.5958/0973-970X.2023.00015.9*

Affiliation: Central Agricultural University, Selesih, Aizawl, Mizoram

2. IAVP-Dr S. Damodaran Award for Best Oncology Paper/Case Report

Title: *Diffuse large B-cell lymphoma with conjunctival involvement in a Dobermann dog: A case report*

Authors: S. Tamizharasan, S. Vairamuthu, N. Pazhanivel, M. Chandrasekar, M. Tirumurugaan and G.V. Sudhakara Rao

Issue: *Indian J. Vet. Pathol., 47(2): 179-183, 2023: DOI: 10.5958/0973-970X.2023.00033.0*

Affiliation: Madras Veterinary College, Chennai, TANUVAS, Tamil Nadu

3. IAVP-Dr B.S. Rajya Award for Best Non-Oncology Short/Rapid Communication

Title: *Pathological and molecular investigation of complex chronic respiratory disease (CCRD) in a broiler farm*

Authors: S. Govindhasamy, Megha Sharma, Sayali Kohale, Kuldeep Dhama and Asok Kumar M.

Issue: *Indian J. Vet. Pathol., 47(2): 169-172, 2023: DOI: 10.5958/0973-970X.2023.00030.5*

Affiliation: ICAR-Indian Veterinary Research Institute, Izatnagar, UP

4. IAVP-Gang-Mana Sharma Award for Best Article/Case Report on Pack Animals

Title: *Strongylus vulgaris induced aneurysm of mesenteric artery complicated with ileal volvulus in a horse*

Authors: M. Thangapandiyan, P. Krishnaveni, V. Kumar, P. Jalantha and G.V. Sudhakar Rao

Issue: *Indian J. Vet. Pathol., 47(2): 155-157, 2023: DOI: 10.5958/0973-970X.2023.00026.3*

Affiliation: Madras Veterinary College, Chennai, TANUVAS, Tamil Nadu

IV. IAVP-Best Post Graduate Thesis Awards

1. IAVP-Best PhD Thesis Award Thesis

Title: Pathomorphological studies on reproductive tract of layer chicken with drop in egg production

Name of Student: M. Sasikala

Major Adviser: P. Srinivasan, Professor and Head, VCRI, TANUVAS, Namakkal

2. IAVP-Dr Patri Rama Rao Memorial Second Best PhD Thesis Award Thesis

Title: Pathomorphological studies on bovine neoplasms with special reference to ocular squamous cell carcinoma

Name of Student: P. Nithya

Major Adviser: G.A. Balasubramaniam, Professor & Head, VCRI, TANUVAS, Namakkal, Tamil Nadu

IAVP-Best MVSc Thesis Awards

1. IAVP-Prof P.K.R. Iyer Memorial Best MVSc Thesis Award

Title: Attenuation of recombinant EHV1 through deletion of glycoprotein I and its pathological and immunological study in murine model for selection of an improved vaccine candidate

Name of Student: K. Supriya

Major Adviser: Nitin Virmani, ICAR-NRCE, Hissar, Haryana

2. IAVP-Dr Ram Raksha-Kiran Shukla Award for Second Best MVSc Thesis

Title: Evaluation of host cellular behaviors to decellularized extracellular matrix based porcine tunica vaginalis scaffolds in rat model

Name of Student: Arathy P.S.

Major Adviser: Dhanush Krishna, CVAS, Thrissur, KVASU, Kerala

V. IAVP-Achievement Awards in Specialty Subjects

1. IAVP-Best Farm Animals Pathologist Award

Rajeev Ranjan, Senior Scientist, ICAR-NIFMD, Bhubaneswar, Odisha

2. IAVP-Best Poultry Pathologist Award

Madhuri S. Hedau, Associate Professor, Nagpur Veterinary College, MAFSU, Nagpur, Maharashtra

3. IAVP-Dr B.L. Purohit Memorial Best Toxicologist-Pathologist Award

Vikram Patial, Scientist, CSIR-Institute of Himalayan Biosource Technology (IHBT), Palampur, Himachal Pradesh

4. IAVP-Best Companion Animal Pathologist Award (Bi-Annual Award)

M. Thagapandiyan, Professor, PDDSL, Namakkal, TANUVAS, Tamil Nadu

5. IAVP-Best Laboratory Animal Pathologist Award (Bi-Annual Award)

R. Madheswaran, Assistant Professor, VC & RI, Udumalpet, TANUVAS, Tamil Nadu

VI. IAVP-Special Encouragement Awards

1. IAVP-Best Veterinary Pathology Teacher Award

Kavitharani, Professor and Head, Veterinary College, Shivamogga, Karnataka

VII. Fellowship of Indian Association of Veterinary Pathologists, 2024

1. **M.K. Gupta**, Professor and Head, Veterinary College, BAU, Ranchi, Jharkhand

2. **B.J. Patel**, Professor & Head, College of Veterinary Sciences & Animal Husbandry, Kamdhenu University, Sardarkrushinagar, Gujarat

3. **Rohitash Dadhich**, Dean, College of Dairy & Food Technology, Jaipur, Rajasthan

VII. IAVP Appreciations/Activities/Recognitions

1. IAVP-Veterinary Pathology Congress - Thematic Lecture

Title: *Climate change and animal diseases*

Speaker: B.N. Tripathi

Affiliation: Vice-Chancellor, SKAUST-Jammu

2. IAVP-Veterinary Pathology Congress - Continuing Veterinary Pathology Education Lecture

Title: *Application of molecular and digital pathology in translational medicine*

Speaker: Manu M. Sebastian

Affiliation: Professor, Department of Veterinary Medicine and Surgery, Department of Translational Molecular Pathology, UT MD Anderson Cancer Centre, Houston, USA

3. IAVP-Dr P.P. Gupta Oration

Title: *Cytopathology of lymphadenopathy: An overview*

Speaker: N.K. Sood

Affiliation: Adjunct Professor, TVCC, GADVASU, Ludhiana, Punjab

4. IAVP-Appreciation to Organizing Secretary and Team

Pankaj Goswami, Organizing Secretary cum Professor and Head, Division of Pathology, Faculty of Veterinary Sciences, SKAUST-Jammu

5. IAVP-President Appreciation Certificate for Best EC Worker/Chapter - Jointly awarded to:

1. **Vitthal Dhayagude**, Organizing Secretary, IAVP-West Zone Conference and Workshop, Veterinary College, Shirwal, MAFSU, Maharashtra

2. **Manjunatha S.S.**, Organizing Secretary, IAVP-South Zone Conference, Veterinary College, Shivamogga, KV AFSU, Karnataka

G.A. Balasubramaniam
(Secretary General, IAVP)

SUPERANNUATION

Dr G. Saikumar

Dr G. Saikumar, a renowned scientist of Veterinary Pathology discipline at ICAR-IVRI, Izatnagar graduated from Orissa Veterinary College, Bhubaneswar and MVSc, PhD from Indian Veterinary Research Institute, Izatnagar. He has vast professional experience and marked contribution on swine diseases, especially infectious viral diseases of economic importance. He worked on Classical Swine Fever (CSF), and developed several new generation molecular diagnostics such as RT-PCR, Real-time RT-PCR, specific DNA and RNA probe-based In-Situ Hybridization techniques. His pioneering studies on the molecular epidemiology of CSFV infections in Indian pigs led to detailed information on emerging genotypes of CSFV in the country. Notable contributions in the field of swine diseases includes pioneering work on occurrence of Porcine circovirus associated diseases, Porcine parvovirus associated reproductive failure, Swine influenza H1N1, Porcine Teschovirus, Porcine Sapelovirus, Swine pox and Porcine Enterovirus G infections. Most notable among his contributions to swine diseases was his research on Japanese encephalitis in pigs, which finally culminated in the development of an inactivated vaccine for use in pigs. He filed a patent application for this innovation.

He has published more than 150 research papers in national and international journals of repute. As a faculty of IVRI Deemed University, he has guided 30 Master's and Doctoral students.

Dr Saikumar also contributed towards research management at ICAR-IVRI by working as In-charge PME Cell for 9 years. During this time, the research output of the institute, both in terms of quality of research publications and IP portfolio improved significantly. He has worked as Chairman of Institute Animal Ethics Committee and Member, Institute Biosafety Committee. He has been a Member in the Institute Management Committee (IMC) of several ICAR institutes; namely ICAR-CIRG, ICAR-CIRB, ICAR-NIHSAD, ICAR-NRC Camel and ICAR-NIVEDI. He is a Member Board of Management of ICAR-IVRI and SVVU, Tirupati. His tenure as Head, Division of Pathology and Joint Director Research (Acting) for 18 Months (from 28.4.2021 to 13.11.2022) is memorable.

He has successfully discharged his professional duties and superannuated on 31.12.2024. The Indian Association of Veterinary Pathologists wish him a healthy, happy and peacefull family life.

OBITUARY

Dr Gopal Yadgirkar Passes Away

Dr Gopal Yadgirkar was a simple, sober, dedicated teacher rendered his services at College of Veterinary Science, Rajendranagar, ANGRAU (erstwhile APAU). He was sincere, very active in Teachers' Association and IAVP activities. His contributions towards the profession were memorable. He passed away on 23.12.2024. IAVP family extends their condolences to the departed soul.

Prof. C.R. Lalitha Kunjamma Passes Away

Prof. C.R. Lalitha Kunjamma belongs to 1970 batch, College of Veterinary and Animal Sciences, Mannuthy. She completed her post graduation in the year 1974-76 and doctorate in the year 1987. She joined as JAP in the year 1977 and served for a long time as Scientist under AICRP on poultry and later as Head of AICRP on poultry farm, further as station Head of LRS, Thiruvazhmkunnu during 2005-2007 and then posted in Department of Veterinary Pathology, CVAS, Mannuthy. She put up an active service of 35 years (1977-2012) and retired in 24.5.2012 as Head of the department. She has guided more than 10 PG students as major advisor and co-guided many PG and PhD students. Her areas of interest were basically rooted in poultry pathology and ethnopharmacology. Through experimentation in lab animals and birds, she had proved the efficacy of lot of indigenous drugs. She was an active member and Programme officer of NSS and was a yoga instructor too.

After retirement in 2012, she also secured an MA in Sanskrit. She was an executive member in VASUTA (Retired Veterinary Teachers Association) and very active in the association until 2022 under various capacities like Joint Secretary. Prof. Lalitha Kunjamma was also a strong advocate of "Art of living" by Sri Ravisankar and practiced yoga throughout her life. The pure soul left us following a brief period of cardiac illness on 11.2.2025. IAVP family extends their condolences to the departed soul.

Dr Anil Purthi Passes Away

Dr Anil Purthi (Ex Dean, Professor (Rtd.) CVSc, LUVAS, Hissar) born on 15.6.1952. He was a simple, sober, philosopher and dedicated teacher who rendered his services as an excellent academician and administrator. He passed away on 16.2.2025. IAVP family extends their condolences to the departed soul.